ated Sample Preparation and Large-Volume Injection for Gas Chromatography with Spectrometric Detection

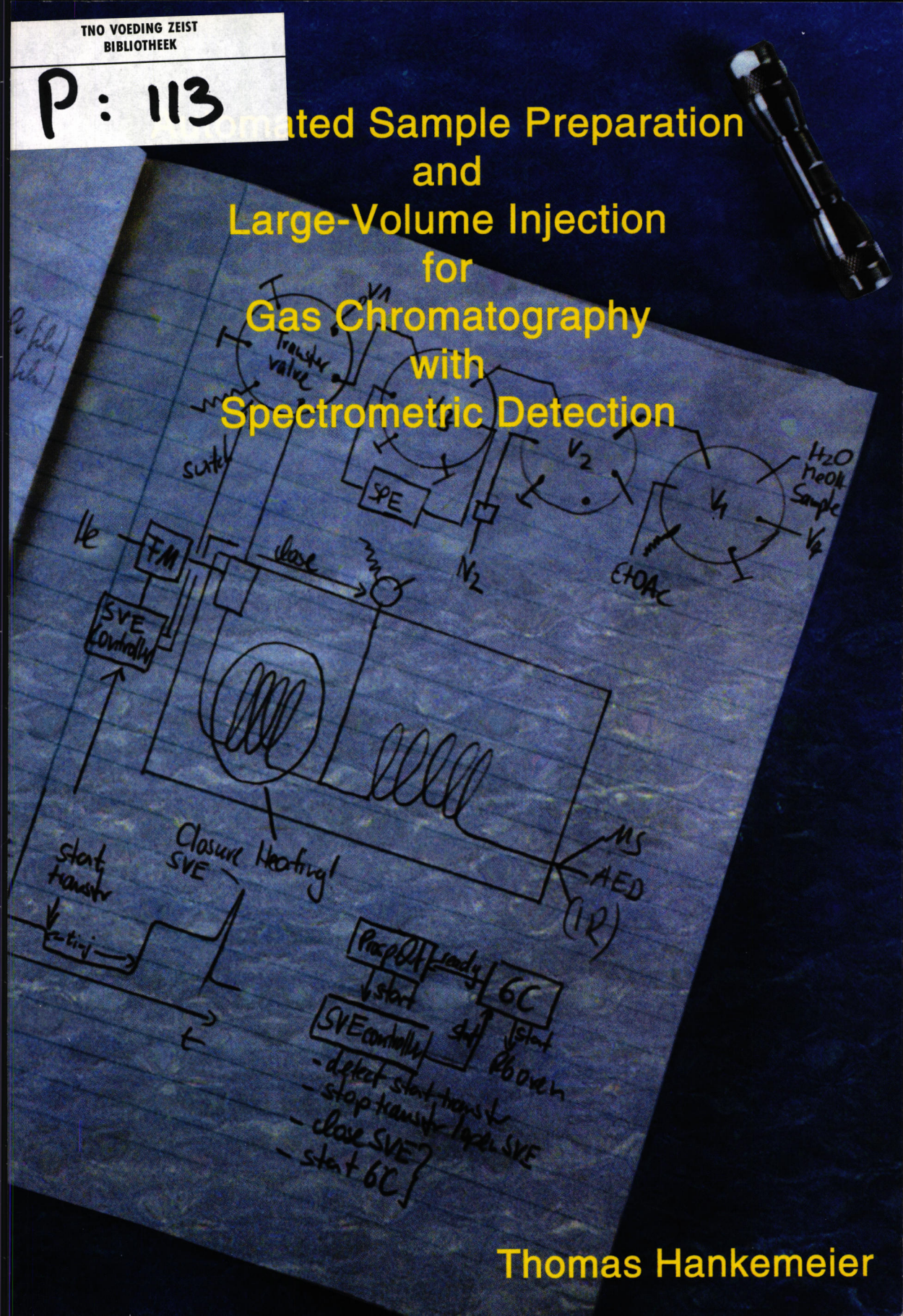

Thomas Hankemeier

Automated Sample Preparation and Large-Volume Injection for Gas Chromatography with Spectrometric Detection

Acknowledgements

The investigations presented in thesis were carried out at the Free University (Amsterdam, The Netherlands). Financial support was generously supplied by the European Union via a Human Capital and Mobility grant (EV5V-CT-93-5225) and the European River Basin Program (Amsterdam/Waldbronn).

VRIJE UNIVERSITEIT

Automated Sample Preparation and Large-Volume Injection for Gas Chromatography with Spectrometric Detection

ACADEMISCH PROEFSCHRIFT

ter verkrijging van de graad van doctor aan
de Vrije Universiteit te Amsterdam,
op gezag van de rector magnificus
prof.dr. T. Sminia,
in het openbaar te verdedigen
ten overstaan van de promotiecommissie
van de faculteit der exacte wetenschappen \ scheikunde
op dinsdag 2 mei 2000 om 13.45 uur
in het hoofdgebouw van de universiteit,
De Boelelaan 1105

door

Thomas Hankemeier

geboren te Detmold, Duitsland

Promotor: prof.dr. U.A.Th. Brinkman
Copromotor: dr. J.J. Vreuls

Aan mijn ouders

ISBN 90-9013682-7

Omslagfoto: Martin van der Vaart
Druk: Febodruk, Enschede

Contents

1

Introduction

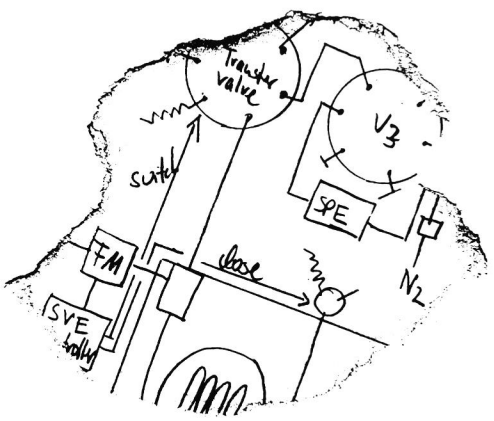

1.1 On-line solid-phase extraction–capillary gas chromatography–mass spectrometry for water analysis

Summary

Current procedures for the on-line sample preparation of aqueous samples for gas chromatography (GC) are discussed. Two approaches can be distinguished. In the heart-cut approach, only a small fraction containing a limited number of analytes is transferred to the GC column after, e.g., a reversed-phase liquid chromatography (LC) separation. This can be done by direct introduction of the water-containing eluent from a micro-LC system, or after elimination of the water by using post-column liquid–liquid extraction or a trapping column. These techniques have met with much less success than the comprehensive approach, with which a wide range of analytes can be isolated in one run by means of solid-phase extraction (SPE) or solid-phase micro extraction (SPME), with subsequent on-line (organic) solvent or thermal desorption.

In this review, most attention is devoted to recent developments in SPE–GC, and the coupling of this technique to mass spectrometric (MS) detection for identification/confirmation purposes. Applications are discussed to highlight the potential of the most powerful approaches for analyte determination at the 0.1–100 ng/l level in surface, tap and waste water.

1.1.1 Introduction [1]

Today, it is widely recognized that for compounds which are amenable to analysis by means of capillary gas chromatography (GC) without prior derivatization, GC should be one's first choice as a separation method because of three main advantages: excellent separation efficiency, a fairly high speed of analysis, and a wide range of sensitive, universal – and often selective – detectors. With regard to these aspects, GC is certainly superior to column liquid chromatography (LC), and supercritical and planar chromatography. In most studies and review papers published in the past decade, it was then immediately added that GC also has one particular weak spot, viz. sample pretreatment/introduction, irrespective of whether samples ending up as organic extracts, or aqueous samples or sample extracts are considered. Fortunately, this is not anymore true today. It is the intention of the present review to briefly discuss recent developments in this area and to highlight current procedures for on-line sample preparation–GC. Emphasis will be on the use of solid-phase extraction (SPE) for sample preparation, and the combination of SPE–GC with mass-spectrometric (MS) detection because of the identification/confirmation potential of such an integrated system. The main application area to be discussed will be (surface, ground, tap and waste) water analysis – an area which attracts increasing attention from governments, health authorities and legislative bodies. However, whenever this is appropriate, related approaches and procedures will be considered in order to illustrate how the use of another injection technique or another type of detector, or the analysis of a different sample type will influence the results or require an adaptation of the analytical strategy.

In most instances, the analyte enrichment required to enable the detection, identification and quantification of the microcontaminants of interest – which are often present at concentration levels of 10^{-8}–10^{-11} g/ml – is carried out by means of liquid–liquid extraction (LLE) or solid–liquid sorption, which is generally called solid-phase extraction (SPE). Even today, the often somewhat laborious procedures frequently are performed manually and, what is more disadvantageous, use rather large volumes of organic solvent (especially LLE), and almost invariably involve partial or complete evaporation of the sample extract, which has the inherent danger of analyte losses. The main drawback, however, is that out of the final extract of, typically, 0.1–1 ml, generally only 1–2 µl are injected into the GC (for many workers this is so routine a procedure, that they frequently omit to state the injection volume in their papers). In other words, in the final step of the sample treatment procedure, some 98–99% of all the collected analyte(s) is discarded. One should note here that the above is true irrespective of the type of sample studied, aqueous or non-aqueous, because all of them end up, in a large majority of all cases, as organic extracts.

Modern injection techniques

Fortunately, in the past decade the situation with regard to sample introduction in GC has improved dramatically and several techniques – such as *on-column*, *loop-type* and *PTV* injection – are available today. These allow the routine introduction of sample volumes of up to, say, 100 µl which is a convenient upper limit for most real-life applications. Since a detailed introduction of these large-volume injection (LVI) techniques is outside the scope of the present review, the essentials are summarized in **Scheme 1** (cf. [1]). It will be obvious

[1] For abbreviations, see glossary at end of this thesis.

that LVI-based procedures can effect a substantial reduction of the amount of sample required – and, consequently, of the time of analysis. In addition, this will make on-line sample preparation–GC easier to accomplish, and will stimulate the miniaturization of sample preparation procedures. For the rest, one should realize that LVI is the basic step in any SPE-to-GC transfer of analytes – which in its turn is the critical step in all SPE–GC procedures. Suitable solvents for LVI–GC include pentane, hexane, methyl acetate and ethyl acetate, and diethyl or methyl-*tert.*-butyl ether. From among these, methyl and ethyl acetate are preferably used in SPE–GC because of their excellent desorption characteristics for a wide variety of organic compounds. For more detailed information, the reader is referred to [2] and [3].

LC versus GC

If we now retrace our steps for a moment, and compare the general situation of sample pretreatment/introduction in LC and GC, it should be clear that, with regard to this aspect, LC is certainly superior. This is especially true if aqueous samples are considered. The use of, either disposable or re-usable, SPE cartridges, which are combined on-line with a (reversed-phase) LC system equipped with, e.g., a diode-array UV–vis, a fluorescence or a mass spectrometric (MS) detector, enables efficient analyte enrichment from 10–100-ml water samples, without analyte breakthrough. The SPE cartridges – which are often called precolumns in on-line procedures – are packed with some 50 mg of an alkyl-bonded silica or highly hydrophobic copolymer sorbent. [Note that the SPE–LC procedure will cause an improved detectability, in terms of concentration units, of three orders of magnitude, compared with 10–100-µl loop injections.] The on-line set-up ensures the transfer of all of the collected analytes rather than a 1–2% aliquot, and facilitates automation. One such system, the SAMOS LC, was developed in our group, and is commercially available from Hewlett Packard (Palo Alto, CA, USA) [4–6]. Similar systems have been developed by other authors [7–9].

Of course, the SPE operations referred to above, do not unavoidably involve hydrophobic interactions. More selective procedures are also in use, with immunoaffinity SPE being the most sophisticated and rewarding option. Examples of this approach will be included in the discussions below.

Conclusions

On the basis of the above considerations, it will be obvious that, for a really powerful GC-based (water) analyser to be built, an LC-type trace enrichment procedure such as SPE should be combined on-line with GC separation-plus-detection. If increased selectivity is deemed more important than improved detectability, LLE and reversed-phase LC (RPLC) are alternatives. Whatever the final choice will be, such on-line water analysers can be readily automated. They are, in addition, fully integrated analytical systems which combine a minimum of sample handling with transfer of the total sample or, at least, the total mass of the analytes of interest. In other words, the full range of sensitive and selective GC detectors is at one's avail and, with quadrupole and ion-trap MS detectors amongst these, it should be possible to use SPE–GC–MS for the simultaneous trace-level (provisional) identification and determination.

Scheme 1

Large-volume introduction techniques for capillary GC (adopted with changes from [1]).

ON-COLUMN INJECTION

For on-column injection, a retention gap is usually connected with an on-column injector. Two types of evaporation techniques can be applied.

* **Conventional retention gap technique**: Sample is injected at a temperature below the solvent boiling point. If the *retention gap* can be wetted by the solvent, a *flooded zone* is formed. The solvent film evaporates from the rear to the front and volatile analytes are reconcentrated by the *solvent trapping effect*. In addition, *phase soaking* effects reconcentration of the analytes due to the increased retention power of the thicker stationary phase. Less volatile components remain spread over the retention gap and are reconcentrated by the *phase-ratio-focusing effect*.

* **Partially concurrent solvent evaporation (PCSE)**: Sample is injected into the GC under conditions that cause the major part of the solvent to evaporate while the remaining solvent floods the retention gap; that is, the solvent introduction rate is higher than the evaporation rate. In this way, up to 90% of the introduced solvent can be evaporated during introduction. Volatile analytes are reconcentrated due to *phase soaking* and *solvent trapping* in the remaining solvent film. Less volatile components remain spread over the retention gap and are reconcentrated by the *phase-ratio-focusing effect*.

Solvent vapour exit

The performance of on-column injection can be improved by using a solvent vapour exit (SVE), a solvent release system which helps to protect the GC detector from vapour and to accelerate solvent evaporation. Since the SVE is usually positioned before the GC column, the major part of the evaporating solvent will go to waste. The moment of closure of the SVE becomes less critical if a short GC column (retaining precolumn) is inserted between the retention gap and SVE, minimizing the loss of volatile analytes.

LOOP-TYPE INJECTION

In this set-up a short *retention gap* is mounted onto a sample valve. The sample present in the loop is pushed into the GC by the carrier gas. Two types of solvent evaporation technique can be applied.

* **Fully concurrent solvent evaporation technique (FCSE)**: Sample is injected at a temperature above the solvent boiling point. The sample is completely evaporated during injection. No *flooded zone* is formed. Volatile analytes co-evaporate with the solvent. Less volatile components remain spread over the retention gap and are reconcentrated by the *phase-ratio-focusing effect*.

* **Co-solvent trapping**: A small amount of a higher boiling co-solvent (e.g. octadecane) is added to the main solvent to create a layer of condensed liquid ahead of the main evaporation site. The main solvent evaporates concurrently, and part of the co-solvent evaporates together with the main solvent. Boiling point and amount of co-solvent must be adjusted such that some co-solvent is left behind as a liquid and spreads into the retention gap. Volatile analytes are reconcentrated due to *solvent trapping* in the co-solvent. Less volatile components remain spread over the retention gap and are reconcentrated by the *phase-ratio-focusing effect*.

As with on-column injection, solvent evaporation can be accelerated by inserting an SVE in front of the column.

Scheme 1 (continued)

Large-volume introduction techniques for capillary GC.

PTV INJECTION

A programmed temperature vaporizer injector (PTV) basically is a split-splitless injector with temperature control, i.e. the vaporizer chamber can be heated or cooled rapidly. Three types of large-volume introduction techniques can be distinguished.

* **PTV solvent split injection**: The sample is injected in a packed liner with an open split exit at an injector temperature below the solvent boiling point. Volatile compounds co-evaporating with the solvent are lost. After solvent evaporation, the analytes retained in the liner are transferred to the GC column. The maximum introduction volume which can be injected 'at once' mainly depends on the liner dimensions: a 1 mm i.d. liner can hold 20–30 µl of liquid, 3–4 mm i.d. liners can hold up to 150 µl of liquid. Higher sample volumes have to be introduced in a speed-controlled manner where the speed is adjusted to the evaporation rate.

* **PTV large-volume splitless injection**: The sample is introduced in a packed liner at a temperature below or close to the solvent boiling point. The split exit is kept closed, i.e. the flow rate through the liner is equal to the column flow rate. The evaporating solvent is vented via the GC column. Volatile components co-evaporating with the solvent are trapped in the swollen stationary phase of the GC column.

* **PTV vapour overflow**: The sample is rapidly injected into a packed liner at a temperature far above the boiling point of the solvent. During solvent evaporation, the split exit is closed but the septum purge is wide open; the evaporating solvent escapes through the purge exit. After solvent evaporation, the injector is heated to effect transfer of the analytes to the GC column. The technique has also been carried out in a conventional split/splitless injector.

EXPLANATION OF TERMS COMMONLY USED IN LC–GC

Retention gap	Uncoated deactivated fused silica capillary injection column, inserted between injector and analytical column (or retaining precolumn) to enable reconcentration of bands broadened in space.
Flooded zone	Length of the capillary zone into which sample liquid flows, expressed as length of solvent film per volume solvent (cm/µl)
Solvent trapping effect	Reconcentration of volatile analytes due to their trapping in solvent film during evaporation of the solvent from the rear end.
Phase soaking	Reconcentration of analytes due to increase of retention caused by swelling of the stationary phase due to presence of solvent vapour.
Phase-ratio-focusing effect	Reconcentration of high-boiling analytes due to increase of retention on going from retention gap to analytical column.
Retaining precolumn	Short piece of coated GC column positioned between the retention gap and the SVE in order to prevent loss of analytes through the SVE

1.1.2 On-line LC–GC-based techniques: heart-cut operation

Over the years, many approaches for combining 'aqueous-type' LC and GC have been studied. An overview is presented in **Table 1**, where two types of goal are distinguished, *heart-cut operation* and *comprehensive analyte isolation*. The first mode will be discussed in this section, the latter mode in Section 1.1.3.

In early years, most attention was devoted to the on-line combination of RPLC with its aqueous–organic eluents and GC. [This was, no doubt, partly due to the fact that the interfacing of normal-phase LC, with its non-aqueous eluents, and GC had rapidly become successful.] The goal of the various published approaches invariably is to collect the RPLC eluent fraction containing the analytes of interest, trap and/or process them in a convenient way (see below), and transfer them on-line to the GC part of the system.

Table 1
Experimental approaches in on-line 'aqueous-type' LC–GC.

Heart-cut operation			
Direct introduction of water	:	micro-LC loop-type interface special retention gaps or stationary phases	
No direct introduction of water	:	liquid–liquid extraction (LLE) post-column trapping column	
Comprehensive analyte isolation			
Using a solvent (mixture)	:	LLE–GC	
Using a sorbent	:	solvent desorption thermal desorption	(SPE–GC) (SPETD–GC)
Using a GC stationary phase	:	solvent desorption thermal desorption	(OTT–GC) (SPME–GC)

Direct introduction of water

Most studies on the direct introduction of water involve the on-line coupling of micro-LC and GC because the LC peak volumes and, consequently, the amount of water-containing eluent that has to be transferred, will then be small. To quote an example, Cortes et al. who used an on-column interface and a non-deactivated retention gap, introduced up to 20 µl of acetonitrile–water (50:50, v/v) and even pure water without serious distortion of the peaks of components eluting near the fully concurrent solvent evaporation (FCSE)[2] transfer temperature. One application dealt with the determination of the toxic bacteriostat, N-Serve, in corn [10]. In another study, chlorpyrifos was determined in well water after a direct large-volume (20 µl) injection into the GC system [11]. However, the risk remains that more polar analytes will be adsorbed on the inner wall of the non-deactivated retention gap, which will result in bad peak shapes.

[2] For the explanation of these, and several other technical terms, the reader is referred to Scheme 1.

Transfer of (partly) aqueous eluents using a loop-type interface does not require wettability of the retention gap: at the high temperatures used for the transfer, water will not destroy the surface of the retention gap. The technique has been used to determine atrazine in a 150-µl heart-cut [12]. Because of the absence of solvent and phase-soaking effects, the method is only suitable for compounds eluting at temperatures more than 100°C above the transfer temperature. That is, it is limited to analytes eluting at very high temperatures. The problem can be partly solved by adding a high-boiling organic co-solvent such as butoxyethanol, which acts as a temporary stationary phase in the retention gap during transfer. Optimization of the procedure has been described [13], but no applications were reported.

Several studies have been published on the use of special stationary phases (using packed GC columns) or special types of deactivated retention gaps [14, 15]. Amongst these, a series of papers by Goosens et al. [16–18] on the use of a Carbowax-deactivated retention gap to transfer acetonitrile–water eluents from the LC to the GC part of the system, merit attention. When using an on-column interface and a solvent vapour exit (SVE), up to 200 µl of aqueous–organic eluent could be introduced, provided that the water content of the eluent did not exceed that of the azeotropic mixture (16 vol. %). Otherwise water will be left in the retention gap after evaporation of the azeotropic mixture and will mar the analysis. In order to remove ion-pairing agents (which would be present in the LC eluents of the applications of interest), an anion-exchange micromembrane device was inserted between the LC and GC parts of the system. The applicability of the set-up was briefly illustrated for the potential drug eltoprazine and, with MS detection, for the impurity profile study of the drug mebeverine. Despite several unfavourable technical aspects, an identification level of 0.1% with respect to mebeverine was achieved. Van der Hoff et al. [19] reported promising results of 1-µl injections into a few metres of an OV-1701-coated retention gap after exposure to water-saturated ethyl acetate. However, this retention gap, which can be also used at higher temperatures than a Carbowax-deactivated retention gap and which is now commercially available, has not been used for RPLC–GC as yet.

Hyötyläinen et al. [20–22] introduced water-containing eluents from RPLC on-line to a GC system by using a vaporizer chamber/precolumn split/gas discharge interface. The water-containing eluent (methanol–water with max. 20% water) was transferred to a vaporizer chamber at 300°C, and the vapour was removed through a retaining precolumn and an SVE. Much attention was paid to the recovery of volatile analytes. Therefore, the oven temperature was kept close to the temperature at which recondensation of the eluent occurs. However, the loss of volatiles could not be prevented. The system was used for the determination of phthalates in drinking and surface water (detection limit, 5–10 ng/l; MS detection) and the determination of pesticides in wine (quantification limit, 5–10 µg/l; FID detection). Blanch et al. [23] transferred up to 2.5 ml of LC fractions to a GC–FID system using a PTV injector with a Tenax TA-packed liner. Chiral lactones in foods were determined by means of RPLC–GC–FID.

No direct introduction of water

With this approach, two routes have been followed, viz. interfacing via an LLE module or via a trapping column.

From a technical point of view, RPLC–LLE–GC is essentially the same as the analysis of a (total) sample by means of LLE–GC, and for some of the technical aspects one is referred to the pertinent section below. An interesting example of the fairly complex instrumentation

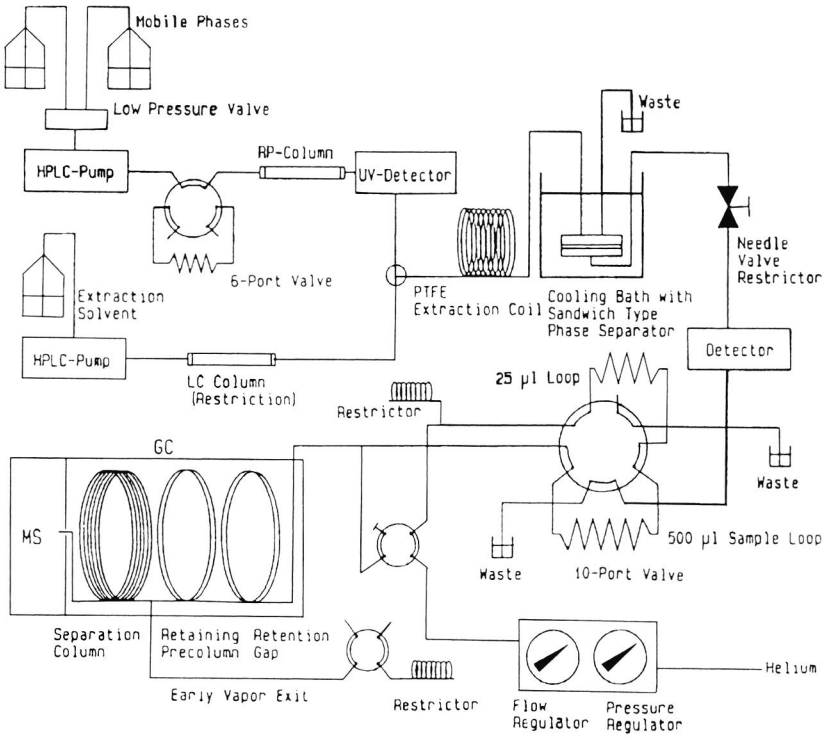

Figure 1

Instrumentation for on-line RPLC–GC–MS using an LLE interface for phase switching [24].

for, in this instance, RPLC–LLE–GC–MS is shown in Figure 1. Ogorka et al. [24, 25] used the technique to identify unknown impurities in pharmaceutical products. Phase separation by means of a sandwich-type phase separator – introduced many years ago to effect phase separation in post-column reaction detection for LC – eliminates all problems arising from the water and buffer salts present in the LC eluent. The procedure was used because LC–MS is less sensitive than GC–MS and, generally, does not produce mass spectra that can be used for identification. Degradation products obtained under alkaline stress of the drug substance ENA 713 were identified as 3-hydroxyacetophenone and 3-hydroxystyrene (Figure 2). For confirmation, simultaneous on-line trimethylation and bromination was included in the procedure by transferring the derivatization reagent into the retention gap by means of a second loop via the loop-type interface at the end of the transfer. The same approach was used for the methylation of carboxylic acids with diazomethane, and the extractive benzoylation of 2,6-dimethylaniline during the LLE extraction process [24]. Similar procedures were used by other workers for non-MS applications. The LC-to-GC transfer volumes often are in the 200–500 µl range.

In RPLC–trapping column–GC, a short SPE-type column is used for post-separation rather than conventional pre-separation purposes [26]. Briefly, the analytes from an up to 2-ml LC heart-cut are retained on the trapping column, the LC eluent is on-line removed by washing with water and the analytes are desorbed with an organic solvent and transferred to the GC. It is somewhat surprising that this procedure, which tolerates the presence of buffer

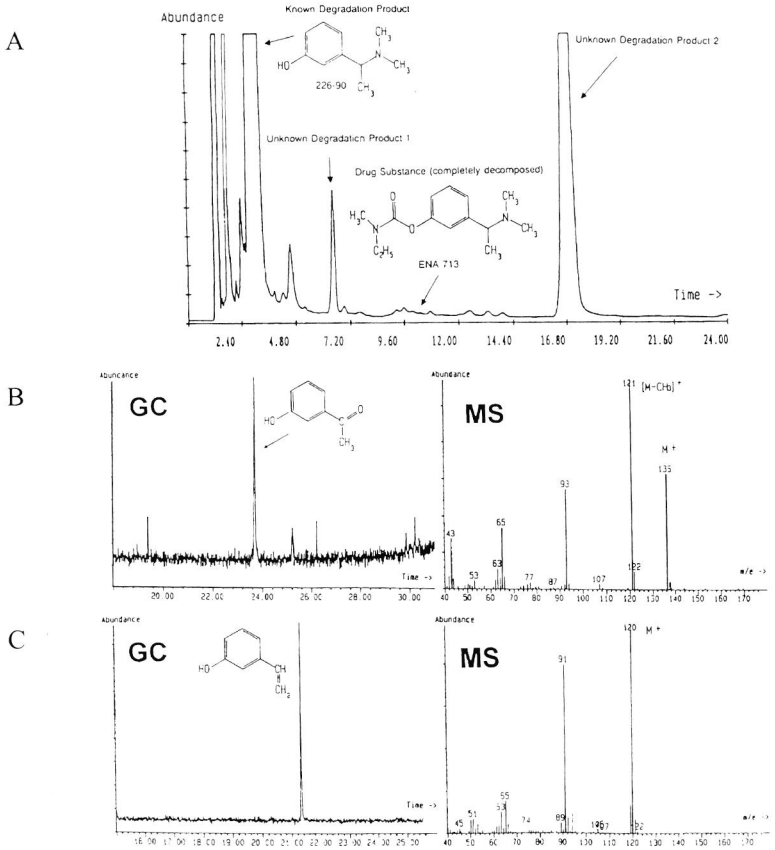

Figure 2
On-line RPLC–LLE–GC–MS for the identification of unknown drug degradation products. (A) RPLC–UV chromatogram of alkaline-stressed ENA 713. RPLC–LLE–GC–MS obtained after transfer of unknown degradation products 1 (B) and 2 (C). Eluent, aqueous potassium dihydrogen phosphate (0.02 M, pH 5)–acetonitrile–triethylamine (87.5:12.5:0.2 for first 5 min; 82.5:17.5:0.2 for 16 min; 70:30:0.2 for 9 min); flow, 1 ml/min; transfer volume, 500 µl [24].

and other salts in the LC eluent, and uses only small volumes of organic solvent (50–75 µl) has been studied only once.

Conclusion

Although quite some research has been carried out in the field of heart-cut-orientated RPLC–GC, it is clear that the two key problems, (i) the rapid and reliable complete removal of water, and (ii) the elimination of additives such as buffer salts and ion-pairing reagents, have not really been solved. The LLE and trapping-column interfacing do provide a solution, but at the cost of an increased complexity of the analytical system. Between both, the trapping-column interface has the advantage of only using a small amount of organic solvent (50–75 µl). Obviously, for the analysis of aqueous samples containing many different types of microcontaminants of interest, like e.g. volatile analytes, one has to look elsewhere for an adequate solution.

1.1.3 Comprehensive analyte isolation

The alternatives to RPLC–GC which we shall discuss now, have attracted attention not only because of their better technical performance, but they also provide a more encompassing answer to the essential question 'which microcontaminants are present in this sample'. In total, or comprehensive, analyte isolation techniques (cf. Table 1), all – or, at least, a wide range of – analytes with divergent physicochemical characteristics are simultaneously isolated from the aqueous sample by means of an LLE or SPE procedure and, next, desorbed with an organic solvent or a thermal gradient, and subjected to GC analysis. That is, instead of a targeted heart-cut-type of analysis, isolation and enrichment of a wide variety of (classes of) compounds is attempted – with the GC separation or, rather, the GC-plus-MS separation and identification being applied to unravel the sample composition. It will be clear that this approach is well suited for general screening, monitoring and early-warning purposes, and is directed at the detection of target compounds as well as unknowns. Finally, it will be obvious that in most instances, a hydrophobic – i.e., a rather non-selective – sorbent will be selected (if an SPE approach is used), because efficient trapping and enrichment, not pre-separation, is the main aim of the first step in the procedure.

The contents of the lower half of Table 1 show that, next to one approach based on solvent extraction (that will be briefly discussed below), there are four alternatives based on liquid–solid sorption. Three of these are closely related, i.e. SPE, SPETD and OTT, and will be discussed in Section 1.1.4. SPME will be discussed separately, in Section 1.1.3.2.

1.1.3.1 LLE–GC

The on-line incorporation of LLE in an analytical system was reported some two decades ago. Typically, an aqueous sample plug is injected into an aqueous carrier. The aqueous phase meets an immiscible organic stream in a segmentor, often a simple T-piece, and segmentation occurs. In the extraction coil the analytes are distributed between the two phases according to their physicochemical characteristics. Next, the phases are separated in a membrane-type phase separator, which is robust but may cause clogging or carry-over problems, or a sandwich-type phase separator, which requires some more skill in handling, separation being effected by wettability and/or gravity. Finally, the organic phase is led to the GC system via one of the injection systems of Scheme 1.

In early continuous-flow LLE–GC studies, pentane was used as extraction solvent for the determination of volatile aromatic hydrocarbons and halocarbons in aqueous samples [27, 28]. Many other applications were reported since then, for example for phenols, N-methylcarbamates, hexachlorocyclohexanes and organo-P pesticides. Special mention should be made of studies in which a derivatization step was included in the LLE–GC procedure to enable the determination of more polar compounds. Phenols, the hydrolysis products of certain methylcarbamates, were derivatized on-line with acetic acid anhydride and pentafluoropropionic anhydride, propionic acid was derivatized by extractive alkylation, and (chlorinated) anilines were acylated with pentafluorobenzoylchloride [29–31]. To our knowledge, hyphenation with a spectroscopic, i.e. an AED, detector has been reported only once: LLE–GC–AED was used for the detection of N-, Cl- and S-containing pesticides and the screening of groundwater samples [32]. In one case, from among four major unknowns detected in a sample, three could be provisionally identified as a di- and trichlorobenzonitrile,

and tetradifon. Although LLE–GC cannot easily be constructed to enable significant analyte enrichment (because the aqueous/organic volume ratio cannot deviate too much from unity) and is, therefore not always useful for real trace-level studies, the reader should keep its practicality for monitoring purposes in mind.

An alternative to using a phase separator is to combine micro-LLE and GC at line by using, e.g., an autosampler vial. After the addition of an appropriate solvent to the sample and gentle shaking or mixing by repetitive drawing up and subsequent dispensing, a large aliquot of the organic solvent (up to 500 µl) can be injected into the GC system. Venema and Jelink added 1 ml of *n*-pentane to 1 ml of sample in an autosampler vial. After 3 min of shaking, the vial was placed in the autosampler tray, and 140 µl of the organic extract were injected into the GC–MS using selected ion monitoring. Hexachlorobenzene and hexachlorobutadiene were detected at the 6 ng/l level [33, 34].

1.1.3.2 SPME

In recent years, SPME–GC has emerged as an alternative to SPE–GC, combining a greater ease of operation (see, e.g. [35–38]) with a more restricted field of application and, often, poorer detection limits. In SPME, trace enrichment is achieved by extraction of the analytes onto a small fiber which is coated with a polymeric films acting as the stationary phasen during a predetermined time, the so-called extraction time. In the direct extraction mode, the fiber is immersed in the sample liquid; in the headspace mode, the fiber is held in the headspace above the liquid phase. If the analytes are sufficiently volatile, the extent of extraction is the same for both modes because of thermodynamic equilibrium, with the headspace mode providing higher selectivity and faster equilibration times [36]. The fiber is placed in a holder which resembles a syringe and allows the fiber to be drawn into the septum-piercing needle for protection. After sampling, the analyte-loaded fiber is inserted in the injection port of the GC and the analytes are thermodesorbed. As the desorption of the analytes from the fiber can take up to 1 min, volatile analytes have to be refocused by using a strongly retaining or thick-film column or by cryotrapping prior to separation-cum-detection.

In SPME, the extraction process reaches an equilibrium and is, in many cases, far from exhaustive. This is the most essential difference with SPE, where quantitative/exhaustive sorption is encountered in (nearly) all situations. Near-exhaustive extraction is generally found in SPME only for analytes with high polymeric film-to-aqueous sample distribution constants, K_d; for most other, notably more polar compounds, the situation is less favourable: extraction yields are frequently less than 10%. Obviously, thermodynamic and kinetic aspects play a major role in SPME and these have, indeed, been studied in much detail [35, 39]: parameters such as extraction time and temperature, pH adjustment, agitation of the sample, influence of the matrix and nature of the fiber coating are of primary importance. To quote a few examples, sample agitation by magnetic stirring or vibration helps to reduce extraction times and a similar result can be obtained by increasing the temperature of the sample solution. However, in the latter case, K_d values will generally decrease and this drawback has to be overcome by cooling the SPME fiber [40]. Even so, extraction times are often 10–60 min depending on the molecular weight and polarity for the analyte, and type and thickness of polymeric coating. Generally, the extraction time is the shorter the thinner the coating and the smaller K_d is [36]. To considerably improve the recovery of especially polar analytes, salt is often added to the sample solution. For quantification, external calibration can be used

only for clean samples; for complex matrices, standard addition techniques or the use of isotopically labelled standards is recommended [41].

More recently, much attention has been paid to the characteristics, and specifically the polarity, of the fibers – which should resemble those of the analytes to achieve efficient extraction. Polydimethylsiloxane coatings have repeatedly been shown to be an excellent choice for the determination of non-polar analytes [42, 43], and the more hydrophilic polyacrylate coatings for analytes such as phenols and medium polar pesticides [44, 45]. Carbowax–divinylbenzene coatings have been used for the extraction of barbiturates from urine [46], and polydimethylsiloxane–divinylbenzene coatings for the determination of alcohols in blood and urine [47]. However, the higher extraction efficiency of the latter phases adversely affected the thermodesorption: even after 6 min at 250°C the barbiturates had not been quantitatively desorbed from the fiber. Two carbon-containing coatings [48, 49] have been recommended for the enrichment of volatiles from aqueous samples. One should add that careful conditioning of the fiber prior to use is required to obtain sufficiently clean blank chromatograms. In addition, due attention should be paid to aspects such as the position of the fiber in the injector (adverse effect of temperature gradients), sample and headspace volumes should be kept constant, and the time between sampling and thermodesorption should be brief.

In summary, mainly because of the simplicity of its set-up, SPME is a promising sample preparation technique, notably for rather volatile analytes such as BETX, substituted benzenes and a number of pesticides. On the other hand, for many other compounds it is more time-consuming and results in less sensitive analytical methods than is sometimes suggested, and careful optimization is recommended.

Applications

A large number of SPME–GC applications for aqueous samples have been published (see, e.g. [35] and Table 4 of [50]) and several types of spectroscopic detectors have been used, such as IR [51], AED [52–54] and MS detectors. Because of the emphasis of the current review, selected applications for the latter detection mode are shown in **Table 2**. In most instances, quadrupole or ion-trap MS detection was performed, but SPME–GC–MS/MS has also been reported [55]. SPME–GC–time of flight MS has successfully been used for the determination of apple flavour volatiles [56]. Generally, the reported repeatabilities (RSDs, 3–20%) are satisfactory [e.g, 60, 62–64, 70, 74].

To quote one study in some more detail, for the analysis of sixty pesticides in water, two different fibers with similar film thickness, polydimethylsiloxane and polyacrylate, were used [57]. For the analytes that were extracted to a large extent by the polydimethylsiloxane fiber, the time to reach equilibrium was generally longer (about 90 min) than for those which were extracted to a lesser extent. As a compromise, an extraction time of 50 min was chosen. **Figure 3** demonstrates the varying extraction efficiency for the sixty analytes which resulted in detection limits from 1 to 60 ng/l (full-scan ITD MS detection; RSDs, generally 5–20%). Figure 3 also shows that the extraction efficiency of a specific compound is generally more or less the same for both fibers; for a few compounds, extraction efficiencies varied 2–10-fold from one fiber to the other. Many of the target analytes were detected in surface snow and ice-core samples of the Russian and Canadian Arctic.

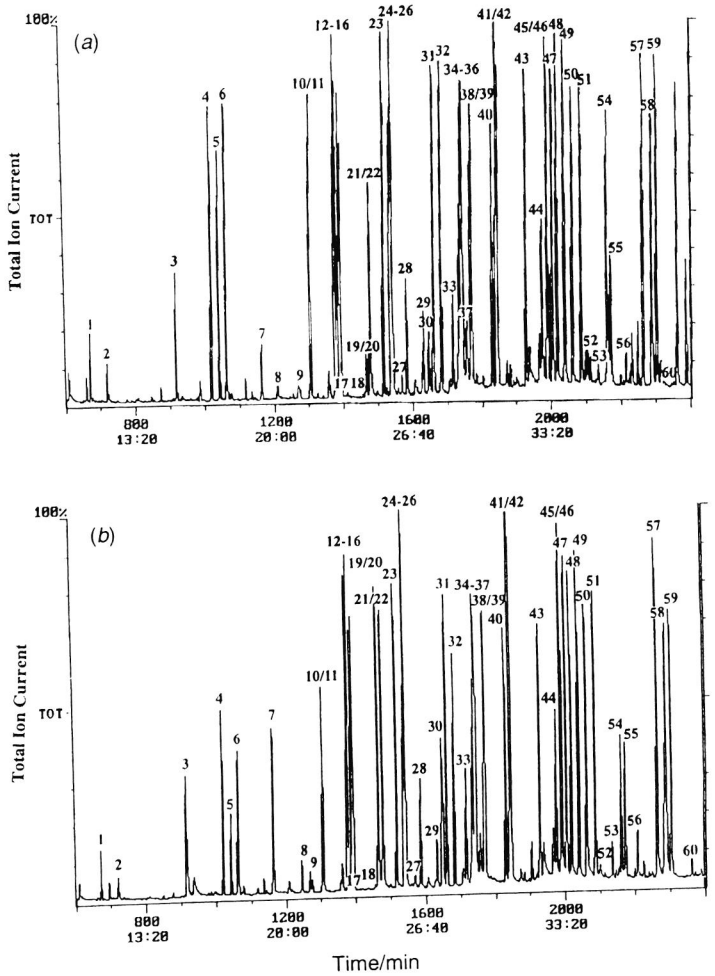

Figure 3
SPME–GC–MS chromatogram of water spiked at the 100 ng/l level using (a) a polydimethylsiloxane (100 μm film thickness) and (b) a polyacrylate (95 μm film thickness) fiber. Conditions: equilibration time, 50 min; agitation, stirring with magnetic bar; desorption, 5 min at 250°C; 25% sodium chloride added. For peak assignment, cf. [57].

Quite some attention has been directed at derivatization combined with SPME. In most studies, the reaction takes place in the aqueous phase. The reaction products are more amenable to the SPME process, and detection limits, consequently, improve. In one study, organomercury, -tin, and -lead compounds were derivatized in water with sodium tetraethylborate. GC with inductively coupled plasma (ICP) MS detection gave detection limits of 0.3–2 ng/l (as Sn) for mono-, di- and tributyltin [58]. In another study, MS/MS was used as detection mode rather than ICP MS [55]. Detection limits improved at least 10-fold compared with ordinary MS detection, and were 7–22 ng/l in urine. An advantage over ICP (MS) detection was that species can be directly identified via their precursor and daughter ions. Inorganic Hg levels in the urine of non-occupationally exposed persons with and

Table 2
Selected applications of SPME of aqueous samples with MS detection.

Analytes	Sample type	MS Detection	LOD (ng/l)	Ref.
BTEX	ground water	Full-scan	30 – 80	60
	urine	SIM	10 – 35	61
Substituted benzenes	water	Full-scan	1 – 10	49
	drinking water	Full-scan	20 – 200	62
Phenols	ground water	Full-scan	4 – 240	44
	sewage water	Full-scan	10 – 1600	63
N-herbicides	water	Full-scan	0.01 – 6	64
N/P-pesticides	water	SIM	5 – 90	65
N/P/Cl-pesticides (EPA 624)	water	Full-scan	1 – 60	57
Geosmin, 2-methylisoborneol	natural water	PCI/EI full scan	1	66
Explosives	seawater	NCI full scan	10 – 300	67
Antifouling agent/fungicide	river water	SIM	50	68
Aliphatic aldehydes	water	Full-scan	5000 – 50000	69
PAHs, PCBs	waste water	Full-scan	1 – 20	70
Fuel hydrocarbons	waste water	Full-scan	30 – 1000	41
Plasticizer, Ibuprofen	waste water	SIM	100	71
Methadone	urine	SIM	20000	72
p-Chlorophenol	urine	SIM	8000	73
Benzophenone-3, metabolites	urine	Full-scan	5000 – 30000	74
Hg(II), alkylated Hg, Pb, Sn	urine	MS/MS	7 – 22	55

LOD, limit of detection; SIM, selected ion monitoring; PCI, positive chemical ionization; NCI, negative chemical ionization; if not stated otherwise, EI ionization was applied.

without dental amalgam were in the 0.1–1.4 µg/l range. In another paper, metabolites of several PAHs were derivatized by silylation with *N,O*-bis(trimethylsilyl)trifluoroacetamid in the headspace. SPME–GC with single-ion monitoring MS was used to profile PAH metabolites in smoker's urine after enzymatic cleavage [59].

1.1.4 On-line SPE–GC

1.1.4.1 General aspects

On-line trace enrichment, and clean-up, by means of SPE using precolumns or (disposable) SPE cartridges is a popular column-switching technique in LC, and most techniques and much of the hardware now becoming in vogue for SPE–GC, were copied from SPE–LC. A brief introduction is as follows.

SPE cartridges have dimensions of, typically, 10–20 mm length x 1–4.6 mm I.D.. In most instances – whether these are LC- or GC-based applications – the cartridges are packed with 10–30 µm sorbents such as C18- or C8-bonded silica or a styrene–divinylbenzene copolymer such as PLRP-S. A typical set-up of equipment to be used for on-line SPE–GC is depicted in **Figure 4**. As regards the SPE part, after conditioning of the SPE cartridge in LC-type fashion – i.e. with methanol or another appropriate organic solvent and, next, with water – a sample volume of, often, 5–10 ml is loaded at a flow-rate of 1–4 ml/min. The loading volume is almost invariably distinctly lower than in SPE–LC (typical range, 30–100 ml), because of the

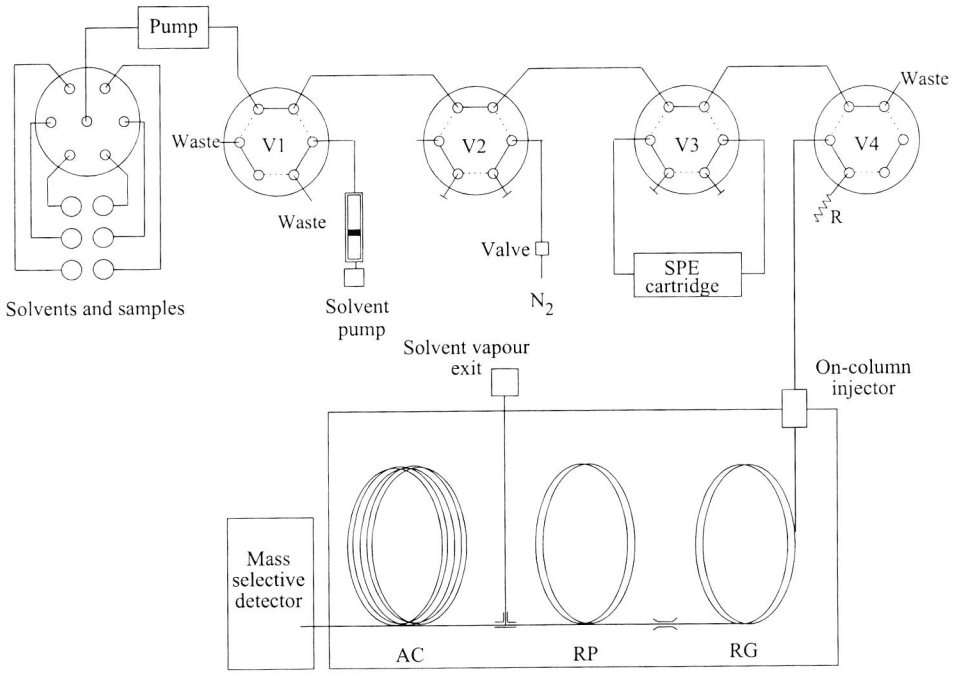

Figure 4
Scheme of on-line SPE–GC–MS system. Abbreviations: AC, analytical column; RG, retention gap; RP, retaining precolumn; R, restriction, V1–4, valves.

better detection performance of GC compared with LC detectors. The analytes of interest, and also many other sample constituents, are preconcentrated on the SPE cartridge. After clean-up, which generally is restricted to washing with water and 15–30-min drying with nitrogen at ambient temperature, the analytes are desorbed with a small amount, typically 50–100 µl, of an organic solvent such as ethyl acetate or methyl acetate and transferred to the GC part of the system for final analysis. Recently, it has even been demonstrated that the transfer volume can be reduced to about 20 µl (see *Volatile analytes* in Section 1.1.4.2). For a brief description of the main steps of such a sample preparation-cum-transfer procedure the reader is referred to **Table 3**.

In early papers on SPE–GC, much attention was devoted to the set-up of such an on-line system. In these studies, conventional (selective) GC detectors rather than a mass spectrometer were used, and essentially technical aspects such as the design and possible re-use of the SPE cartridges, optimization of the drying step and the SPE-to-GC transfer were studied in much detail. To give an impression of the analytical performance then achieved, selected applications are shown in **Table 4**. The most relevant technical aspects are discussed in the next section.

Table 3
Typical time schedule of sample preparation programme of on-line SPE–GC–MS.

Time [min:sec]	Solvent selection valve [a]	Flow [b] [ml/min]	Valves [c]				Auxiliary events [d]			Comment
			V1	V2	V3	V4	1	2	3	
00:00	2	2.5	1	0	0	0	on	off	off	flush tubing with MeOAc/flush pump with *i*-PrOH
01:00	1				1					condition cartridge with MeOAc
02:00			0				off			condition cartridge with water
03:00	3	5			0					flush pump/tubing with sample
04:00		2.5			1					preconcentrate 10 ml of sample
08:00	1	5			0					clean pump/tubing with water
08:30		2.5			1					clean-up with water
09:00		0		1				on		drying cartridge for 20 min
25:00							on			start of MeOAc pump
29:00								off		stop drying/depressurize cartridge
29:30			1	0	0					flush tubing with MeOAc
31:30					1	1			on	transfer of analytes with 50 µl MeOAc at 120 µl/min
32:25						0			off	clean cartridge with MeOAc
34:30					0					end of sample preparation

[a] 1, water; 2, *i*-PrOH; 3, sample.
[b] Flow of solvents/sample pump.
[c] V1–V4: position 0 refers to reference position in Figure 4.
[d] 1, Syringe pump (for desorption solvent) on/off; 2, nitrogen valve on/off; 3, start of SVE controller.
Abbreviations: *i*-PrOH, isopropanol; MeOAc, methyl acetate (desorption solvent).

Table 4
Selected applications of on-line SPE–GC procedures with conventional detection.

Analytes	Sample type	Detection	Sample volume (ml)	LOD (ng/l)	Ref.
PCBs, pesticides	River water	ECD	1–12	1	75, 76
Musk ketone and xylene	River water	ECD	10	15	77
Medium polar analytes	Water	FID	1	100	78, 79
Steroid hormones	Urine	FID	5	100	80
Triazines	Waste water/ orange juice	NPD	10	10	81
Triazines, organo-P pesticides	River water	NPD	2.5–10	1–100	82, 83
Triazines organo-P/S pesticides	River water	FPD	10	1–40	84

1.1.4.2 Optimization of SPE–GC procedure

Stationary phase for trace enrichment

In SPE–GC, the SPE part of the procedure is in most cases only used to effect trace enrichment and no attempt is made to improve selectivity (which is taken care of by the GC separation-plus-detection procedure). Consequently, in actual practice only two types of sorbent are used, hydrophobic C18-bonded silicas and highly hydrophobic copolymers. According to abundant literature information, breakthrough volumes[3] of non- and medium-polar analytes, and even many polar analytes, on SPE cartridges packed with these sorbents, and with dimensions of 10–20 mm length x 1–4.6 mm I.D., are much higher than 10 ml. Polystyrene copolymers typically provide 20–30-fold more retention than the alkyl-bonded silicas. In other words, it is safe to state that the sorption step of the SPE process will not cause a noticeable loss of most analytes. In addition, because of the reliable information already available in the literature, there is no need for the analytical chemist tackling a new problem, to start with a rather time-consuming collection of experimentally determined breakthrough data. For a more detailed discussion, the reader is referred to texts such as ref. [9].

In recent years, cartridge holders containing one or a few small (diameter, 3–4.6 mm; thickness, 0.5 mm) membrane extraction disks have been recommended as an alternative to conventional precolumns or cartridges for both LC and GC analyses [85, 82]. The disks contain ca. 90 wt. % of a hydrophobic sorbent held in a PTFE mesh, and can be loaded at fairly high speed. Drying with nitrogen at room temperature proceeds rapidly. The commercial Empore (3M, St. Paul, MN, USA) extraction disks, which have a diameter of 47 mm, are often recommended for field studies. It will be clear that a single 47 mm I.D. disk – after having been used for field sampling and, subsequently, having been transported to the laboratory – can be used for a large number of 4.6-mm-diameter-based SPE–GC analyses!

Abundant experimental evidence shows that analyte desorption from the loaded cartridges or disks (an aspect that is equally important for the final recovery to be obtained as is the sorption step), is easily achieved with less than 100 µl of methyl or ethyl acetate, applied at a flow-rate of 50–100 µl/min. This is well within the conditions of ordinary LVI procedures and does not present any technical problems.

So far, hydrophobic sorbents have been used in essentially all SPE–GC procedures. One main reason why the additional selectivity provided by modified SPE sorbents, which is frequently studied in SPE–LC, is less popular in GC-based analyses, no doubt is the much higher efficiency of conventional GC compared with LC separations. Still, two papers have been devoted to the on-line combination of immunoaffinity SPE (IASPE) and GC [80, 81]. In IASPE, desorption from an antibody-loaded SPE cartridge has to be carried out with, typically, several millilitres of methanol–water (95:5, v/v). Since it is impossible to introduce such a solution directly into the GC part of the system, it is on-line diluted with an excess of HPLC-grade water and the mixture led through a conventional C-18-bonded silica SPE cartridge as trapping column, as in RPLC–GC. The gain in breakthrough volume of the analytes, due to increased retention caused by the considerably decreased modifier percentage, easily outweighs the volume increase. Consequently, the analytes are

[3] The breakthrough volume V_b can be influenced by the retention factor k because of:

$V_b = V_o\,(k+1)\,(1-3/\sqrt{N_p})$, with N_p the plate number and V_o the void volume of the SPE cartridge.

quantitatively trapped on this second precolumn. Desorption from this trapping column and the further procedure are as for conventional SPE–GC. The method was applied to steroid hormones in 5–25 ml of urine. The detection limit of 19-ß-nortestosterone was about 0.1 µg/l (FID detection). A similar approach, which combined an antibody-loaded first, and a copolymer-packed second precolumn was used for the trace-level determination of triazines in river and waste water, and orange juice. The detection limits were about 10 ng/l when 10-ml samples were analysed using nitrogen–phosphorus detection (NPD). It is interesting to add that, although IASPE–GC has not yet been combined with MS detection, setting up such a hyphenated system is not expected to cause any technical problems. We shall then have an instrumental set-up which permits highly selective analyte isolation *and* structure-based identification or, in other words, identification and confirmation, in one run.

Removal of water by drying

Problems caused by the presence of water in the retention gap can be overcome by inserting a drying cartridge or drying the SPE cartridge for about 15–30 min with nitrogen gas (at ambient temperature). Nitrogen drying has the advantage that it is a well-known and simple procedure and is, therefore, generally preferred. Volatile compounds such as chlorobenzene are not lost to a significant extent [86]. It is interesting to add that drying of copolymers is distinctly more rapid, and has a somewhat more reliable outcome than that of C18-bonded silicas. The insertion of a drying cartridge containing silica or sodium sulphate between the SPE cartridge and the GC part of a system is an interesting alternative to reduce the drying time. Both silica and sodium sulphate can be re-used many times if they are regenerated between runs by (external electrical) heating. Since analyte losses appear to be negligible for a wide variety of compounds, e.g., triazines, alkylbenzenes, chlorobenzenes and chlorophenols, even at the trace level, the use of a drying cartridge is a viable approach [87, 83, 84]. Recently, the design of the drying cartridge was improved to enable higher temperatures during regeneration, and volatile analytes up to tetrachloroethylene could be included (methyl acetate as desorption solvent) [88]. Although molecular sieves and sodium sulphate have a higher drying capacity, silica was found to be the best choice in actual practice.

SPE-to-GC transfer

When using the SPE cartridges described above, the analytes are generally transferred with 50–100 µl of organic solvent (preferably ethyl or methyl acetate) from the cartridge to the GC. This volume is required to desorb the analytes and to prevent memory effects due to adsorption of analytes in the transfer capillary.

If relatively volatile analytes have to be included in the set of compounds that has to be determined, on-column interfacing is the preferred technique if the sample extract is not too dirty [89, 90]. The main problem is that with highly contaminated samples such as e.g. waste water, the retention gap easily looses its performance: distorted peak shapes and/or lower analyte responses for, especially, the more polar analytes, can already show up after a few GC runs. To maintain the quality of the analyses, the retention gap should be heated prior to starting the temperature programme of the analytical column. This can be done by putting the retention gap in a separate GC oven [91, 92] or by wrapping it with heating wire [93]. Recently, the retention gap was placed in a low-weight oven in the GC oven itself and no loss

of performance was observed after more than 200 on-line SPE–GC–MS analyses of river water samples [94].

Recent studies recommend the use of a PTV injector in on-line SPE–GC if highly contaminated samples have to be analysed [95]. Exchange of the packed liner of such an injector is straightforward and takes little time. The main real drawback is that the separation of volatile analytes from the (desorption) solvent is less good than with a retention gap [90]. Staniewski et al. used a PTV injector as interface in on-line SPE–GC and 50 µl of ethyl acetate for desorption [96]. Several herbicides were determined in water at about the 1 µg/l level with recoveries of 20–90 %.

If volatile analytes do not play a prominent role in the samples to be analysed, the use of a loop-type interface – which is rather easy to use – can be recommended [97, 98]. In order to somewhat increase the application range at the volatile end, Noij et al. [97] desorbed the analytes with 500 µl of methyl *tert.*-butyl ether–ethyl acetate (90:10, v/v), and the eluate was injected together with 50 µl of *n*-decane as co-solvent into the GC. The most volatile analyte included in the study was mevinphos. Another approach to extend the application range of loop-type injections, is to use an Autoloop (Interchro, Bad Kreuznach, Germany) interface, which essentially consists of an SPE cartridge and two loops for storing organic solvent which are mounted on a 14-port valve [77, 99–101]. Solvent transfer for desorption to the GC is achieved by the carrier gas, which can be diverted via a 6-port valve. The solvent in the first loop effects phase swelling of the retaining precolumn to increase the application range to more volatile analytes. The solvent in the second loop is used to desorb the analytes and transfer them to the retention gap. Because a rather long retention gap and a total transfer volume of about 200 µl are used, a transfer temperature of 90° C can be used which is lower than that usually applied with ethyl acetate.

As has repeatedly been mentioned, one of the incentives of on-line SPE–GC is that the total analyte-containing fraction is transferred to the GC column. There are, however, a few studies in which this was not done. For example, Ballesteros et al. [102, 103] desorbed the analytes from a copolymer SPE cartridge with 100 µl of ethyl acetate and, after homogenisation of the extract by means of a mixing coil, injected 5 µl of the eluent via a loop and a capillary in a splitless injector. When 50-ml water samples were analysed by GC–FID, detection limits of 0.7–1 µg/l were achieved for *N*-methylcarbamates and their phenolic degradation products. The quoted procedure is elegant, but one should keep in mind that using a (small) aliquot of the total sample will, in most instances, cause a considerable loss of detectability expressed in concentration units.

Finally, analyte desorption and, consequently, SPE-to-GC transfer, can also be performed without any organic solvent being used – that is, by thermal desorption (TD). The two options, SPETD and SPME, are discussed in Sections 1.1.4.4 and 1.1.3.2, respectively.

At-line operation

Sample enrichment by SPE, or LLE, and GC analysis can also be integrated into one set-up by at-line coupling: the sample extract is transferred from the sample preparation module to the gas chromatograph via, e.g., an autosampler vial using an ASPEC (Gilson, Villiers-le-Bel, France) or a PrepStation (Hewlett-Packard, Palo Alto, CA, USA). The main disadvantage of most of the published procedures is that, after elution of the SPE cartridge and collection of the solvent in a vial, only an aliquot is injected. In some studies, such as those on organochlorines and pyrethroids in surface water [104, 105] and benzodiazepines in

plasma [106], 100–200 µl were injected out of 2–5 ml. In another paper, only 1 µl out of 1 ml was injected to determine barbiturates in urine [107]. Not surprisingly, detection limits in the latter PrepStation–GC–MS study were in the sub-to-low mg/l range. Similar sensitivity problems were encountered by the authors [108] when serum had to be analysed and, by other workers, in a PrepStation-based study on the determination of organic acids [109].

In view of the above, it is interesting to quote another study [110, 111] which was directed at improving the performance of the PrepStation–GC set-up by introducing several modifications, viz. (i) increasing the aqueous sample volume from 1.5 to 50 ml, (ii) using 50-µl 'at-once' on-column LVI rather than 1-µl injections and (iii) decreasing the desorption volume to 300 µl by reducing the amount of sorbent in the SPE cartridge. The redesigning was markedly successful: an overall 300-fold improvement had been calculated, and a 150–300-fold improvement was observed in actual practice. An initial problem was that, as a

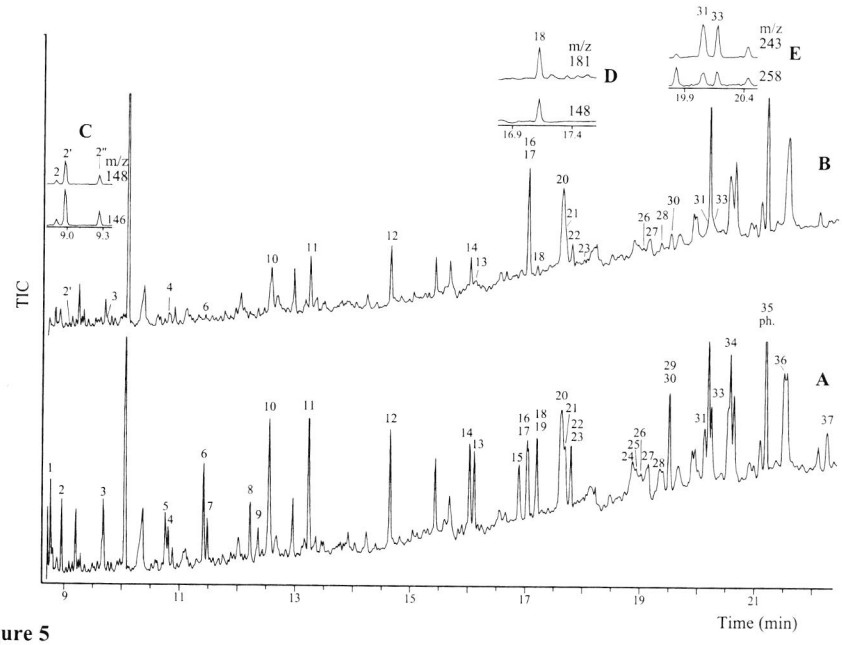

Figure 5

Full-scan PrepStation–GC–MS obtained after preconcentration of 50 ml of river Meuse water (B) without and (A) with spiking with 37 micropollutants at the 0.18 µg/l level. 100 µl out of the 300 µl extract were injected. The inserts show the reconstructed-ion chromatograms of two characteristic masses of 1,3-dichlorobenzene (C), 2-methylthiobenzothiazole (D) and Musk G and T (E); the time scale is enlarged 2-fold compared to the full-scan chromatogram. The response scales for each of the two reconstructed-ion chromatograms of the same compound are identical except for the mass trace m/z 258, which is enlarged twice compared to m/z 243. The following compounds were detected in the non-spiked river water: 2, 1,3-dichlorobenzene (0.2 ng/l); 2', 1,4-dichlorobenzene (1.5 ng/l); 2'', 1,2-dichlorobenzene (0.6 ng/l); 3, acetophenone (6 ng/l); 4, decamethylcyclopentasiloxane (7 ng/l); 6, naphthalene (4 ng/l); 10, isoquinoline (74 ng/l); 11, 2-methylquinoline (30 ng/l); 12, 2,4,7,9-tetramethyl-5-decyne-4,7-diol (190 ng/l); 13, dibenzofuran (7 ng/l); 14, triisobutyl phosphate (52 ng/l); 15, *N,N'*-diethyl-3-methylbenzamide (15 ng/l); 16, 2,2,4-trimethylpentane-1,3-dioldiisobutyrate (110 ng/l); 17, diethyl phthalate (75 ng/l); 18, 2-methylthiobenzothiazole (9 ng/l); 20, tetraacetylethylenediamine (430 ng/l); 21, tributyl phosphate (33 ng/l); 22, ethyl citrate (145 ng/l); 23, desethylatrazine (42 ng/l); 25, simazine (10 ng/l); 26, atrazine (27 ng/l); 27, tris(2-chloroethyl) phosphate (46 ng/l); 28, *N*-butylbenzenesulfonamide (40 ng/l); 30, tris(2-chloroisopropyl) phosphate (66 ng/l); 31, Musk G (3 ng/l); 33, Musk T (3 ng/l) [111].

result of the increased sensitivity, the PrepStation was found to be less inert than expected: several interferences from impurities extracted from the septa and also the commercial cartridges showed up. A cartridge made from stainless steel and polychlorotrifluoroethylene and a 2-needle system were constructed to eliminate these interferences. Several micropollutants were detected in 50 ml of (unfiltered) river water at the 0.2–400 ng/l level using full-scan MS acquisition (**Figure 5**).

In summary, with carefully designed and operated at-line sample preparation–GC systems, analyte detectability can be made similar to that in on-line SPE–GC set-ups. However, interferences due to contamination and analyte losses will always be more serious.

Medium- and non-polar analytes

Consciously or unconsciously, most conventional GC, and also LVI–GC and SPE–GC procedures have been designed for the determination of the medium-polar compound range which comprises analytes from typically, simazine and *N,N*-dimethylaniline to trichlorobenzene and dibutylphthalate. With such sets of compounds, it is highly unlikely that any sort of technical problems will be encountered. If, for a certain application, the range of analytes has to be extended to include really non-polar compounds such as organochlorine pesticides, ethion or bromophos-ethyl, one should add 20–30 vol.% of methanol to the aqueous sample to prevent adsorption of these analytes to the inner walls of capillaries and valves [112, 113]. It will be clear that, in the end, a situation may arise in which too wide a range of analytes has to be determined. In such a case, one can of course compromise with regard to the recoveries on either the polar or non-polar end. However, for a more robust operation, it is recommended to carry out two separate runs, with conditions optimized for the former (purely aqueous sample) and the latter (modifier addition) group, respectively. To quote an example, the addition of 30 vol.% of methanol to surface water samples did not interfere with the determination of a set of non- and medium-polar pesticides. However, the most polar analyte in the test set, dimethoate, was largely lost [112].

Volatile analytes

Recently, our understanding of the processes involved in the on-column LVI–GC [114–117] and on-line SPE–GC [86] analysis of volatile compounds has improved. Due to the pressure drop along the solvent film in the retention gap which occurs when an SVE is used, solvent evaporation takes place not only at the rear end, but also along the whole length and even at the front of the solvent film. Loss of volatiles can therefore be severe, especially in SPE–GC, because these analytes are mainly present in the front part of the desorption solvent. To improve performance, after conventional sample loading and drying with nitrogen, one should introduce some pure organic solvent, the so-called presolvent, into the retention gap prior to the actual desorption (using the lower boiling methyl rather than ethyl acetate). A solvent film will now have been formed before the analytes arrive as a result of the SPE-to-GC transfer, and will ensure their retention also during evaporation of the solvent film. The beneficial effect is vividly illustrated in **Table 5**: with some 30 µl of presolvent analytes as volatile as monochlorobenzene are quantitatively recovered even at the 0.5 µg/l level [86][4].

[4] Recently, it was found that satisfactory recoveries (70–90%) can be obtained for volatile analytes such as monochlorobenzene and the xylenes with a mere 20–25 µl of methyl acetate even without the use of a presolvent. Preconditions are the use of an 0.53 mm I.D. retention gap, and closure of the SVE during SPE-to-GC analyte transfer [94].

Table 5
Dependence of analyte recoveries of on-line SPE–GC transfer on amount of presolvent [a].

Compound	Recoveries (%) for a presolvent volume of			
	0 µl	10 µl	20 µl	30 µl
Volatile				
Monochlorobenzene	5	7	70	**97**
p/m-Xylene	7	8	72	**95**
Styrene	22	34	**86**	**100**
o-Xylene	9	14	**85**	**99**
Methoxybenzene	40	66	**95**	**100**
o-Chlorotoluene	33	54	**94**	**96**
Semi-volatile				
Benzaldehyde	70	**102**	**100**	**103**
1,2-Dichlorobenzene	62	**89**	**95**	**97**
Indene	64	**94**	**96**	**101**
Nitrobenzene	**88**	**100**	**95**	**100**
Naphthalene	**89**	**96**	**95**	**99**
High-boiling				
Methylnaphthalene	**95**	**94**	**95**	**96**
Acenaphthene	**99**	**100**	**99**	**101**
Metolachlor	**99**	**100**	**102**	**99**

[a] Pure methyl acetate introduced as presolvent into the GC prior to desorption with 50 µl methyl acetate [86]. Recoveries values above 80% are shown in bold print.

Self-controlled set-up

When using an on-column interface for the SPE-to-GC transfer, until recently, the injection speed, and the timing of the start of the transfer and the SVE closure had to be determined prior to analysis.

It has now been demonstrated that the SVE closure can also be performed in an automated fashion [114]. As an example, **Figure 6** shows the carrier gas (helium) and solvent vapour flow (FID response) profiles during a 54-µl on-column injection of ethyl acetate into a 0.53 mm I.D. retention gap. At the start of the injection, the helium flow sharply decreases and the solvent flow sharply increases, while at the end of the evaporation process the helium flow sharply increases and the solvent flow decreases. The sharp increase of the carrier gas flow (or, better, of its first derivative) observed when evaporation is complete, can be used to trigger SVE closure. For 30-µl injections of *n*-alkanes (C_7–C_{20}) in *n*-hexane under partially concurrent solvent evaporation (PCSE) conditions, no analytes were lost with the automated procedure when compared with (the conventional) closing of the SVE 0.1 min prior to completion of the evaporation process.

Automation does not only make pre-optimization superfluous, but also improves the robustness of the SPE–GC procedure (and, any LVI–GC procedure in general): if the evaporation time slightly changes due to, e.g., small changes of the injection speed or injection volume, the SVE will still be closed just in time without undue loss of volatiles or a significant change of the solvent peak width at the detector. The latter aspect is important when working with a mass-selective detector, because the delay time for switching on the

filament can now be kept constant. As additional advantages, the repeatability of the retention times of volatile analytes is improved [94] and the capacity of the retention gap is significantly larger when the SVE is closed at the last possible moment [117].

As regards the desorption of the SPE cartridge within the SPE–GC procedure, the introduction of the sorption solvent into the retention gap will cause a similar decrease of the helium flow as depicted in Figure 6 for the start of the sample introduction. This allows the introduction of the desired volume of desorption solvent without the need of (re-)assessing the proper timing of the start of the introduction when using e.g. a new type of SPE cartridge. The transfer is stopped after the preprogrammed delay time by switching the transfer valve [94].

The final parameter to be optimized in SPE–GC using an on-column interface is the injection speed. As regards this aspect, recent research [94] has shown that (i) with an optimised desorption-plus-transfer-line-flushing strategy only 20–25 µl of methyl acetate are required per run, and (ii) the closure of the SVE at the very end of the evaporation process considerably increases the capacity of the retention gap (cf. above). Both improvements allow significant reduction of the amount of solvent evaporated during injection without using too long a retention gap. This implies that the injection speed will, in any case, be higher than the evaporation rate – which makes injection speed optimization superfluous!

In summary, there is no parameter left that has to be optimized when exchanging the retention gap or the SPE cartridge or, in other words, one now has a truly 'self-controlled system'.

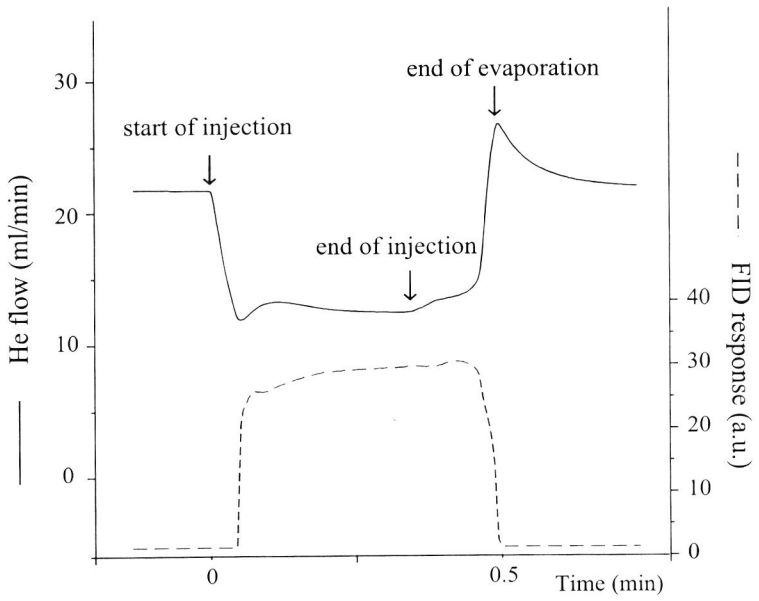

Figure 6
(A) Helium flow rate and (B) solvent peak profile for injections of ethyl acetate into a 0.53 mm I.D. retention gap. Injection time, 20 sec; injection speed, 160 µl/min; evaporation rate, 130 µl/min; 10 µl were left as solvent film in the retention gap at end of injection. Helium flow is measured by means of a flow meter in the carrier gas tubing, and the solvent flow by means of an FID at the end of the retention gap [114].

1.1.4.3 OTT–GC

Another possibility to extract analytes from an aqueous phase is by retaining them in the stationary phase of an open tubular trapping (OTT) column, which essentially is a piece of GC column. After enrichment from 0.2–10 ml of water, clean-up with 0.15–0.5 ml distilled water and removal of the water by a slow nitrogen flow during 1 min, the analytes are desorbed with an organic solvent and directly transferred to the GC via, e.g., a PTV injector as interface [118]. To obtain acceptable breakthrough volumes of 0.5 ml or higher for apolar analytes like PAHs at reasonable flow rates (ca. 0.2 ml/min) and with desorption volumes compatible with LVI (75–250 µl), a narrow-bore column of 2 m x 0.32 mm I.D. with a polysiloxane film of 5 µm thickness was used. More recently, it was demonstrated that with coiled or stitched columns much higher sample flow rates up to 4 ml/min can be used, because the secondary flow in deformed capillaries enhances radial dispersion [119].

The breakthrough volume and, thus, the sample volume can be significantly increased if the stationary phase is substantially swollen prior to sampling by a solvent, which is generally the desorption solvent [120]. Obviously, this solvent should not dissolve in water, nor should water dissolve in the organic solvent. OTT columns swollen with pentane were

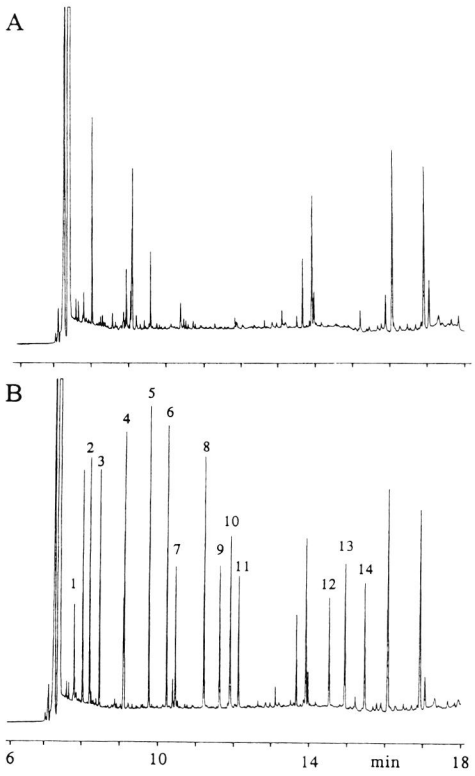

Figure 7
OTT–GC–FID of 2.25 ml of river Dommel water (A) without and (B) with spiking at the 5 µg/l level. Peak assignment: 1, toluene: 2, ethylbenzene; 3, methoxybenzene; 4, *p*-dichlorobenzene; 5, dimethylphenol; 6, dimethylaniline; 7, *p*-chloroaniline; 8, indole; 9, dichlorobenzonitrile; 10, trichlorophenol; 11, dinitrobenzene; 12, trifluralin; 13, atrazine; 14, phenanthrene [120].

found to be the most promising option with non-polar analytes; breakthrough volumes exceeded 10 ml when using a 2-m OTT column with a 5 μm thick polysiloxane film. Chloroform was the preferred solvent for swelling the OTT column if more polar compounds like dimethylphenol, dimethylaniline and atrazine had to be included. **Figure 7** shows the OTT–GC–FID analysis of 2.25 ml of river Dommel water spiked with 14 analytes at the 5 μg/l level and using chloroform as swelling agent. Analyte recoveries were satisfactory and detection limits were at the low- and sub-ng/ml level. OTT–GC–FID was also applied to the determination of six compounds such as toluene, trichlorobenzene and lindane in urine and serum samples. Satisfactory repeatabilities (1.5–10%) and quantitative recoveries were obtained which indicates that no adverse matrix effects occurred.

It can be stated that the main advantage of OTT–GC is the ease of water elimination, and the absence of clogging problems. It is somewhat surprising that this rather simple approach has not attracted more attention.

1.1.4.4 SPETD–GC

An alternative to desorption of the analytes trapped on an SPE cartridge with an organic solvent, is thermal desorption (SPETD). In the first on-line SPETD set-up, 100–500 μl of aqueous sample were injected, directly or via a loop system, into the packed liner of a PTV [121]. The water was evaporated at a high gas flow rate and a backflush set-up inserted between the PTV and the analytical GC column ensured that no water entered the analytical column. Next, the analytes were desorbed and transferred to the analytical column by rapidly increasing the injector temperature. Tenax GR and TA were found to be suitable sorbents [122]. That is, they combined sufficient retention power for analytes in the liquid phase (sorption), poor interaction with water (drying) and good thermal stability (desorption). The potential of the method was demonstrated by the analysis of 10 μg/l standard solutions of *n*-alkanes and phenols. In a similar set-up, micropollutants were determined in up to 1-ml water samples with satisfactory recoveries even for compounds as volatile as methoxybenzene and dichlorobenzene [123]. In an improved SPETD–GC set-up [124], the liner of the PTV was re-designed and the water evaporated by a vent similar to an SVE rather than through the purge exit of the PTV. Drying times were reduced to 2 min, and washing with HPLC-grade water was used to prevent degradation of the analytes due to remaining constituents of the matrix. The analysis of river and harbour water using this set-up and ion-trap tandem MS detection will be described in Section 1.1.5.1.

Recently, larger liners placed in a separately heated module (TDS, Gerstel, Mühlheim, Germany) were used for sample enrichment and thermal desorption [125]. The advantage of this approach is that longer sampling tubes and, therefore, larger sample volumes can be processed. After sampling, clean-up, drying of the stationary phase and thermal desorption in the backflush mode, the analytes were trapped in a PTV injector at -100°C in order to refocus the analytes prior to GC analysis. Polydimethylsiloxane was used as stationary phase. The system was fully automated. The analysis of tap water spiked with 45 test analytes at the 0.4–8 μg/l level is shown in **Figure 8**. All test analytes showed up in the GC–MS chromatogram; however, many disturbing peaks caused by the polydimethylsiloxane also showed up. Even though they did not interfere with the pesticides and PAHs of interest, their presence seems to indicate a certain instability of the set-up. With 10-ml samples, the procedure gave detection limits of about 10 ng/l using full-scan MS detection.

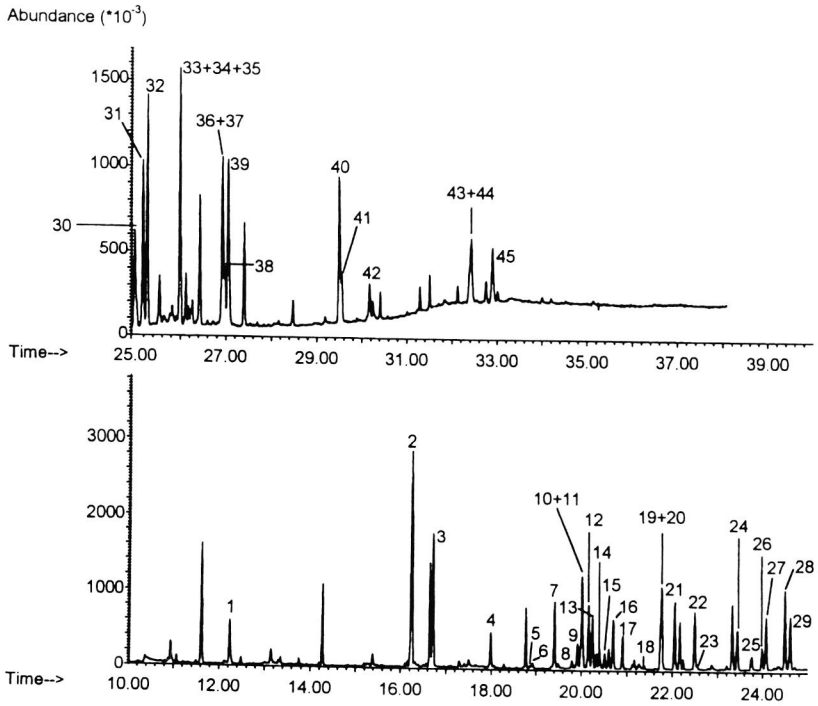

Figure 8
SPETD–GC–MS of 10 ml tap water spiked at the 0.4–8 μg/l level. Stationary phase, 340 mg of 240–400 μm particles of polydimethylsiloxane; ID of liner, 4 mm; thermal desorption, 50°C - 1°C/s - 225°C (5 min) [125].

Finally, analytes can also be enriched on a stationary phase in the PTV insert after the evaporation of the water in the PTV [126–128]. Also in this mode, Tenax appeared to be the best choice [129]. However, sampling took a rather long time due to the low evaporation rate of water (ca. 10 μl/min) [127], and the insert had to be exchanged rather often, because deposition of matrix constituents such as salts in the liner caused the decomposition of chemically less stable compounds [128]. If proper precautions were taken, analyte recoveries were, however, fully satisfactory (80–104%), and detection limits of 10–20 ng/l were obtained (0.5-ml samples; NPD detection). Actually, the procedure seems to be interesting mainly for compounds with high water solubility.

In one application [130], OTT trapping has been combined with thermal desorption. Volatile halocarbons were extracted from 8 ml of water by a 1.8 m x 0.56 mm I.D. column with a polysiloxane film of 95 μm thickness. Next, the analytes were thermally desorbed from the trapping column and refocused by a cold trap in the second GC oven prior to analysis by GC–FID.

1.1.5 SPE–GC using spectrometric detection

1.1.5.1 SPE–GC–MS

Next to trace-level detection, unambiguous confirmation of the presence of target compounds and the provisional identification of unknowns is rapidly gaining importance. Some five years ago, several papers were published which demonstrated that SPE–GC–MS can do just that, and can do it in a fully automated fashion. In an early study [131], atrazine and simazine were determined by means of SPE–GC–MS, in both the selected ion monitoring (SIM) and full-scan (FS) mode, as well as SPE–GC–NPD, using 1- and 10-ml samples. Briefly, quantification of the microcontaminants at levels of around 10–50 ng/l presented no real problems with RSDs of 3–8% (n=4) and limits of detection as low as 0.5 ng/l (SIM), 3 ng/l (FS) and 4 ng/l (NPD) for 10-ml samples. The MS- and NPD-based data showed good agreement (with differences generally being less than 10 ng/l at the 10–70 ng/l level) and linear calibration curves were obtained in both instances.

Attention was also devoted to non-target analysis. A mere 1-ml sample of river Rhine water was spiked with 1 µg/l of each of a mix of 168 microcontaminants, and a 1-min window selected for further study [131]. By selecting a number of individual masses found in the mass spectra of the apex of each of the six major peaks, it was possible to record rather undisturbed mass traces such as those shown in **Figure 9**. From these traces, it was apparent that at least nine peaks eluted in the selected time window. The mass spectra of the nine peaks were recorded at their apexes and compared with the NBS library. The data presented in **Table 6** show that the final result is quite satisfactory. Problems apparently started to

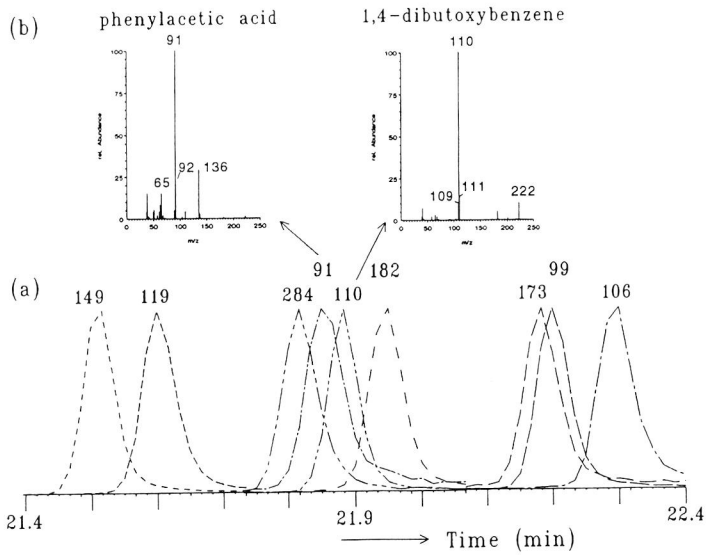

Figure 9
(a) Nine reconstructed ion traces (masses indicated above each peak) of on-line SPE–GC–MS of 1 ml of river Rhine water spiked at the 1 µg/l level with each of 168 micropollutants and (b) mass spectra of phenylacetic acid and 1,4-dibutoxybenzene, which elute at 21.83 and 21.86 min, respectively [131].

Table 6
Compounds identified in the time window of 21.4–22.4 min after SPE–GC–MS of 1 ml of river water spiked at 1 µg/l [131].

Retention time (min)	Main mass (m/z)	Compound	Library search fit [a]
21.50	149	Diethyl phthalate	0.94
21.58	119	*N,N*-Diethyl-3-methylbenzamide	0.91
21.80	284	Hexachlorobenzene	0.85
21.83	91	Phenylacetic acid	0.95
21.87	110	1,4-Dibutoxybenzene	0.96
21.93	182	Benzophenone	0.95
22.17	173	1-Nitronaphthalene	0.66
22.18	99	3-Chloro-4-nitrophenol	0.61
22.28	106	3-Aniliniopropionitril	0.95

[a] Library search fit factor on a scale of 1.00.

occur when the peak maxima were merely 0.01–0.02 min apart, as is demonstrated by the pair 1-nitronaphthalene/3-chloro-4-nitrophenol.

In subsequent papers, the development and use of an automated benchtop instrument received much attention. The final system (cf. Figure 4) consisted of a Prospekt (Spark Holland, Emmen, the Netherlands) automated sample-handling module for trace enrichment, drying of the SPE cartridge, and analyte transfer under PCSE conditions using an SVE and an on-column injector, coupled on-line to a GC–MS. The total system was completely software-controlled under Microsoft Windows and was used to analyse a variety of water samples. The further development and subsequent upgrading of that set-up, with a self-controlled system as the ultimate goal, was discussed in Section 1.1.4.2. The next paragraphs, therefore, mainly emphasize the detection/identification performance that can be achieved in hyphenated SPE–GC systems.

Table 7
Selected applications of on-line SPE–GC with MS or tandem MS detection for river and tap water.

Analytes	MS detection	Sample volume (ml)	LOD (ng/l)	Ref.
Atrazine, simazine, various micropollutants	SIM	10	0.5	131
	Full-scan		3	
Various micropollutants	Full-scan	10	2 – 50	86, 88, 99, 113, 135, 136, 132
Pesticides, phenols	SIM	10	1 – 20	112, 101
Chlorinated pesticides	EI full-scan	100	1 – 30	137
	NCI full-scan		0.1 – 3	
Pesticides	MS/MS	10	0.01 – 2	100
Hetero-atom containing pesticides/micropollutants	AED/full-scan MS [a]	5–50	1 – 15	143, 144

[a] At-line set-up because of necessary repeated injections for AED analysis.
SIM, selected ion monitoring; NCI, negative chemical ionization; if not stated otherwise, EI ionization was applied.

Table 7 summarizes relevant analytical data on the sensitivity of the SPE–GC–MS analysis of, chiefly, aqueous environmental samples such as tap, surface and waste water. The main conclusions that can be drawn from the tabulated data, are rather promising. Sample volumes of about 10 ml suffice to obtain full-scan MS traces such as are shown in **Figure 10**. Detailed study indicated that detection limits were in the 20–50 ng/l range or lower for essentially all compounds. As a demonstration of the identification power of the procedure, the traces of the four characteristic ions of peak No. 11 (benzaldehyde) in the raw, i.e. non-spiked, water are included. Comparison with the 0.5-µg/l spiked trace shows that benzaldehyde was present at a level of approx. 40 ng/l. This system appears to be well suited for the screening of rather volatile as well as high(er)-boiling compounds, i.e. for automated monitoring procedures.

While monitoring studies often aim at detecting 'all' microcontaminants present above a threshold level (estimated from, e.g., an FID or a total-ion-current trace), there are also situations in which targeted analysis is the main goal. Then it is, of course, beneficial to use (time-scheduled) selected ion monitoring (SIM) and other, related, techniques. **Figure 11** shows a relevant example which does not require much explanation. The detectability of the compounds of interest improved some 3–10-fold upon going from the total ion chromatogram to post-run ion extraction, and improved a further 10-fold upon going from full-scan acquisition to SIM detection (two ions per analyte) [113]. Detection limits of 0.2–1.1 ng/l were achieved for 10-ml surface water samples. However, one should always consider that the improved selectivity and detectability are accompanied by a serious loss of information on the general composition of the sample.

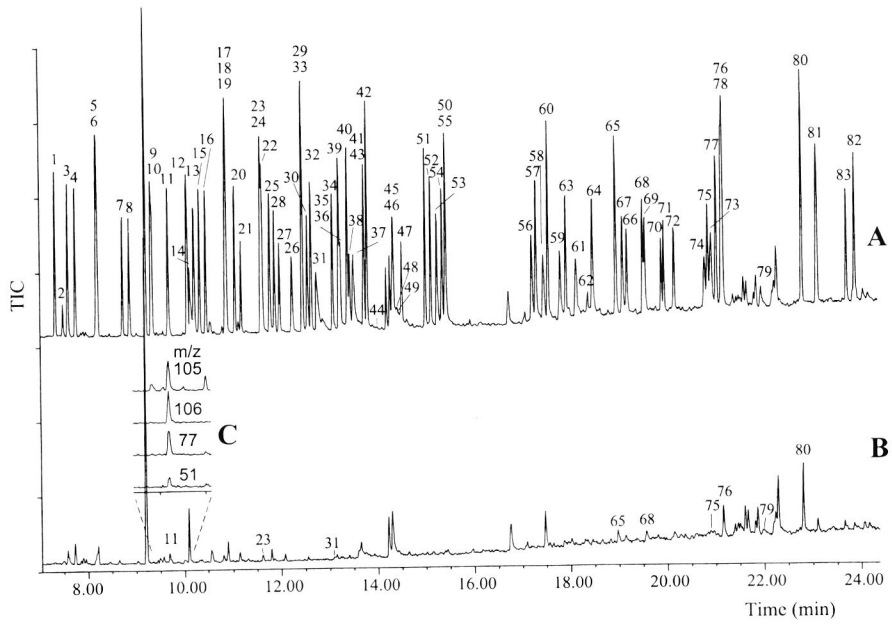

Figure 10
Total ion chromatogram for SPE–GC–MS of 10 ml of river Rhine water (B) non-spiked and (A) spiked at the 0.5 µg/l level with 86 microcontaminants. 50 µl of methyl acetate were used as presolvent. The insert (C) shows the extracted ion chromatograms of four characteristic masses of benzaldehyde (m/z 51, 77, 105 and 106). The time scale for the ion chromatogram is twice as large as for the TIC chromatogram [86].

Jahr [101] used Autoloop–GC–MS for the trace analysis of phenols in water at the low ng/l level. The phenols were derivatized by in-sample acetylation with acetic acid anhydride prior to fully automated SPE–GC–MS. The method was validated with 26 alkyl-, chloro- and mononitrophenols; these included 4-nonylphenol and 17-ethinylestradiol. Repeatability was good and the sensitivity in the time-scheduled selected ion monitoring mode was excellent.

On-line dialysis–SPE–GC–MS was developed for the determination of benzodiazepines in plasma [133]. Clean-up was achieved by dialysis of 100-µl samples for 7 min using water as the acceptor, and trapping the diffused analytes on an SPE column. After drying, the analytes were desorbed with 375 µl of ethyl acetate on-line to the GC–MS via a loop-type interface. Sample clean-up was very efficient and offered the possibility of adding chemical agents which can help to reduce drug–protein binding. The benzodiazepines were determined in plasma at the 1 ng/ml level which is relevant for forensic or pharmacokinetical studies.

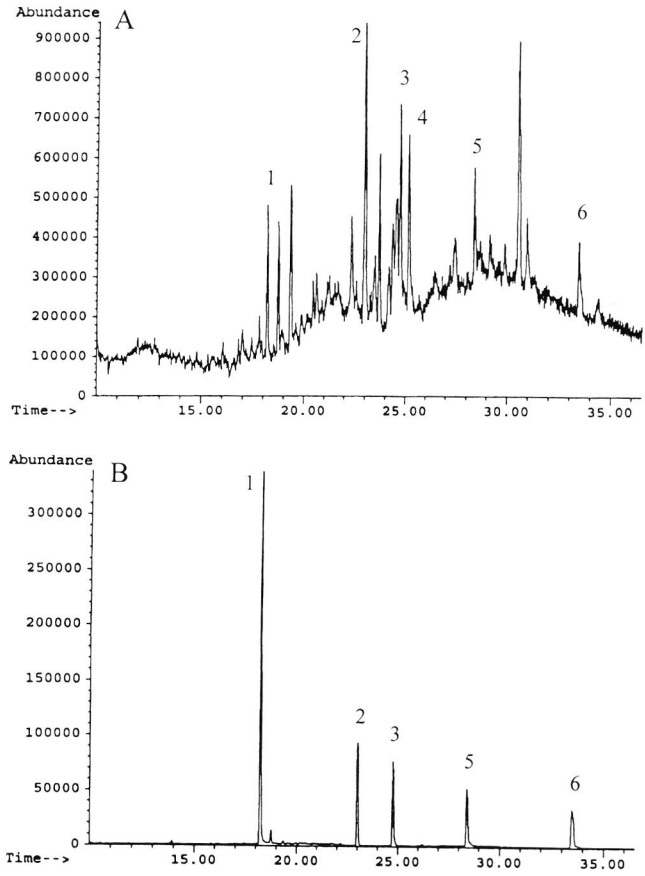

Figure 11

SPE–GC–MS chromatograms obtained after trace enrichment of 10 ml of river Rhine water spiked at the 0.1 µg/l level. (A) Full-scan mode (m/z 50–375) and (B) time-scheduled SIM. Peak assignment and ions used: 1, mevinphos (m/z 127/192); 2, diazinon (m/z 197/204); 3, fenitrothion (m/z 277/260); 4, fenthion (not determined with SIM); 5, triazophos (m/z 161/257); 6, coumaphos (226/362) [113].

SPE–GC–MS/MS

In recent years, GC–ion trap detection (ITD) systems which can perform tandem MS (MS/MS) on a routine basis have become commercially available [134]. Because ITD provides good sensitivity as well as increased selectivity in the MS/MS mode, an on-line SPE–GC–ITD system was optimized for the trace-level determination of polar and apolar pesticides [100]. The Autoloop interface (see Section 1.1.4.2) was operated at an injection temperature of 90°C which permitted the determination of thermolabile pesticides such as carbofuran and carbaryl. With sample volumes of 10–30 ml and a copolymer SPE cartridge, linear calibration curves were obtained for several pesticides over the range of 0.1–500 ng/l. Fully satisfactory tandem mass spectra were obtained at levels as low as 0.1 ng/l level in tap and river water samples. The system was used to analyse samples from several European and Asian rivers, and the determination of microcontaminants such as alachlor and metolachlor at 8 ng/l and 16 ng/l levels did not cause any problems (**Figure 12**). Relevant analytical data are presented in **Table 8**. Actually, one conclusion may be that, for this target-compound type of analysis, a sample volume of 1 ml *or less* will be sufficient to comply with governmental directives.

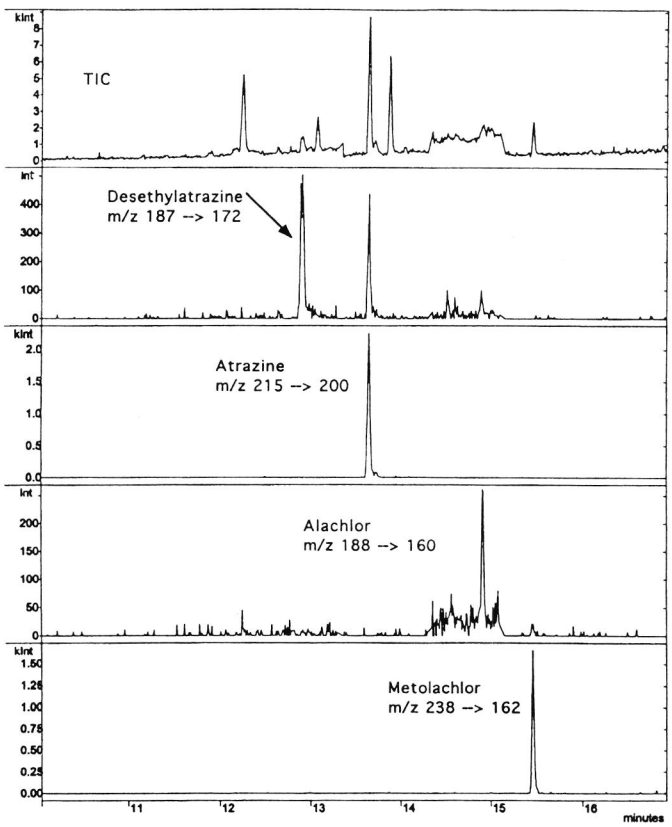

Figure 12

Total ion current and reconstructed ion chromatograms obtained after SPE–GC–MS/MS of 10 ml river Rhine water at m/z 172 (desethylatrazine), 200 (atrazine), 160 (alachlor) and 162 (metolachlor) [100].

Table 8
SPE–GC–MS/MS of pesticides in 10 ml tap water [100].

Analyte	Linear range (ng/l)	R^2	RSD [b] (%)	LOD (ng/l)
Desethylatrazine [a]	2 – 200	0.9941	18	0.5
Atrazine	1 – 200	0.9993	10	0.2
Metolachlor	1 – 200	0.9997	6	0.04
Trifluralin	0.1 – 200	0.9993	6	0.01
Carbofuran	0.1 – 200	0.9981	7	0.1
Parathion-methyl	2 – 200	0.9991	7	1
Alachlor	0.1 – 200	0.9996	6	0.05
Fenitrothion	0.1 – 200	0.9961	7	0.1
Fenthion	0.1 – 200	0.9969	6	0.1
Parathion-ethyl	5 – 200	0.9993	6	2
Carbaryl	1 – 200	0.9979	6	0.1

[a] Less good results for this polar analyte mainly due to integration problems.

[b] RSD determined at 10 ng/l analyte concentration (n=7).

In another application [124], SPETD–GC–ion trap MS/MS was optimized for alachlor and metolachlor. Appropriate precursor ions with a high m/z value were selected from the EI and PCI spectra, and the CID voltage optimized so that the highest abundance of a selective product ion was observed to achieve maximum sensitivity. Due to the use of tandem MS detection, detection limits of 0.1 µg/l were reported for alachlor and metolachlor for 100-µl samples. As an example, **Figure 13** shows the analysis of 100 µl of Rotterdam harbour water, in which metolachlor was suspected to be present. Figure 13 A shows the extracted ion SPETD–GC–MS chromatogram of mass m/z 162 and the mass spectrum of the peak at the retention time of metolachlor. The result cannot be called fully satisfactory. If, however, the analysis was performed in the MS/MS mode (Figure 13 B), the sample background had completely disappeared, and identification of the compound as metolachlor was perfectly straightforward due to the much higher selectivity. Quantification on the basis of the response of m/z 162 gave closely similar results for MS and MS/MS detection, i.e. 1.3 and 1.2 µg/l, respectively. The presence of metolachlor was also confirmed by SPETD–GC–PCI–MS(/MS).

1.1.5.2 Combined SPE–GC–MS and SPE–LC–MS

In many research projects and monitoring programmes, a mixture of compounds has to be addressed, a number of which can be analysed by means of GC–MS, while others require an LC-based approach, i.e. LC–MS. If, on the LC side, a particle beam interface is used, i.e. LC–PB-MS, the two chromatographic techniques can be combined in one set-up, sharing the sample-handling unit as well as the MS detector. With this so-called Multianalysis system [135, 136], two subsequent runs are performed per sample. First, the analytes from an about10-ml sample trace enrichment are desorbed and sent to the GC–MS; in the next run, a 100–200-ml sample (with the larger volume compensating for the lower sensitivity) is preconcentrated, desorbed, and analysed by LC–DAD-UV–MS. In both instances, classical EI spectra are generated which can be searched by using any GC library. In one example, nine test compounds, triazines, anilides and organo-P pesticides, were added to tap water.

Detection limits were 0.005–0.1 μg/l for SPE–GC–MS (10-ml samples) in the full-scan mode, and 0.5–7 μg/l for SPE–LC–PB-MS (100-ml samples) in the full-scan, and 0.05–1 μg/l in the SIM mode. It will be obvious that there is an urgent need to improve the performance – which, presumably, means the transfer efficiency – of the PB interface, but this is a topic outside the scope of the present discussion. Finally, when using negative chemical ionization (NCI) MS, with methane as a reagent gas, the detection limits for SPE–GC–MS and SPE–LC–PB-MS could be improved 10–30-fold for most of the chlorinated pesticides studied [137].

The Multianalysis system was used to monitor the pollution at a number of sampling sites along the river Nitra (Slovak Republic), a tributary of the Danube, during a 2-year surveillance programme. All three techniques mentioned above were found to be robust and no serious maintenance problems occurred. More than 500 compounds frequently showed up in the sample chromatograms, and about 30% of these could be identified by at least one technique. One example is shown in **Figure 14**: in April 1994, the compound of interest suddenly appeared in the chromatograms recorded for the sampling site Cechynce and for the downstream sites. The acridone is a degradation product of acridine, which is widely used in the production of plastics. There is, indeed, a large plastics producer just a few kilometres upstream from the sampling site [136].

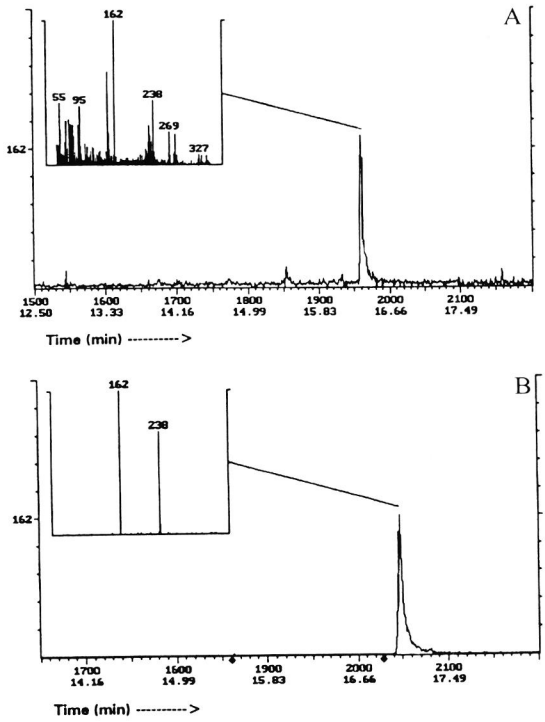

Figure 13
(A) SPETD–GC–MS ion chromatogram (m/z 162) of 100 μl of Rotterdam harbour water. Insert shows the mass spectrum of the prominent peak. (B) SPETD–GC–MS/MS daughter chromatogram (m/z 162; parent mass, m/z 238) of same sample. Insert shows the mass spectrum of the prominent peak [124].

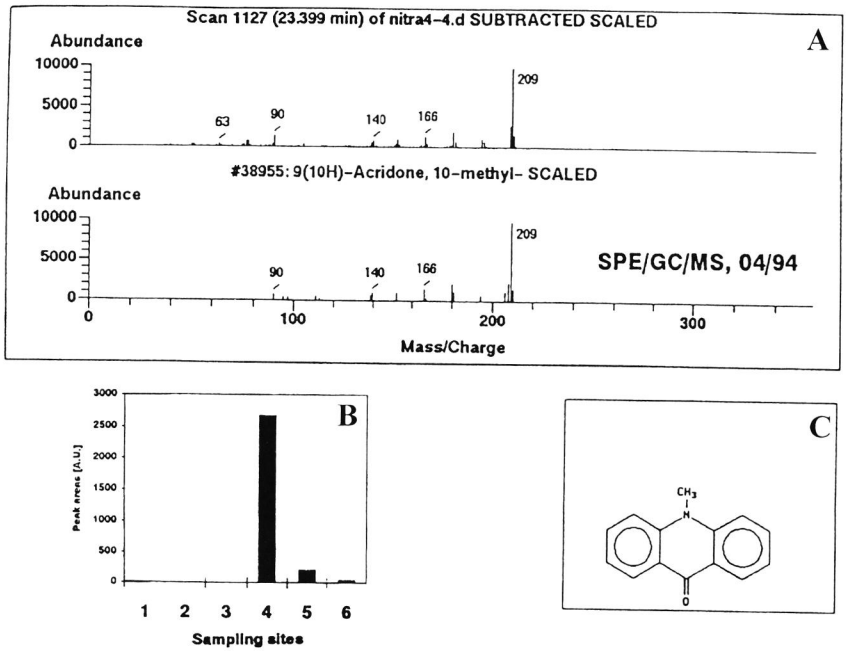

Figure 14
(A) Result of spectrum library search for compound detected in the Nitra river (site 4, Cechynce, April 1994) by SPE–GC–MS; (B) pollution profile, site 1 is farthest upstream, site 6 farthest downstream; (C) structure of identified 9,10-dihydro-N-methyl-10-acridone [136].

1.1.5.3 SPE–GC–AED/MS

A recent extension of the scope of SPE–GC concerns the use of AED detection. With its distinct element selectivity, such a detector can provide information which is complementary to that of a mass-selective detector. An additional advantage of the AED is that the response per mass unit of an element is more or less independent of the structure of the analyte of interest. This allows the use of the universal calibration concept [138, 139], although this statement is not uncontested for, at least, some elements [140]. The AED is not as delicate a detector as is sometimes thought: injections of 100 µl of ethyl acetate, and also of other organic solvents such as iso-octane, toluene and even dichloromethane do not cause problems such as flame-outs [141]. Consequently, an on-line SPE–GC–AED set-up was constructed [142]. With 10-ml water samples, detection limits of 5–20 ng/l were obtained for organo-P pesticides.

Because of the promising results obtained in the early studies, the combination of AED and MS detection was considered as the next stage. Data obtained by on-line SPE–GC–AED and on-line SPE–GC–MS using a similar set-up are ideally suited for the (non-target) screening of hetero-atom-containing compounds in aqueous samples [143]. First, the partial

molecular formula for a peak detected at the same retention time in one or more of the AED traces, was calculated using the universal calibration concept. Next, the corresponding mass spectrum, i.e. at the same retention index, was obtained from the SPE–GC–MS chromatogram. After (provisional) identification by an MS library search and with the partial formula obtained by GC–AED, the compound was quantified by means of AED-based universal calibration. This concept was successfully used for the detection of S-, Br-, Cl- and/or P-containing compounds present above the 0.02 µg/l-level in tap water, and above the 0.2 µg/l-level in waste water. **Figure 15** shows that, in the latter case, seven peaks were detected above the threshold concentration(s) for the SPE–GC–AED analysis of 7 ml of the effluent of a municipal wastewater treatment plant. All peaks could be identified on the basis of the combined partial molecular formulae and mass spectral information (**Table 9**). In a more advanced set-up, AED and MS detection were combined in a single SPE–GC–AED/MS instrument with a split of approx. 1:1 of the GC effluent [144]. Retention times could then be kept the same to within, typically, 0.5 sec, which made correlation even more straightforward. The system was applied to the analysis of vegetables and the (non-target) analysis of river water. Several hetero-atom-containing microcontaminants were identified and quantified down to the 20 ng/l level. On-going work in the same area, the analysis of wastewater, further confirms the practicality of this approach [145].

Table 9

Identification and quantification of hetero-atom-containing microcontaminants by means of their partial formulae and universal calibration (AED) and corresponding mass spectra and standard addition (MS) in waste water [143].

SPE–GC–AED			SPE–GC–MS				Concentration (µg/l)				
No.	RI	Partial formula	RI	Library search [b] Identified compound	Q [b]	Formula	AED S	P	Cl	Br	MS
1	1662	P	1663	Tributylphosphoric acid	64	$C_{12}H_{27}O_4P$		0.10			0.21
2	1782	$Cl_{2.5}P$	1781	Tris(2-chloroethyl) phosphate	91	$C_6H_{12}Cl_3O_4P$		0.36	0.30		0.54
3	1792	Cl	1778	Hexachlorocyclohexane [a]	32	$C_6H_6Cl_6$			0.12		
4	1818	$Cl_{2.5}P$	1814	Tris(2-chloro-1-methyl-ethyl) phosphate		$C_9H_{18}Cl_3O_4P$		0.25	0.21		
5	1831	$Cl_{2.3}P$	1828	Bis(2-chloro-1-methyl-ethyl) (2-chloropropyl) phosphate		$C_9H_{18}Cl_3O_4P$		0.09	0.06		
6	2148	$Br_{1.1}Cl_{1.9}P_{1.1}S$	2135	Bromophos-ethyl [c]	38	$C_{10}H_{12}BrCl_2O_3PS$	1.1	1.2	1.0	1.2	
7	2427	P	2425	Tris(2-butoxyethyl) phosphate	40	$C_{18}H_{39}O_7P$		0.07			

[a] Isomer not further identified.

[b] NBS library was used for library search and determination of match qualifier (Q) on a scale of 100. Identified compounds always were No. 1 on hit list.

[c] Bromophos-ethyl, spike of 1.0 µg/l corrected for low recovery.

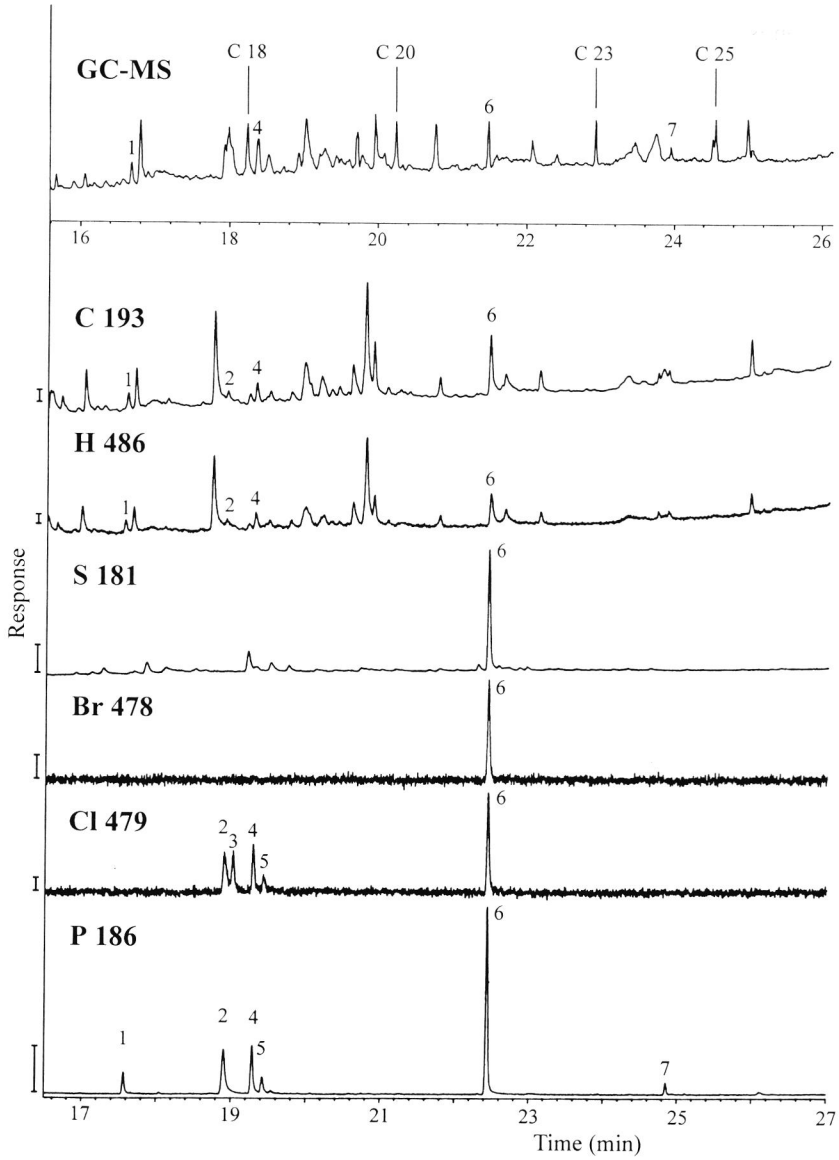

Figure 15

Element-selective SPE–GC–AED chromatograms and full-scan SPE–GC–MS chromatogram of 7 ml of waste water (C, H, S, P, Cl and Br traces). The sample was spiked with bromophos-ethyl (no. 6) at the 1.86 µg/l level. The sample analysed by GC–MS was also spiked with some *n*-alkanes. For peak assignment, see Table 9. The bars indicate the peak height of a (hypothetical) compound containing one of each hetero-atoms at the 0.2 µg/l level [143]. Numbers indicate wavelength in nm.

1.1.5.4 SPE–GC–IR

Infrared detection is ideally suited for the identification and determination of isomers and the screening for functional groups and is, in this regard, more powerful than is MS. A sample storage interface such as the cryotrapping module, with its GC effluent immobilization on a ZnSe window at 80 K and on-the-fly detection or post-run scanning, is some two orders of magnitude more sensitive than the conventional light-pipe interface, but is still rather insensitive compared with other GC detectors. As will be obvious by now, analyte detectability can be improved by coupling LVI and/or SPE, and GC–IR. This has recently been done with quite some success for a GC–cryotrapping-IR system [146, 147]. To reduce the background due to organic solvent and water, which is much more critical for a sample-

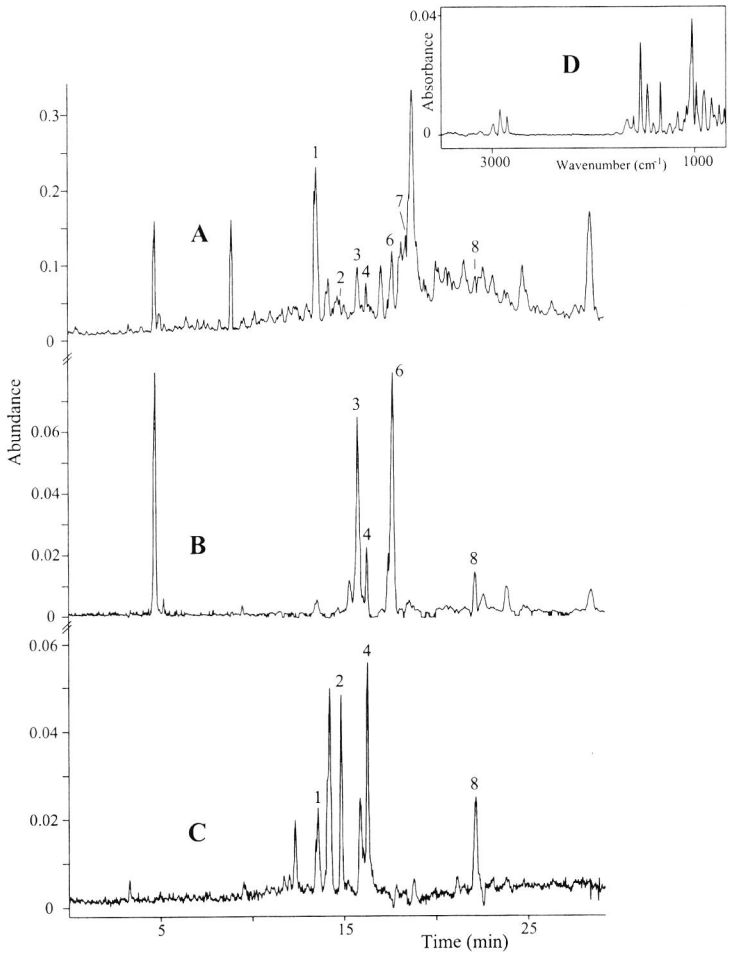

Figure 16
On-line SPE–GC–IR analysis of 20 ml of harbour water spiked at the 1.0 µg/l level with several microcontaminants. The (A) Gram–Schmidt, two functional-group chromatograms, viz. (B) (1520–1580 cm^{-1}) and (C) (1000–1050 cm^{-1}), and the (D) 'post-run' IR spectrum of peak No. 8 (triazophos) are shown. Peak assignment: 1, diethylphthalate; 2, sulfotep; 3, atrazine; 4, diazinon; 5, caffeine; 6, simetryn; 7, metolachlor; 8, triazophos [147].

storage-type cryotrapping interface than for a light-pipe interface, an column-switching device was inserted between the GC column and the IR detector and the leak-tightness of the overall system improved.

With SPE–GC–cryotrapping-IR, sample volumes of only 20 ml sufficed to identify microcontaminants in tap and surface water at the 0.1–1 µg/l level. For tap water, detection limits were even on the order of 15 ng/l when using appropriate functional-group chromatograms rather than the Gram–Schmidt GC–IR chromatogram, which is mainly determined by the summed absorption. **Figure 16** demonstrates the potential of SPE–GC–IR for the screening for functional groups – i.e. for selected classes of compounds – present in 20 ml of harbour water spiked at the 1.0 µg/l level. In the 1520–1580 cm^{-1} chromatogram, a wavelength region which correlates with the C=N structural feature of triazines, atrazine and simetryn show up, and in the 1000–1050 cm^{-1} chromatogram, which is characteristic for organo-P pesticides, major peaks could be assigned to sulfotep, diazinon and triazophos. Despite the complexity of the matrix, the IR spectra obtained were of good quality (Figure 16 D). Until now, no paper on SPE–GC–IR/MS has been published. However, in view of the detailed studies published by Wilkins and his group on various GC–IR/MS, and even multi-GC–IR/MS, set-ups [148], it is obvious to conclude that this next step will, and should be, made in the near future.

1.2 Conclusions and future trends

In the present chapter, a number of sample preparation techniques that can be coupled on-line to GC have been discussed. Special attention was devoted to *SPE–GC* as the preparation-plus-separation procedure, to the analysis of *aqueous samples*, and to analyte identification, i.e. to the use of *mass spectrometric* detection.

One way of sub-dividing on-line sample preparation–GC techniques is into solvent-free techniques and techniques requiring the introduction of some 10–100 μl of an organic solvent into the GC. As regards the latter sub-group, five to ten years ago, such amounts of solvent were called 'very large'. Today, large-volume injection (LVI) has become a really routine procedure. This, by itself, is a major step forward for, essentially, all GC-based separation procedures and can be called a distinct breakthrough. As a consequence, LLE–phase separator–GC is an easily accessible technique. However, it does not provide noticeable analyte enrichment and is, therefore, not always well suited for trace-level analysis. Normal-phase LC–GC (not a topic discussed in this chapter) has also become markedly successful but, here, the main limitations are the heart-cut nature of the set-up and the restricted use of NPLC separations. Somewhat disappointingly, the counterpart of NPLC–GC, reversed-phase LC–GC, has yet failed to become an analytical technique of interest. Clearly, the problems created by most typical RPLC eluents keep jeopardizing the LC-to-GC interface performance and, thus, the LVI into the GC. This leaves us with today's favoured option within the LVI-based sub-group, SPE–GC.

The past history of SPE–GC clearly shows that introducing new technology invariably requires much time and effort. As was remarked in an earlier review [1], setting up an on-line technique is not simply the coupling of two well established 'sub'techniques, but will generally require adaptation and subsequent optimization as well as a profound knowledge of the underlying principles. Several recent papers [114–117] have clearly demonstrated just that. A better understanding of the LVI–GC and SPE-to-GC transfer processes has allowed an optimization of the analytical procedures and, next, a higher sample throughput, wider application range and improved robustness, and has made optimization essentially superfluous. One can safely state that SPE–GC has become a mature technique, making traditional *off-line* SPE-plus-GC correspondingly less attractive (mainly because of better analyte detectability, improved precision, easier miniaturization and automation, and less solvent consumption). In many cases, SPE–GC should also be preferred over the at-line combination of micro-LLE and LVI–GC for much the same reasons and, in addition, because

of its wider application range. As a consequence, one can now fully profit from (i) the wealth of information provided in the LC-oriented literature on SPE to facilitate method development, and (ii) the essentially quantitative isolation of analytes which cover a very wide polarity/boiling-point range, to perform extensive screening (and, with MS detection, identification/confirmation) studies at ultra-trace levels.

A rather similar type of picture emerges for the solvent-free sub-group. Although supercritical fluid extraction (SFE)–GC (not discussed in this chapter) seemed to be a most promising option a decade ago, especially because interfacing was considered to be straightforward, on-line SFE–GC has not become a viable approach. A series of operational and design problems, and the unexpectedly complicated nature of supercritical fluid–analyte–matrix interactions are primarily responsible for this outcome. Another, more recent addition to the list, SPME, has on the other hand become remarkably successful in a couple of years. Being a solvent-free technique, SPME can be coupled rather easily with GC, and sorption is rapid, and close to exhaustion for BTEX, substituted benzenes and other, similar analytes (it is a combination of high hydrophobicity and sufficient volatility which works best to achieve efficient sorption/desorption). The main drawback of SPME is that extending the application range to, e.g., medium polar or higher-molecular-weight analytes often causes a dramatic increase in the sample preparation time. In addition, the non-equilibrium conditions frequently used, the disturbing role of sample matrix constituents and the rather high viscosity of the sample solution after the, often necessary, addition of NaCl make relatively extensive optimization unavoidable. Furthermore, the precision is satisfactory (RSDs, 3–20%), but often not as good as in SPE–GC (RSDs, 1–10%). Still, one can conclude already now that SPME–GC is an attractive technique.

Because of the preferred application range of SPME indicated above, SPME–GC and SPE–GC may well become complementary rather than competitive techniques. The simplicity of the set-up (SPME), the relative ease of method development and optimization (SPE or SPME), the wider application range (SPE) and the better analyte detectability (SPE) will be main debating points. In this context, it may be interesting to mention SPETD–GC as an alternative: SPETD combines the solvent-free operation of SPME with the exhaustive analyte isolation of SPE. Surprisingly, this approach has received very little attention in the scientific literature. Further exploration of this 'middle of the road' option is therefore indicated.

As regards the final step of the analytical procedure, until quite recently conventional selective GC detectors were predominantly used. Probably also today, an element-selective detector is a proper choice for many screening studies in which the number of negatives far exceeds that of the positives. However, with (i) the advent of much less expensive MS detectors with, simultaneously, improved analytical characteristics, and (ii) the increasing demand for analyte identification/confirmation on the basis of structural information, GC–MS is becoming the method of choice for a rapidly increasing number of applications. In the field being reviewed in this paper, this is especially manifest in the area of SPE–GC and, recently also, SPME–GC. Moreover, studies on the target-compound-oriented use of ion-trap-type MS/MS detection start to appear. Analyte identification at or below the 1 ng/l level has been accomplished for ca. 10-ml aqueous samples.

With SPE–GC–MS rapidly becoming a recognized standard, there is also enhanced interest in alternative hyphenated procedures, notably in the use of atomic emission detection (AED) with its multi-element detection capability and unusually high selectivity. The

recently introduced SPE–GC–AED/MS with its confirmation-plus-identification potential in one run, has been remarkably successful for pesticide analysis in a variety of complicated samples. This, in its turn, brings another alternative, IR detection, to our attention. Several studies are now available which indicate that, with deposition-based detection, e.g. with cryofocusing, trace-level identification is possible at or below the 1 μg/l level with ca. 10-ml aqueous samples. This is, by itself, a rewarding result. In view of the wide application range of IR and its frequent complementarity to MS detection, e.g. when screening for analytes containing certain functional groups, one would like to see more studies regarding this detection mode being performed in the near future. Now that the notoriously high detection limits have disappeared because of the introduction of SPE and LVI, the practicality and robustness of the approach need confirmation.

Finally, let us take SPE–GC–MS as the model system to attempt quantification of what has been achieved, and to indicate a few trends that start to emerge. In many instances, aqueous samples of about 10 ml are analysed. Sample preparation and separation-plus-detection each take about 30 min, so that, with the parallel set-up almost invariably used, throughput can be 40–45 samples per day. Detection limits in full-scan MS (of special importance if unknowns are expected) are on the order of 5–50 ng/l (TIC) or 1–10 ng/l (reconstructed ion chromatogram), and with target-orientated MS/MS, 0.1–1 ng/l. Since regulatory requirements often are in the range of 0.1–1 μg/l, it will be obvious that sample volumes can frequently be reduced 10–100-fold. This is a rather challenging conclusion, because it opens the possibility to design completely different ways of sample introduction, and removal of (only a few hundreds of microlitres) of water. On the other hand, designing improved, i.e. faster, sample-handling procedures is rapidly becoming urgent because of the introduction of fast GC techniques which can effect an about 10-fold shorter GC run time: with a 5–6 min GC run-plus-reequilibration time, a similarly reduced sample handling/introduction time-span is required. Loading smaller volumes and accelerating the drying step will obviously be especially important. Finally, with such advanced systems, MS detection has to be accelerated correspondingly. Here, time-of-flight MS will probably be the solution to the problem. It is, as yet, too early, to give a final verdict. However, it seems fair to state that the rapidity of data acquisition of this MS technique meets all present-day demands [149].

In summary, we have arrived at the stage where modest sample volumes are sufficient for the automated analysis of a variety of water samples. From among the approaches available, SPE–GC–MS probably has the widest application range, and detection/identification limits are consistently below those set by governmental bodies. At the same time, there are several indications that each of the three steps involved - sample introduction, separation, and detection - will be considerably improved in the near future. Should this indeed be true, then a next challenge will become immediately apparent: how should one interpret, use and store the avalanche of data produced?

1.3 Scope of the thesis

The primary objective of the studies described in this thesis was the development of automated and robust water analysers based on GC separations combined with MS, AED and/or IR detection for the screening, identification and quantification of micropollutants below the 0.1 µg/l level.

For sample preparation, SPE was preferred because of its potential to enrich analytes which cover a wide range of volatility and polarity. In order to obtain an integrated system in which SPE and GC are coupled on-line, SPE had to be optimized so that the amount of organic solvent required for on-line desorption could be directly transferred to the GC via an LVI interface. At the start of the project, several LVI interfaces had been described in the scientific literature. However, not all of them could be called user-friendly, one main shortcoming being the time-consuming optimization often required to find the proper injection conditions. From among the several interfaces available, we selected on-column injection because it was the only interface allowing LVI of volatile and high-boiling analytes at the same time. When the present research project was started, the general principles of on-line SPE–GC were well known, but the operational details were not well understood. Most papers published at that time dealt with the determination of medium-polar analytes using element-selective and, in a few cases, MS detection.

One set of goals of the present project was to extend the application range of on-line SPE–GC to volatile analytes like monochlorobenzene, to improve the robustness of SPE–GC and to reduce the time required for optimization of the overall procedure. To accomplish this, the underlying principles of SPE–GC had to be understood and important steps in the SPE–GC procedure like the drying of the SPE cartridge and the several stages of the transfer procedure had to be studied in detail. Secondly, a sophisticated water analyser should combine SPE–GC with spectrometric detection in order to enable selective and sensitive detection as well as identification and confirmation of suspected analytes. Next to MS detection, the obvious first choice, AED and IR detection were studied. The aim was the (non-target) screening for micropollutants containing particular hetero-atoms or functional groups, and identification/confirmation of identity in combination with information obtained form SPE–GC–MS.

In Chapter 1.1 the literature on hyphenated GC techniques for water analysis and related techniques is critically reviewed. The coupling of reversed-phase LC and GC, on-line LLE–GC and SPME are discussed and various applications described. Relevant aspects of SPE–

GC interfacing are reviewed considering also the results obtained in this thesis. Alternative interfaces such as OTT–GC and SPETD–GC are included in the discussion. Several applications using spectrometric detection are descibed. At the end, the most promising approaches are critically compared for their suitability for water analysis, and some future trends are discussed.

Chapter 2 deals with the optimization of the injection conditions (injection speed and temperature) and SVE closure time for large-volume on-column injections. In Chapter 2.1 two strategies are described for the optimization of the injection speed or temperature for 100-µl injection–GC–MS using partial concurrent solvent evaporation (PCSE) conditions during injection and an SVE. The former strategy relies on the programmable speed of an infusion pump, which is adapted such that it is just above the evaporation rate of the solvent used. With the second procedure, which can be used for a commercially available autosampler, the evaporation speed is adjusted to the fixed speed of injection by varying the temperature during injection. Optimization was achieved by subsequent injections of an n-alkane standard and monitoring of the peak shapes and heights. Then, the additional SVE time, i.e. the time elapsed between completion of injection and SVE closure, was increased until loss of the volatile analytes started to occur. The system was used for the determination of micropollutants at or below the 100 ng/l level in 20–100 ml of tap or surface water by off-line SPE enrichment and subsequent injection of a 100-µl aliquot from the 0.5–1-ml SPE extract using the developed procedures. To reduce the time required for optimization, monitoring of the helium flow into the GC was studied in Chapters 2.2 and 2.3. A procedure was developed in Chapter 2.2 that ensures automated closure of the SVE when the carrier gas flow increases at the very end of the evaporation process. It was demonstrated that with this new procedure – which makes all optimization of the SVE closure superfluous – the volatile analytes are recovered quantitatively. In Chapter 2.3 first experimental evidence is presented (and a mathematical model used) which shows that the evaporation rate changes during large-volume on-column injections when using an SVE. Then two methods which take that effect into account are suggested for the rapid optimization of the injection speed and temperature for large-volume on-column injections under PCSE conditions. With the first method, the evaporation rate is determined and subsequently an appropriate injection speed calculated, with the second method the injection temperature is varied to adapt the evaporation rate to the injection speed. Both methods require some four injections of pure organic solvent and optimization of the injection conditions now takes less than one hour.

Chapter 3 discusses modifications of the SPE–GC procedure aimed at extending the application range and improving the robustness of the set-up. In Chapter 3.1, the losses of volatile analytes occurring with 'conventional' SPE procedures are explained and the introduction of 30–50 µl of 'pure' solvent prior to the actual desorption is recommended to eliminate this problem. The so-called presolvent ensures that a solvent film is present in front of the analytes at the start of the transfer and during evaporation of the solvent. With the modified procedure, about 80 micropollutants were determined in 10-ml river water samples with good analytical performance (typically: recoveries, 90–115%; RSDs, 1–9 %; LODs, 20–50 ng/l using full-scan MS detection). However, optimization of the system still required some time. Therefore, in Chapter 3.2, the SPE–GC procedure was further improved by (i) seriously reducing the amount of organic solvent transferred during SPE-to-GC transfer of the analytes, (ii) (automated) detection of the start of the transfer into the GC by monitoring of the helium carrier gas flow, (iii) opening of the SVE only after the transfer of the

desorption solvent, (iv) the use of a separate retention gap oven and (v) applying the automated SVE closure developed in Chapter 2.2. As a result, the system became self-controlled; that is, no correction for different dead volumes of different SPE cartridges and optimization of the injection speed or temperature and SVE closure time are necessary any more. In addition, the quality of the retention gap is now much less critical than before, the precision of the retention times of volatile analytes improves and the system is more tolerant to variations of, e.g., the desorption solvent flow rate. Even without the introduction of a presolvent, analytes as volatile as toluene and chlorobenzene can now be recovered without significant losses. The analytical characteristics were fully satisfactory and similar to those found in Chapter 3.1.

Chapter 4 deals with the at-line coupling of SPE and GC by means of a PrepStation. The system combines several advantages of on-line and off-line SPE–GC: an integrated and closed system is used and the SPE extract is transferred from the sample preparation module to the autosampler via an autosampler vial. As the sensitivity of the original set-up was not sufficient for the analysis of aqueous samples, the set-up was modified in Chapter 4.1 by (i) increasing the sample volume to 50 ml, (ii) increasing the injection volume to 50 µl by 'at-once' on-column injections and (iii) decreasing the desorption volume to 300 µl by modifying the original SPE cartridge. Because of the much improved sensitivity, interferences due to compounds extracted from the commercial SPE cartridges and septa of the autosampler vial had to be removed by extensive pre-cleaning. In Chapter 4.2 the set-up was redesigned: a cartridge made of stainless steel and polychlorotrifluoroethylene and a 2-needle system were constructed which allowed the determination of micropollutants at the low-ng/l level without any precleaning. The analytical characteristics were satisfactory and comparable to those of on-line SPE–GC systems. Even though analyte detectability was somewhat poorer and analysis times were longer, the at-line approach has obvious merits like its ease of operation.

SPE–GC–AED is discussed in Chapter 5. The AED is an attractive detector because of its high element selectivity and because the response of each element is more or less independent of the structure of the analyte tested. In Chapter 5.1, the coupling of SPE–GC and AED is described. It was shown that the phosphorus channel, which has medium sensitivity, can be used for the determination of organophosphorus pesticides at the 5–30 ng/l level in 10 ml of an aqueous sample. The suitability of SPE–GC–AED for screening purposes of complex samples was illustrated by analysing an effluent sample from a municipal waste water plant. In Chapter 5.2 a procedure is described for the (non-target) screening of hetero-atom-containing compounds by correlation of SPE–GC–AED and SPE–GC–MS data. The screening was carried out for compounds containing at least one hetero-atom above a predetermined concentration level. Micropollutants at or above the 0.05 µg/l (tap water) or 0.5 µg/l (waste water) level could be identified by their partial formulae (AED) and the corresponding mass spectra, which were obtained via the retention index concept. Although an identical set-up and procedure were used for both systems, slight differences in retention indices were observed, which was attributed mainly to minor differences in the column flow due to pressure differences at the end of the GC columns. Retention times could be kept the same to within 0.5 sec by combining AED and MS in one system as described in Chapter 5.3. This made correlation fully straightforward. The system proved to be a powerful means for screening and identification of micropollutants in vegetables, tap and surface water.

Chapter 6 discusses the potential of GC–cryotrapping-IR for trace-level analysis when combined with LVI and SPE. An IR detector is attractive because of its selectivity for functional groups and its identification potential. A sample storage interface such as a cryotrapping GC–IR interface is about 100-fold more sensitive than the conventional lightpipe interface. Unfortunately, it is also much more sensitive to disturbances such as an ice-background caused by water or solvent crystallisation. In Chapter 6.1 a loop-type interface was used to enable 100-µl injections, thereby enhancing analyte detectability by some two orders of magnitude. The system permitted the determination of PAHs in river water at the 0.5 µg/l level by micro-LLE/LVI–GC–cryotrapping-IR. However, a water background (caused by leakage of press-fit connections and/or a six-port valve) and, in some cases, a solvent background somewhat disturbed the IR chromatograms and spectra. In Chapter 6.2 the robustness of the set-up was improved by improving the leak-tightness of the system and by using an open-split interface between the GC column and the IR detector. Next, the system was combined on-line with SPE. 20 ml of a surface water sample now sufficed to detect and identify microcontaminants at the 0.1–1 µg/l. The potential for the screening of environmental samples on a functional-group basis, i.e. in terms of classes of compounds, was clearly demonstrated.

References

[1] E.C. Goosens, D. de Jong, G.J. de Jong and U.A.Th. Brinkman, *Chromatographia*, 47 (1998) 313.

[2] K. Grob, in W. Bertsch, W.G. Jennings and P. Sandra (eds.), *On-line coupled LC–GC*, Hüthig, Heidelberg, 1991.

[3] W. Engewald, J. Teske and J. Efer, *J. Chromatogr. A*, 842 (1999) 143.

[4] J. Slobodnik, E.R. Brouwer, R.B. Geerdink, W.H. Mulder, H. Lingeman and U.A.Th. Brinkman, *Anal. Chim. Acta*, 268 (1992) 55.

[5] J. Slobodnik, M.G.M Groenewegen, E.R. Brouwer, H. Lingeman and U.A.Th. Brinkman, *J. Chromatogr.*, 642 (1993) 359.

[6] P.J.M. van Hout and U.A.Th. Brinkman, *Europ. Water Poll. Control*, 3 (1993) 29.

[7] R. Reupert, I. Zube and E. Ploeger, *LC·GC Intern.*, 5 (1992) 6.

[8] J.M. Huen, R. Gillard, A.G. Mayer, B. Baltensberger and H. Kern, *Fresenius J. Anal. Chem.*, 348 (1994) 606.

[9] D. Barceló and M.-C. Hennion, *Trace determination of pesticides and their degradation products in water*, Elsevier, Amsterdam, 1997.

[10] H.J. Cortes, C.D. Pfeiffer, G.L. Jewett and B.E. Richter, *J. Microcol. Sep.*, 1 (1989) 28.

[11] B.B. Gerhart and H.J. Cortes, J. Chromatogr., 506 (1990) 377.

[12] K. Grob Jr. and Z. Li, *J. Chromatogr. A*, 473 (1989) 423.

[13] K. Grob and E. Müller, *J. Chromatogr. A*, 473 (1989) 411.

[14] D. Duquet, C. Dewaele, M. Verzele and M. McKinley, *J. High Resolut. Chromatogr. Chromatogr. Commun.*, 11 (1988) 824.

[15] G. Audunsson, *Anal. Chem.*, 60 (1988) 1340.

[16] E.C. Goosens, D. de Jong, G.J. de Jong and U.A.Th. Brinkman, *J. Microcol. Sep.*, 6 (1994) 207.

[17] E.C. Goosens, I.M. Beerthuizen, D. de Jong, G.J. de Jong and U.A.Th. Brinkman, *Chromatographia*, 40 (1995) 267.

[18] E.C. Goosens, K.H. Stegman, D. de Jong, G.J. de Jong and U.A.Th. Brinkman, *Analyst*, 121 (1996) 61.

[19] G.R van der Hoff, P. van Zoonen and K. Grob, *J. High Resolut. Chromatogr.*, 17 (1994) 37.

[20] T. Hyötyläinen, K. Grob, M. Biedermann and M.-L. Riekkola, *J. High Resolut. Chromatogr. 20 (1997)* 410.

[21] T. Hyötyläinen, K. Grob and M.-L. Riekkola, *J. High Resolut. Chromatogr.*, 20 (1997) 657.

[22] T. Hyötyläinen, K. Janho and M.-L. Riekkola, *J. Chromatogr. A*, 813 (1998) 113.

[23] G.P. Blanch, M.L. Ruiz del Castillo and M. Herraiz, *J. Chromatogr. Sci.*, 36 (1998) 589.

[24] P. Wessels, J. Ogorka, G. Schwinger and M. Ulmer, *J. High Resolut. Chromatogr.*, 16 (1993) 708.

[25] J. Ogorka, G. Schwinger, G. Bruat and V. Seidel, *J. Chromatogr. A*, 626 (1992) 87.

[26] J.J. Vreuls, V.P. Goudriaan, G.J. de Jong and U.A.Th. Brinkman, *High Resolut. Chromatogr.*, 14 (1991) 475.

[27] J. Roeraade, *J. Chromatogr. A*, 330 (1985) 263.

[28] E. Fogelqvist, M. Krysell and L.-G. Danielsson, *Anal. Chem.*, 58 (1986) 1516.

[29] E. Ballesteros, M. Gallego and M. Valcárcel, *Anal. Chem.*, 65 (1993) 1773.

[30] E. Ballesteros, M. Gallego and M. Valcárcel, *J. Chromatogr. A*, 633 (1993) 169.

[31] E.C. Goosens, M.H. Broekman, M.H. Wolsters, R.E. Strijker, D. de Jong, G.J. de Jong and U.A.Th. Brinkman, *J. High. Resolut. Chromatogr.*, 15 (1992) 243.

[32] E.C. Goosens, D. de Jong, G.J. de Jong, F.D. Rinkema and U.A.Th. Brinkman, *J. High Resolut. Chromatogr.*, 18 (1995) 38.

[33] A. Venema and J.T. Jelink, in P. Sandra (ed.), *Proc. 17th Internat. Symp. Capillary Chromatogr., Riva del Garda 1994*, Hüthig, Heidelberg, Germany (1994), p. 1035.
[34] A. Venema and J.T. Jelink, *J. High Resolut. Chromatogr.*, 19 (1996) 234.
[35] J. Pawliszyn, *Solid Phase Microextraction, Theory and Practice,* Wiley–VCH, New York, USA, 1997.
[36] R. Eisert and J. J. Pawliszyn, *Crit. Rev. Anal. Chem.*, 27 (1997) 103.
[37] C. Arthur, D. Potter, K. Buchholz, S. Motlagh and J. Pawliszyn, *LC-GC,* 10 (1992) 656.
[38] A. Peñalver, E. Pocurull, F. Borrull and R.M. Marcé, *Trends Anal. Chem.*, 18 (1999) 557.
[39] H. Prosen, *Trends Anal. Chem.*, 18 (1999) 272.
[40] Z. Zhang and J. Pawliszyn, *Anal. Chem.*, 67 (1995) 34.
[41] J.J. Langenfeld, S.B. Hawthorne and D.J. Miller, *Anal. Chem.,* 68 (1996) 144.
[42] I. Valor, C. Cortada and J.C. Moltó, *J. High Resolut. Chromatogr.*, 742 (1996) 472.
[43] T. Nilsson, F. Pelusio, L. Montanarella, B. Larsen, S. Facchetti and J.O. Madsen, *J. High Rolut. Chromatogr.*, 18 (1995) 617.
[44] K.D. Buchholz and J. Pawliszyn, *Environ. Sci. Technol.,* 27 (1993) 2844.
[45] R. Eisert and K. Levsen, *Fresenius J. Anal. Chem.*, 351 (1995) 555.
[46] B.J. Hall and J.S. Brodbelt, *J. Chromatogr. A*, 777 (1997) 275.
[47] T. Kumazawa, H. Seno, X.P. Lee, A. Ishii, O. Suzuki and K. Sato, *Chromatographia*, 43 (1996) 393.
[48] P. Popp and A. Paschke, *Chromatographia,* 46 (1997) 419.
[49] F. Mangani and R.Cenciarini, *Chromatographia*, 41 (1995) 678.
[50] J.J. Vreuls, A.J.H. Louter and U.A.Th. Brinkman, *J. Chromatogr. A*, 856 (1999) 279.
[51] J. Auger, S. Rousset, E. Thibout and B. Jaillais, *J. Chromatogr. A*, 819 (1998) 45.
[52] C. Struppe, B. Schäfer and W. Engewald, *Chromatographia*, 45 (1997) 138.
[53] R. Eisert, K. Levsen and G. Wünsch, *J. Chromatogr. A*, 683 (1994) 175.
[54] A. Wenner and M. Wortberg, *J. High Resolut. Chromatogr.*, 21 (1998), 661.
[55] L. Dunemann, H. Hajimiragha and J. Begerow, *Fresenius J. Anal. Chem.*, 363 (1999) 466.
[56] J. Song, B.D. Gardner, J.F. Holland and R.M. Beaudry, *J. Agr. Food Chem.*, 45 (1997) 1801.
[57] A.A. Boyd-Boland, S. Magdic and J.B. Pawliszyn, *Analyst,* 121 (1996) 929.
[58] L. Moens, T. Desmaele, R. Dams, P. Vandenbroeck and P. Sandra, *Anal. Chem.,* 69 (1997) 1604.
[59] G. Gmeiner, C. Krassnig, E. Schmid and H. Tausch, *J. Chromatogr. B*, 705 (1998) 132.
[60] D. Potter and J. Pawliszyn, *J. Chromatogr. A,* 625 (1992) 247.
[61] S. Fustinoni, R. Giampiccolo, S. Pulvirenti, M. Buratti and A. Colombi, *J. Chromatogr. B*, 723 (1999) 105.
[62] T. Nilsson, F. Pelusio, L. Montarella, B. Larsen, S. Fachetti and J.O. Madsen, *J. High Resolut. Chromatogr.,* 18 (1995) 617.
[63] K.D. Buchholz and J. Pawliszyn, *Anal. Chem.,* 66 (1994) 160.
[64] A.A. Boyd-Boland and J.B. Pawliszyn, *J. Chromatogr. A,* 704 (1995) 163.
[65] R. Eisert and K. Levsen, *J. Am. Soc. Mass Spectrom.,* 6 (1995) 1119.
[66] R. McCallum, Ph. Pendleton, R. Schumann and M.-U. Trink, *Analyst*, 123 (1998).
[67] S.A. Barshick and W.H. Griest, *Anal. Chem.*, 70 (1998) 3015.
[68] A. Penalver, E. Pocurull, F. Borrull and R.M. Marce, *J. Chromatogr. A*, 839 (1999) 253.
[69] Á. Keszler and K. Héberger, *J. Chromatogr. A*, 845 (1999) 337.
[70] D.W. Potter and J. Pawliszyn, *Environ. Sci. Technol.,* 28 (1994) 298.
[71] N. Huppert, N. Wurtele and H.H. Hahn, *Fresenius J. Anal. Chem.*, 362 (1998) 529.
[72] M. Chiarotti and R. Marsili, *J. Microcol. Sep.,* 6 (1994) 577.
[73] M. Guidotti, G. Ravailo and M. Vitali, *J. High Resol. Chromatogr.*, 22 (1999) 427.

[74] T. Felix, B.J. Hall and J.S. Brodbelt, *Anal. Chim. Acta,* 371 (1998) 195.

[75] E. Noroozian, F.A. Maris, M.W.F. Nielen, R.W. Frei, G.J. de Jong and U.A.Th. Brinkman, *J. High Resolut. Chromatogr. Chromatogr. Commun.,* 10 (1987) 17.

[76] Th.H.M. Noij, E. Weiss, T. Herps, H. Van Cruchten and J. Rijks, *J. High Resolut. Chromatogr. Chromatogr. Commun.*, 11 (1988) 181.

[77] P. Enoch, A. Putzler, D. Rinne and J. Schlüter, *J. Chromatogr. A*, 822 (1998) 75.

[78] J.J. Vreuls, W.J.G.M. Cuppen, E. Dolecka, F.A. Maris, G.J. de Jong and U.A.Th. Brinkman, *J. High Resolut. Chromatogr.,* 12 (1989) 807.

[79] J.J. Vreuls, W.J.G.M. Cuppen, G.J. de Jong and U.A.Th. Brinkman, *J. High Resolut. Chromatogr.,* 13 (1990) 157.

[80] A. Farjam, J.J. Vreuls, W.J.G.M. Cuppen, G.J. de Jong and U.A.Th. Brinkman, *Anal. Chem.,* 63 (1991) 2481.

[81] J. Dallüge, Th. Hankemeier, J.J. Vreuls, G. Werner and U.A.Th. Brinkman, *J. Chromatogr. A*, 830 (1999) 377.

[82] P.J.M. Kwakman, J.J. Vreuls, U.A.Th. Brinkman and R.T. Ghijsen, *Chromatographia*, 34 (1992) 41.

[83] Y. Picó, J.J. Vreuls, R.T. Ghijsen and U.A.Th. Brinkman, *Chromatographia*, 38 (1994) 461.

[84] Y. Picó, A.J.H. Louter, J.J. Vreuls and U.A.Th. Brinkman, *Analyst*, 119 (1994) 2025.

[85] E.R. Brouwer, D.J. van Iperen, I. Liska, H. Lingeman, and U.A.Th. Brinkman, *Intern. J. Environ. Anal. Chem.*, 47 (1992) 257.

[86] Th. Hankemeier, S.P.J. van Leeuwen, J.J. Vreuls and U.A.Th. Brinkman, *J. Chromatogr. A*, 811 (1998) 117.

[87] J.J. Vreuls, R.T. Ghijsen, G.J. de Jong and U.A.Th. Brinkman, *J. Chromatogr. A,* 625 (1992) 237.

[88] Th. Hankemeier, A.J.H. Louter, J. Dallüge, J.J. Vreuls and U.A.Th. Brinkman, *J. High Resolut. Chromatogr.*, 21 (1998) 450.

[89] J.J. Vreuls, H.G.J. Mol, J. Jagesar, R. Swen, R.E. Hessels and U.A.Th. Brinkman, in P. Sandra and G. Devos (Editors), Proc. 17th Intern. Symp. Cap. Chromatogr., Riva del Garda, September 1994, Hüthig, Heidelberg (1994), p. 1181.

[90] K Grob and M Biedermann, *J. Chromatogr. A*, 750 (1996) 11.

[91] E.C. Goosens, D. de Jong, J.H.M. van den Berg, G. J. de Jong and U.A.Th. Brinkman, *J. Chromatogr.*, 552 (1991) 489.

[92] G. Hagman and J. Roeraade, *J. Microcol. Sep.*, 5 (1993) 341-346.

[93] J.F. Hiller, T. McCabe and P.L. Morabito, *J. High Resolut. Chromatogr.*, 16 (1993) 5.

[94] Th. Hankemeier, S. Ramalho, S.J. Kok, J.J. Vreuls and U.A.Th. Brinkman, submitted for publication.

[95] H.G.J. Mol, M. Althuizen, H.-G. Janssen, C.A. Cramers and U.A.Th. Brinkman, *J. High Resolut. Chromatogr.*, 19 (1996) 69.

[96] J. Staniewski, H.-G. Janssen, C.A. Cramers and J.A. Rijks, *J. Microcol. Sep.*, 4 (1992) 331.

[97] Th.H. M. Noij and M.M.E van der Kooi, *J. High. Resolut. Chromatogr.,* 18 (1995) 535.

[98] A.J.H. Louter, P. Jones, D. Jorritsma, J.J. Vreuls and U.A.Th. Brinkman, *J. High Resolut. Chromatogr.*, 20 (1997) 363.

[99] A.J.H. Louter, S. Ramalho, J.J. Vreuls and U.A.Th. Brinkman, *J. Microcol. Sep.*, 8 (1996) 469.

[100] K.K. Verma, A.J.H. Louter, A. Jain, E. Pocurull, J.J. Vreuls and U.A.Th. Brinkman, *Chromatographia*, 44 (1997) 372.

[101] D. Jahr, *Chromatographia*, 47 (1998) 49.

[102] E. Ballesteros, M. Gallego and M. Valcárcel, *Environ. Sci. Technol.,* 30 (1996) 2071.

[103] M.A. Crespín, E. Ballesteros, M. Gallego and M. Valcárcel, *Chromatographia,* 43 (1996) 633.

[104] G.R. van der Hoff, S.M. Gort, R.A. Baumann and P. van Zoonen, *J. High Resolut. Chromatogr.*, 14 (1991) 465.

[105] G.R. van der Hoff, F. Pelusio, U.A.Th. Brinkman, R.A. Baumann and P. van Zoonen, *J. Chromatogr. A*, 719 (1996) 59.

[106] A.J.H. Louter, E. Bosma, J.C.A. Schipperen, J.J. Vreuls and U.A.Th. Brinkman, *J. Chromatogr. B*, 689 (1997) 35.

[107] A. Namera, M. Yashiki, K. Okada, Y. Iwasaki, M. Ohtani and T. Kojima, *J. Chromatogr. B*, 706 (1998) 253.

[108] A. Namera, M. Yashiki, Y. Iwasaki, M. Ohtani and T. Kojima, *J. Chromatogr. B*, 716 (1998) 171.

[109] I.M. Bengtsson, D.C. Lehotay, *J. Chromatogr. B*, 685 (1996) 1.

[110] Th. Hankemeier, P.C. Steketee, J.J. Vreuls and U.A.Th. Brinkman, *J. Chromatogr. A*, 750 (1996) 161.

[111] Th. Hankemeier, P.C. Steketee, J.J. Vreuls and U.A.Th. Brinkman, *Fresenius J. Anal. Chem.*, 364 (1999) 106.

[112] E. Pocurull, C. Aguilar, F. Borrull and R.M. Marcé, *J. Chromatogr. A*, 818 (1998) 85.

[113] A.J.H. Louter, C.A. Beekvelt, P. Cid Montanes, J. Slobodnik, J.J. Vreuls and U.A.Th. Brinkman, *J. Chromatogr. A*, 725 (1996) 67.

[114] Th. Hankemeier, S.J. Kok, J.J. Vreuls and U.A.Th. Brinkman, *J. Chromatogr. A*, 811 (1998) 105.

[115] E. Boselli, B. Grolimund, K. Grob, G. Lercker and R. Amadò, *J. High Resolut. Chromatogr.*, 21 (1998) 355.

[116] B. Grolimund, E. Boselli, K. Grob, R. Amadò and G. Lercker, *J. High Resolut. Chromatogr.*, 21 (1998) 378.

[117] Th. Hankemeier, S.J. Kok, J.J. Vreuls and U.A.Th. Brinkman, *J. Chromatogr. A*, 841 (1999) 75.

[118] H.G.J. Mol, J. Staniewski, H.-G. Janssen, C.A. Cramers, R.T. Ghijsen and U.A.Th. Brinkman, *J. Chromatogr. A*, 630 (1993) 201.

[119] H.G.J. Mol, H.-G. Janssen, C.A. Cramers and U.A.Th. Brinkman, *J. Microcol. Sep.*, 7 (1995) 247.

[120] H.G.J. Mol, H.-G. Janssen and C.A. Cramers, *J. High Resolut. Chromatogr.*, 16 (1993) 413.

[121] J.J. Vreuls, U.A.Th. Brinkman, G.J. de Jong, K. Grob and A. Artho, *J. High Resolut. Chromatogr.*, 14 (1991) 455.

[122] J.J. Vreuls, R.T. Ghijsen, G.J. de Jong and U.A.Th. Brinkman, *J. Microcol. Sep.*, 5 (1993) 317.

[123] H.G.J. Mol, H.-G.M. Janssen, C.A. Cramers and U.A.Th. Brinkman, *J. High Resolut. Chromatogr.*, 16 (1993) 459.

[124] A.J.H. Louter, J. van Doornmalen, J.J. Vreuls and U.A.Th. Brinkman, *J. High Resolut. Chromatogr.*, 19 (1996) 679.

[125] E. Baltussen, F. David, P. Sandra, H.-G. Janssen and C.A. Cramers, *J. Chromatogr. A.*, 805 (1998) 237.

[126] G. Schomburg, E. Bastian, H. Behlau, H. Husmann and F. Weeke, *J. High Resolut. Chromatogr. Chromatogr. Commun.*, 7 (1984) 4.

[127] J. Teske, J. Efer and W. Engewald, *Chromatographia*, 46 (1997) 580.

[128] J. Teske, J. Efer and W. Engewald, *Chromatographia*, 47 (1998) 35.

[129] S. Müller, J. Efer and W. Engewald, *Chromatographia*, 38 (1994) 694.

[130] S. Blomberg and J. Roeraade, *J. High Resolut. Chromatogr.*, 13 (1990) 509.

[131] A.-J. Bulterman, J.J. Vreuls, R.T. Ghijsen and U.A.Th. Brinkman, *J. High Resolut. Chromatogr.*, 16 (1993) 397.

[132] A.J.H. Louter, F.D. Rinkema, R.T. Ghijsen and U.A.Th. Brinkman, Intern. J. Environ. Anal. Chem., 56 (1994) 49.

[133] R. Herraez Hernandez, A.J.H. Louter, N.C. van de Merbel and U.A.Th. Brinkman, *J. Pharm. Biomed. Anal.*, (1996) 1037.

[134] A. Saraf and L. Larsson, *J. Mass Spectrom.*, 31 (1996) 389.

[135] J. Slobodnik, A.C. Hogenboom, A.J.H. Louter and U.A.Th. Brinkman, *J. Chromatogr. A,* 730 (1996) 353.

[136] J. Slobodnik, A.J.H. Louter, J.J. Vreuls, I. Liska and U.A.Th. Brinkman, *J. Chromatogr. A,* 768 (1997) 239.

[137] A.J.H. Louter, A.C. Hogenboom, J. Slobodnik, J.J. Vreuls and U.A.Th. Brinkman, *Analyst*, 122 (1997) 1497.

[138] S. Pedersen-Bjergaard, T.N. Asp, T. Greibrokk, *Anal. Chim. Acta,* 265 (1992) 87.

[139] N.L. Olson, R. Carrell, R. Cummings, R. Rieck, S. Reimer, *J. Assoc. Offic. Anal. Chem. Intern.*, 78 (1995) 1464.

[140] J. Th. Jelink, A. Venema, *J. High Resolut. Chromatogr.*, 13 (1990) 447.

[141] E.C. Goosens, D. de Jong, G.J. de Jong, F.D. Rinkema and U.A.Th. Brinkman, *J. High Resolut. Chromatogr.*, 18 (1995) 38.

[142] Th. Hankemeier, A.J.H. Louter, F.D. Rinkema and U.A.Th. Brinkman, *Chromatographia,* 40 (1995) 119.

[143] Th. Hankemeier, J. Rozenbrand, M. Abhadur, J.J. Vreuls and U.A.Th. Brinkman, *Chromatographia*, 48 (1998) 273.

[144] H.G.J. Mol, Th. Hankemeier and U.A.Th. Brinkman, *LC–GC Intern.*, 12 (1999) 108.

[145] L.L.P. van Stee, P.E.G. Leonards, R.J.J. Vreuls and U.A.Th. Brinkman, *Analyst*, 134 (1999) 1547.

[146] Th. Hankemeier, H.T.C. Van der Laan, J.J. Vreuls, M.J. Vredenbregt, T. Visser and U.A.Th. Brinkman, *J. Chromatogr. A,* 732 (1996) 75.

[147] Th. Hankemeier, E. Hooijschuur, R.J.J. Vreuls, U.A.Th. Brinkman and T. Visser, *J. High Resolut. Chromatogr.* 21 (1998) 341.

[148] N. Ragunathan, K.A. Krock, C. Klawun, T.A. Sasaki and C.L. Wilkins, *J. Chromatogr. A*, 703 (1995) 335.

[149] R.J.J. Vreuls, J. Dallüge and U.A.Th. Brinkman, *J. Microcol. Sep*, 1999, in press.

2

Large-volume on-column injection in GC

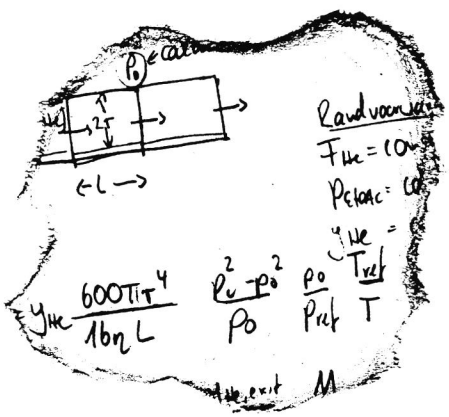

2.1 Optimization of large-volume on-column injections for GC

Summary

Large-volume injection is an attractive means to improve detection limits when analysing dilute sample extracts. There is now no need to achieve enrichment by means of solvent evaporation. The latter would make the total analytical procedure less reliable and less robust due to loss of volatile compounds.

In this study large-volume injection was carried out using an on-column injector in combination with a deactivated uncoated fused silica capillary (retention gap) and an early SVE. Two strategies for the optimization of the injection conditions are described. The first one relies on the programmable speed of an infusion pump, which is adapted such that it lies just above the evaporation rate of the extraction solvent used. With the second procedure, which can be used with a commercially available autosampler, the evaporation speed is adjusted to the fixed speed of injection by varying the temperature during injection. During optimization the additional solvent evaporation time was determined. The optimum conditions for an injection volume of 100 µl of either *n*-hexane or ethyl acetate are reported. Large-volume injection was used for simplified and miniaturized solid-phase extraction procedures. The procedures were used to determine various organic micropollutants, such as organophosphorus pesticides and triazine herbicides, in tap and surface water extracts, using a flame photometric and a mass spectrometric detector. For both methods good recovery for most of the analytes (70–87%), linear calibration curves (0.01–5 µg/l range) and relative standard deviations of less than 10% were obtained. Detection limits typically were in the range of 1–10 ng/l for GC–FPD and 10–150 ng/l for GC–MS. When working in the time-scheduled selected ion monitoring detection mode detection limits in GC–MS were one order of magnitude lower.

2.1.1 Introduction

Gas chromatography (GC) is frequently used for the trace analysis of organic micropollutants. High separation efficiency, a high speed of analysis and a wide range of detectors are the main advantages of this separation technique compared with column liquid chromatography (LC). Many of the detectors, such as the nitrogen–phosphorus detector, the flame photometric detector (FPD) and the electron-capture detector are more or less element-selective, while another one, the mass spectrometer (MS), provides excellent detection and identification possibilities for amounts of analytes of, typically, 1 ng or less.

However, even today it is still true that in many cases only a small amount (1–2 µl) of the total sample extract is introduced into the analytical system. This means that after careful sample preparation which often comprises analyte isolation by extraction and changing to a GC-compatible solvent, only 1–2% of the extract will be injected and reach the detector. The analyte concentration required to achieve low detection limits is obtained by the volume ratio (water/organic solvent) during extraction, and/or by evaporation of the extraction solvent [1]. Already several years ago Grob and Müller [2] illustrated that solvent evaporation is a rather critical step during sample preparation in which as a result of coevaporation the more volatile compounds were lost from the sample extract with the main solvent.

Several techniques have been reported that allow the injection of sample extracts of up to at least 100 µl, which implies that detection limits can be decreased by two orders of magnitude or that, on the other hand, concentration steps become superfluous. Such techniques were initially developed to couple LC on-line with GC [3], viz. partially concurrent solvent evaporation (PCSE) using an on-column interface [4] and fully concurrent solvent evaporation (FCSE) with a loop-type interface [5]. On-column injection has successfully been used for confirmatory GC–MS with full scan acquisition of various compounds at the sub-µg/l level in water extracts [6]. Polycyclic aromatic hydrocarbons could be detected in surface water at the 5 ng/l level after extraction of 1 l of sample with twice 0.8 ml of *n*-hexane. The presence of atrazine was confirmed in tap water at a level of 0.05 µg/l after off-line solid-phase extraction (SPE) of 100 ml of sample with subsequent desorption with 2 ml of ethyl acetate. In both cases, the injection volume was 100 µl. By using special features of an autosampler, viz. adapting the insertion depth of the syringe needle in the autosampler vial, Venema and Jelink [7] achieved in-vial extraction of hexachlorobutadiene and hexachlorobenzene into *n*-pentane. A similar approach was used for the determination of phenolic compounds in water [8]. Large-volume injection using the loop-type interface has been combined with GC–AED [9–13] for analytes covering a limited volatility range. It was used to confirm GC–MS data and for element specific screening of ground, tap and surface water samples with limits of detection below 1 µg/l. Programmed temperature vaporizer (PTV) injection, which was developed already in 1979 [14], has been used for large-volume injection into a gas chromatograph only in the past few years [15,16].

The key parameters of the optimization process are essentially the same for each of the above injection techniques. During injection of the sample extract most or all of the solvent is evaporated and no liquid solvent should reach the stationary phase in the analytical GC column. Furthermore, in order to protect the detector, most of the solvent vapours should be released either *via* a split vent as for the PTV injector, or *via* an early solvent vapour exit (SVE) as for the other two injection techniques [17]. After the injection has been completed the time of "solvent release system open" has to be optimized in order not to lose the early

eluting compounds and at the same time to transfer as small an amount of solvent as possible to the analytical GC column and detector.

It is evident that increasing the retention power during solvent elimination will greatly improve the recovery of more volatile analytes. Although several routes are open to achieve increased retention, creation of a temporary solvent film on the wall of the retention gap or PTV liner is of most interest. During injection this solvent film is an efficient trap for the analytes, while after evaporating, what remains is a bare wall with low retention.

In our group on-column injection, which uses a retention gap [18,19] in combination with an on-column injector, is the preferred technique. Introduction of the analyte-containing solvent then has to take place at a temperature below the solvent boiling point, in order to prevent solvent vapour backflush into the injector. The introduction speed is usually higher than the evaporation rate to ensure the formation of a solvent film on the surface of the retention gap. Until recently rather long retention gaps (10 m or longer) were used to prevent the liquid film from reaching the stationary phase of the analytical GC column. The principles developed by Munari et al. for eluent transfer from LC to GC under PCSE conditions [20] indicated that larger volumes could be injected. In PCSE, under optimized conditions some 90% of the injected solvent is evaporated during injection. Because only a minor part is introduced as liquid, which floods the retention gap, retention gaps could be drastically decreased in length [21], which reduces the price of the analytical system. The main advantage of the on-column interface is that it can be used for non-volatile as well as volatile analytes, while alternatives such as FCSE or PTV are restricted to compounds eluting at relatively high temperatures. It can be used without any hardware modifications (except for the early SVE) for a wide range of analytes, i.e. for compounds eluting just after the solvent peak up to very non-volatile compounds. Moreover, no discrimination of high-boiling compounds occurs. The most serious problem encountered is that high-boiling "dirt", which remains spread out in the retention gap after completion of the solvent evaporation process, can cause analyte adsorption, deteriorated peak shapes and even loss of analytes due to catalytic degradation. This implies that sample extracts have to be rather clean, which is usually true for surface and tap water extracts.

This paper reports two strategies for the optimization of large-volume on-column injection. One can be used if the injection speed can be controlled with an accuracy of 1 µl/min or better, e.g. when using an infusion pump for injection. With the other procedure the temperature during injection is reduced such that ca. 90% of the injected solvent evaporates during injection. To this end, the speed of injection is initially preset at a fixed value such that all the solvent evaporates at the standard boiling point. In this case a commercially available autosampler was used which had an injection speed programmable in 60-µl/min steps. Values for the additional solvent evaporation times, and optimum conditions for 100-µl injections of *n*-hexane and ethyl acetate were determined using *n*-alkanes as test compounds. Large-volume injection made it possible to modify extraction procedures. Avoiding the solvent evaporation step and total miniaturization of the extraction procedure are described. These new procedures were applied to the determination of organophosphorus pesticides (OPPs) by injecting 100 µl out of a 10-ml extract into a GC–FPD system, and 100 µl out of a 1-ml extract containing various other micropollutants into a GC–MS system. Extracts of tap and surface water samples were analysed.

2.1.2 Experimental

Chemicals and stock solutions

Stock solutions containing the C_8–C_{20} *n*-alkanes (except for C_{16}) were prepared in *n*-hexane at a concentration of about 20 µg/ml. The standard mixtures for optimization of the parameters for large-volume injections were prepared by diluting this stock solution 100-fold in *n*-hexane or ethyl acetate. Another stock solution containing eleven OPPs was prepared in ethyl acetate. This was directly added to water samples for spiking purposes. All chemicals were of 99% purity or better. Freshly distilled solvents were used to prepare the standard solutions and subsequent dilutions.

Bromophos-ethyl, diazinon, ethion, fenchlorphos, fenitrothion, mevinphos, parathion-ethyl, pyrazophos, sulfotep, tetrachlorvinphos and triazophos were purchased from Riedel de Haën (Seelze, Germany). Various analytes were used in GC–MS experiments: 1,2,4-trichlorobenzene, 1,2,4,5-tetrachlorobenzene, propachlor, trifluralin, prometon, atrazine, diazinon, prometryn, metolachlor, parathion-ethyl and chlorpyriphos. Stock solutions of the standards were made by weighing and dissolving them in ethyl acetate. Ethyl acetate and *n*-hexane (J.T. Baker, Deventer, the Netherlands) were freshly distilled before use. HPLC-grade water was freshly prepared using a Milli-Q system (Millipore, Bedford, MD, USA).

Large-volume on-column injection

The set-up of the system is schematically shown in **Figure 1**. A Carlo Erba 8000 series gas chromatograph equipped with an on-column injector, an FID-40 or FPD-80 and Chromcard data storage system (CE Instruments, Milan, Italy) was used. A 1.0–2.5 m x 0.53 mm i.d. diphenyltetramethyldisilazane-deactivated retention gap (DPTMDS; BGB Analytik, Zürich, Switzerland) was used for the introduction of 100 µl of sample extract under PCSE conditions. It was connected to a 2-m retaining precolumn and a 10-m analytical GC column (both 0.32 mm i.d. DB-1, d_f =1 µm) *via* a glass press-fit and a Y-piece connector, respectively. The SVE valve, which was actuated *via* a remote event of the gas chromatograph, was connected to the Y-piece. Helium was used as the carrier gas at an inlet pressure of 50 kPa, which resulted in a flow rate of 2.3 ml/min, which was measured at the detector outlet with the SVE closed. The detector settings were optimized according to the Carlo Erba manual: FID (air, 350 ml/min; hydrogen, 25 ml/min) and FPD (air, 120 ml/min; hydrogen, 100 ml/min; make-up, 20 ml/min). Helium was used as make-up gas.

When using a mass spectrometer (MD 800; CE Instruments), a similar set-up as described above was used. Now, a 1–1.5-m long DPTMDS-deactivated retention gap was connected to 2 m x 0.25 mm i.d. retaining precolumn (d_f = 0.25 µm), which in its turn was connected to the SVE and a 25 m x 0.25 mm i.d. HP-5-MS column (d_f = 0.25 µm) via a glass Y-piece. Since the MassLab programme, which is used for data handling and programming of the GC–MD800 system, has not yet been adapted for large-volume on-column injection, the autosampler and the SVE closure time were programmed manually after down-loading a sequence.

For optimization of the injection speed an automated syringe pump (Harvard Apparatus 22, SO. Natick, MA, USA) was used. The injection speed could be controlled in the 1–390 µl/min range at intervals of 1 µl /min. The 500-µl syringe with a PTFE plunger tip was

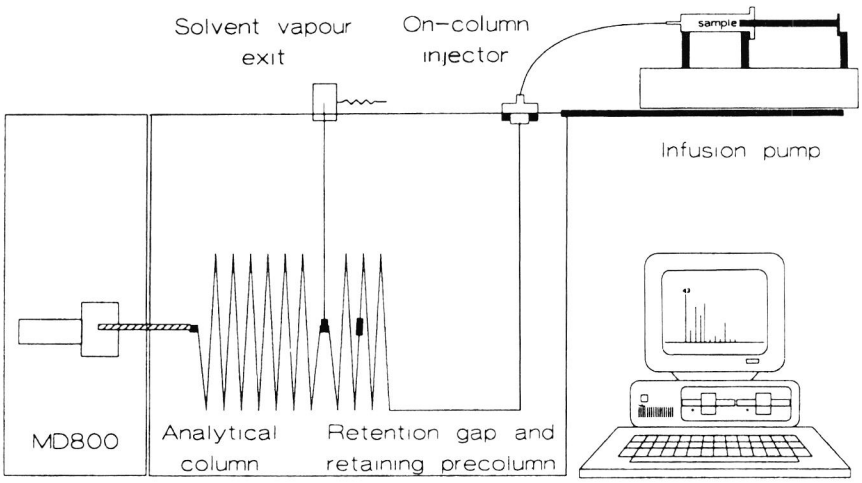

Figure 1
Schematical set-up for on-column injection with an infusion pump (Harvard Apparatus 22).

manually filled and after mounting it in the Harvard apparatus the sample was transferred to the injector via 50 cm x 0.10 mm i.d. PEEK tubing and a syringe needle, which were coupled by means of a stainless-steel connector. The Harvard apparatus was actuated via two remote events of the gas chromatograph. After completion of the injection and evaporation of the solvent, the SVE was closed and the temperature programme started from the initial temperature to 300°C at a rate of 10°C/min. When *n*-hexane or ethyl acetate were used the initial temperatures were 69°C and 77°C, respectively.

For optimization of the evaporation rate with the AS-800 autosampler (CE Instruments) and when injecting at a speed of 1 µl/s, the temperature was varied in order to meet PCSE conditions (evaporation rate, ca. 0.9 µl/s). The 250-µl syringe with a PTFE plunger tip was first cleaned with solvent, then washed with sample extract and finally the syringe was debubbled five times. After completion of the injection and evaporation of the solvent, the SVE was closed after 110 sec and the temperature programme started from the injection temperature to 300°C at 10°C/min.

Off-line solid-phase extraction of OPPs using Empore™ extraction disks

One 47 mm diameter extraction disk containing Biobeads SM-2 particles in a mesh of PTFE (BioRad, Richmond, CA, USA) was mounted in a laboratory-made filtration unit consisting of a glass filter which could be connected to a vacuum system mounted on top of a 2-l vessel; the disk was held in position by clamping. The extraction disk was conditioned with 10 ml of ethyl acetate and 10 ml of HPLC-grade water. Next, 2 l of water sample were passed through at a rate of about 100 ml/min, and the disk was dried for 15 min at ambient temperature. The analytes were desorbed with 10 ml of ethyl acetate. Extracts were used without further treatment.

In a later stage of the study the size of the extraction disks and the filtration unit were decreased to a diameter of 12 mm. The disks were cut from the original 47 mm pieces. This allowed the 10–20-fold reduction of the procedure: conditioning with 1 ml of ethyl acetate and 1 ml of HPLC-grade water, sampling of 100 ml at a rate of about 10 ml/min. The drying step was maintained constant at 15 min. Desorption was carried out with 0.5 ml of ethyl acetate directly into the autosampler vial.

Off-line solid-phase extraction of various analytes using packed cartridges

Standard SPE cartridges for off-line sample treatment containing 1000 mg of C-18 modified silica in an all-glass holder (J.T. Baker) were conditioned with 10 ml of ethyl acetate, 3 ml of methanol and 10 ml of HPLC-grade water. Next, 20 ml of water sample were passed through at a rate of about 10 ml/min, and the cartridge was dried for 15 min at ambient temperature. The analytes were desorbed with 1 ml of ethyl acetate. Extracts were used without further treatment.

2.1.3 Results and discussion

Optimization of parameters

Optimization of large-volume on-column injection consists of two essential steps: (i) the speed of injection is adapted to the evaporation rate of the solvent (or vice versa) in order to enable the analysis of volatile compounds, since the application range on the "volatile end" strongly depends on the presence of solvent and a phase soaking effect, and the additional solvent evaporation time; (ii) since the SVE is kept open during and even after completion of the injection until almost all the solvent has evaporated, closure of this exit has to be optimized carefully in order to prevent loss of the most volatile analytes. Two mixtures of *n*-alkanes in *n*-hexane and in ethyl acetate were used to study these effects. The parameters were optimized for as wide an application range as possible.

Adjusting the injection speed to the evaporation rate

The evaporation rate was determined by injecting 100 µl of solvent containing about 20 ng of each of the *n*-alkanes (C_{10}–C_{20}; except for C_{16}) while varying the speed of injection during subsequent GC runs (10 µl/min increase). Closing of the SVE was done precisely at the end of the injection to prevent any loss due to an open exit. **Figures 2**A and B show the results of two subsequent experiments carried out with ethyl acetate as solvent and using injection speeds of 50 and 60 µl/min, respectively. In Figure 2A the absence or the deteriorated peak shapes of the early eluting volatile compounds indicate that there is no solvent effect. The sample is obviously introduced into the retention gap at a speed below the evaporation rate. Injection at 60 µl/min resulted in formation of a solvent film on the wall of the retention gap, which in its turn created the desired solvent effects that produce sharp peaks, also for the volatile compounds, i.e. starting from C_{10} as can be seen Figure 2B. Besides, the peak areas were found to be the same as for 1-µl injections of the stock solution (typical differences, 1–4%). The evaporation rate obviously is between 50 and 60 µl/min. Although it is not really necessary, the evaporation rate can be determined more accurately by this trial-and-error

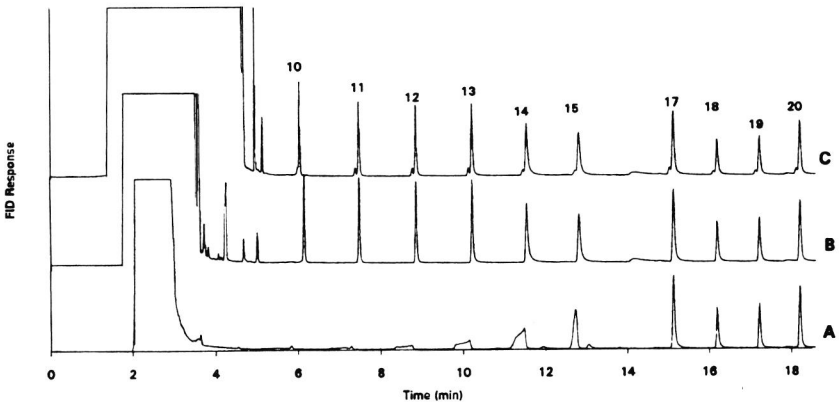

Figure 2
GC–FID chromatograms obtained after injection of 100 µl of a C_{10}–C_{20} *n*-alkane test mixture in *n*-hexane injected at a speed of (A) 50, (B) 60, and (C) 85 µl/min. For details , see Experimental section.

method, viz. by increasing the injection speed in smaller steps. The evaporation rates for *n*-hexane and ethyl acetate determined in this way were 84 and 58 µl/min, respectively. For a more rapid optimization, it is convenient to use a test mixture with only volatile compounds (C_9–C_{12}) to keep analysis time rather short.

The injection speed should not be increased in too large steps, because this will result in broad and distorted peaks when too much solvent is introduced into the GC system as a liquid. When the increase is made on the basis of the length of the retention gap, there is almost no risk of flooding the analytical GC column [22]. The following rule of thumb may be used [23]: for wetting solvents the length of the length of the flooded zone will certainly be less than 10 cm/µl for 0.53 mm i.d. retention gaps and less than 30 cm/µl for 0.32 mm i.d. retention gaps. This means that the injection speed can be increased in steps of 10 and 3 µl/min per meter of retention gap installed in the GC system for a 0.53 and 0.32 mm i.d. capillary, respectively.

Adjusting the evaporation rate to the injection speed
If the speed of injection cannot be varied at all or only in too large steps, as is the case for the present commercially available autosampler (steps of 60 µl/min), rather long retention gaps have to be used in order to retain the amount of solvent that is introduced as liquid. Therefore, as an alternative, the temperature was lowered to adjust the evaporation rate to the injection speed. The injection speed of the autosampler was set to a value which is below the evaporation rate at the standard boiling point, in this case to 1 µl/s. The resulting chromatogram, which was similar to that of Figure 2A, showed the absence of, or distorted peak shapes for the volatile compounds, but still perfect peak shapes for the non-volatile compounds. In subsequent runs the temperature was decreased stepwise. Closing of the SVE was done precisely at the end of the injection to prevent any loss due to an open exit. The chromatogram obtained at an injection temperature of 71°C showed good peak shapes for all the C_{10}–C_{20} *n*-alkanes.

Additional solvent exit time

As can be expected, solvent peaks can be rather broad. Unfortunately, this can not be tolerated by all GC detectors. It is possible to close the SVE some time after the injection has been completed, i.e. to use an additional SVE time. Part of the evaporating solvent film, which still is in the retention gap after the injection has been stopped, will then be vented to waste, i.e. will not enter the GC column. However, this process can not be unduly prolonged, since delayed closure of the SVE will result in the loss of volatile compounds. **Figure 3** shows that delayed closure of the SVE on the order of only a few seconds already results in a complete loss of the volatile compounds which, in this case, elute at t_r < ca. 5 min.

Application of large-volume injection

For water samples current European Union (EU) directives dictate that the concentration of, e.g., individual pesticides in tap water should not exceed 0.1 μg/l [24]. Meeting these limits is a challenging task. More economical use of the total extract by injecting larger volumes will help to meet these criteria. Transfer of the total extract can best be carried out with on-line procedures [25,26]

GC–FPD

Large-volume on-column injection was applied for the determination of OPPs using an FPD for selective detection. River Meuse water samples and Amsterdam tap water were tested for the presence of eleven OPPs. **Figures 4**A and B show results obtained with on-column injection of the extracts of 2-l Meuse river water samples (Eysden, the Netherlands) without and with spiking at the 50 ng/l level, respectively. The recovery for the spiked compounds were in the 70–90% range. Figure 4A revealed, next to some unknown peaks, the presence of a peak ("3?") with the same retention time as diazinon in river Meuse water. The calculated

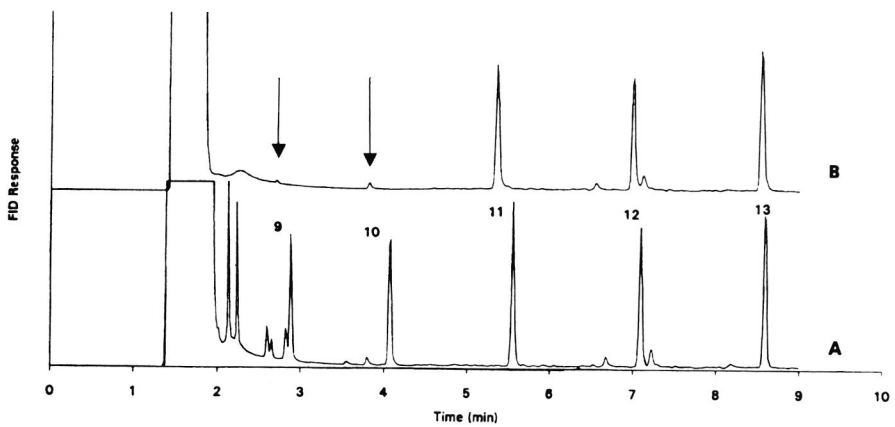

Figure 3

GC–FID chromatograms obtained after 100 μl-injection of *n*-hexane containing *n*-alkanes (C_9–C_{13}) using an additional solvent vapor exit time of (A) 13 and of (B) 15 s. Injection speed: 100 μl/min; evaporation rate: 84 μl/min. For other details, see Experimental section.

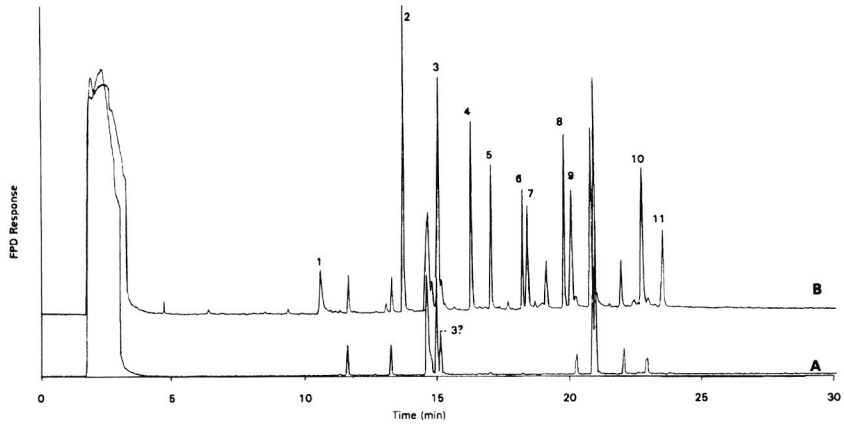

Figure 4
GC-FPD chromatogram of a river Meuse water extract (A) without and (B) with spiking at the 50 ng/l level. Sample volume: 2 l; extraction volume: 10 ml; injection volume: 100 µl. For other details, see *Experimental* section. Peak assignment: (1) mevinphos, (2) sulfotep, (3) diazinon, (4) fenchlorfos, (5) parathon-ethyl, (6) bromophos-ethyl, (7) tetrachlorvinphos, (8) ethion, (9) triazophos, (10) pyrazophos, and (11) coumaphos.

concentration was between 10 and 15 ng/l. Estimating the concentration of the unknown compounds based on responses of the eleven OPPs, showed that most compounds were present in the surface water sample at below the 10–25 ng/l level. Two compounds with retention times of 20.86 and 20.96 min were present at a level of about 50 ng/l; even this is far below the alert and alarm levels of 1 and 3 µg/l, respectively, commonly used for individual compounds in surface water. For the Amsterdam tap water (data not shown) all peaks that showed up in the chromatogram, were much below the tolerance level of 0.1 µg/l of the EU.

In a next step, the total procedure was miniaturized in such a way that the overall concentration factor remained the same, i.e. 100 ml of sample and 0.5 ml of ethyl acetate for desorption (cf. Experimental part). **Table 1** summarizes some analytical data for nine analytes studied with this new procedure. The recovery and the relative standard deviation (RSD) for the total SPE plus large-volume injection GC–FPD analysis are satisfactory. For all compounds except the rather apolar bromophos-ethyl (50–72%) which tended to adhere to the wall of the extraction device, the recovery was over 70% at the 0.1 µg/l level. It is interesting to add that, for all analytes, the recoveries were essentially the same at all spiking levels tested in the 0.05–5 µg/l range. As is to be expected, the RSD values slightly increased with decreasing spiking levels, but values never were higher than 10%, which is fully satisfactory. Linearity was tested by preconcentrating spiked Amsterdam tap water and river Meuse water at four different concentrations levels in the 0.05–5 µg/l range. For all analytes the regression coefficients were better than 0.985. For the OPPs studied the detection limits (signal-to-noise ratio, 10:1) in GC–FPD were about 1–10 ng/l when using 100-ml samples. Limits of detection were extrapolated from the peak heights recorded at the 50 ng/l level.

Table 1
Analytical data (n=6) for the total procedure of off-line SPE and large-volume on-column injection GC–FPD of riverwater extracts.

Compound	Recovery (%) at 0.1 µg/l	RSD (%)	Regression coefficient [a]	Detection limits [b] (ng/l)
Mevinphos	70	10	0.985	1.5
Diazinon	87	4	0.999	0.8
Fenchlorfos	78	7	0.998	1.2
Parathion-ethyl	84	4	0.995	1.2
Bromophos-ethyl	61	12	0.989	2
Ethion	72	5	0.999	1.4
Triazophos	78	8	0.997	2.3
Pyrazophos	82	8	0.999	5
Coumaphos	80	7	0.997	12

[a] Regression coefficient from the linear plot of peak area vs. injected amount of OPP.
[b] Detection limit extrapolated for signal-to-noise ratio of 10 (sample volume, 100 ml).

GC–MS

In order to demonstrate the potential of the present system for the identification of (unknown) pollutants at the trace level, standard solutions containing a set of about 200 analytes of interest - among them triazines, OPPs, anilines, chlorobenzenes, trialkylphosphates, polycyclic aromatic hydrocarbons (PAHs), N-methylcarbamates and phthalates - were injected into the system under full-scan conditions. An absolute amount of 10–1000 pg was injected in the conventional 1-µl, and in the large-volume mode. **Figure 5** shows a typical chromatogram obtained under full-scan conditions (mass range, *m/z* 35–385) for the 100-µl injection of a standard solution containing 200 pg of each of eleven test compounds (cf. legend to Figure 5). At this level of 200 pg, ca. 85% of the compounds showed spectra of such a good quality with both types of injection, that there was satisfactory agreement with spectra from the NBS library, viz. with match factors above 900 on a scale of 1000. The inherent power of large-volume injection is that even at the 2 pg/µl level rather good-quality spectra were obtained. As examples, Figures 5B and C show mass spectra of 1,2,4,5-tetrachlorobenzene and diazinon, respectively. Further it was found that several groups of compounds, i.e. PAHs and anilines, gave good-quality spectra even at a level of about 10 pg, i.e. 0.1 pg/µl. For most other compounds, detection - although, not identification - was possible for injected amounts of 10–20 pg by reconstruction of their most intense ion traces.

A considerable improvement in analyte detectability as well as selectivity was obtained by using time-scheduled selected ion monitoring (SIM) with 4–20 ions per window and, next, reconstructing a single ion trace. For each of the eleven test compounds of Figure 5 four ions were selected which had a relatively high intensity and, preferably, isotope clusters. This mode of operation resulted in detection limits of about 1–2 pg injected amount. These multiple-ion spectra were still good enough for tentative identification of all test compounds (cf. [27]).

With the SPE procedure using packed SPE cartridges, 100 µl out of 1-ml extracts of 20 ml of Amsterdam tap water were analyzed with and without spiking, using the eleven selected compounds of Figure 5. As regards the analytical data for the total procedure, i.e. extraction of a 20-ml sample, drying with air, desorption with 1 ml of ethyl acetate, and sub-

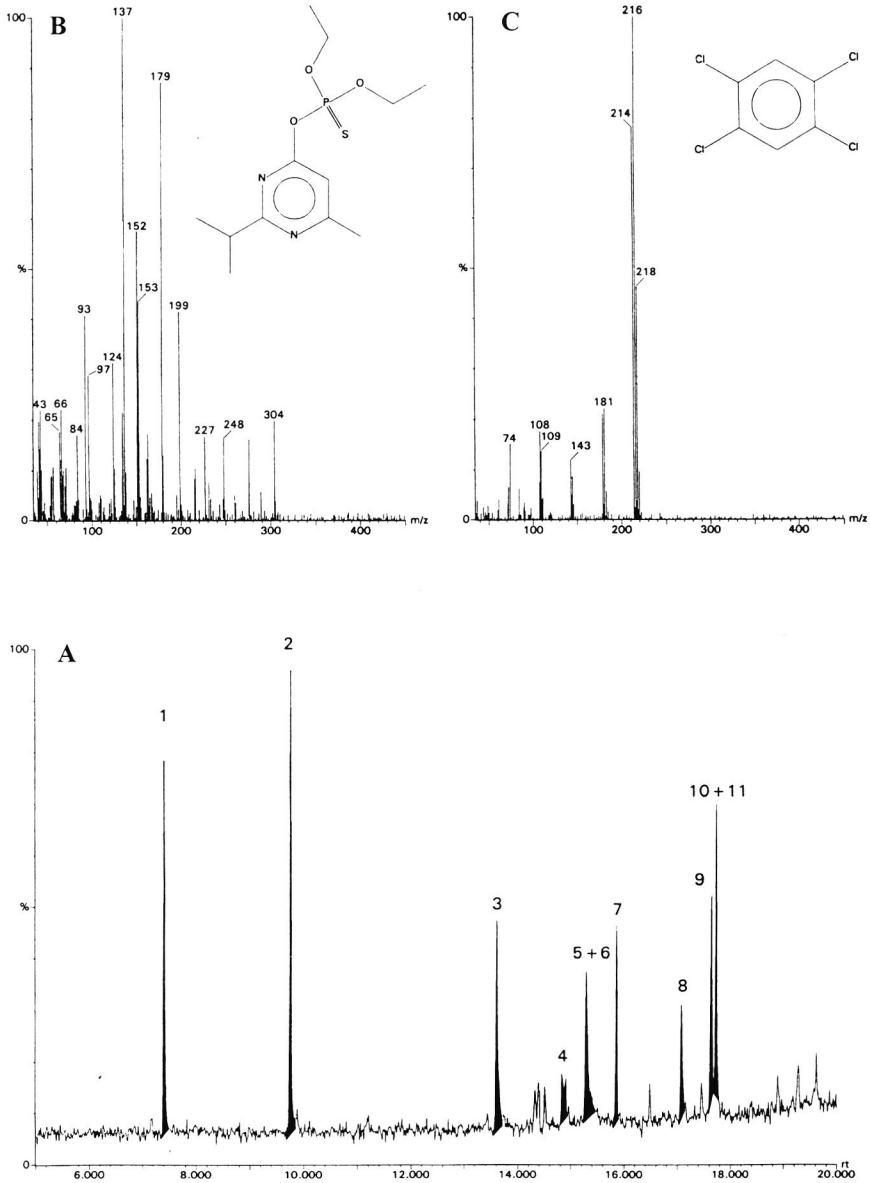

Figure 5

(A) Reconstructed multiple-ion GC-MS chromatogram acquired in full-scan mode and obtained after 100 µl-injection of a standard solution containing 200 pg of each of the following compounds: (1) 1,2,4-trichlorobenzene, (2) 1,2,4,5-tetrachlorobenzene, (3) propachlor, (4) trifluralin, (5) atrazine, (6) prometon, (7) diazinon, (8) prometryn, (9) metolachlor, (10) parathion-ethyl, and (11) chlorpyriphos. The recorded MS spectra of diazinon (B) and 1,2,4,5-tetrachlorobenzene (C) are shown.

Table 2
Analytical data for SPE of 20 ml of Amsterdam tap water followed by 100-µl on-column injection and GC–MS analysis.

Compound	Recovery (%) at 0.1 µg/l	RSD (%)	Regression coefficient [b]	Detection limits (ng/l) full-scan
1,2,4-Trichlorobenzene	91	3	0.999	10
1,2,4,5-Tetrachlorobenzene	90	5	0.999	10
Propachlor	93	3	0.999	30
Trifluralin	88	15	0.999	50
Atrazine	112	6	0.999	30
Prometon	91	17	0.999	50
Diazinon	83	7	0.999	30
Promethryn	80	7	0.997	50
Metolachlor	86	13	0.999	20
Parathion-ethyl [a]	95	10	0.996	150
Chlorpyriphos	61	5	0.999	30

[a] Recovery obtained by SIM mode because of low response in full-scan mode.
[b] Regression coefficient from the linear plot of peak area vs. injected amount of analyte.

sequent GC–MS analysis of 100 µl, **Table 2** lists the recoveries, RSD values, and linearity data obtained with Amsterdam tap water extracts. Except for chlorpyriphos (61%), all analytes gave recoveries of 80–95% at the 0.1 µg/l level. The high apparent recovery for atrazine is due to the presence of this compound in the tap water. The repeatability of the total SPE/GC–MS procedure was tested at the 0.1 µg/l level. RSD values were in the range of 3–17%, which is quite acceptable. For parathion the response in the full-scan mode was too low to enable detection and quantification in the real-life samples at the 0.1 µg/l level. In both the full-scan and SIM acquisition mode, the calibration curves (signal *vs.* amount of analyte) were linear in the 20-2000 pg range. The limits of detection were on the order of 10–50 ng/l in the full-scan, and 1–5 ng/l in the time-scheduled ion-extraction mode, respectively.

Typical results for the total SPE/GC–MS analysis of a spiked (0.1 µg/l) sample are shown in the reconstructed ion chromatograms of **Figure 6** for nine compounds. From among the eleven test solutes, only atrazine was found to be present in the water sample itself, viz. at a concentration of 60–70 ng/l. This agrees with earlier findings [28, 29].

It should be added that serious problems were encountered at the 0.01 µg/l level because interferences from the packing material and the frits of the SPE cartridge were eluted during desorption. The interfering peaks were mainly due to alkanes and commonly used plasticisers and additives in polymer materials. The analyte peaks could only be detected after reconstructing their ion traces, and identified by their spectra obtained after baseline subtraction. Rigorous cleaning of the SPE cartridges by flushing with ethyl acetate did help, but the chromatogram still contained several disturbing peaks. Obviously, the sensitivity of the present GC–MS set-up is such that SPE starts to become the weakest link in the total procedure.

SPE/GC–MS analysis was also performed with the extract of river Meuse water, which was earlier analyzed by means of GC–FPD (cf. Figure 4A) to confirm the presence of diazinon. Analysis of the full-scan chromatogram revealed that there was no diazinon

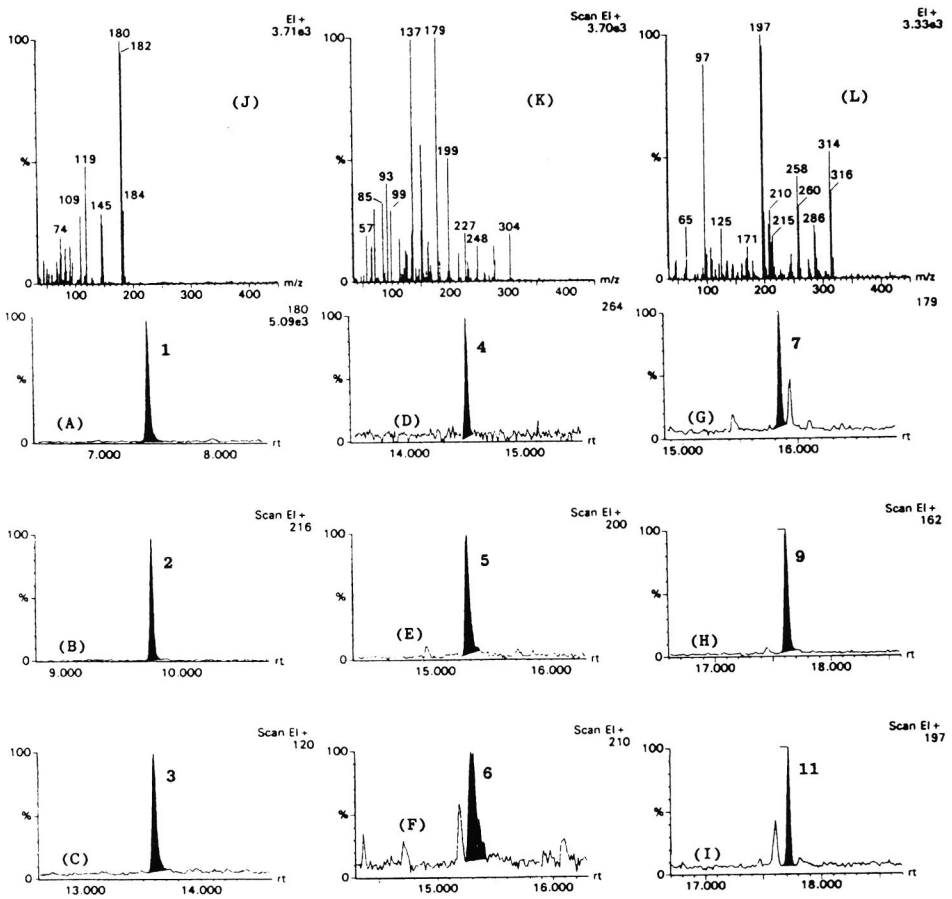

Figure 6

(A–I) Reconstructed ion GC–MS chromatograms obtained after 100 µl-injection of a tap water extract spiked at the 0.1 µg / l level. Peak assignment as in Figure 5. Mass spectra for (1) 1,2,4-trichlorobenzene (J), (7) diazinon (K), and (11) chlorpyriphos (L). For other details, see *Experimental* section.

present. The indicated concentration of 10–15 ng/l estimated on the basis of GC–FPD, would have resulted in the injection of 200–300 pg in the 100-µl extract, which without any doubt would have resulted in a spectrum comparable to that of Figures 5C and 6K. Diazinon could not even be detected in the SIM mode (m/z 304, 199, 179 and 137), while analysis of a standard solution containing 2 pg in 100 µl showed a peak with a signal-to-noise ratio of about 8. It can therefore be stated that no diazinon was present in the river Meuse water at a level higher than 1–5 ng/l.

2.1.4 Conclusions

Large-volume injection is an elegant way to analyse very diluted sample extracts by means of GC. During optimization special care has to be taken with regard to the evaporation rate, the injection speed and the length of the flooded zone. With the two procedures presented in this study such optimization becomes rather simple and can be carried out within a few hours for each different solvent used in the extraction.

Combining the present large-volume injection technique with a GC–MS, or GC–FPD, procedure with its high separation efficiency, and selective and sensitive detection, offers a powerful tool for ultratrace analysis of contaminants in aqueous samples. Mass spectrometric detection provides the means to detect and quantify target compounds, and to identify unknowns, at levels of typically 0.01–0.1 µg/l which are at or below the EU threshold values for tap water and much below the alert level for surface water. Further improvement for the detection of target compounds can be achieved by using time-scheduled SIM detection. In the present study, no attempt has been made to reduce sample volumes as much as possible. Rather, the potential of the procedure has been demonstrated by omitting any concentration step involving solvent evaporation, and by still using modest aliquots of the final extracts for analysis. Even so, it turns out that sample volumes of approx. 20 ml are all that is required.

References

[1] W. Dünges, *Prächromatographische Methoden*, Hüthig, Heidelberg, Germany 1979, pp 33–48.
[2] K. Grob and E. Müller, *J. Chromatogr.*, 404 (1987) 297.
[3] K. Grob, in W. Bertsch, W.G. Jennings, and P. Sandra (eds.), *On-line coupled LC-GC*, Hüthig, Heidelberg, 1991, pp. 2769.
[4] K. Grob, D. Fröhlich, B. Schilling, H.-P. Neukom and P. Nägeli, *J. Chromatogr.*, 295 (1984) 55.
[5] K. Grob and J.-M. Stoll, *J. High Resolut. Chromatogr./Chromatogr. Commun.*, 9 (1986) 518.
[6] J.J. Vreuls, S. Ramalho, M. de Jong and U.A.Th. Brinkman, poster presented at *17th Internat. Symp. Capillary Chromatogr., Riva del Garda, 1994.*
[7] A. Venema and J.T. Jelink, in P. Sandra (ed.), *Proc. 17th Internat. Symp. Capillary Chromatogr., Riva del Garda, 1994,* Hüthig, Heidelberg (1994) p. 1035.
[8] F. Munari, P.A. Colombo, P. Magni, G. Zolioli, S. Trestianu and K. Grob. Jr., in P. Sandra (ed.), *Proc. 17th Internat. Symp. Capillary Chromatogr., Riva del Garda, 1994,* Hüthig, Heidelberg (1994) p.1212.
[9] E.C. Goosens, D. de Jong, G.J. de Jong, F.D. Rinkema and U.A.Th. Brinkman, *J. High Resolut. Chromatogr.,* 18 (1995) 38.
[10] F.D. Rinkema, Th. Hankemeier, A.J.H. Louter and U.A.Th. Brinkman, in P. Sandra (ed.), *Proc. 17th Internat. Symp. Capillary Chromatogr., Riva del Garda, 1994,* Hüthig, Heidelberg (1994) p. 1422.
[11] F.D. Rinkema, A.J.H. Louter and U.A.Th. Brinkman, *J. Chromatogr.*, 678 (1994) 289.
[12] A.J.H. Louter, F.D. Rinkema, R.T. Ghijsen and U.A.Th. Brinkman, *Intern. J. Environ. Anal. Chem.*, 56 (1994) 49.
[13] A.J.H. Louter, F.D. Rinkema and U.A.Th. Brinkman, in P. Sandra (ed.), *Proc. 17th Internat. Symp. Capillary Chromatogr., Riva del Garda, 1994,* Hüthig, Heidelberg (1994) p. 1423.
[14] W. Vogt, K. Jacob and H.W. Obweber, *J. Chromatogr.*, 174 (1979) 437.
[15] J. Staniewski and J.A. Rijks, in P. Sandra (ed.), *Proc. 11th Internat. Symp. Capillary Chromatogr., Riva del Garda, 1989,* Hüthig, Heidelberg, Germany, 1989, p. 1334.
[16] J. Staniewski and J.A. Rijks, *J. High Resolut. Chromatogr.*, 16 (1993) 182.
[17] K. Grob, H.-G. Schmarr and A. Mosandl, *J. High Resolut. Chromatogr.*, 12 (1989) 375.
[18] K. Grob Jr., G. Karrer and M.-L. Riekkola, *J. Chromatogr.*, 334 (1985) 129.
[19] K. Grob, in W.G. Jennings, W. Bertsch and P. Sandra (eds.), *On-Column Injection in Capillary Gas*

Chromatography, Hüthig, Heidelberg, 1987.

[20] F. Munari, A. Trisciani, G. Mapelli, S. Trestianu, K. Grob Jr. and J.M. Colin, *J. High Resolut. Chromatogr./Chromatogr. Commun.*, 8 (1985) 601.

[21] J.J. Vreuls, H.G.J. Mol, J. Jagesar, R. Swen, R.E. Hessels and U.A.Th. Brinkman in P. Sandra (ed.), *Proc. 17th Internat. Symp. Capillary Chromatogr., Riva del Garda, 1994,* Hüthig, Heidelberg, Germany, 1994, p. 1181.

[22] K. Grob Jr., G. Karrer and M.-L. Riekkola, *J. Chromatogr.*, 334 (1985) 129.

[23] K. Grob, in W. Bertsch and P. Sandra (eds.), *On-line LC–GC* , Hüthig, Heidelberg, 1991, p. 191.

[24] *EEC Drinking Water Guidelines, 80/779/EEC, EEC No. L229/11-29*, EEC, Brussels, August 30, 1980.

[25] J.J. Vreuls, G.J. de Jong, R.T. Ghijsen and U.A.Th. Brinkman, *J. Assoc. Off. Anal. Chem.*, 77 (1994) 306.

[26] H.G.J. Mol, H.-G.M. Janssen and C.A. Cramers, J.J. Vreuls and U.A.Th. Brinkman, *J. Chromatogr.*, 703 (1995) 277.

[27] J.J. Vreuls , A.-J. Bulterman, R.T. Ghijsen and U.A.Th. Brinkman, *The Analyst*, 117 (1992) 1701.

[28] H. Bagheri, J.J. Vreuls, R.T. Ghijsen and U.A.Th. Brinkman, *Chromatographia*, 34 (1992) 5.

[29] A.J. Bulterman, J.J. Vreuls, R.T. Ghijsen and U.A.Th. Brinkman, *J. High Resolut. Chromatogr.*, 8 (1993) 397.

2.2 Monitoring the actual carrier gas flow during on-column LVI to automate closure of the SVE

Summary

Monitoring of the helium flow into a gas chromatograph (GC) by means of an electronic flow meter has been used to optimize and control large-volume on-column injections. The nature of the observed carrier gas flow rate profiles is discussed in some detail. A rather strong dependence of the evaporation rate on the injection speed was found for injections into a 0.32 mm I.D. retention gap, which can be attributed to the pressure drop along the retention gap when using a solvent vapour exit (SVE). The variation of the evaporation rate with the injection speed was found to be less critical for a 0.53 mm I.D. retention gap.

The carrier gas flow rate profile during the actual injection was used to effect the automated closure of the SVE precisely at the end of the evaporation process. Retention gaps of 0.53 mm I.D. were preferred over 0.32 mm I.D. retention gaps, as 0.53 mm I.D. retention gaps allowed a clearer detection of the end of the evaporation process. Compared with the conventional procedure which involves closure of the SVE at a predetermined time, the present approach is more robust and hardly any optimization is required; it did not cause losses of volatile analytes. The procedure considerably simplifies the use of large-volume on-column injections. Large-volume injections of alkanes were used to study the potential of the large-volume injection–GC system.

2.2.1 Introduction

The use of large-volume injections (LVI) in gas chromatography (GC), i.e. the injection of a larger aliquot of a sample extract than the conventional 1–5 µl, is attractive from several points of view. The sensitivity (in terms of concentration units) of existing analytical procedures will be increased, which is especially welcome when relatively insensitive detectors such as an infrared detector [1] or certain element channels of an atomic emission detector [2, 3] are being used. Next, it allows new strategies in sample preparation, i.e., (i) circumvention of solvent evaporation which often is the final step in off-line procedures; (ii) miniaturization of existing procedures using smaller sample and extraction solvent volumes and/or (iii) on-line coupling of sample preparation and GC analysis.

Several concepts for the injection of large sample volumes into a GC have been reported. Two techniques can be used for most types of application, i.e., large-volume on-column [4–6] and programmed temperature vaporizer (PTV) [7, 8] injection. If the sample extract is not too dirty, on-column injection is preferred, because it allows the determination of volatile as well as high-boiling analytes without any hardware modifications (except for the installation of an early solvent vapour exit, see below) such as cooling with CO_2, which is necessary for PTV injection.

With large-volume on-column injections, the solvent is injected into a retention gap which is installed in front of the analytical column. An early solvent vapour exit (SVE) is generally used to increase the evaporation rate and to protect the detector from excessive amounts of solvent vapour [9]. In order not to loose the volatile analytes, the SVE exit has to be closed at a predetermined time, i.e. just before the evaporation of the last part of the solvent. This point in time can be determined by monitoring the effluent leaving the SVE by a flame or a flame ionization detector (FID) at high attenuation [10, p. 127]. Alternatively, the closure time of the SVE can be derived from a series of injections performed at different closure times, viz. by determining at which closure time the volatile analytes are quantitatively recovered [4]. However, after optimization, slight changes of, for example, the carrier gas pressure, the injection speed and/or the injected volume due to the presence of, e.g., a small bubble in the syringe of an autosampler, will easily result in too late a closure and, consequently, loss of volatile analytes. In practice, even the exchange of a press-fit can influence the optimum conditions or, in other words, the procedures are not really robust.

Obviously, it is desirable to make optimization less time-consuming or even superfluous. One instrument manufacturer developed a software package which calculates appropriate parameters for a fixed set-up [5]. However, the algorithm of the software is not described, and only one type of retention gap can be used. In principle, it is also possible to calculate the evaporation rate for a specific instrument set-up [11]. However, as such calculations of the evaporation rate are only approximately correct, the closing of the SVE still has to be optimized. Obviously, automated closure of the SVE at the correct moment is highly desirable.

In the present study, the changes in the actual flow rate of the carrier gas during and at the end of the evaporation process were used to optimize and control large-volume on-column injections. The helium flow into the GC was measured by means of an electronic flow meter. Relevant theoretical aspects, such as the influence of the internal diameter of the retention gap, the head pressure and injection temperature and the injection speed, were studied in detail. The goal was to automate the closure of the SVE at the proper moment in time on the

basis of the flow rate profile of the carrier gas during injection and evaporation. The performance of the new concept was compared with that of the conventional procedure.

2.2.2 Experimental

Chemicals

Ethyl acetate and hexane (both p.a., J.T. Baker, Deventer, the Netherlands) were distilled before use. A 1 μg/μl stock solution of several *n*-alkanes in the C_8–C_{20} range (cf. Table 3 below) was prepared in *n*-hexane and stored in the dark at 4°C. For large-volume on-column injections, it was diluted to a concentration of 0.5 ng/μl.

Set-up of large-volume injection–GC system

The large-volume injection–GC system (**Figure 1**) consisted of a Carlo Erba Series 8000 gas chromatograph equipped with an on-column injector and an FID-80 (CE Instruments, Milan, Italy). A Model F101D-HA mass flow meter (Bronkhorst, Ruurlo, the Netherlands) was installed between the pressure regulator and the on-column injector; the flow was determined by means of thermal conductivity and the measurement was independent of the pressure. A 3-m diphenyltetramethyldisilazane-deactivated retention gap (DPTMDS; BGB Analytik, Zürich, Switzerland) was connected to a 2-m retaining precolumn and a 28-m analytical column (both DB-XLB, 0.25 mm I.D., film thickness 0.25 μm; J&W, Folsom, CA, USA) via a press-fit connector and a Y-piece, respectively. The SVE, an electronically controlled 6-port valve (Valco Instruments, Houston, TX, USA), was connected to the T-piece. The SVE was either controlled by a pre-programmed remote event of the GC, or by the SVE controller,

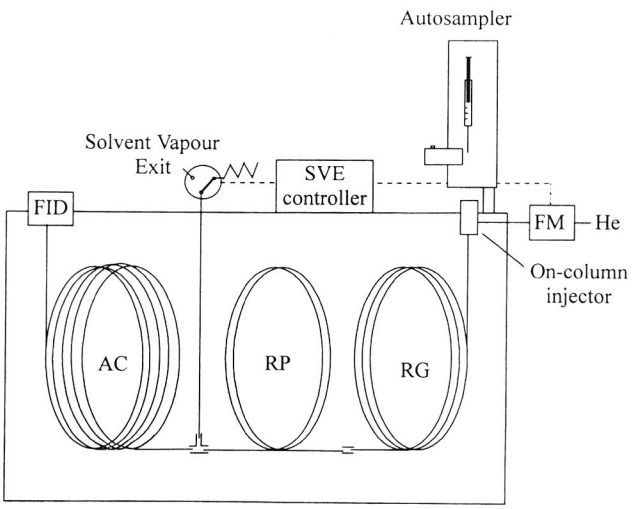

Figure 1
Set-up of the large-volume injection–GC system. Abbreviations: AC, analytical column; RP, retaining precolumn; RG, retention gap; FM, flow meter; He, helium; SVE, solvent vapour exit.

which was developed during the present project. The FID detector settings for the acquisition of chromatograms were chosen according to the manual (air, 350 ml/min; hydrogen, 25 ml/min). The standard boiling point of a solvent was used as the initial GC temperature, i.e. 77°C for the injection of ethyl acetate and 69°C for hexane. Helium 5.0 (Hoekloos, Schiedam, The Netherlands) was used as carrier gas; unless it is stated differently in the text, the head pressure was 110 kPa.

Unless stated differently, injections were performed with an automated syringe pump (Harvard Apparatus 22, So. Natick, MA, USA) using a 500-µl syringe with a PTFE-coated plunger. After filling and mounting it on the Harvard pump, the sample was transferred to the on-column injector via a stainless-steel needle (O.D. 0.25 mm).

For injections with the AS 800 autosampler (CE Instruments), a 250-µl syringe with a PTFE plunger and an injection needle of 0.5 mm O.D. were used. The appropriate settings for the autosampler were programmed by means of Chromcard Ver. 1.33 (CE Instruments). For injections with the AS 800 autosampler the injection speed was 2 µl/s.

After the automated closure of the SVE by the SVE controller, the temperature programme of the GC was started with a delay of 2.5 min. The temperature was increased to 280°C at 20°C/min, and held at 280°C for 1 min.

FID monitoring of solvent peak

Next to the carrier gas flow rate profile, the solvent peak was monitored, viz. with the FID. A press-fit splitter was connected to the retention gap. A 0.2 m x 0.1 mm I.D. fused silica restriction was used to direct about 0.5% of the gas flow to the FID. The other outlet of the T-splitter was connected to 0.9 m of a 0.32 mm I.D. retention gap. In order to record the whole solvent peak, the air flow of the FID was increased to 1500 ml/min by removing the restriction in front of the pressure controller, and the range was set to 10^3.

Automated detection of end of evaporation and SVE closure

A microprocessor-based SVE controller with a small keyboard and LCD display was constructed and a programme written in C to actuate the closure of the SVE. The helium flow was registered by the programme every 200 µsec via an A/D converter. Communication with the AS 800 autosampler and GC instrumentation was achieved by means of contact closure events.

When ready for a next run, the GC instrumentation gave a start signal to the AS 800 autosampler. When the autosampler was ready for injection, a signal was given to the SVE controller to open the SVE. After a delay time of 0.05 min, the injection was started. The syringe was removed 0.05 min after completion of the injection. After an additional delay time of 0.05 min to allow stabilization of the helium flow, monitoring of the helium flow by the SVE controller was initiated. As soon as the first derivative of the helium flow [which was calculated by subtracting the one-but-last from the last value] exceeded a preset threshold value, the SVE was closed and the GC run started. All relevant parameters, i.e. the pre-injection delay time, the injection time, the post-injection delay time and the threshold value, could be programmed in the SVE controller and were stored in its memory. The closure times of the SVE were stored in the memory of the SVE controller and could be displayed for 50 injections.

2.2.3 Results and discussion

In order to achieve the goals outlined in the Introduction, two major aspects were studied. Firstly, the helium flow rate and the solvent evaporation profile for large-volume injections recorded for 0.32 and 0.53 mm I.D. retention gaps were compared. Next, the usefulness of monitoring the helium flow to achieve automated closure of the SVE was studied and the results compared with those of conventional procedures.

Helium flow rate profile and solvent evaporation profile for large-volume injections

Injection of ethyl acetate into a retention gap was studied by monitoring the helium flow into the on-column injector of the GC with a flow meter, while the solvent vapour leaving the retention gap was monitored with an FID. This type of injection resembles a large-volume injection with the SVE open and in the absence of a retaining precolumn. For the study of the helium profiles (Figures 1 and 2, and data of Tables 1 and 2), the injection syringe remained in the injector during solvent evaporation after the injection had been completed. Injections were done with the Harvard pump.

The influence of parameters such as the internal diameter of the retention gap, injection speed and head pressure on the helium flow rate profile and the profile of the solvent peak were studied. The main focus was on the use of the helium flow rate profile to detect the start and end of the evaporation process.

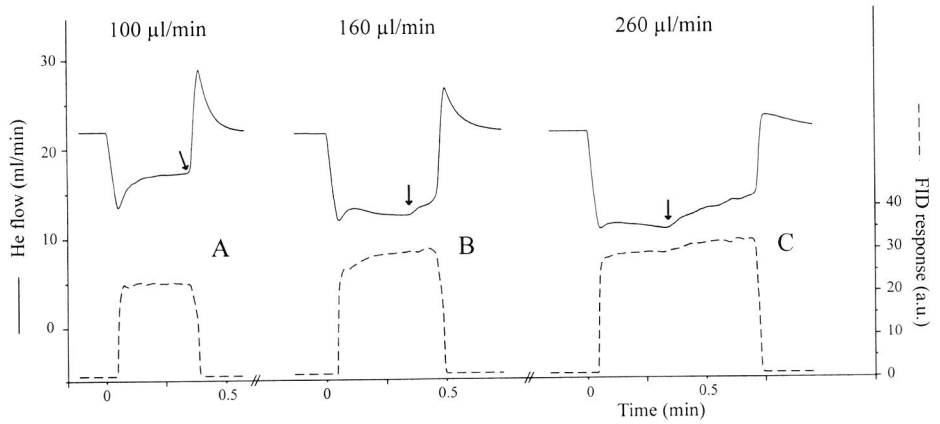

Figure 2
Helium flow rate profile (full-drawn lines) and solvent peak profiles (broken lines) for injections of ethyl acetate into a 0.53 mm I.D. retention gap. Injection time, 20 sec; injection speed: (A) 100 µl/min, (B) 160 µl/min and (C) 260 µl/min. As the evaporation rate was determined to be 130 µl/min, with the latter two injections 10 µl and 43 µl were estimated to be left as solvent film in the retention gap, respectively (calculated as described in footnote [b] of Table 1). The syringe was not removed from the injector after the injection. The end of the injection is indicated by an arrow.

Diameter of retention gap

Injections of 0.33 min into a 4 m x 0.53 mm I.D. retention gap were carried out at a head pressure of 46 kPa. Using the set-up described (see Experimental), a helium flow rate of 21.9 ml/min was obtained.

For all injection speeds studied, the helium flow decreased rapidly at the very moment that solvent entered the retention gap. The helium flow rate profiles in the top part of **Figure 2** show several typical examples, which were recorded under different conditions. When injecting at a speed below the evaporation rate, e.g. 100 µl/min, the helium flow sharply increased at the end of the injection (Figure 2A, full-drawn line). As was to be expected, when injecting at a speed above the evaporation rate, e.g. 160 or 260 µl/min (Figures 2B and 2C; full-drawn lines), the helium flow rate increase was delayed: it sharply increased 0.12 min or 0.55 min after the end of the injection (the arrows in Figure 2 indicate completion of the injection), respectively, because the residual 10 or 43 µl of solvent film left in the retention gap at the end of the injection had to evaporate.

The solvent peak which was recorded simultaneously by the FID began to show up 0.05 min after the start of an injection (Figure 2, broken lines) because of the delay due to the transport of the solvent vapour from the point of injection through the retention gap and restriction to the FID. The solvent peak decreased abruptly 0.01–0.03 min after the increase of the helium flow at the end of the evaporation process. This delay is shorter than that at the start of the injection because, at the end of the evaporation process, evaporation occurs further down in the retention gap than at the start of an injection. Consequently, the width of the solvent peak recorded by the FID is somewhat shorter than the signal recorded by the helium flow meter. The more solvent is left in the retention gap at the end of the injection, the further does the solvent film extend into the retention gap, and the shorter will be the second delay time (since the small difference cannot easily be seen from Figure 2, see especially discussion of Table 1 below).

Next, injections of 0.33 min were carried out into a smaller-bore, i.e. a 5.1 m x 0.32 mm I.D. retention gap (connected to a 0.9 m x 0.32 mm I.D. capillary) at a head pressure of 63 kPa. With the injection needle inserted, a helium flow rate of 6.5 ml/min was obtained.

The helium flow rate profiles in the top part of **Figure 3** show sharp decreases and increases in the helium flow at the start and end of the evaporation process, respectively; these are comparable to those of Figure 2. In the present example, about 12 µl and 39 µl were left in the retention gap at the end of the injection, and the helium flow started to increase with a delay of 0.30 min (Figure 3A) and 0.60 min (Figure 3B), respectively. The solvent peak recorded by the FID again started to show up 0.05 min after the decrease of the helium flow. However, different from the injections into a 0.53 mm I.D. retention gap, the helium flow rate changed significantly during the injection and evaporation process. The large increase of the helium flow after the injection had been completed was especially remarkable (cf. Figure 3B, arrow indicates completion of injection). It will be discussed in more detail in the *Discussion* section below.

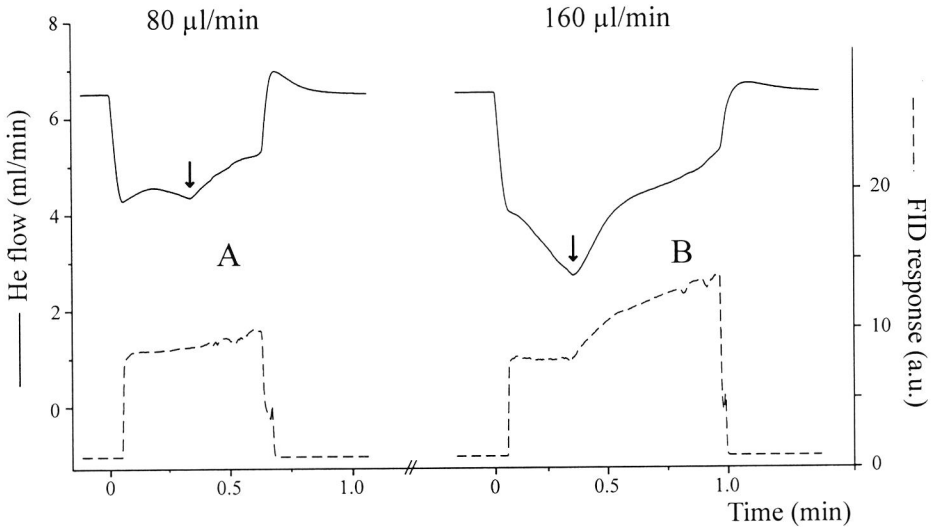

Figure 3
Helium flow rate profile (full-drawn lines) and solvent peak profiles (broken lines) for injections of ethyl acetate into a 0.32 mm I.D. retention gap. Injection time, 20 sec; injection speed: (A) 80 µl/min and (B) 160 µl/min. As the evaporation rate was determined to be 43 µl/min, 12 µl and 39 µl were estimated to be left as solvent film in the retention gap after injection, respectively. The syringe was not removed after injection. The end of the injection is indicated by an arrow.

Injection speed

In order to check if the evaporation rate was independent of the position of the solvent film in the retention gap, two 36-µl injections were carried out at 180 and 360 µl/min into a 0.53 mm I.D. retention gap, so that 10 µl or 23 µl of solvent were left in the retention gap at the end of the injection (**Table 1**). The evaporation as indicated by the helium flow rate profile took 0.48 and 0.49 min. In other words, the evaporation rate depended only slightly on the position and length of the solvent film in the 0.53 mm I.D. retention gap. However, for the same two injections the solvent peak widths recorded by the FID showed a somewhat larger increase, viz. from 0.50 min to 0.52 min. As explained above, this is due to the fact that the farther down the last portion of solvent is in the retention gap at the end of the evaporation process, the shorter the hold-up time to the FID will be. This suggests that monitoring the injection by means of the helium flow will be more precise than with an FID, because the helium flow will start to increase immediately after the evaporation process is completed, irrespective of the position of the last drop of solvent in the retention gap.

The situation was, however, rather different for injections into a 0.32 mm I.D. retention gap. When varying the injection speed of the 36-µl injections causing from 6 to 32 µl of solvent to be left in the retention gap after injection, the duration of the evaporation as monitored by means of the helium flow changed significantly, i.e. from 0.68 min to 0.84 min and, if monitored with the FID, even more, i.e. from 0.59 min to 0.82 min (Table 1). The results suggest that for injections into the 0.32 mm I.D. retention gap the evaporation rate depends rather strongly on the position and/or the thickness of the solvent film.

Table 1
Characteristics of solvent evaporation for 36-µl injections into a 0.53 and 0.32 mm I.D. retention gap using different injection speeds [a].

Retention gap	Injection speed (µl/min)	Solvent film in RG [b] (µl)	Evaporation time (min)	
			He flow	FID [c]
0.53 mm I.D.	360	23	0.48 ± 0.01	0.50 ± 0.01
	180	10	0.49 ± 0.01	0.52 ± 0.01
0.32 mm I.D.	360	32	0.68 ± 0.02	0.59 ± 0.02
	180	27	0.76 ± 0.02	0.71 ± 0.02
	60	6	0.84 ± 0.02	0.82 ± 0.02

[a] Set-up and head pressure same as for injections shown in Figs. 2 and 3; syringe left in injector after injection.
[b] Estimated amount of solvent left in retention gap (RG) at end of injection, V_s, calculated from: $V_s=(\upsilon_{inj}-\upsilon_{evap})*t_{inj}$ with υ_{inj}, injection speed; t_{inj}, injection time, υ_{evap}, evaporation rate (determined from repetitive injections of pure solvent at increasing injection speed [10]).
[c] Solvent peak width at half maximum.

Discussion

The above observations can be explained by taking into account the dependence of the helium flow, F_{He}, on the following three parameters: (i) the ratio of the partial pressures of helium and the solvent used, (ii) the viscosity of the gas mixture, and (iii) the flow resistance of the system. The helium flow through a small segment of the retention gap is according to [12]:

$$F_{He} = y_{He}(600\ \pi\ r^4 / 16\ \eta_m\ L)\ [(p_i^2 - p_o^2) / p_o]\ [p_o / p_{ref}]\ [T_{ref} / T] \qquad (I)$$

with: F_{He}, flow rate of helium, ml/min; y_{He}, mole fraction of helium; r, internal radius of retention gap, cm; η_m, viscosity of the helium and solvent gas mixture calculated according to Wilke's approximation, Poise [11, 12]; L, length of segment of retention gap, cm; p_i and p_o, pressures at beginning and end of a small segment of the retention gap, Pa; p_{ref}, reference pressure, 1.013 x 10^5 Pa; T, column temperature, K; T_{ref}, reference temperature, 298.15 K. Ideal gas behaviour of the solvent vapour and saturation of the gas phase with solvent vapour are assumed. A possible decrease of the retention gap temperature due to the evaporating solvent was not taken into account. Because the molar fraction, the viscosity and the solvent film thickness may vary along the length of the retention gap (see discussion below), Equation I is only valid for an infinitesimally small part of the retention gap, and we therefore had to calculate the helium flow iteratively. In addition, the pressure drop due to the insertion of the injection needle had to be taken into account.

At the start of the injection, the mole fraction of helium and the viscosity of the gas mixture start to change. The mole fraction of helium starts to decrease, and the viscosity of the mixture of helium and solvent vapour will become lower than that of pure helium, because the viscosity of the solvent vapour, i.e. ethyl acetate or hexane, is significantly lower than that of helium. Equation I reveals that in most cases the helium flow will be lower during the injection and evaporation process than prior to the injection. [An increase of the

helium flow will occur only if a solvent with a very low-viscosity vapour is slowly introduced at a temperature much below the boiling point.] The helium and solvent vapour flows are also reduced by the increase of the restriction of the retention gap caused by the presence of the solvent film. To give an example, for the injection of ethyl acetate into a 0.53 mm I.D. retention gap, a flooded zone of 5.6 cm/µl has been found [13], which corresponds with an average film thickness of about 11 µm. According to Equation I, a decrease of the internal diameter of a segment of the retention gap by 22 µm at the same pressure difference would result in a decrease of the flow by 15% for a retention gap of 0.53 mm I.D. and 25% for one of 0.32 mm I.D.

When injecting at a speed below the evaporation rate, after the initial change of the mole fraction of helium and of the viscosity of the helium and solvent gas mixture at the start of the injection, both will not change significantly during injection any more, because no solvent film of significant length is created in the retention gap. Therefore, the helium flow rate and, also, the height of the solvent peak will be essentially constant during injection (Figure 2A). However, we invariably observed a noticeable dip of the helium flow rate at the very beginning of the injection, and a rapid increase occurred at the end of the evaporation before the flow returned to its initial value. These dips and peaks of varying intensity (cf. Figures 2C and 3A) are probably connected with the rapid change of the contents of the retention gap, which occurs when part of the helium is suddenly replaced by solvent vapour, or vice versa, and the viscosity suddenly changes dramatically.

If the injection speed is above the evaporation rate, the mole fraction of helium, the viscosity of the gas mixture, and the restriction caused by the solvent film, keep changing during injection and evaporation, which further complicates matters and causes the rather complex helium flow rate and solvent peak profiles of Figures 2B and C and Figure 3. In that part of the retention gap in which there is a solvent film, the partial pressure of the solvent, i.e. the solvent vapour pressure, remains constant (**Figure 4**, trace B), and the ratio (partial helium pressure/partial solvent pressure) (Figure 4, trace C) will decrease due to the total pressure drop along the retention gap (Figure 4, trace A). Consequently, the viscosity will also change in that part of the retention gap. However, from the front of the solvent film to the SVE, the ratio (partial helium pressure/partial solvent pressure) does not change any more (Figure 4, trace C) and the viscosity will therefore remain constant.

For an injection speed higher than the evaporation rate, a further increase will cause the solvent film at the injection point to become thicker and to reach farther into the retention gap. During the injection, the helium flow will continue to decrease as the film reaches farther into the retention gap, and this decrease will be larger for higher injection speeds. To quote a few examples, Equation I predicts that for the 80-µl/min injection of Figure 3A into a 0.32 mm I.D. retention gap the helium flow will decrease from 6.8 ml/min to 4.7 ml/min at the start of the injection (decrease from 6.5 to 4.8 ml/min experimentally measured) and to 4.2 ml/min at the end of the injection (4.4 ml/min measured) (**Table 2**). For the 160-µl/min of Figure 3B, a decrease to 3.1 ml/min at the end of the injection is predicted (2.7 ml/min measured). After the injection, the solvent film is pushed farther into the retention gap [13, 15] and it can be assumed that its thickness becomes more uniform and, of course, also starts to decrease. The solvent evaporates mainly from the rear end till just prior to the end of the evaporation only a short thin film of solvent is left. Both effects result in an increase of the helium flow (cf. Equation I). As an example, just prior to the end of the evaporation of the

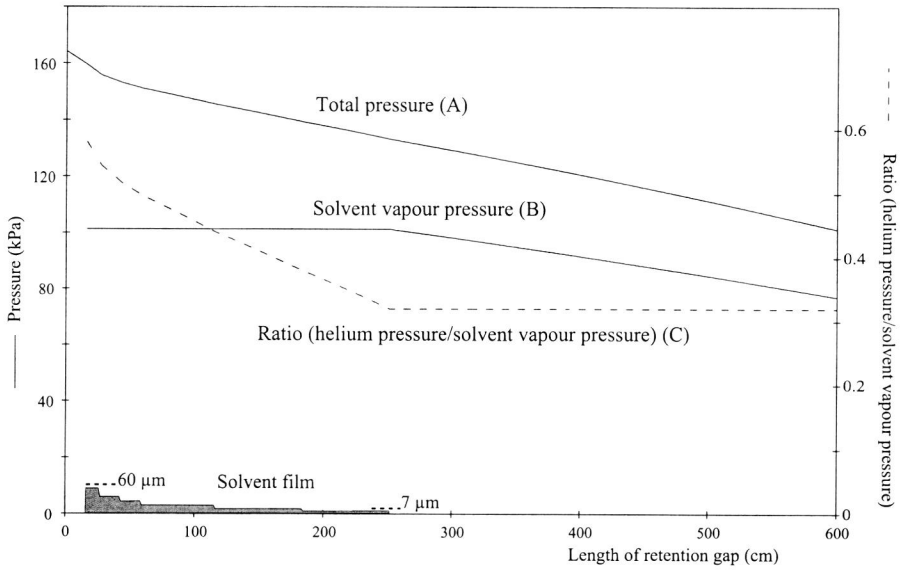

Figure 4

Theoretical profile of (A) the total pressure, (B) the partial solvent pressure and (C) the ratio (partial helium pressure/partial solvent pressure) in the retention gap at the end of the 160-µl/min injection of Figure 3B. The profiles were (iteratively) calculated by means of Equation I using the solvent film distribution as shown. For more details, see text and footnotes of Table 2.

160-µl/min injection of Figure 3B, the helium flow rate is predicted to be 5.2 ml/min (5.3 ml/min measured). Table 2 provides more details concerning these calculations.

For injections into the 0.53 mm I.D. retention gap (cf. Figure 2), Equation I predicts the change of the helium flow between the sharp decrease at the start of the injection and the sharp increase at the end of the evaporation to be less than for the 0.32 mm I.D. retention gap. To quote an example, the helium flow of the 260-µl/min injection of Figure 2C was calculated to decrease at the start of the injection from 22.4 ml/min to 13.2 ml/min (decrease from 21.9 ml/min to 11.9 ml/min measured). The flow at the end of the injection was calculated to be 11.8 ml/min (10.9 ml/min measured), and that just prior to the end of the evaporation to be 13.9 ml/min (14.6 ml/min measured).

The predicted and experimentally measured helium flow rates agree rather satisfactorily, and the up to 15% differences can be primarily attributed to the approximations briefly mentioned above when introducing Equation I (also see footnotes to Table 2).

In other words, the calculated values predict the changes of the helium flow rate during the injection rather well, notably the sharp decrease at the start of the injection, the slower changes during the injection and evaporation process and the final sharp increase when evaporation is complete. The fact that the change of the helium flow rate during injection and evaporation is smaller for a 0.53 mm I.D. than a 0.32 mm I.D. retention gap is also correctly predicted.

Table 2
Calculation of helium flow rates at various moments during injections into a 0.32 mm I.D. (cf. Figure 3) or a 0.53 mm I.D. (cf. Figure 2) retention gap [a].

Retention gap (mm I.D)	Situation	He flow (ml/min)	
		Calculated	Measured
0.32	Prior to injection [b]	6.8	6.5
	80 µl/min (Fig. 3A)		
	Start of inj.	4.7	4.8 [c]
	End of inj.	4.2	4.4
	End of evap.	4.8	5.2
	160 µl/min (Fig. 3B)		
	Start of inj.	4.5	4.1 [c]
	End of inj.	3.1	2.7
	End of evap.	5.2	5.3
	After end of evap. [b]	6.8	6.5
0.53	Prior to injection [b]	22.4	21.9
	160 µl/min (Fig. 2B)		
	Start of inj.	13.4	14.1 [c]
	End of inj.	13.1	12.6
	End of evap.	13.4	14.3
	260 µl/min (Fig. 2C)		
	Start of inj.	13.2	11.9 [c]
	End of inj.	11.8	10.9
	End of evap.	13.9	14.6
	After end of evap. [b]	22.4	21.9

[a] Helium flow calculated by means of Equation I. Solvent film thickness distributions used for calculations were estimated, as no exact experimental data were available. Position of last portion of solvent just prior to end of evaporation was calculated by multiplying amount of solvent left in retention gap at end of injection (cf. Table 1, footnote b) with flooded zone (expressed in cm/µl; 5.6 and 9.3 cm/µl for 0.53 and 0.32 mm I.D. retention gaps, respectively), assuming a constant flooded zone. Front of solvent film at end of injection was assumed to be at 70% of distance into retention gap of position of last portion of solvent just prior to end of evaporation (cf. above; comparable data found in [15]). As an example, estimated solvent film thickness distribution at end of injection of Figure 3B is given in Figure 4. Solvent film thickness distributions for other injections were obtained in a similar way as that of Figure 3B; data available from the authors upon request.

[b] 15 cm of 0.25 mm O.D. needle of syringe inserted into retention gap.

[c] Negative peak at start of injection is ignored.

As with the helium flow rate, the evaporation rate of the solvent depends on the ratio (partial helium pressure/partial solvent pressure), the viscosity of the gas mixture and the restriction caused by the solvent film in the retention gap. As these parameters keep changing during injection and evaporation if injection is done at a speed above the evaporation rate, the evaporation rate depends on the injection speed and the amount of solvent injected. As demonstrated for the helium flow rate, Equation I predicts this dependence to be larger for injections into a 0.32 mm I.D. than into a 0.53 mm I.D. retention gap. The larger variation of

the evaporation rate with the injection speed for injections into a 0.32 mm I.D. was confirmed by the experiments of Table 1. This aspect will be discussed in more detail in Chapter 2.3.

Automated closure of the SVE

Since it was our intention to use the sharp increase of the flow rate at the end of the evaporation process for the automated closure of the SVE, we compared the loss of volatiles occurring when (i) closing the SVE on the basis of the helium flow rate profile and (ii) using a pre-set closure time at which not all solvent had evaporated as yet. A retention gap of 0.53 mm I.D. was preferred over one with 0.32 mm I.D., because the helium flow rate profile then is simpler and the completion of the evaporation process, consequently, can be detected more easily.

Figure 5 shows that using the first derivative of the helium flow rate profile (trace A) is a simpler alternative than using the profile itself (trace B) for the (automated) indication of the end of the evaporation process because of the better stability of the signal during evaporation, and the shaper final increase. In a first experiment the SVE was manually closed at the end of the evaporation process as indicated by the helium flow rate profile. Since a comparison of

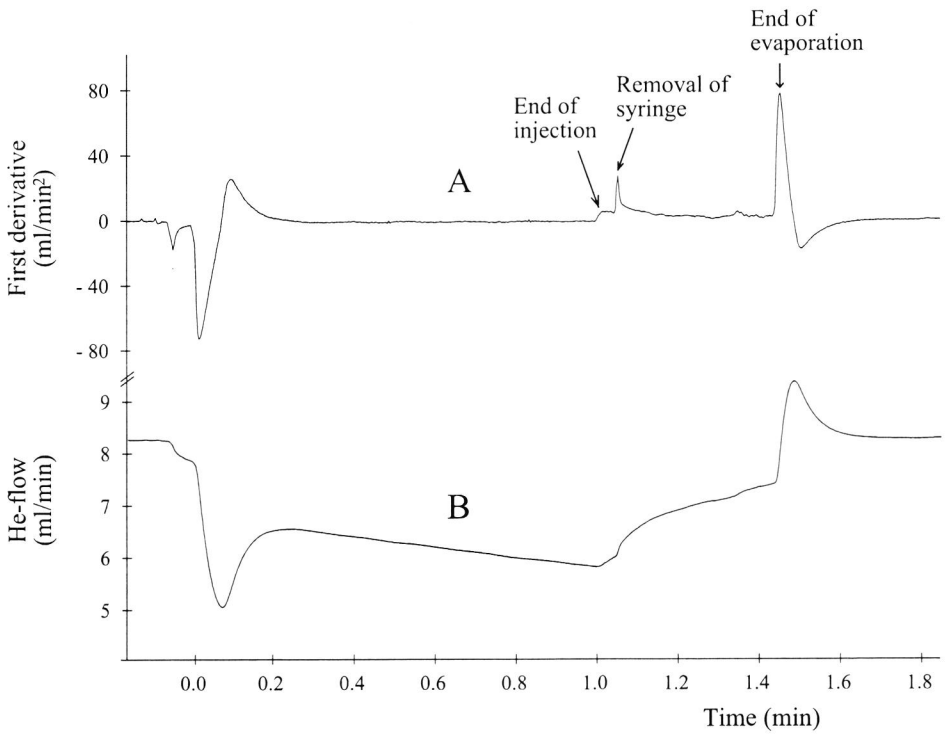

Figure 5
Helium flow rate profile (B) and its first derivative (A) for a 60-µl injection of *n*-hexane in a 6 m x 0.32 mm retention gap connected to a 1.5 m x 0.32 mm retaining precolumn. Injection started at 0 min, needle inserted into injector 0.05 min before start of injection, and removed 0.05 min after end of injection; SVE left open all the time.

Table 3

Recoveries and repeatability of peak areas of several *n*-alkanes for 30-µl injections in *n*-hexane using automated closure of the SVE.

Compound	Recovery [a] (%)	RSD (%, n = 42)
C_8	99	3.2
C_9	98	2.9
C_{10}	101	3.1
C_{11}	100	4.1
C_{15}	99	3.4
C_{17}	99	4.3
C_{18}	98	0.9
C_{19}	100	0.8
C_{20}	98	1.0

[a] The recoveries were calculated by using as a reference a 30-µl injection with which the SVE was closed by the GC programme rather than the SVE controller 0.1 min prior to completion of the evaporation process. For further details, see text.

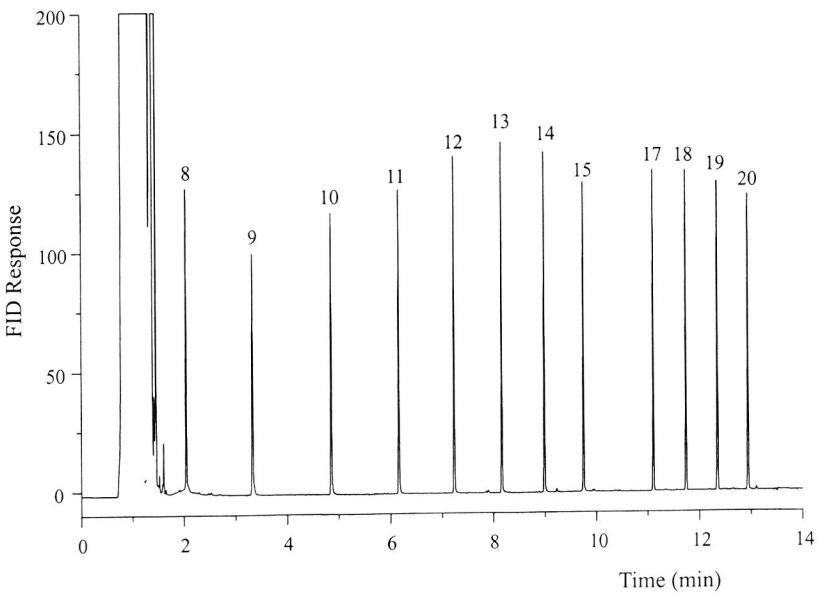

Figure 6

GC–FID chromatogram of a 30-µl injection of *n*-alkanes in *n*-hexane. The closure of the SVE was automated by means of a laboratory-made microprocessor-based controller. For more details, see text.

the results obtained for injections of *n*-alkanes (C_8–C_{20}) in ethyl acetate made under these conditions and of injections made when the SVE was closed 0.05–0.1 min prior to completion of the evaporation process did not indicate any loss of even C_9 or C_{10}, a microprocessor-based controller was built to monitor the flow to automate the closure of the SVE.

The SVE was (automatically) closed when the first derivative exceeded a pre-set threshold value; the influence of the choice of this threshold value was studied using 30-µl injections of *n*-alkanes in ethyl acetate at 120 µl/min and threshold values from 10 to 80 ml/min^2 [the evaporation rate was found to be 47 µl/min]. This resulted in a closure of the SVE 0.01–0.02 min (for 10–50 ml/min^2) or 0.04 min (for 80 ml/min^2) after evaporation was completed, i.e. after the helium flow started to increase. In all cases, the recoveries of the relatively volatile C_8–C_{11} *n*-alkanes were between 94 and 98% compared with a 30-µl injection with which the SVE was closed 0.07 min before evaporation was complete. Not unexpectedly, when the SVE was closed 0.15 min too late, the volatile *n*-alkanes up to C_{14} were completely lost. As a compromise between too early closure and late closure (or no closure at all), a threshold value of 30 ml/min^2 was selected for further work. Monitoring of the first derivative was started 0.05 min after withdrawal of the syringe, because the helium flow by then was stable again after the peak caused by the withdrawal of the syringe (cf. Figure 5, trace B). It should be mentioned that, when starting monitoring of the flow only with a delay after the end of injection, some solvent has still to be left in the retention gap at the moment monitoring of the helium flow is started. With other words, the injection speed has to be higher than the evaporation rate to allow automated closure. However, when monitoring is started immediately at the end of the injection, i.e. without a delay, automated closure also occurs when the injection speed is equal to or slightly below the evaporation rate. In the latter case, the needle should be withdrawn with a certain delay after completion of the injection to assure that solvent evaporation is complete when withdrawing the needle.

The reliability of the automated SVE closure was tested by performing 42 30-µl injections of a standard solution of *n*-alkanes in *n*-hexane by means of the GC autosampler. All *n*-alkanes from *n*-octane on showed up in the GC–FID chromatogram (**Figure 6**). Comparison with an injection with which the SVE was closed 0.05 min before the end of the evaporation showed that they were quantitatively recovered (recoveries, 98–101%; cf. **Table 3**). The relative standard deviation (RSD) of the SVE closure time was 0.09% at an average SVE closure time of 0.48 min, and the RSD values of the peak areas were quite good (1–4.5%, cf. Table 3) and comparable to those obtained with a pre-set SVE closure time. One should add that, even if the injection or evaporation process would show a poorer precision than in the present instance, the SVE controller will still close the SVE just at the end of the evaporation process. This will cause the retention times to remain constant and no loss of volatiles will occur, whereas with closure at a pre-programmed time, retention times may well shift and/or volatile analytes may be lost.

During over 300 injections, no automated closure was ever observed which occurred too early due to changes of the helium flow during evaporation of the solvent.

2.2.4 Conclusions

Monitoring of the helium carrier gas flow allows the (automated) control of large-volume on-column injections. The end of the evaporation process can be detected (as a sharp helium flow increase) without any delay due to a hold-up time. Actually, for nearly all large-volume injections into 0.32 or 0.53 mm I.D. retention gaps, the helium flow will sharply decrease at the start of the injection and sharply increase when evaporation is complete. This is especially true for a 0.53 mm I.D. retention gap which was therefore selected for use in the automated SVE closure set-up. Pre-optimization or calculation of a fixed time for the SVE closure now is superfluous. In addition, even when the evaporation time slightly changes due to, e.g., small changes of the injection speed or injection volume, the SVE will be closed just in time without undue loss of volatiles or a significant change of the solvent peak width at the detector. The latter aspect is important when working with a mass-selective detector, because the delay time for switching-on the filament can now be kept constant.

Implementation of (automated) helium flow monitoring is an important step towards a self-optimizing large-volume on-column injection system. A self-optimizing system is to be preferred to a system in which all parameters are pre-optimized (or calculated), because the latter is rather vulnerable if small changes in the experimental conditions or set-up occur.

References

[1] Th. Hankemeier, H.T.C. van der Laan, J.J. Vreuls, M.J. Vredenbregt, T. Visser and U.A.Th. Brinkman, *J.Chromatogr. A*, 732 (1996) 75.
[2] F.D. Rinkema, A.J.H. Louter and U.A.Th. Brinkman, *J. Chromatogr. A*, 678 (1994) 289.
[3] H.-J. Stan and M. Linkerhägner, *J. Chromatogr. A*, 727 (1996) 275.
[4] S. Ramalho, Th. Hankemeier, M. de Jong, U.A.Th. Brinkman and J.J. Vreuls, *J. Microcol. Sep.*, 7 (1995) 383.
[5] F. Munari, P.A. Colombo, P. Magni, G. Zilioli, S. Trestianu and K. Grob, *J. Microcol. Sep.*, 7 (1995) 403.
[6] A. Venema and J.T. Jelink, *J. High Resolut. Chromatogr.*, 19 (1996) 234.
[7] H.G.J. Mol, H.-G. Janssen, C.A. Cramers and U.A.Th. Brinkman, *J. High Resolut. Chromatogr.*, 18 (1995) 19.
[8] H.G.J. Mol, H.-G. Janssen, C.A. Cramers and U.A.Th. Brinkman, *Trends Anal. Chem.*, 15 (1996) 206.
[9] K. Grob, H.-G. Schmarr and A. Mosandl, *J. High Resolut. Chromatogr.*, 12 (1989) 375.
[10] K. Grob, in W. Bertsch, W.G. Jennings and P. Sandra (eds.), *On-line coupled LC–GC*, Hüthig, Heidelberg, 1991, p. 127.
[11] J. Staniewski and K. Alejski, poster presented at *18th Intern. Symp. Cap. Chromatogr 1996, Riva del Garda.*
[12] R.C. Reid, J.M. Prausnitz and Th.K. Sherwood, *The Properties of Gases and Liquids*, 3rd ed., McGraw-Hill, New York, N.Y., 1977.
[13] Th. Hankemeier, S.J. Kok, J.J. Vreuls and U.A.Th. Brinkman, *J. Chromatogr. A*, 841 (1999) 75.
[14] K. Grob, Jr., G. Karrer and M.-L. Riekkola, *J. Chromatogr.*, 334 (1985) 129.
[15] Appendix of Chapter 2.2 of this thesis.

Appendix: Use of a flooding detector

Introduction

The aim of this study was to investigate whether the injection of large-volume on-column injections using PCSE can be optimized by injections of pure solvent, or even during the actual injection itself. The idea was to construct a *flooding detector* to monitor the length of the solvent film formed during the injection, i.e. to prevent that the solvent film reaches the retaining precolumn. The flooding detector should detect the presence of the solvent film at a certain position, i.e. at a quartz press-fit inserted between two parts of the retention gap, by observing the scattering of the light of a diode laser with a photodiode. Until now, visualization of (the movement of) the solvent film is possible only by using etched glass [1]. Admittedly, flooding of the retaining precolumn by the solvent film can be detected by disturbed peaks in a GC chromatogram, but injection of standards rather than of pure solvent is then required. A second goal was to study the movement of the solvent film during injection in order to better understand large-volume on-column injections.

Experimental

The same set-up and conditions were used as in Chapter 3.1. The only difference was that two pieces of 3 m and 2.5 m long retention gap of 0.32 mm I.D. (DPTMDS deactivated; BGB Analytik, Zürich, Switzerland) were used rather than a single retention gap. A modified press-fit was inserted between both retention gaps. The press-fit was made from quartz, and was somewhat 'blown up' in the middle. The press-fit was placed in a light metal holder, and two light fibres (one coming from a diode laser, one going to a photodiode) were positioned and fixed by means of fingertights onto the holder such that they were perpendicular to the press-fit, and that a large proportion of the laser light was sent to the photodiode. The laser light from the diode laser (10 mW, 670 nm, Model ROLD9215, Toshiba, Tokyo, Japan) was coupled into the light fibre by means of a home-made box outside of the GC oven. The laser light was detected with a BPW34 silicon photodiode (Siemens, München, Germany) outside of the GC oven and, after amplifying with a home-made amplifier, visualized on a recorder (Kipp & Zonen, Delft, The Netherlands, Model BD101).

Results and discussion

Design of flooding detector

The flooding detector consisted of a laser diode (670 nm), a photodiode as detector and a press-fit, which was part of the column system within the GC oven, as optical cell. The light from the laser diode was transferred through a light fibre to the press-fit, and after passing the press-fit, part of the light entered the light fibre to the detector. If solvent vapour or a solvent film was present in the press-fit, a deflection of the light beam occurred and a different amount of light entered the light fibre to the detector. The light fibres were surrounded by metal tubing to reduce disturbances caused by vibrations of the fibre.

Figure 1 shows the change of the signal typically observed when solvent vapour or the solvent film enters the press-fit. Obviously, the presence of a solvent film can clearly be

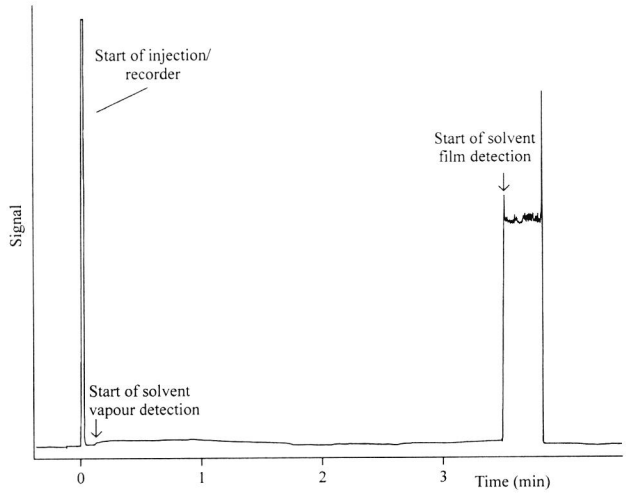

Figure 1
Signal of flooding detector for 35-µl/min injection (injection time 176 sec; head pressure, 95 kPa; flow through SVE, 7.9 ml/min; v_{evap}, ca. 27 µl/min); arrows indicate start of detection of solvent vapour and solvent film.

detected, but unambiguous detection of vapour is not really possible. This actually is an advantage for the purpose we had in mind. Changing the positions of the light fibres or using an UV lamp as light source (up to 400 nm, the upper limit for the light fibre) did not improve performance.

Movement of solvent film
With the flooding detector inserted between the two retention gaps, methyl acetate was injected into the retention gap at an injection speed of 60 µl/min, and for varying injection times (head pressure, 95 kPa; flow through SVE, 12 ml/min; v_{evap}, ca. 39 µl/min). With an injection time of 70 sec, the solvent film did not reach the flooding detector at all, while for an injection time of 75 sec the solvent film reached the flooding detector after 108 sec. When increasing the injection time to 80, 90 or 110 sec, the solvent film reached the flooding detector also after 108 sec. Obviously, the movement of the solvent film is essentially the same for injections with injections times of 75–110 sec. If one assumes a constant movement of the solvent film (which is probably a simplification, but may be used as an approximation), the front end of the solvent film can be calculated to move into the retention gap over a considerable distance of up to ca. 40% of the total length of the film at the end of the injection [((110–75)/75) x 100%]. On the other hand, when the injection is terminated just when the solvent film reaches the flooding detector (i.e. 3 m after the point of injection), the solvent film does not reach the retaining precolumn (at a distance of 2.4 m from the flooding detector), as could be seen from the undisturbed peaks of *n*-alkanes in the GC–MS chromatogram. In other words, the front end of the solvent film does not move more than 80% [(2.4/3) x 100%] further into the retention gap after completion of the injection. It should be mentioned that, of course, many parameters like, e.g., the evaporation rate, gas flow, solvent type and temperature, influence the extent of the movement of the solvent film.

Conclusion

The flooding detector can be used to detect the presence of a solvent film at a pre-selected position in the retention gap, without giving a disturbing signal caused by solvent vapour. The experimental results show that after the injection and until evaporation is complete, the solvent film moves over a considerable distance. Consequently, it is not possible to adjust the injection speed *during* a large-volume on-column injection to prevent flooding of the retaining precolumn. Even if the injection speed is reduced when the solvent film reaches the flooding detector, the solvent film will keep moving. Actually, from the data obtained, an estimation can be made of the distance travelled by the solvent film after completion of the injection.

The installation of the flooding detector, and especially the coupling of the light from the press-fit into the fibre to the photodiode, requires some experience. On the other hand, optimization of the injection conditions by means of a helium flow controller has meanwhile been shown to be straightforward (Chapter 2.3). The use of a flooding detector for optimization of the injection conditions has therefore been discontinued. For a recent alternative solution based on the use of a thermocouple positioned on the outer wall of the retention gap to detect solvent recondensation and evaporation, the reader is referred to refs. [2] and [3]. With the latter set-up, only the passage rather than the presence of a solvent film can be detected.

References

[1] K. Grob, in W. Bertsch, W.G. Jennings and P. Sandra (eds.), *On-column Injection in Capillary Gas Chromatography*, Hüthig, Heidelberg, 1987, p. 12.

[2] T. Hyötyläinen, K. Grob and M.-L. Riekkola, *J. High Resol. Chromatogr.*, 20 (1997) 657.

[3] B. Grolimund, E. Boselli, K. Grob, R. Amadò and G. Lercker, *J. High Resol. Chromatogr.*, 21 (1998) 378.

2.3 Optimization of large-volume on-column injection conditions by monitoring the actual carrier gas flow

Summary

The change of the evaporation rate of the solvent during injection and evaporation is the most critical aspect during optimization of large-volume on-column injection conditions in gas chromatography (GC). The change is caused by the pressure drop along the retention gap when using an early solvent vapour exit (SVE) and can be described by a mathematical model.

Four procedures for the optimization of the injection conditions were compared. It was found that different procedures often yield different evaporation rates, which may also depend on the injection speeds used during optimization. For optimization of a new set-up, i.e. if little is known about the optimal injection conditions, the evaporation rate should be determined by increasing the injection time at a fixed injection speed, injection temperature and head pressure; subsequently, an appropriate injection speed can be calculated. If a mere re-optimization is required as e.g. after the exchange of the retention gap, adjusting the evaporation rate to the injection speed by varying the injection temperature at a constant injection speed is the preferred procedure. With both methods, optimization can be achieved by means of 2–5 injections of pure solvent and monitoring the helium carrier gas flow. That is, optimization of the injection conditions takes less than 1 hour. When using this strategy, analytes as volatile as monochlorobenzene can be determined in aqueous samples by in-vial liquid–liquid extraction–GC–mass spectrometry.

Closing the SVE at the very end of solvent evaporation results in a considerable increase of the capacity of the retention gap compared to closing the SVE before all solvent is evaporated.

2.3.1 Introduction

Large-volume on-column injection and aim of the study

Today, large-volume injections, i.e. the injection of volumes larger than 1–5 µl, are increasingly used in gas chromatography (GC) to improve analyte detectability (in concentration units) [1–3]. This approach also allows the use of new strategies in sample preparation [4]. To quote an example, the injection of a larger aliquot of an extract makes in-vial liquid–liquid extraction (LLE) much more attractive, because the sample volume can be decreased from 100–1000 ml to 1–10 ml [5].

On-column injection is the preferred technique for the introduction of larger volumes up to 250 µl of sample if the determination of volatile analytes is the main goal and the sample extract is not too contaminated. The solvent is injected into a retention gap, which is connected to a retaining precolumn or, directly, to the analytical column. For the on-column injection of larger volumes, two parameters have to be carefully chosen. (i) An early solvent vapour exit (SVE) is generally inserted between the retaining precolumn and the analytical column to allow faster evaporation and to protect the detector from the solvent vapour. The SVE has to be closed at an appropriate moment in time [6]. (ii) If a considerable part of the solvent evaporates during injection, so-called injection under partially concurrent solvent evaporation (PCSE) conditions [7], the injection speed has to be chosen to be larger than the evaporation rate to ensure the formation of a solvent film in the retention gap so that volatile analytes will be trapped without, however, the solvent film reaching the end of the retention gap [8].

SVE closure

Usually, the SVE is closed at a predetermined time just before the last of the solvent evaporates, in order not to loose the volatile analytes. This moment in time is usually determined by monitoring the effluent leaving the SVE by a flame or by performing a series of injections at different closure times [viz. by determining when losses of the volatile analytes start to occur] [9, 10]. Recently, we demonstrated that monitoring the helium flow into a GC by means of an electronic flow meter can be used to register the end of the evaporation process and effect the automated closure of the SVE [11]. During the injection and evaporation process the helium flow rate decreases, mainly because of the presence of solvent vapour in the gas phase, and the completion of the evaporation process is indicated by a steep increase of the helium flow to its original value. Our approach makes optimization of a fixed point in time for the SVE closure superfluous. The system also becomes more robust: even when the evaporation time varies due to small changes of the injection speed or volume, closure of the SVE occurs just in time without loss of volatiles or a significant change of the solvent peak width in the detector.

Procedures for optimization of injection speed

There are two types of strategies to find the appropriate PCSE on-column injection conditions, viz. by means of injections of standard solutions of, e.g., *n*-alkanes or pure solvent. With the former approach, the injection speed is stepwise increased until solvent trapping causes reconcentration of the volatile analytes [10]. The set-up does not have to be changed, but the optimization procedure can take up to one day, even for an experienced

analyst. We therefore focused on strategies which use injections of pure solvent and determination of the evaporation time to reduce the time required for optimization.

With all of the proposed methods (which are described in *Procedures for optimization of injection speed*, below), the evaporation time can be determined from the solvent peak width registered with an FID (modification of the set-up required) or a flame or, more precisely (cf. [11]), by the (automated) monitoring of the helium flow. It is, also, tacitly assumed that the evaporation rate is independent of the injection speed. However, recently we demonstrated that this is not true. The dependence of the evaporation rate on the injection speed could be attributed to a pressure drop along the length of the retention gap and the restriction of the gas flow by the formation of a solvent film within the retention gap [11]. Recently, this phenomenon was also reported by Grob *et al.* [12]. This makes evaporation rates as were calculated by Staniewski and Alejski [13], who did not consider the influence of the solvent film, somewhat unreliable.

Aim of the study

In the present paper, critical aspects of the optimization of the conditions for large-volume on-column injection are discussed. Monitoring of the helium carrier gas flow was used to study the influence of the moment of SVE closure on the length of the flooded zone and the role of inserting and withdrawing the injection needle on the evaporation rate. A mathematical model was developed to help interpret the change of the evaporation rate during injection and to study the influence of this phenomenon on the determination of the evaporation rate by means of various methods. The aim was to find an efficient strategy for the optimization of the injection conditions by (automated) monitoring of the carrier gas flow. The practicality of the new approach was demonstrated by the determination of volatile microcontaminants in water by in-vial LLE–GC–MS.

Procedures for optimization of injection speed

Three procedures are based on the determination of the evaporation rate and subsequent calculation of an appropriate injection speed (Methods A1, A2 and B, see below). When the evaporation rate, v_{evap} (µl/min), the length of the retention gap, L_{RG} (cm), and the flooded zone, FZ (cm/µl), are known, one can calculate the injection speed, v_{inj} (µl/min) at which a certain length of the solvent film in the retention gap (expressed as the fraction, f, of the total length of the retention gap) for a given sample volume, V_{inj} (µl), is obtained, from (cf. [9, 14]):

$$v_{inj} = \frac{v_{evap}}{1 - \frac{f \times L_{RG}}{V_{inj} \times FZ}} \qquad \text{(I)}$$

Method A

One option is to determine the evaporation rate by increasing the injection speed at a constant injection time and head pressure, and plotting the evaporation time *vs.* the injection volume. As is depicted in **Figure 1** below, the evaporation rate then equals the injection speed at the point of intersection of the two parts of the plot (Method A1). Alternatively, the evaporation rate can be calculated from the slope of the high-injection speed part of the same plot,

because it is equal to the inverse of that slope expressed as (Δ evaporation time/Δ injection volume) [9, p. 255] (Method A2).

Method B

As an alternative, the evaporation rate can be calculated from the slope of a plot of evaporation time *vs.* injection time, recorded at constant injection speed, where the evaporation rate again equals the inverse of the slope expressed as (Δ evaporation time/Δ injection volume). Obviously, the evaporation time has to be longer than the injection time, as otherwise injections will be made under fully concurrent evaporation conditions and no significant amount of solvent will be left in the retention gap during injection.

Method C

If only slight changes of the set-up have to be made – that is, if the optimal injection conditions are rather well known – a simpler strategy can be used. In this case, the evaporation rate is varied by changing the injection temperature at a fixed injection speed and head pressure to adjust the evaporation rate to the injection speed. The injection temperature

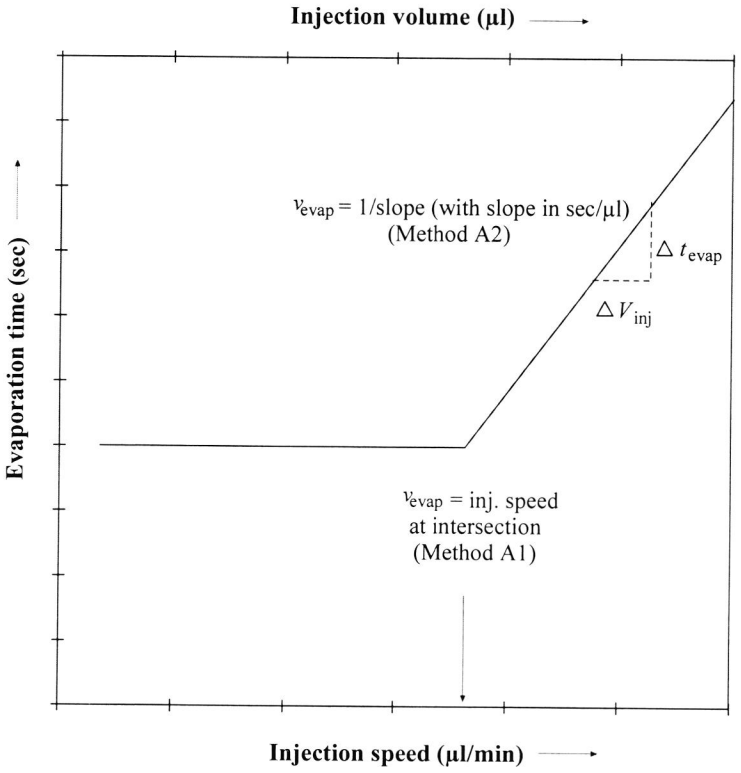

Figure 1

Theoretical plot of evaporation time (t_{evap}) *vs.* injection speed and volume (V_{inj}) at a constant injection time, temperature and head pressure. The determination of the evaporation rate according to methods A1 and A2 is shown. The evaporation rate is assumed to be constant during injection and evaporation (for more details, see text). For an example, see Figure 5.

is varied and the ratio (injection time/evaporation time), called ϑ, which is identical with the percentage of solvent evaporated during injection, is determined for the injection of pure solvent until a pre-selected target value is obtained (for details, see Section *Adjusting the evaporation rate to the injection speed*, below).

2.3.2 Experimental

Chemicals

Ethyl acetate and *n*-hexane (both p.a., J.T. Baker, Deventer, the Netherlands) were distilled before use. For the test analytes, which came from various sources and were all of p.a. quality, one is referred to Table 6 below. For on-column injections and spiking purposes, stock solutions were diluted to 1 ng/µl. Spiking of water samples was done just prior to analysis. The samples were spiked in the autosampler vial prior to extraction.

Set-up of large-volume injection–GC system

The large-volume injection (LVI)–GC system consisted of a Carlo Erba Series 8000 gas chromatograph equipped with an on-column injector and an FID-80 (CE Instruments, Milan, Italy) or an MD 800 mass spectrometer (CE Instruments); for a figure of the set-up one is referred to [11]. A Model F101D-HA flow meter (Bronkhorst, Ruurlo, The Netherlands) was inserted between the pressure regulator and the on-column injector. A 3-m diphenyltetramethyldisilazane-deactivated retention gap (0.53 mm I.D.; BGB Analytik, Zürich, Switzerland) was connected to a 2-m retaining precolumn and an 28-m analytical column (both DB-XLB, 0.25 mm I.D.; film thickness, 0.25 µm; J&W, Folsom, CA, USA) via a press-fit connector and a T-piece, respectively. The SVE, an electronically controlled 6-port valve (Valco Instruments, Houston, TX, USA), was connected to the T-piece and was controlled by the SVE controller [11; also see below]. Helium 5.0 (Hoekloos, Schiedam, The Netherlands) was the carrier gas. If not otherwise stated, the standard boiling point of a solvent was used as initial GC temperature, i.e. 77°C for ethyl acetate and 69°C for *n*-hexane, and the head pressure was 100 kPa.

For injections with an automated syringe pump (Harvard Apparatus 22, So. Natick, MA, USA), a 500-µl syringe with a PTFE-coated plunger was used. After filling and mounting it in the Harvard pump, the sample was transferred to the on-column injector via a stainless-steel needle (O.D. 0.25 mm).

For LLE/LVI–GC–MS of aqueous samples, an AS 800 autosampler (CE Instruments) and a 250-µl syringe with PTFE plunger and an injection needle of 0.5 mm O.D. were used. The proper settings for the autosampler were programmed by means of Chromcard Ver. 1.33 (Fisons Instruments, Manchester, UK) for FID detection, and on the controller of the autosampler in the case of MS detection.

After optimization had been achieved and sample analyses were being performed, the injection needle was removed 0.05 min after completion of the injection (during optimization the needle was removed only after the end of the evaporation). After the automated closure of the SVE by the controller, the temperature programme of the GC was started after a delay of 2 min. The temperature was increased to 280°C at 10°C/min, and held at 280°C for 5 min.

FID monitoring of solvent peak

Next to the carrier gas flow rate profile, the solvent peak was monitored, viz. with the FID. A press-fit splitter was connected to the retention gap. A 0.6 m x 0.05 mm I.D. fused silica restriction was used to direct about 0.04% of the gas flow to the FID. The other outlet of the T-splitter was connected to 0.3–0.5 m of a 0.32 mm I.D. retention gap. In order to record the whole solvent peak, the air flow of the FID was increased to 1500 ml/min by removing the restriction in front of the pressure controller, and the range was set to 10^3.

Automated detection of end of evaporation and SVE closure

A laboratory-made and microprocessor-based SVE controller with a small keyboard and LCD display was constructed to actuate the closure of the SVE. As soon as the first derivative of the helium flow exceeded a pre-set threshold value, the SVE was closed and the GC run started. All relevant parameters, i.e. the threshold value and delay times could be programmed in this controller and were stored in its memory. The closure times of the SVE were stored in the memory of the SVE controller and could be displayed for 50 injections (for more details, cf. [11]).

When ready for a next run, the GC instrument gave a start signal to the AS 800 autosampler. When the autosampler was ready for injection, a signal was given to the SVE controller to open the SVE. After a delay of 0.05 min, the injection was started. The syringe was removed. After an additional delay of 0.05 min to allow stabilization of the helium flow, monitoring of the helium flow by the SVE controller was initiated.

Determination of flooded zones

The flooded zone was determined by injecting a 1 ng/µl (experiments with SVE closed during injection) or 0.2 ng/µl (experiments with SVE open during injection) solution of *n*-alkanes in ethyl acetate, and recording at which injected volume prepeaks due to flooding of the retaining precolumn started to occur. The head pressure was 115 kPa and the helium flow 12.5 ml/min (SVE open) or 1.5 ml/min (SVE closed). With the SVE open, the evaporation rate was found to be 45 µl/min. Injections with the SVE closed during injection were done with the AS 800 autosampler at a speed of 120 µl/min (injection volumes for SVE closed also during evaporation: 10–22 µl; for SVE open during evaporation: 30–70 µl). For experiments with the SVE open during injection, injection was done with the Harvard pump at 71 µl/min (injection volumes: 118–178 µl).

2.3.3 Results and discussion

Influence of injection needle diameter

When the original injection syringe of the AS 800 autosampler with an O.D. of 0.5 mm was inserted into the on-column injector, the helium flow decreased ca. 12% at a head pressure of 50 kPa due to the increased resistance in the gas-flow system (**Figure 2**, all traces). At the start of the injection, the helium flow rate sharply decreased, as is evident from traces B and C; with trace A no injection was made. If the syringe was removed at the end of the injection (traces A and B), the helium flow increased again. The end of the evaporation process was indicated by another, sharp, increase of the helium flow rate, which is the basis of our current procedure of automated closure (traces B and C). The time required for the evaporation of the solvent left in the retention gap was less if the syringe was removed at the end of the injection (trace B) than when it was not removed (trace C). This can be attributed to elimination of the pressure drop along the length of the injection needle in the retention gap upon removal of the needle and, consequently, in an increase of the helium flow and the evaporation rate.

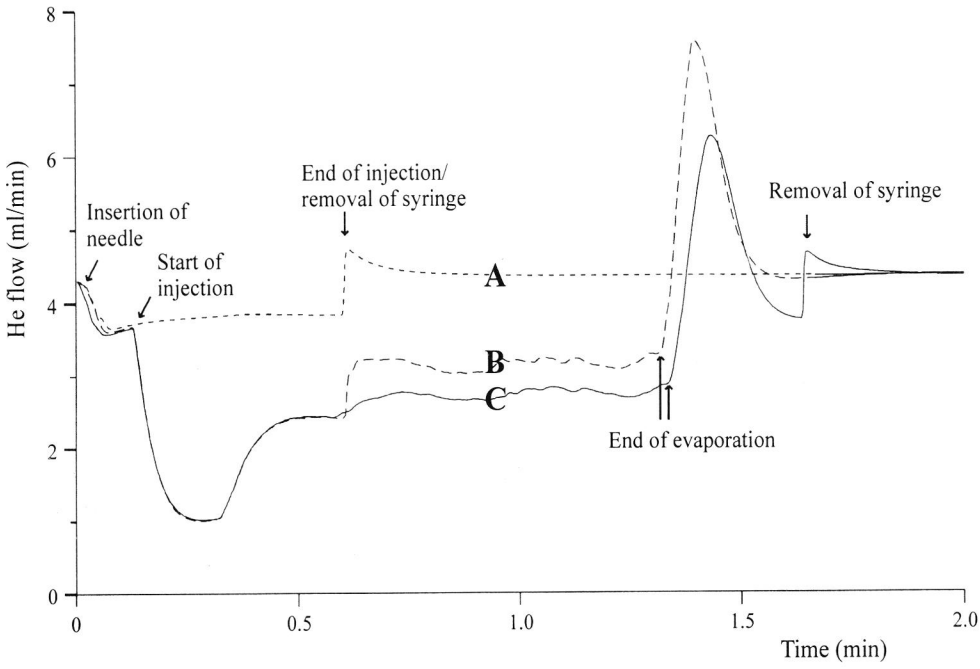

Figure 2
Helium flow-rate profile for (A) inserting and withdrawing of needle without injection, and (B and C) a 30-µl injection of ethyl acetate with SVE open and with (B) and without (C) removing the injection needle at the end of the injection. Injection speed, 60 µl/min; head pressure, 50kPa; for further details, see text.

When using a custom-made injection needle of 0.25 instead of 0.5 mm O.D., the helium flow decreased only about 1% upon needle insertion, and there was no noticeable change of the evaporation rate or time upon needle insertion/removal.

Dependence of flooded-zone length on SVE closure time

The solvent film formed during injection is slowly pushed farther into the retention gap by the carrier gas flow after the injection is complete and, the longer the solvent evaporation takes, the farther will the film extend into the retention gap [9, 15]. That is, the longer evaporation takes, the longer will be the flooded zone, and the less solvent will fit in the retention gap without flooding the retaining precolumn or, in other words, the smaller will be the 'capacity' of the retention gap. When studying the dependence of the flooded-zone length on the closure time of the SVE, one should consider that, if the determination of volatile analytes is the goal, the SVE should be closed before the last drop of liquid disappears [6]. This implies that, in practice, one closes the SVE somewhat too early to be on the safe side.

The influence of the time of SVE closure on the flooded zone of a 3.1 m x 0.53 mm I.D. DPTMDS-deactivated retention gap was determined for three sets of conditions: (i) the SVE was kept closed during injection and evaporation, (ii) the SVE was open during injection and closed just when evaporation was complete, and (iii) the SVE was opened only at the end of the injection and closed just when evaporation was complete. Closure was initiated by the SVE controller.

When the SVE was kept closed, the flooded zone was found to be 15.5 cm/µl. However, when the SVE was open after the injection, i.e. during the final part of the evaporation, the flooded zones were much smaller, viz. 6.0 cm/µl (SVE open at end of injection) and 5.6 cm/µl (SVE open during injection and evaporation). The large differences illustrate the major influence of having the SVE open after completion of the injection and not closing the SVE too early.

The flooded zones reported over the years in the literature for injections with the SVE open during injection, but (probably) being closed before evaporation was complete, are in between the values of ca. 6 cm/µl and ca. 15 cm/µl found by us. Vreuls *et al.* reported a flooded zone of 10 cm/µl for ethyl acetate into a DPTMDS-deactivated retention gap of 0.53 mm I.D at an injection temperature of 83°C [16]. Grob reported a flooded zone of about 11 cm/µl for a wetted and uncoated retention gap of 0.53 mm I.D. if the injection temperature is less than 20°C below the pressure-corrected boiling point [9, p. 209]. Only recently, Boselli *et al.* reported flooded zones of about 3 cm/µl for large-volume injections into a 0.53 mm I.D. retention gap [12].

Obviously, closing the SVE just in time causes a considerable reduction of the flooded zone and thereby maximizes the capacity of the retention gap. This will allow a considerable reduction of the length of the retention gap or the injection of a larger volume, or it will provide a larger margin with regard to variations of; e.g., the injection volume. Therefore, in the rest of the study, the SVE was always closed at the very end of the solvent evaporation.

Calculation of evaporation rate during injection and evaporation

The helium flow depends on three parameters, (i) the ratio of the partial pressures of helium and the solvent used, (ii) the viscosity of the gas mixture, and (iii) the flow resistance of the system [11]. The helium flow can be calculated from:

$$F_{He} = y_{He}(600\ \pi\ r^4 / 16\ \eta_m\ L)\ [(p_i^2 - p_o^2) / p_o]\ [p_o / p_{ref}]\ [T_{ref} / T] \qquad \text{(II)}$$

and the evaporation rate of the solvent, $v_{evap,}$ from:

$$v_{evap} = 1000\ [(1 - y_{He,\ exit}) / y_{He,\ exit}]\ [M / (V_m\ d)]\ F_{He} \qquad \text{(III)}$$

with: d, density of solvent, g/ml; F_{He}, flow rate of helium, ml/min; η_m, viscosity of the helium and solvent gas mixture calculated according to Wilke's approximation, Poise [13, 17]; L, length of retention gap, cm; M, molecular weight of solvent, g/mol; p_i and p_o, pressures at beginning and end of a small segment of the retention gap, Pa; p_{ref}, reference pressure, 1.013 x 10^5 Pa; r, internal radius of retention gap, cm; T, column temperature, K; T_{ref}, reference temperature, 298.15 K; v_{evap}, evaporation rate of the solvent, µl/min; V_m, molar gas volume at T_{ref} and p_{ref} (101.3 kPa), ml/mol; y_{He}, mole fraction of helium; $y_{He,\ exit}$, mole fraction of helium at exit of retention gap. The same assumptions were made as in the previous study, i.e. ideal gas behaviour of the solvent vapour and saturation of the gas phase with solvent vapour; a possible decrease of the retention gap temperature due to solvent evaporation was not considered. A pressure drop due to the insertion of the injection needle was accounted for by using a smaller internal diameter for that length of the retention gap in which the injection needle was inserted.

When injecting at a speed above the evaporation rate, v_{evap}, the latter may change during the injection. The change itself will be dependent on the injection speed because of the pressure drop along the solvent film which causes a change of the ratio (partial helium pressure/partial solvent pressure) and of the viscosity of the helium/solvent gas mixture. Eq. II is therefore valid for an infinitesimally short part of the retention gap only, and the helium flow was calculated iteratively for a given moment in time [11]. The evaporation rate was calculated by incrementally increasing the time and calculating the actual solvent film distribution and the evaporation rate at that time. The (iterative) calculation was done by means of a programme written as visual basic macro and a spreadsheet programme as shown in **Table 1**.

It is possible to calculate the *solvent vapour flow* at any position in the retention gap (which is a kind of cumulative evaporation rate up to that specified point and is expressed in µl liquid/min; **Figure 3**, curves *d* and *h*) at any moment in time by using the mole fraction of helium at that position rather than at the exit of the retention gap as in Eq. III. [In the latter case, the evaporation rate is obtained.] In Figure 3 this is shown in the upper frame for the final moment of a 120-µl/min injection into a 5.95 m x 0.32 mm I.D. retention gap.

Whereas the partial solvent pressure is constant along the solvent film (Figure 3, curve *c*), the solvent vapour flow increases along the length of the solvent film. This is primarily due to the (total) pressure drop (Figure 3, curve *a*) along the retention gap and the resulting increase of the molar fraction of solvent in the gas phase (which is reflected by the increasing ratio (partial solvent pressure/partial helium pressure) of Figure 3, curve *b*). The farther the

Table 1
Programme used to calculate evaporation rate.

No.	Step	Comment
1	Read variables	Variables read, e.g., head pressure, injection speed, injection time, length and I.D. of retention gap (RG), retaining precolumn and capillary to SVE
2	Calculate evaporation rate at start of injection ($t = 0$)	Solvent film of 15 cm length is assumed for calculation of evaporation rate at start
3	Repeat until end of evaporation:	
	A: Increase time, t	t is iteratively increased by 0.02 min
	B: Calculation of amount of solvent in RG	$V_{s,t} = (v_{inj} - v_{evap,t\text{-}dt})*dt + V_{s,t-dt}$ with $V_{s,t}$, amount of solvent in RG at time t; dt, time increment; v_{ini}, injection speed; $v_{evap,t-dt}$, evaporation rate at time $t - dt$.
	C: Check if evaporation is finished	If $V_{s,t} = 0$, then go to step 4.
	D: Calculation of solvent film	Solvent film distribution is estimated, as it cannot be measured exactly. Calculation by algorithm during injection: solvent film thickness proportional to difference $v_{ini} - v_{evap,t}$, length dependent on $v_{ini} - v_{evap,t}$ and $V_{s,t}$. The (calculated) flooded zone depends on amount of solvent left in RG at end of injection and solvent film length at end of injection. Position of last drop depends on injection speed, evaporation rate and volume injected. Flooded zones were (during injections of Table 2) 7.5–9.2 cm/µl for 0.32 mm I.D. and 3.6–4.8 cm/µl for 0.53 mm I.D. RGs. Film thicknesses were between 40 µm (at front end) and 10 µm (at end of evaporation). [For examples, cf. Figure 2; details upon request from authors.]
	e: Calculation of evaporation rate	For given solvent film distribution and helium flow, pressure profile along RG is calculated by iteratively increasing position along length of RG by means of Eq. II, using mole fraction and viscosity from previous segment. Helium flow is iteratively increased until pressure at SVE exit is 1.013×10^5 Pa; evaporation rate calculated from Eq. III.
	f: Write data to spreadsheet	
4	Calculate average evaporation rate, $v_{evap,\ average}$	$v_{evap,\ average} = (\Sigma_t\ v_{evap})/n$ with n, number of time increments
5	End of programme	

solvent film reaches into the retention gap during the injection, the higher will the evaporation rate become. This effect is enhanced by the decrease of the viscosity connected with the higher mole fraction of the solvent vapour which has a lower viscosity than helium. This increase is only partly annulled by the increased restriction due to the presence of the solvent film. This does not only result in evaporation at the rear end of the film, but also along the whole solvent film. After the injection, evaporation of solvent occurs (mainly) from the rear end of the solvent film, which therefore moves towards the end of the retention gap (Figure 3, lower frame) until all of the solvent has evaporated. The evaporation rate increases as the rear end moves farther into the retention gap, due to the smaller pressure drop along that part of the retention gap where there is no solvent film compared with the part with a

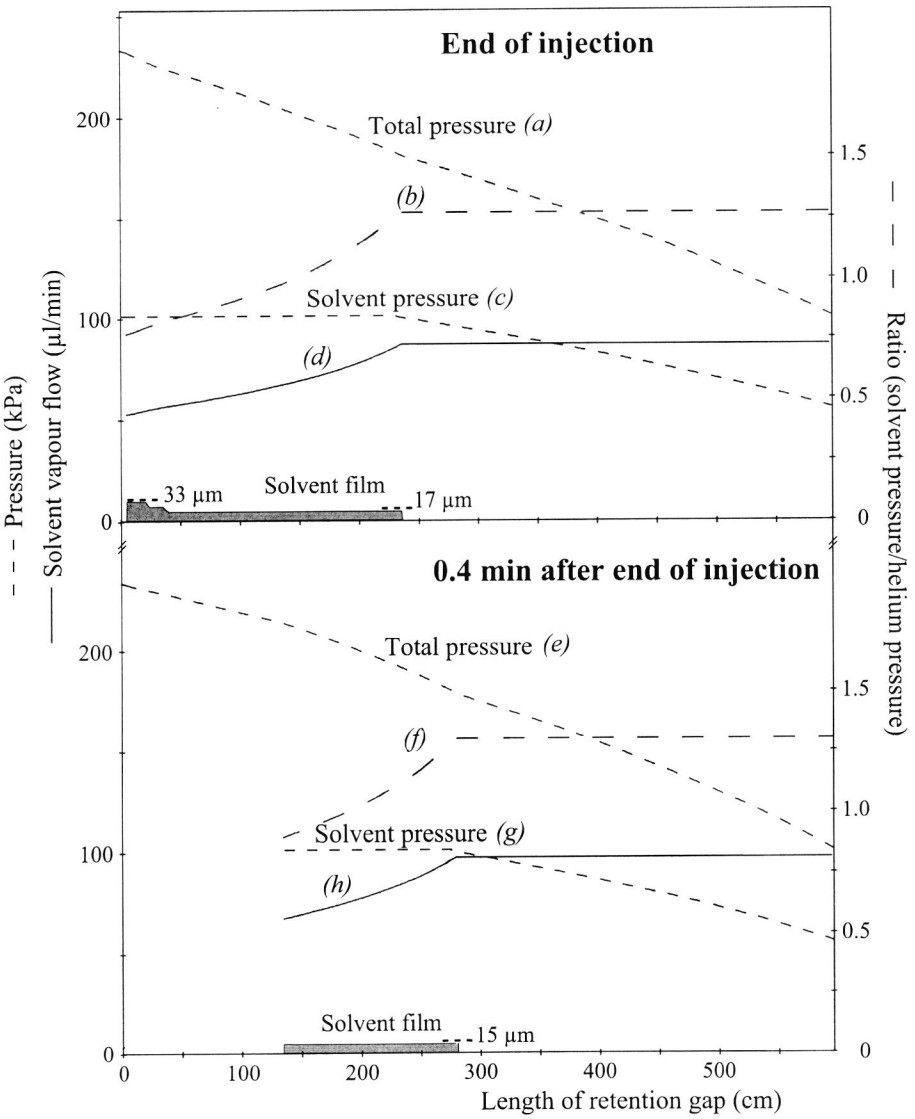

Figure 3

Theoretical profiles of the solvent film distribution, the total pressure (a, e), the partial solvent pressure (c, g), the ratio (partial solvent pressure/partial helium pressure) (b, f) and the solvent vapour flow (d, h) for a 120-µl/min injection of ethyl acetate into a 5.95 m x 0.32 mm I.D. retention gap at a head pressure of 132 kPa. Injection time, 1 min. The situation at the end of the injection (*a–d*) and 0.4 min after the end of the injection (*e–h*) are shown. The profiles were calculated by the programme of Table 1 and using Eqs. II and III.

a solvent film (caused by the lower viscosity of pure helium) (Figure 3, curve *e*).

Data for 0.32 mm I.D. retention gap

The change of the evaporation rate, i.e. the cumulative solvent vapour flow at the end of the retention gap, during injection was determined by splitting a small part of the eluting helium/solvent gas mixture via a restriction to an FID. Relevant results are shown in **Figure 4** and **Table 2**. [Due to the dead time through the restriction of 0.04 min (solvent/helium mixture) up to 0.18 min (pure helium), start and end of injection and end of evaporation are recorded by the FID with a delay of 0.04–0.18 min relative to the real time of the injection which is presented on the *x* axis of Figure 4.] To quote an example, as is to be expected from the above discussion, the experimentally observed increase of the evaporation rate of 18 µl/min (calculated with programme of Table 1: 12 µl/min) during the 120-µl/min injection into the 0.32 mm I.D. retention gap of set-up 1 (Table 2) is larger than that of 11 µl/min (calculated: 4 µl/min) for a 90-µl/min injection (Table 2, Figure 4). After the injection, the increase of the evaporation rate up to the end of the evaporation is 17 µl/min (calculated: 22 µl/min), which is larger than the 8 µl/min (calculated: 4 µl/min) of the 90-µl/min injection. Figure 4 also shows that the evaporation rate increases more strongly after, than during, the injection.

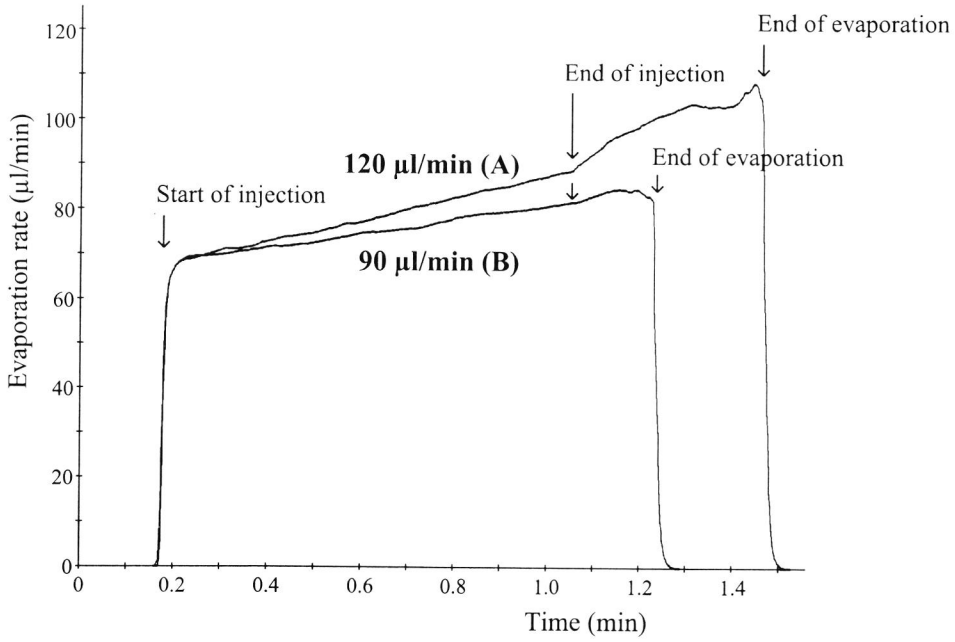

Figure 4

Evaporation rate during 1-min injection of ethyl acetate at (A) 120 µl/min and (B) 90 µl/min into the 0.32 mm I.D. retention gap of set-up 1 of Table 2. The solvent peak was monitored with an FID (for more details and the time *x* axis, see text). Head pressure, 132 kPa. The injection needle was not removed after the injection.

Data for 0.53 mm I.D. retention gap

A similar trend in the evaporation rate is observed for injections into a 0.53 mm I.D.. However, the changes are less pronounced (see data of set-ups 2 and 3 of Table 2). To quote an example, for a 230- and a 320-µl/min injection into a 3.95 m x 0.53 mm I.D. retention gap, the evaporation rate increases only 12 and 3 µl/min, respectively (1 and 3 µl/min calculated). This increase is significantly lower than with the injections into a 0.32 mm I.D. retention gap described above, although more solvent is left in the retention gap after the injection is complete. After the injection, the evaporation rate increases more than during the injection, viz. 22 and 59 µl/min (calculated: 13 and 43 µl/min) for the 230- and 320-µl/min injections, respectively. This is, again, less than for the injections into the 0.32 mm I.D. retention gap of set-up 1 of Table 2.

To sum up, the differences between experimental and calculated evaporation rates at different moments during injection are less than 10% (Table 2). [Of course, the per cent differences between the experimental and calculated *increases* of the evaporation rate, which are obtained by subtraction, are considerably larger.] The differences between the experimental and calculated values can be attributed to assumptions made with regard to Eqs. II and III and to the solvent film distribution (cf. above), to contributions of the dynamics of solvent film formation, e.g. the formation of waves [9], and the imprecision of the numerical

Table 2

Evaporation rate during large-volume on-column injections of ethyl acetate.

Set-up [a]				Solvent	Evaporation rate, **experimental** [b] or *calculated* (µl/min)			
No.	ID (mm)	RG P (kPa)	Injection speed (µl/min)	at end of injection [c] (µl)	at start of injection [d]	at end of injection	at end of evaporation	mean [e]
1	0.32	132	90	*14*	**70**	**81**	**89**	**77**
					75	*79*	*83*	*77*
			120	*41*	**70**	**88**	**105**	**86**
					75	*87*	*109*	*85*
2	0.53	25.2	250	*26*	-	-	-	**197**
					197	*190*	*231*	*201*
			350	*77*	-	-	-	**212**
					197	*207*	*318*	*219*
3	0.53	38.7	230	*21*	**192**	**204**	**214**	**172**
					187	*188*	*200*	*188*
			320	*67*	**193**	**196**	**252**	**178**
					187	*190*	*230*	*196*

[a] Set-up 1: 5.95 m x 0.32 mm I.D. retention gap (RG); after 5.65 m T-splitter for 0.05 mm I.D. capillary to FID; injection time, 1 min. Set-up 2: 4.85 m x 0.53 mm I.D.; injection time, 30 sec; no experimental data for evaporation rate at various moments of injection available as no FID was installed at end of RG. Set-up 3: 3.95 m x 0.53 mm I.D. RG connected to a T-splitter via a 0.54 m x 0.05 mm I.D. capillary to the FID and a 0.48 m x 0.32 mm I.D. RG; injection time, 30 sec.

[b] From FID response.

[c] Calculated with computer programme of Table 1.

[d] Evaporation rate at 0.05 min after start of injection.

[e] Calculated by dividing injected volume by evaporation time; value which can easily be measured in practice (correction for dead time is necessary).

values used for calculation. With regard to the last aspect, the examples included in **Table 3** indicate that imprecisions in the evaporation rate of 1–6% can be expected as a result of the imprecision of individual parameters. The internal diameters of the retention gap and retaining precolumn, the length of the retaining precolumn, the outlet pressure and, especially, the head pressure appear to be most critical in this respect. Calculating the viscosity of the gas mixture may result in some imprecision; using Reichenberg's method rather than Wilke's as approximation results in a 4% higher evaporation rate.

In conclusion, the calculated values agree rather well with the experimental values, and the present model can be used for the (semi-quantitative) description of the change in the evaporation rate occurring during injection and evaporation. This knowledge can, in its turn, be used to find the best strategy to optimize injection conditions in actual practice and to evaluate its robustness.

Optimization of PCSE on-column injection conditions

As discussed in the *Introduction*, optimization of the injection conditions of PCSE on-column injections with, in principle, a series of injections of pure solvent can be achieved by (i) determining the evaporation rate (Method A1, A2 or B) and subsequently selecting an appropriate injection speed with Eq. I or (ii) adjusting the evaporation rate to the injection speed by varying the injection temperature (Method C). However, as we now know, the change of the evaporation rate during injection and, especially, during subsequent

Table 3
Influence of imprecision of parameters on calculated evaporation rate and helium flow rate [a].

Parameter	Value taken	Uncertainty [b]	Per cent change of	
			evaporation rate	Helium flow rate
Internal diameter of retention gap (mm)	0.53	0.01	–4.3	–4.4
Length of retention gap (m)	3.95	0.10	1.4	1.3
Internal diameter of retaining precolumn (mm)	0.32	0.01	–6.0	–5.7
Length of retaining precolumn (m)	0.48	0.05	5.3	6.0
Solvent film thickness (µm)	22	2	0.7	1.5
Solvent film length (m)	2.0	0.2	0.9	–2.6
Head pressure [c] (kPa)	38.7	5.0	–11	–22
		1.0	–2.2	–4.7
Column temperature (°C)	77.0	0.4	0.9	4.0
Approximate viscosity of mixture (µPoise)	93.5	4.3 [d]	4.0	4.0
Outlet pressure (kPa)	101.3	2.0 [e]	4.4	5.0

[a] Set-up 3 of Table 2; injection speed, 320 µl/min. Change of evaporation rate and helium flow calculated with computer programme of Table 1 for situation 0.04 min after start of injection.

[b] Expected uncertainty of 'value taken'; for calculation of per cent changes, uncertainty was given negative sign.

[c] Uncertainty of reading manual manometer found to be about 5 kPa.

[d] Difference of viscosity obtained when using Reichenberg's rather than Wilke's method for calculation [17].

[e] Typical maximum variation of atmospheric pressure in North-Western Europe in one month [19].

evaporation has to be considered. The various strategies will be compared especially with regard to the latter effect. In all cases the end of evaporation was detected by means of the SVE controller.

As outlined above, one has to consider that the introduction of the injection needle may decrease the gas flow and, therefore, the evaporation rate. This is especially the case when a rather thick injection needle, as e.g. with an autosampler, is used. Therefore, during optimization, the injection syringe was left in the injector until the end of the evaporation process (in practice, the syringe was kept in the injector for 1 min after injection), because otherwise a 'mixture' of the evaporation rates with the needle inserted and withdrawn would be measured, while for the calculation of the appropriate injection speed the evaporation rate with the needle in the injector is required. For the development of the optimization strategies it was assumed that the capacity of the retention gap used was at least 20% of the injection volume.

Determination of evaporation rate to select appropriate injection speed (Methods A–B)

For the same set-up, identical evaporation rates should be obtained with Methods A1, A2 and B, if the evaporation rate were constant during injection and evaporation. However, the experimental value determined by Method A1 was significantly lower than those obtained by Methods A2 and B (**Table 4**), and the latter two also depended on the injection speed. This was not unexpected after the above discussion, because there is not one 'true' evaporation rate, as it keeps changing during injection. A tentative explanation is as follows.

The evaporation rate determined by Method A1, which is equal to the injection speed at which the time of evaporation starts to exceed the injection time (**Figure 5**), is identical with the evaporation rate at the start of the injection when there is, as yet, no significant solvent film present in the retention gap. When increasing the injection speed above the evaporation rate at a constant injection time, most of the additional volume injected is deposited in the

Table 4
Determination of evaporation rate by variation of injection speed or injection time.

Set-up [a]			Evaporation rate, **experimental** or *calculated* by							
No.	I.D. RG (mm)	P (kPa)	Method A1	Method A2			Method B			
			Evap. rate (µl/min)	Injection speed (µl/min)	Solvent at end of injection [b] (µl)	Evap. rate (µl/min)	Injection speed (µl/min)	Solvent at end of injection (µl)	Injection time (s)	Evap. rate (µl/min)
1	0.32	132	**73**	80–100	*5–23*	**106**	100	*5–12*	10–30	**76**
			75			*100*				*77*
				100–120	*23–41*	**140**		*16–23*	40–60	**86**
						125				*83*
3	0.53	38.7	**175**	200–260	*6–37*	**195**	240	*10–26*	10–30	**179**
			187			*202*				*190*
				260–320	*37–67*	**209**		*36–51*	40–60	**190**
						221				*200*

[a] See footnote (a) of Table 2.

[b] Calculated with computer programme of Table 1.

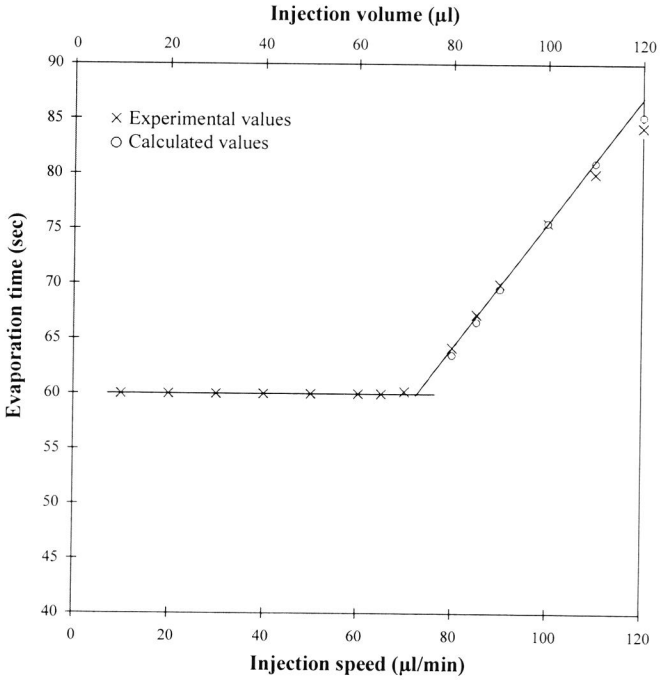

Figure 5

(X) Experimental and (O) calculated (with programme of Table 1) evaporation times for 1-min injections performed at various injection speeds to determine the evaporation rate according to Methods A1 and A2 (for details, see text). Slope of the high-injection speed part of evaporation rate *vs.* injection volume plot obtained by linear regression of experimental data obtained at 80–100 µl/min injection speeds. Injection was done via a 0.25 mm O.D needle into a 5.95 m x 0.32 mm I.D. retention gap of set-up 1 of Table 2. The injection needle was not removed after the injection.

retention gap. This results in an increase of the evaporation rate during, but especially, after the injection, so that the remaining additional solvent evaporates at a higher evaporation rate. Because of this, the use of Method A2 will result in a value for the evaporation rate (which is equal to the inverse of the slope of the high-injection speed part of the evaporation time *vs.* injection volume plot expressed as Δ evaporation time/ Δ injection volume; see Figure 5) which is larger than the evaporation rate during injection. The more solvent is left at the end of the injection (that is, the higher the injection speed is), the larger is the increase of the evaporation rate. This is reflected by the decrease of the slope of the high-injection speed part of the evaporation time *vs.* injection volume plot of Figure 5. In other words, the experimentally determined value depends on the range of injection speeds chosen. With Method B (see **Figure 6**), a significantly larger amount of the additional volume injected during the increased injection time evaporates during injection than with Method A2. Since the evaporation rate increases much less during, than after, injection, the evaporation time per injected solvent volume for the additional volume injected does not decrease as much as with Method A2. Consequently, the experimentally determined value for the evaporation rate does not depend on the injection speed as much as for Method A2, and will be closer to that of Method A1 than of Method A2.

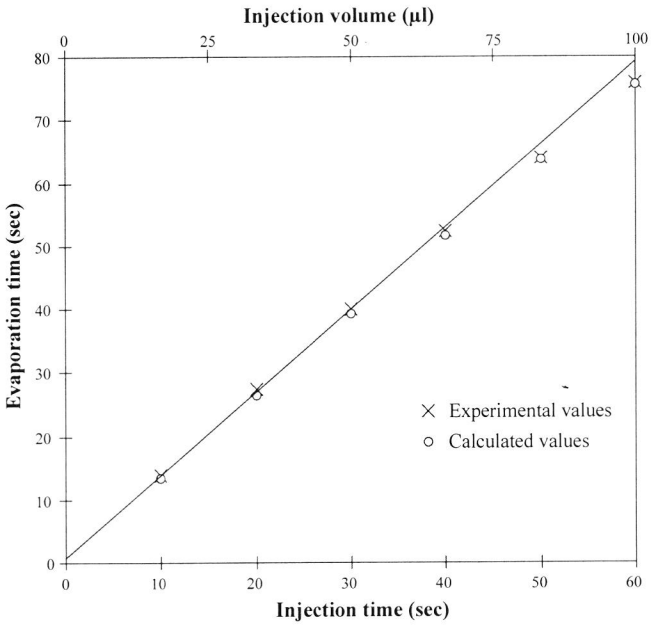

Figure 6

(X) Experimental and (O) calculated (with programme of Table 1) evaporation time for 100-µl/min injections performed during various injection times to determine the evaporation rate of ethyl acetate by means of Method B (for details, see text). Slope obtained by linear regression of experimental data obtained for 10–30 sec injection times. Evaporation time does not increase exactly linearly with injection volume; therefore, measurements should be made such that evaporation time does not exceed injection time more than 30–40%. Injection was done via a 0.25 mm O.D needle into 5.95 m x 0.32 mm I.D. retention gap of set-up 1 of Table 2. The injection needle was not removed after the injection.

Relevant experimental data from Table 4 can be quoted in order to illustrate the above explanation. For injection conditions which leave similar amounts of solvent in the retention gap at the end of the injection, the evaporation rates determined with Method B vary less than those obtained with Method A2: as the data of set-up 1 of Table 4 show, with Method A2 values of 106 µl/min (5–23 µl solvent left at end of injection in retention gap) and 140 µl/min (23–41 µl solvent left) were obtained as against 76 µl/min (for injection times of 10–30 sec leaving 5–12 µl in the retention gap) and 86 µl/min (for injection times 40–60 sec leaving 16–23 µl) for Method B. The value of 73 µl/min obtained with Method A1 (which is identical to the evaporation rate at the start of the injection) is below the mean evaporation rate during the injection and evaporation (77 µl/min for a 90-µl/min injection and 86 µl/min for a 120-µl/min injection; cf. Table 2). The values obtained with Method B (76 and 86 µl/min) are below the evaporation rate at the end of the evaporation (89 µl/min for a 90-µl/min injection and 105 µl/min for a 120-µl/min injection; cf. Table 2) and are closely similar to the mean evaporation rates. The values obtained with Method A2 are, on the other hand, significantly higher than the mean evaporation rates, and actually, can even exceed the evaporation rate at the end of the evaporation!

In all instances do the experimental data agree well with the data calculated with the programme of Table 1 (see Table 4 and Figures 5 and 6). The mutual differences of less than 10% demonstrate the good agreement between theory and experiment. It can be added that a similar trend was found for the determination of the evaporation rate for injections into a 0.53 mm I.D. retention gaps (Table 4, set-up 3), with the mutual differences being somewhat smaller than for the 0.32 mm I.D. retention gap.

Obviously, when trying to select an appropriate injection speed, Method A2 cannot be recommended to determine the evaporation rate: overestimation of the mean evaporation rate will easily occur, which can result in choosing an injection speed at which flooding of the retaining precolumn may occur. This can, e.g., be the case when using the experimentally determined value of the evaporation rate of 140 µl/min (Table 4, set-up 1) for the selection of the appropriate injection speed from Eq. I: for a 200-µl injection and $f = 0.60$ (cf. below), an injection speed of 173 µl/min is then calculated. However, as the calculation programme of Table 1 readily shows, with this injection speed the length of the solvent film will exceed the length of the retention gap just after completion of injection, i.e. when the solvent film is pushed farther into the retention gap during its evaporation. For practical reasons, we prefer Method B over Method A1, because a smaller number of injections of pure solvent is required - typically, 3–4 against 5–8, according to our experience.

Finally, as regards the calculation of an appropriate injection speed from Eq. I, a compromise has to be made to assure that a solvent film of sufficient (but not excessive; cf. above) length is formed to retain the volatile analytes and there has to be a safety range to compensate for small changes of, e.g., the injection volume during a series of analyses and differences between the calculated and experimentally solvent film length (see Section 3.4.3.). Therefore, we generally prefer $f = 0.6$ to calculate the appropriate injection speed.

Adjusting the evaporation rate to the injection speed (Method C)

As discussed above, Method B is recommended for the optimization of the injection conditions of a new set-up or when using a new solvent for injection. However, if only slight changes have to be made, such as after the exchange of the retention gap, and the optimal injection conditions are therefore rather well known, the simpler Method C (see *Introduction*) can be used. Here, the evaporation rate is varied by varying the injection temperature at a fixed injection speed and head pressure to adjust the evaporation rate to the injection speed until the targeted value of ϑ = injection time/evaporation time is obtained. Optimization is started with the injection temperature used prior to the minor modification of the system (and with the injection volume selected for the subsequent, or on-going, real-life analyses).

Similarly to what was said above about the desired value of f (Method B), in the case of selecting a proper value of ϑ, one has to consider that the solvent film in the retention gap should be of sufficient length, but should not exceed the length of the retention gap. When taking small experimental changes and possible differences of calculated and experimental values of ϑ into account, according to our experience it is advisable to select the value of ϑ such that $f = 0.5$ (for both 0.32 and 0.53 mm I.D. retention gaps), or, in other words, that half of the capacity of the retention gap is used.

To illustrate the above, a 100-µl injection of ethyl acetate into a 5.65 m x 0.32 mm I.D. retention gap with a capacity of about 60 µl is considered. For $f = 0.5$, 70% of the solvent has to be evaporated during injection or, in other words, the targeted value of ϑ should be 0.7. As a demonstration of the variation of ϑ with the (injection) temperature, **Table 5** lists values for

Table 5
Optimization of injection temperature for ethyl acetate by adjusting evaporation rate [a].

Injection temperature	Ratio ϑ [b]		Calculated [c] per cent solvent evaporated during injection
(°C)	Experimental	calculated [c]	
88	1.00	1.00	100
86	0.98	1.00	100
84	0.95	1.00	100
82	0.89	0.94	94
80	0.85	0.88	87
78	0.81	0.82	80
76	0.77	0.77	74
74	0.73	0.72	69
72	0.70	0.68	63

[a] Set-up 1 of Table 2; 100-µl injections at 100 µl/min; head pressure, 132 kPa He. Injection needle left in injector after injection for further 60 s.

[b] ϑ (= injection time / evaporation time) equals fraction of solvent evaporated during injection if evaporation rate should be constant during injection and evaporation. Evaporation time determined by SVE controller (time of closure of SVE).

[c] Using programme of Table 1. Simple experimental determination of percentage of solvent evaporated during injection is not possible (e.g., possible with FID only when splitting very small flow to FID because of limited linear range of detector).

temperatures from 88°C down to 72°C. As is to be expected, a decrease of the injection temperature results in a decrease of ϑ. The mutual differences of less than 10% between the experimental values and the values calculated with the programme of Table 1 demonstrate the good agreement between theory and experiment. Values such as those shown in Table 5 are, strictly speaking, of course valid for one set-up ('the present retention gap and press-fit') only. Experience shows that the difference in the injection temperatures at which the targeted ϑ value was obtained prior to, and after, the exchange of a retention gap, was only ±(0–1)°C.

Finally, it is interesting to emphasize that $100*\vartheta$ is not exactly equal to the percentage of solvent evaporated during injection - which it would be if the evaporation rate were constant - but is somewhat higher, as is obvious from the data of Table 5. That is, more solvent is left in the retention gap after the injection than is suggested by ϑ. This can be attributed to the increase of the evaporation rate after the injection: a higher percentage of solvent evaporates after the injection than is suggested by the experimental value of ϑ, which reflects the *average* evaporation rate/injection rate ratio. To quote an example obtained by using the calculation programme of Table 1, for a 100-µl injection at 76°C, $\vartheta = 0.77$, but only 74% of the solvent evaporates during the injection. Screening of the data in the table shows that, in order to be on the safe side, one has to assume that up to 5% more solvent may be left in the retention gap than is suggested by ϑ if 65–85% solvent evaporation during injection. This is actually the reason for choosing ϑ such that $f = 0.5$ (and $f = 0.6$ for calculation of appropriate injection rate with Method B), because then solvent film lengths of 55–70% of the total length of the retention gap are predicted by the calculation programme of Table 1.

It is interesting to add that, if the injection speed can be chosen only in rather large steps - e.g. with the AS 800 autosampler injections speeds of only 1, 2, 3 etc. µl/sec can be chosen - selecting an appropriate injection speed after determination of the evaporation rate is not

possible. In this case, Method C is also preferred when the optimal injection conditions are not known. The temperature at which optimization is started should then be just below the boiling point of the solvent at the selected head pressure and some 4–8 injections are required.

Analysis of aqueous samples by LLE/large-volume injection (LVI)–GC–MS

The potential of the present LVI–GC approach was demonstrated for the analysis of aqueous samples using mass-selective detection. The use of LVI–GC allows the miniaturization and simplification of sample preparation by in-vial LLE: 0.16 mg sodium chloride was weighed into a 2-ml vial, a 0.8-ml aqueous sample and 0.8 ml of *n*-hexane were added and mixed by shaking for 2 min and placed in the autosampler tray for analysis. Next, 100 µl of the organic extract were injected into the GC–MS system. The SVE was automatically closed by the SVE controller, and the injection conditions were optimized by means of Method C using an injection speed of 120 µl/min and $\vartheta = 0.7$. Actually, after exchange of the retention gap, a maximum of only two injections were required to find the injection temperature resulting in the targeted vale of ϑ, which was in most cases 70°C.

Table 6
Recovery of micropollutants after LLE/LVI–GC–MS of 0.8-ml HPLC-grade water spiked at the 10-µg/l level.

No.	Compound	Recovery [a] (%)	No.	Compound	Recovery [a] (%)
1	Monochlorobenzene	102	27	Nitrobenzene	100
2	Chlorohexane	111	28	*N,N*-Dimethylphenol	97
3	Ethylbenzene	106	29	Triethyl phosphate	65
4	*p/m*-Dimethylbenzene	97	30	*N*-Ethylaniline	101
5	Styrene	100	31	Isoforon	100
6	*o*-Dimethylbenzene	100	32	1,3,5-Trichlorobenzene	101
7	Methoxybenzene	101	33	1,4-Dimethoxybenzene	101
8	1,2,3-Trichloropropane	100	34	2,4 + 2,6-Dimethylaniline	98
9	Propylbenzene	101	35	2,4-Dichlorophenol	88
10	*o*-Chlorotoluene	99	36	2-Methoxyaniline	82
11	Benzaldehyde	99	37	1,2,4-Trichlorobenzene	102
12	1,2,3-Trimethyl thiophosphate	96	38	Naphthalene	104
13	2,4,6-Trimethylpyridine	96	39	Hexachlorobutadiene	102
14	Benzonitrile	94	40	1,2,3-Trichlorobenzene	102
15	*m*-Dichlorobenzene	101	41	*α,α,α*-Trichlorotoluene	107
16	*p*-Dichlorobenzene	96	42	1-Chlorodecane	99
17	5-Ethyl-2-methylpyridine	121	43	Quinoline	108
18	Indane	103	44	1-Chloro-4-nitrobenzene	101
19	o-Dichlorobenzene	100	45	1-Chloro-2-nitrobenzene	102
20	Indene	102	46	Isoquinoline	96
21	Butylbenzene	97	47	1H-Indole	91
22	*N*-Methylaniline	85	48	1,4-Diethoxybenzene	93
23	2-Methylphenol	97	49	1-Methylnaphthalene	105
24	2-Methylbenzeneamine	101	50	Ferrocene	102
25	Acetophenone	92	51	2-Methylisoquinoline	100
26	*N,N*-Dimethylamine	100	52	1,2,4,5-Tetrachlorobenzene	101

[a] 4, 4'-Difluorobiphenyl used as internal standard. Recoveries calculated using a 100-µl standard injection as reference.

The aim was the determination of analytes as volatile as monochlorobenzene. Recently, we demonstrated that the determination of monochlorobenzene is not possible with conventional on-line SPE–GC. This was attributed to the non-uniform distribution of the analytes in the solvent film during an on-line SPE–GC transfer, i.e. to the fact that the major part of the analytes is deposited in the front part of the solvent film [18]. Quantitative recovery of monochlorobenzene could be achieved only if a so-called presolvent was introduced prior to desorption.

A preliminary series of injections of a 100 µl-injection of the test mixture in *n*-hexane showed that the recoveries of all analytes - i.e., also of the more volatile compounds - were at least 80% compared with a standard 1-µl injection. This demonstrated that the present optimization strategy and the use of a controller for the closure of the SVE indeed allows the determination of volatile analytes. As regards the results of the total procedure, the recoveries were very good (85–110%) for 50 out of the 52 test compounds (**Table 6**). Somewhat lower recoveries were obtained only for compound Nos. 36 (82%) and 29 (65%). This can be attributed to their rather polar nature, which is reflected by their low octanol–water coefficients (K_{OW}): their log K_{OW}s are 1.2 and 0.8, respectively. The relative standard deviation of the recovery data was found to be satisfactory for all test compounds (1–9%; n = 6). **Figure 7** shows the total ion chromatogram of the LLE/LVI–GC–MS analysis of 0.8-ml HPLC-grade sample spiked with 10 µg/l of the test analytes. The detection limits using the reconstructed ion chromatograms were typically 20–250 ng/l.

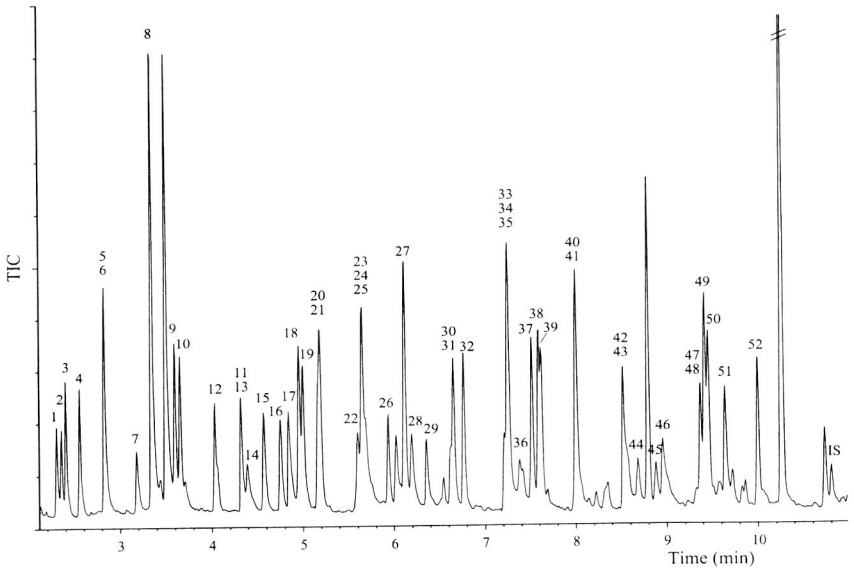

Figure 7
Total ion current LLE/LVI–GC–full-scan MS of a 0.8-ml water sample spiked with 52 micropollutants at the 10-µg/l level. For peak assignment, see Table 6. Unknown compounds are co-eluting with analytes Nos. 8 and 27.

2.3.4 Conclusions

Recent studies indicate that monitoring of the helium flow rate is a simple and reliable method to control large-volume on-column injections in GC. Closure of SVE at the very end of evaporation increases the capacity of the retention gap. This is readily (and automatically) achieved by means of the SVE controller, while closing at a pre-determined value at the very end can result in loss of volatiles when the evaporation time slightly shifts, e.g., due to small changes in the injection volume.

Experiments show, and theory can explain, that the evaporation rate changes during injection and, even more so, during subsequent evaporation, and that this change is more significant for injections into a 0.32 mm I.D., than into a 0.53 mm I.D. retention gap. This effect significantly influences the optimization of injection conditions of PCSE on-column injections. A comparison of four methods which are commonly used to determine the proper injection conditions showed that two of these can be recommended for practical work:

- determination of the evaporation rate by increasing the injection time at a constant injection speed and subsequent calculation of an appropriate injection speed from Eq. I (Method B) is preferred when the optimal conditions are essentially unknown;
- if re-optimization of an on-column injection after, e.g., exchange of the retention gap, is required and the optimal conditions are known fairly well, adjusting of the evaporation rate to the injection speed by variation of the injection temperature at a constant injection speed (Method C) is preferred.

Although the experimentally determined values of the amount of solvent evaporated during injection and evaporation (*g*, Method C), or the length of the solvent film in the retention gap (*f*, Method B, no data shown) may differ somewhat from the targeted values due to the change of the evaporation rate during injection and evaporation, both methods can be used without any risk of flooding or losing volatile analytes if the injection conditions are calculated from the experimental values as described above. With both strategies, optimization of the injection speed is straightforward and rapid: two (Method C) to five (Method B) injections of pure solvent are required without any reconstruction of the set-up. A logical next step seems to be the development of appropriate software which will enable automated system optimization without the assistance of an operator.

References

[1] Th. Hankemeier, H.T.C. van der Laan, J.J. Vreuls, M.J. Vredenbregt, T. Visser and U.A.Th. Brinkman, *J. Chromatogr. A*, 732 (1996) 75.
[2] F.D. Rinkema, A.J.H. Louter and U.A.Th. Brinkman, *J. Chromatogr. A*, 678 (1994) 289.
[3] H.-J. Stan and M. Linkerhägner, *J. Chromatogr. A*, 727 (1996) 275.
[4] H.G.J. Mol, H.-G. M. Janssen, C.A. Cramers, J.J. Vreuls and U.A.Th. Brinkman, *J. Chromatogr. A*, 703 (1995) 277.
[5] A. Venema and J.T. Jelink, *J. High Resolut. Chromatogr.*, 19 (1996) 234.
[6] K. Grob, H.-G. Schmarr and A. Mosandl, *J. High Resolut. Chromatogr.*, 12 (1989) 375.
[7] F. Munari. A. Trisciani, G. Mapelli, S. Trestianu, K. Grob and J.M. Colin, *J. High Resolut. Chromatogr.*, 8 (1985) 601.
[8] K. Grob, Jr., G. Karrer and M.-L. Riekkola, *J. Chromatogr.*, 334 (1985) 129.
[9] K. Grob, in W. Bertsch, W.G. Jennings and P. Sandra (eds.), *On-line coupled LC–GC*, Hüthig, Heidelberg, Germany, 1991.

[10] S. Ramalho, Th. Hankemeier, M. de Jong, U.A.Th. Brinkman and J.J. Vreuls, *J. Microcol. Sep.*, 7 (1995) 383.
[11] Th. Hankemeier, S.J. Kok, J.J. Vreuls and U.A.Th. Brinkman, *J. Chromatogr. A*, 811 (1998) 105.
[12] E. Boselli, B. Grolimund, K. Grob, G. Lercker, R. Amadò, *J. High Resolut. Chromatogr.*, 21 (1998) 355.
[13] J. Staniewski and K. Alejski, poster presented at *18th Intern. Symp. Cap. Chromatogr., Riva del Garda, 1996.*
[14] J.J. Vreuls, G.J. de Jong, R.T. Ghijsen and U.A.Th. Brinkman, *J. Ass. Off. Anal. Chem, 77 (1994) 306.*
[15] Appendix of Chapter 2.2 of this thesis.
[16] J.J. Vreuls, W.J.G.M. Cuppen, G.J. de Jong and U.A.Th. Brinkman, *J. High Resolut. Chromatogr.*, 13 (1990) 157.
[17] R.C. Reid, J.M. Prausnitz and B.E. Poling, *The Properties of Gases and Liquids*, 4th ed., McGraw-Hill, New York, NY, USA, 1987.
[18] Th. Hankemeier, S.P.J. van Leeuwen, J.J. Vreuls and U.A.Th. Brinkman, *J. Chromatogr. A*, 811 (1998) 117.
[19] Data from WWW site of Institute for Meterology of Free University Berlin; Internet: http://user.cs.tu-berlin.de/~eserte/met/wetter-1998.

3

On-line SPE–GC–MS of aqueous samples

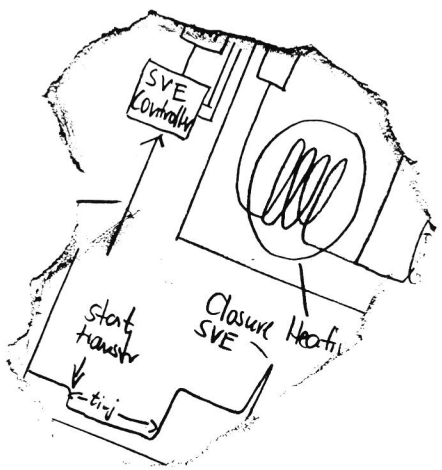

3.1 Use of a presolvent to include volatile organic analytes in the application range of on-line SPE–GC–MS

Summary

The application range of the on-line solid-phase extraction–gas chromatographic (SPE–GC) analysis of aqueous samples has been extended to volatile analytes. In the new set-up, after conventional aqueous-sample loading and drying of the SPE cartridge with nitrogen gas, 30–50 µl of an organic solvent, the so-called presolvent, such as methyl acetate or ethyl acetate are introduced into the retention gap prior to the actual desorption to ensure that a solvent film is already present in the retention gap when the introduction of the analyte-containing desorption solvent starts. This procedure allows the recovery of analytes as volatile as monochlorobenzene and xylene. Aspects such as the type of retaining precolumn, and the type and amount of presolvent have been studied systematically to explain the performance of the novel set-up. Actually, when using 50 µl of presolvent, the use of a retaining precolumn did not have any significant influence on the recovery of the volatile analytes.

The modified SPE–GC procedure was tested by analysing 10 ml of river Rhine water spiked at the 0.5 µg/l level with about 80 microcontaminants covering a wide range of volatility. The test compounds included chlorobenzenes, substituted and non-substituted aromatic compounds, anilines and phenolic compounds and organonitrogen and organophosphorus pesticides. The system performance in terms of recovery (typically 70–115% at the 0.5 µg/l level) and repeatability (RSD values typically 1–9%; n = 7) was satisfactory, even for monochlorobenzene, the most volatile analyte of the test mixture. Low recoveries due to early breakthrough (polar analytes) or adsorption to the tubing (apolar analytes) were observed for a few analytes only. The detection limits in SPE–GC–MS using full-scan acquisition generally were 20–50 ng/l.

3.1.1 Introduction

The trace-level analysis of aqueous samples to determine organic microcontaminants requires fast, sensitive and selective methods. In this context, the on-line coupling of the sample-preparation and the separation-cum-detection procedure in one integrated system is desirable to allow automation and increase sensitivity. In such a system, solid-phase extraction (SPE) is preferred for the transfer of the analytes from the aqueous phase into an organic solvent. The analytes are desorbed from the SPE cartridge into the GC system with 50–100 µl of organic solvent. Several applications have been reported for the SPE–GC analysis of pesticides using an on-column [1, 2] or a loop-type [3] interface and a variety of selective detectors, including mass-selective (MS) [1, 4] and atomic-emission [5] detectors.

Fully automated on-line SPE–GC is ideally suited as an early-warning system for the at-site screening of river water quality. In this case, it is desirable to have volatile analytes such as lower chlorinated benzenes included in the procedure. MS detection generally is preferred because of its identification potential. When the application range has to cover volatile analytes, an on-column interface should be one's first choice because of the solvent effects then operational for trapping of the analytes [6]. However, also with large-volume on-column injection, the loss of a not fully-trapped analyte, e.g., toluene in pentane, was observed by Grob and Neukom when injecting 70 µl instead of 0.7 µl on-column [7]. They attributed the loss to incomplete reconcentration of partially solvent-trapped bands by phase soaking, because phase soaking only slows down the migration of early escaped volatiles, but does not stop it, and is therefore only active up to a certain injection volume. Deans [8] proposed the introduction of pure solvent in front of the sample plug to serve as a barrier against escaping solvent and showed an example for a 40 µl injection in packed-column GC. Several related studies [9–12] have been reported, but none of these used the approach for large-volume on-column injections into a retention gap in a GC.

On-line SPE–GC of volatile analytes has not been studied in much detail. Only Picó et al. reported the on-line SPE–GC determination of some chlorobenzenes and other rather volatile analytes [13]. In their set-up, a drying cartridge was inserted between the SPE module and the GC to remove traces of water from the organic SPE extract. However, the recoveries of 3-chlorotoluene and 1,2-dichlorobenzene were only 34 and 50%, respectively. In addition, in one of the real-life examples shown several other dichlorobenzenes also showed up with rather low recoveries. These results indicate that there is an experimental problem.

The goal of this study was to extend the application range of on-line SPE–GC of aqueous samples to include volatile analytes next to higher-boiling compounds. To this end, the role of the drying step which is necessary to remove the water left in the SPE cartridge after the sampling step, the choice of the desorption solvent and the use of a so-called presolvent (i.e. the transfer of pure organic solvent into the GC prior to the analyte-containing fraction) were studied. The total system was used for the SPE–GC–MS determination of some eighty microcontaminants covering a wide volatility range, i.e. from monochlorobenzene to dioctyl phthalate, in river water at the sub-µg/l level.

3.1.2 Experimental

Chemicals

HPLC-grade water, ethyl acetate, methyl acetate and isopropanol, all of p.a. grade, were purchased from J.T. Baker (Deventer, the Netherlands). The organic solvents were glass-distilled prior to use. A stock solution of all test compounds at a concentration of about 20 ng/µl in dichloromethane, which was a gift from the Institute for Inland Water Management and Waste Water Treatment (RIZA, Lelystad, the Netherlands), was kept at -20°C. For the microcontaminants used as test analytes, which came from various sources and were all of p.a. quality, one is referred to Table 6 below. For the optimization of the amount of presolvent and the comparison of several retaining precolumns, a stock solution of 29 test compounds in methyl acetate or hexane was prepared (Nos. 1, 4, 5, 6, 7, 9, 11, 13, 15, 16, 18, 20, 22, 23, 25, 26, 27, 35, 39, 40, 51, 54, 55, 60, 66, 70, 77, 81 and 82 of Table 6). Water samples were spiked prior to analysis by adding an aliquot of a (diluted) stock solution. River water samples were filtered through 0.45 µm membrane filters (Schleicher & Schüll, Dassel, Germany).

Equipment

The total system (**Figure 1**) consisted of a Prospekt (Spark Holland, Emmen, the Netherlands) equipped with a solvent delivery unit (SDU), for sample preparation, and a GC–MSD for analysis.

SPE system
The Prospekt system consisted of three pneumatic six-port valves, an automatic cartridge exchanger and an SDU equipped with a six-port solvent selection valve and a single-piston HPLC pump. All timed events were programmed via a software package (Hewlett Packard, Waldbronn, Germany) into the Prospekt controller unit. Additional equipment was programmed via auxiliary contact closure events of the Prospekt. A Phoenix 30 syringe pump (Carlo Erba Strumentazione, Milan, Italy) used for the delivery of the organic desorption solvent was modified to switch the flow on/off by an auxiliary event. An electrically actuated Must six-port valve (Spark Holland) was used as transfer valve, and a 24 V solenoid gas valve for actuating the nitrogen flow for drying of the cartridge. The nitrogen was purified with a carbon trap (20/40 mesh Carbotrap C; Supelco, Bellefonte, PA, USA). The water samples were preconcentrated on a commercial 10 mm x 2 mm I.D. cartridge packed with 20 µm, 100 Å PLRP-S styrene–divinylbenzene copolymer (Spark Holland). One cartridge could be used for at least 50 water analyses. The tubing between valves V3 and V4 had a dead volume of 6 µl, and was occasionally used as sample loop for the simulation of an SPE–GC transfer. The SPE module was interfaced to the on-column injector of the GC system via a 0.25 m x 75 µm I.D. deactivated fused silica capillary.

GC–MS system
A Hewlett Packard (Palo Alto, CA, USA) Model 5890 Series II gas chromatograph equipped with a pressure-programmable on-column injector and a Model 5972 mass selective detector (MSD) was used for GC–MS. MS ionization was achieved by electron impact, and ions with m/z 47–335 were monitored at 1.5 scans/sec. The electron multiplier voltage was set at 1800 V. The injector was connected to a 5 m x 0.32 mm I.D. retention gap (BGB Analytik, Zürich,

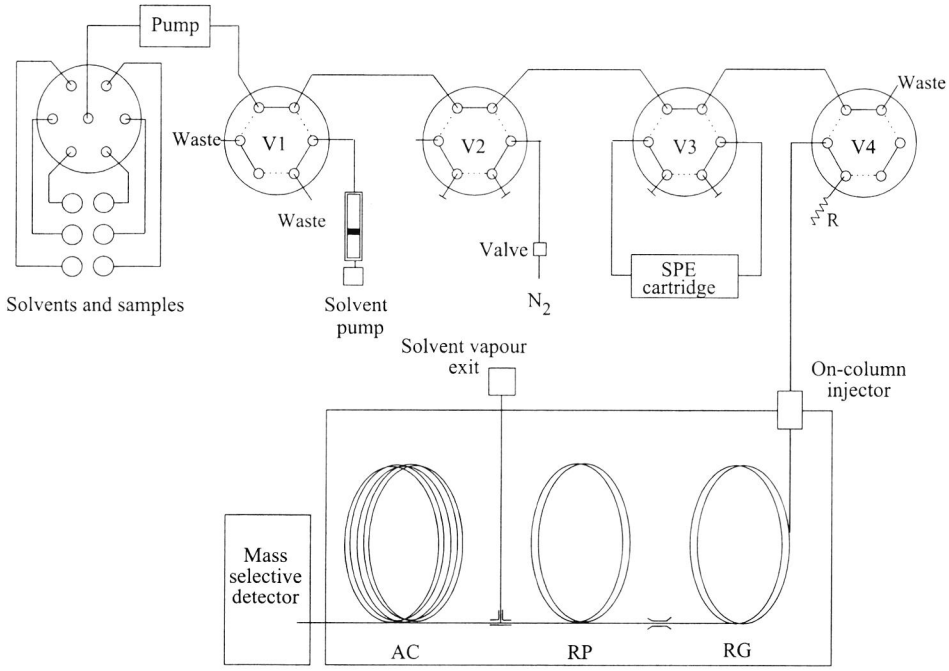

Figure 1
Scheme of the on-line SPE–GC–MS system. Abbreviations: AC, analytical column; RG, retention gap; RP, retaining precolumn; R, restriction, V1–4, valves.

Switzerland) and a 1.5 m x 0.32 mm I.D. retaining precolumn containing PS-264 (5% diphenyl-polysiloxane and 95% dimethyl-siloxane) with a film thickness of 0.25 μm. An early solvent vapour exit (SVE) was inserted between the retaining precolumn and the GC column (HP5MS, 27 m x 0.25 mm I.D., 0.25 μm film) to vent most of the solvent vapour [14]. The SVE was connected to the press-fit T-splitter (BGB Analytik) between the retaining precolumn and GC column (see Figure 1). The home-made SVE was installed on the top of the split/splitless injector and kept at 150°C to prevent solvent condensation.

One other retention gap and several other retaining precolumns were used in a brief comparative study (see Table 5 below). The OV-1701-OH coated retention gap (0.32 mm I.D.) and the retaining precolumn (0.32 mm I.D.) coated with PS-264 (5% phenyl, 95% methylsilicone) with several film thicknesses were obtained from BGB. The retaining precolumns (0.32 mm I.D.) coated with DB-1701 (0.25 μm film thickness) and DB-1 (1 μm film thickness) were from J&W (Folsom, CA, USA).

Procedures

SPE procedure

The final time schedule of the SPE procedure is shown in **Table 1**. Each run started with conditioning of the SPE cartridge with 100 μl of desorption solvent and, next, 2.5 ml of HPLC-grade water. The HPLC pump and all connecting capillaries up to valve V3 were then flushed with 10 ml of sample in order to cover active sites and, thus, reduce the loss of apolar

analytes due to adsorption on capillary walls and the HPLC pump during sampling. Next, 10 ml of sample were loaded on the SPE cartridge at 2.5 ml/min. Some clean-up to remove salts and very polar compounds was effected by flushing the cartridge with 1.9 ml of HPLC-grade water. The cartridge was then dried for 30 min with 70 ml/min of nitrogen at ambient temperature. During drying, the HPLC pump was cleaned with 2.5 ml of isopropanol, which will remove all air from the pump and, thus, prevent malfunctioning. The analytes were subsequently desorbed with 50 or 100 µl of methyl or ethyl acetate and transferred via the transfer line to the GC at the optimized flow rate (see below). The modification of the SPE procedure required when using a presolvent, which is discussed in Section *Use of a presolvent*, is included in Table 1. To increase sample throughput, pretreatment of the next sample was started after the transfer and subsequent cleaning of the SPE cartridge with 200 µl of methyl or ethyl acetate. This reduced the sample throughput time from 79 to 47 min.

Table 1
Time schedule of sample preparation programme of on-line SPE–GC–MS.

Time [min:sec]	Solvent selection valve	Flow[a] [ml/min]	Valves[b]				Auxiliary events[c]			Comment
			V1	V2	V3	V4	1	2	3	
00:00	1	2.5	1	0	1	0	off	off	off	condition cartridge with MeOAc
02:00			0							condition cartridge with water
03:00	3	5			0					preflush pump/tubing with sample
04:55		2.5								decrease flow of pump
05:05					1					preconcentrate 10 ml of sample
09:05	1	5			0					clean pump with water
09:25		2.5								decrease flow of pump
09:35					1					clean-up with 1.9 ml of water
10:20		0		1				on		start drying for 30 min
10:30	2	5	1							clean pump with i-PrOH
11:30	1									clean pump with water
12:30		0								stop flow of pump
37:00							on			start of MeOAc pump
40:20								off		depressurize after drying
40:50				0						fill cartridge with MeOAc
42:37					0					preflush tubing with MeOAc
43:18									on	start of GC
43:30						1			off	transfer of 50 µl pure MeOAc as presolvent
44:22					1					transfer of analytes with 50 µl MeOAc
45:39						0				end of transfer, cleaning of cartridge with MeOAc
47:00							off			stop flow of MeOAc pump
47:00										end of sample preparation

[a] Flow of SDU pump.
[b] V1–V4: position 0 refers to position in Figure 1.
[c] 1, Syringe pump on/off; 2, nitrogen valve on/off; 3, start of GC.
Abbreviations: i-PrOH, isopropanol; MeOAc, methyl acetate.

SPE–GC transfer

During the transfer of solvent into the GC under partially concurrent solvent evaporation conditions, the SVE was open. The oven temperature was 54°C or 75°C when using methyl or ethyl acetate, respectively. The SVE was closed just before the last microlitres of solvent evaporated. The head pressure of the GC was increased from 60 kPa to 130 kPa at 500 kPa/min before the transfer, and decreased at 300 kPa/min to 60 kPa after the transfer. During the temperature programme of the GC run, the head pressure was programmed to provide constant flow. After 6 min the GC oven temperature was increased from the injection temperature to 280°C at 10°C/min, and then kept at 280°C for 5 min. The same temperature and pressure programme was used for 2-µl or 5-µl on-column injections carried out for reference purposes, except for the fact that the pressure was kept constant at 60 kPa during injection. Only during the study of several retaining precolumns (see Table 5 below), the head pressure was kept constant at 80 kPa during the transfer and the whole run. When injecting ethyl acetate, the head pressure was 90 kPa and programmed to provide constant flow during the GC run, and the GC oven temperature was increased 5 min after the start of the transfer at 10°C/min as described above.

Optimization of introduction flow rate

The flow rate used to introduce the solvent, methyl or ethyl acetate, into the retention gap of the on-column injector was optimized by means of repetitive 100-µl injections of an *n*-alkane standard solution. For these (and other) 100-µl injections, a 120-µl loop was inserted between valves V3 and V4. This loop and the tubing between valves V2 and V3 was filled by means of a syringe, which was mounted on valve V2 and replaced the nitrogen line. Next, the sample was pushed into the retention gap by organic solvent from the syringe pump.

The introduction flow rate was stepwise increased until peak distortion of the analytes was observed, which indicated flooding of the retaining precolumn with solvent [15]. The flow rate was then set at a value 4 µl/min below that for which flooding has been observed. This procedure ensured that a solvent film was always created in the retention gap during the transfer step without undue risk of flooding of the retaining precolumn. Typical flow rates were 40–50 µl/min.

3.1.3 Results and discussion

In the present paper, we first studied the loss of volatile analytes occurring with a conventional SPE–GC set-up. Next, the procedure was improved by including the addition of a presolvent and examining various related aspects. Finally, the optimized method was put to the test by analysing spiked surface water.

Loss of volatile analytes with conventional on-line SPE–GC

On-line SPE–GC: critical parameters

To investigate the potential of conventional on-line SPE–GC for the determination of volatile analytes, a 2-µl on-column injection of a standard solution of a test mixture (**Figure 2**C) was used for comparison. Next, 10 ml of HPLC-grade water spiked with the same test mixture at the 0.2 µg/l level were analysed (Figure 2A). [To ensure that the SVE would not be closed

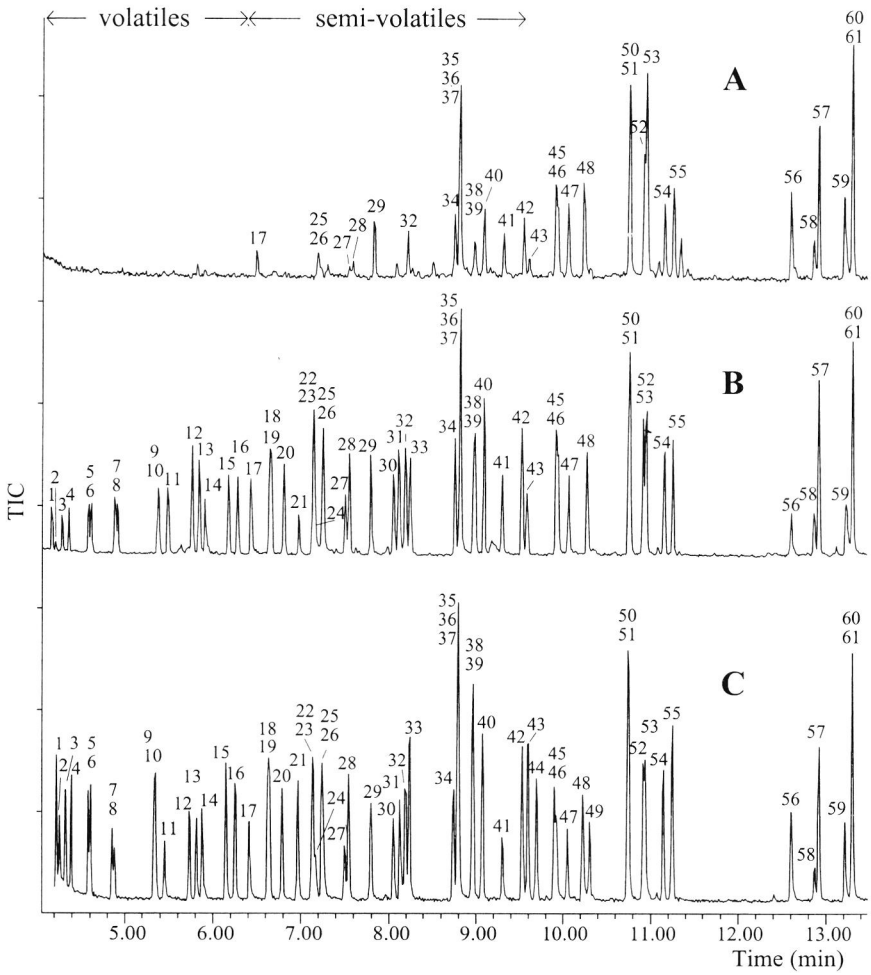

Figure 2

On-line SPE–GC–MS of 10 ml HPLC-grade water spiked at the 0.2 µg/l level (A) and off-line SPE/GC–MS of 10 ml HPLC-grade water spiked at the 1 µg/l level (B). In the latter case, 100 µl out of the 250-µl extract were injected. For comparison, a 2-µl on-column standard injection of the test mixture is shown (C). In all cases, the total ion current (TIC) GC–MS chromatograms are shown. For peak assignment, see Table 6.

too late, i.e., that some solvent would still be left in the retention gap at the moment of closure, the time difference between the end of the solvent peak, monitored by the pressure gauge of the MSD, and the moment of closure of the SVE, was made 0.5–1 min longer than the dead time of the analytical column.] Comparison of the chromatograms shows that the more volatile analytes (compounds Nos. 1–21 in Figure 2) did not show up in the on-line SPE–GC–MS chromatogram at all, and that most of the semi-volatiles (Nos. 22–44) were only partly recovered. From quinonine (No. 45) on, most analytes were recovered quantitatively. For practical reasons, the chromatogram is shown up to 3-nitroaniline (No. 60).

The observed loss of volatile analytes can occur during several stages of the total SPE–GC procedure. One possibility is early breakthrough during sample loading on the SPE

cartridge [16]. Another possibility, strong adsorption to the walls of the tubing [5, 17] is much less likely with the present set of compounds. Self-evidently, losses may also be due to the drying with nitrogen [16, 18] or to incomplete desorption of the SPE cartridge. Finally, losses of volatile analytes can occur during their transfer to the GC. The transfer temperature and the open time of SVE time are critical parameters in this respect.

As regards the role of the SPE procedure, the trace enrichment of a 10-ml HPLC-grade water sample was repeated at the spiking level of 1 μg/l. In this instance, desorption of the analytes was carried out with 260 μl of ethyl acetate into an autosampler vial and a 100-μl aliquot of the extract was injected into the GC. Figure 2B shows that the volatile analytes now all show up in the full-scan GC–MS chromatogram. Actually, all analytes that were eluted later than trimethyl thiophosphate (No. 12) were quantitatively recovered. This result indicates that the losses of volatile analytes observed in the SPE–GC procedure occurs during the transfer into the GC. However, the losses cannot be attributed to the transfer temperature or the SVE open time, because they were the same as in the earlier experiment. Obviously, the essential remaining difference between the off-line large-volume injection and the on-line transfer is the distribution of the (volatile) analytes over the length of the solvent film which is uniform in the former case, but probably not in the latter.

Since the loss of volatiles obviously is a critical aspect, methyl acetate was used as desorption solvent in the rest of this study. With this solvent, the polar and apolar analytes were desorbed from the SPE cartridge with a efficiency similar to that of ethyl acetate (see **Table 2** below). However, because the boiling point of methyl acetate is 20°C [19] below that of ethyl acetate, the more volatile analytes will be recovered more efficiently [20].

Table 2
Elution profile of several analytes in on-line SPE–GC [a].

Compound	Recovery (%) in fraction (in μl)				
	0–10	10–20	20–30	30–50	Σ 0–50
N,N-Dimethylphenol	78	10	4	0	92
Isoforon	79	9	7	0	95
Triethyl phosphate	95	0	0	0	95
1,2,4-Trichlorobenzene	83	2	0	0	85
Naphthalene	91	6	2	0	98
m-Nitrotoluene	90	7	0	0	97
Hexachlorobutadiene	64	9	0	0	73
1-Chloro-2-nitrobenzene	87	12	0	0	99
1,4-Diethoxybenzene	86	9	0	0	95
2-Methylisoquinoline	90	1	0	0	91
Ferrocene	86	6	4	1	97
1-Nitronaphthalene	99	6	0	0	105
Tributyl phosphate	90	10	5	2	107
Trifluralin	45	2	2	2	51
Hexachlorobenzene	40	5	1	0	46
Dimethoate	121	0	0	0	121
Atrazine	87	16	0	0	103
Phenanthrene	76	6	3	0	85
Diazinon	84	11	4	3	102

[a] After drying of the PLRP-S cartridge, a predetermined volume of desorption solvent (50, 30, 20, 10 or 0 μl) was flushed to waste before a 100-μl fraction was transferred to the GC; methyl acetate was used as desorption solvent.

Desorption and transfer profiles

The elution profile of a selected series of analytes from the SPE cartridge was determined by a number of on-line SPE–GC analyses of a spiked HPLC-grade water sample. The procedure was as follows. After drying of the SPE cartridge, a predetermined volume of desorption solvent (methyl acetate; 100, 50, 30, 20, 10 or 0 µl) was flushed to waste before a 100-µl fraction was transferred to the GC. The amount of each analyte in the 0–10 µl, 10–20 µl, etc., fractions was calculated by subtraction (Table 2). No analytes were found anymore in desorption solvent collected after over 50 µl had been led to waste; no data for the 50–150 µl fraction are therefore given in Table 2. Actually, most of each analyte was desorbed in the 0–10 µl fraction and desorption generally was complete within 30 µl. However, to prevent carry-over due to memory effects in the transfer line, a desorption volume of 50 µl was chosen for the SPE–GC procedure used in further experiments.

Next, in order to further study the distribution of analytes in the solvent film in the retention gap during an on-line SPE–GC transfer, we deliberately transferred a series of *n*-alkanes (C_6–C_{20}) in the first or last microlitres (cf. below) of a 100-µl injection, and investigated whether they were deposited at the front end, or in any other part, of the solvent film. The presence of the alkanes at the front end will be indicated by peak distortion if conditions are selected which cause flooding of the retaining precolumn. In a first experiment, the analytes were 'located' in the first 6 µl of a 100-µl injection. By first transferring the content of the 6-µl loop between valves V3 and V4 (cf. Figure 1) and, subsequently, 94 µl of pure solvent into the retention gap. As peak distortion was observed at a flow rate at which flooding for a standard 100-µl injection just occurred (38 µl/min; cf. Section *Optimization of introduction flow rate*), it was evident that a considerable part of the alkanes was deposited in the front part of the solvent film. When, on the other hand, the analytes were transferred in the final 6 µl of a 100-µl injection, i.e. after the introduction of 94 µl of pure solvent, no peak distortion was observed even at a flow rate of 80 µl/min, i.e. when about 60 µl of solvent flooded the retaining precolumn.

In conclusion, during an on-line SPE–GC transfer, the major part of all analytes tested will be situated in the front part of the solvent film in the retention gap, because they are desorbed and transferred with the first 10–20 µl of the desorption solvent (cf. Table 2).

Influence of the desorption volume

We next studied whether the amount of desorption solvent had an important influence on the loss of volatiles. When using 100 µl rather than 50 µl of methyl acetate for the on-line desorption step, and using the same injection temperature, pressure and injection rate, the loss of volatiles was higher. This was demonstrated for on-line SPE–GC of a 10-ml HPLC-water sample spiked at the 0.5 µg/l level. To quote two examples, the recoveries of o-chlorotoluene and indene decreased from 42 to 11% and 78 to 29%, respectively, when increasing the desorption volume from 50 µl to 100 µl. However, even with 50 µl, the losses were still significant for all analytes with an elution temperature of ca. 100°C or below (**Table 3**). The results of the on-line SPE–GC transfer were essentially the same as those obtained by means of a large-volume injection used to simulate an on-line SPE–GC transfer; here, the analytes were transferred in a plug of 6 µl, followed by 44 or 94 µl of pure solvent. This result further supports the hypothesis that the desorption-cum-transfer profile is the main cause of the loss of volatile compounds, and suggests that one should use only 50 µl of desorption solvent, as was found to be necessary above.

Table 3
Recoveries of fourteen test compounds using on-line SPE–GC of 10 ml water or a transfer simulated by a large-volume injection (LVI)[a].

No.	Compound	Elution temperature (°C)	Recoveries (%) for desorption volume (µl) of			
			50 µl		100 µl	
			LVI transfer	10 ml water	LVI transfer	10 ml water
1	Chlorobenzene	54	8	8	0	1
4	*p/m*-Xylene	54	8	11	0	1
5	Styrene	57	23	27	0	4
6	*o*-Xylene	64	14	16	0	1
7	Methoxybenzene	72	45	47	7	17
9	*o*-Chlorotoluene	80	37	42	3	11
11	Benzaldehyde	84	74	73	42	51
18	1,2-Dichlorobenzene	99	70	74	31	50
20	Indene	101	71	78	32	29
27	Nitrobenzene	112	91	99	84	90
40	Naphthalene	127	92	94	79	87
51	Methylnaphthalene	144	97	99	91	95
60	Acenaphthene	170	99	98	98	98
81	Metolachlor	225	100	102	102	102

[a] In LVI, the first 5 µl of desorption solvent contained all analytes. For further details on desorption with 50 µl or 100 µl of methyl acetate, see text. All experiments were carried out in duplicate.

Summary

The combined results of the present section allow us to improve our earlier (cf. Section *Loss of volatile analytes with conventional on-line SPE–GC*) classification of the analytes in three groups, i.e. volatile (compounds Nos. 1–10), semi-volatile (compounds Nos. 11–49) and high-boiling (compounds Nos. 50–81) analytes.

The volatile analytes are lost more or less completely (recovery below 20%) when using 100 µl of desorption solvent. With 50 µl, recoveries are still below 50%. Because they have an elution temperature 0–26°C above the injection temperature, these analytes are only partly trapped by the solvent film [21].

The semi-volatile analytes (elution temperatures 30–85°C above the injection temperature) showed recoveries between 29 and 99% depending on the analyte and the amount of desorption solvent. To quote examples, from analytes such as nitrobenzene, recoveries were above 90% for desorption with 50 µl, and above 75% for desorption with 100 µl of methyl acetate, while for analytes such as 1,2-dichlorobenzene the corresponding recoveries were ca. 70% and ca. 40%, respectively. In nearly all cases, peak deformation could be observed in the mass chromatogram; some fronting, taking the shape of a very low seat, was observed in front of the actual peak. These analytes are partially up to nearly fully trapped by the solvent film [21]. If no solvent film is present, as will occur when the SVE is closed only after all solvent has evaporated, these analytes are easily lost. It should be added that the analytes cover a wide polarity range with many of them having a polarity considerably different from that of the solvent. This obviously somewhat hampered solvent trapping.

The high-boiling analytes (elution temperature 90–171°C above the injection temperature) invariably showed recoveries of, at least, 91%. They were not lost if the SVE

was closed too late, i.e., after evaporation of the last drops of solvent, and, no prepeaks were observed. These analytes are fully reconcentrated by the retention gap effect, i.e. during their transfer from the retention gap to the retaining precolumn which displays much higher retention [22, p. 184], and do not require any solvent trapping. This is in agreement with data reported by Grob: analytes move through the retention gap at temperatures 100–140°C below their elution temperature and the reconcentration of analytes by internal cold-trapping on the analytical column requires a temperature difference of about 90°C between the injection and elution temperature ([22], p. 215).

Obviously, analytes showing low recoveries due to the SPE procedure itself have not been considered in the above discussion.

Use of a presolvent

Two aspects may be considered to be the cause of the (partial) loss of the volatile and semi-volatile analytes: (i) a delay in the formation of the solvent film at the start of the injection and (ii) an early escape of non-fully-trapped analytes deposited at the front end of the solvent film. Grob has reported that some of the solvent introduced into the retention gap will evaporate concurrently, because eluent evaporation starts immediately upon starting the transfer to the GC. However, Grob also found that this concurrent evaporation is a rather minor effect ([22], p. 246). Actually, the experiments of Table 3 on the much larger losses found with 100 µl rather than 50 µl of desorption solvent suggest that the amount of solvent introduced after the analytes themselves have been transferred is also important. During the transfer, a solvent film of about 3 m length (see footnote (c) of Table 5) containing about 20 µl of solvent was deposited in the retention gap (assuming a flooded zone of about 10 µl/min [23]). Although there was a strong pressure drop along this solvent film due to the presence of the SVE, there was no risk that the eluent reached a zone in which the boiling point equaled the column temperature ([22], p. 218), as the injection temperature of 54°C was below the boiling point of methyl acetate at atmospheric pressure, 57°C [19]. Therefore, a delay in the formation of the solvent film at the start of the injection or concurrent evaporation of the solvent film further in the retention gap cannot fully explain our observations. The increase of the pressure during the transfer was not of much influence, as transfers at a constant head pressure of 80 kPa resulted in a similar loss of the volatile and semi-volatile analytes (see Table 5, 0-µl presolvent data).

If an analyte is not fully trapped by the solvent film in the retention gap, i.e., if it is also present in the gaseous phase, it will move through the retention gap with a higher velocity than the front end of the solvent film. If such a compound catches up with this front, it will not be retarded anymore and will be lost through the SVE. This is schematically shown in Figures 3A and B which depict this situation for a volatile compound which is deposited at the front end of the solvent film. During injection, that amount of the analyte already injected moves towards the front end of the film and then is lost through the SVE (Figure 3A). At the end of the solvent evaporation process, the analyte has been lost completely (Figure 3B). It should be kept in mind here that the loss of non-fully-trapped volatiles is more critical in on-line SPE–GC than with conventional large-volume injections because of the non-uniform distribution of the analytes in the solvent film, i.e. because the major part of the analytes is deposited in the front part of the solvent film.

The creation of a solvent barrier in front of the sample plug by introducing a small amount of organic solvent, so-called presolvent, to ensure that a solvent film is already present in the retention gap when the introduction of the analyte-containing desorption solvent starts (Figure 3C), should prevent the loss of volatiles in on-line SPE–GC. To our best knowledge, the concept of a solvent barrier in front of the sample plug (although suggested by Dean for 40-µl injections in packed-column GC [8]) has not been applied to large-volume on-column injections yet. For the loop-type interface, injection of a co-solvent has been reported [24]. However, this approach was not studied by us, because the solvent peak of the additional higher boiling solvent may well obscure the early eluting compounds.

If the velocity of the analyte through the retention gap is lower than the movement of the rear end of the solvent film due to evaporation after the injection has been completed, and enough solvent is present in front of the analyte, the analyte will be enriched in the rear part of the solvent film (Figure 3D). It will only start to move through the retention gap towards the retaining precolumn after the last drop of solvent has evaporated. Analyte loss due to a delayed formation of the solvent film will also be prevented by the introduction of the presolvent prior to the desorption.

Amount of presolvent

The potential of using a presolvent for SPE–GC of volatile analytes was studied by simulating the analyte desorption by large-volume injections, i.e. a 6-µl sample plug containing the analytes and, next, 44 µl of pure methyl acetate were introduced into the GC (cf. above). Different from the earlier experiments, volumes of 10 to 50 µl of pure methyl acetate, the so-called presolvent, were introduced into the retention gap prior to the analyte transfer. The SVE was switched to the 'open' position prior to the introduction of the

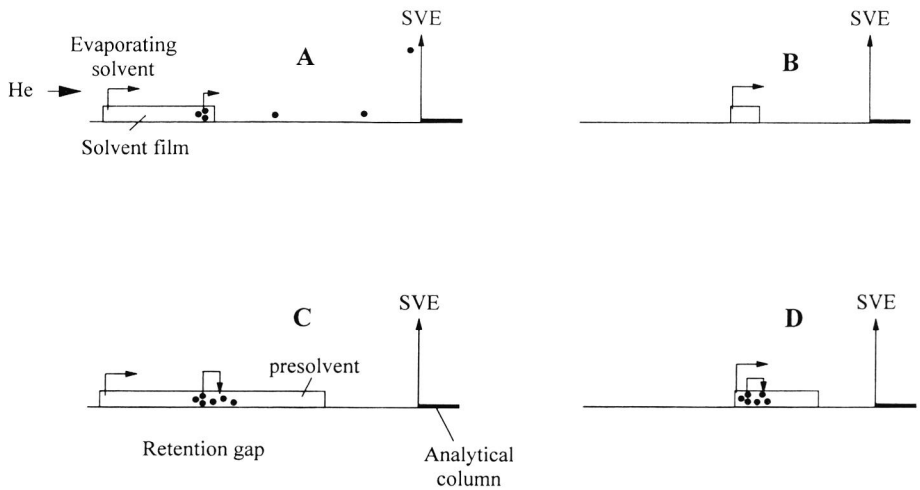

Figure 3

Scenario for analytes (indicated by •) which are not fully trapped by the solvent film during an on-line SPE–GC transfer. During injection these analytes are deposited (A) at the front of the solvent film if there is no presolvent, or (C) behind a solvent barrier if a presolvent is used. At the end of solvent evaporation, analytes (B) have been lost without presolvent, but (D) are recovered with presolvent.

Table 4
Dependence of analyte recoveries of a large-volume injection simulating an on-line SPE–GC transfer on amount of methyl acetate introduced as presolvent into the GC prior to desorption with 50 µl methyl acetate [a].

No.	Compound	Recoveries (%) for a presolvent volume of			
		0 µl	10 µl	20 µl	30 µl
1	Chlorobenzene	5	7	70	**97**
4	*p/m*-Xylene	7	8	72	**95**
5	Styrene	22	34	**86**	**100**
6	*o*-Xylene	9	14	**85**	**99**
7	Methoxybenzene	40	66	**95**	**100**
9	*o*-Chlorotoluene	33	54	**94**	**96**
11	Benzaldehyde	70	**102**	**100**	**103**
18	1,2-Dichlorobenzene	62	**89**	**95**	**97**
20	Indene	64	**94**	**96**	**101**
27	Nitrobenzene	**88**	**100**	**95**	**100**
40	Naphthalene	**89**	**96**	**95**	**99**
51	Methylnaphthalene	**95**	**94**	**95**	**96**
60	Acenaphthene	**99**	**100**	**99**	**101**
81	Metolachlor	**99**	**100**	**102**	**99**

[a] For the sake of convenience, not all analytes present in the test mixture are given in this table. Recoveries above 80% are shown in bold print. For more details, cf. text.

presolvent and closed before the last drop of solvent had evaporated. A 5 m x 0.32 mm I.D. DPTMDS-deactivated retention gap and a 1.5 m x 0.32 retaining precolumn (PS-264, 0.25 µm film thickness) were used. The test mixture contained twenty compounds.

As the data of **Table 4** show, in the absence of presolvent, only methylnaphthalene, acenaphthene and metolachlor were recovered quantitatively. Even if only 10 µl of presolvent were used, the situation changed considerably. Now benzaldehyde, indene and all later eluted analytes were recovered quantitatively. With 20 µl of presolvent, the recoveries of the volatile compounds (Nos. 1–10) improved markedly, and with 30 µl all analytes were recovered quantitatively. A further increase to 50 µl of presolvent did not have any further beneficial influence. Chromatograms which vividly illustrate the marked effect of the presolvent are given in **Figure 4**.

The above results indicate that mixing of the sample plug and the presolvent which may occur to some extent [10], does not ruin the effect of the introduction of the presolvent. Obviously, in the on-line SPE–GC–MS procedure, the SPE cartridge has to be filled nearly completely with desorption solvent prior to the transfer of presolvent and desorption of the analytes (cf. Table 1).

Influence of retention gap and retaining precolumn

Next, the influence of the retention gap and the type of coating and film thickness of the retaining precolumn (for details, see **Table 5**) were studied by varying the amount of presolvent used. In this case, a total volume of 100 µl of methyl acetate, i.e. of presolvent plus desorption solvent, was always injected, because the same amount of solvent would then be left in the GC provided the SVE was closed at the same time.

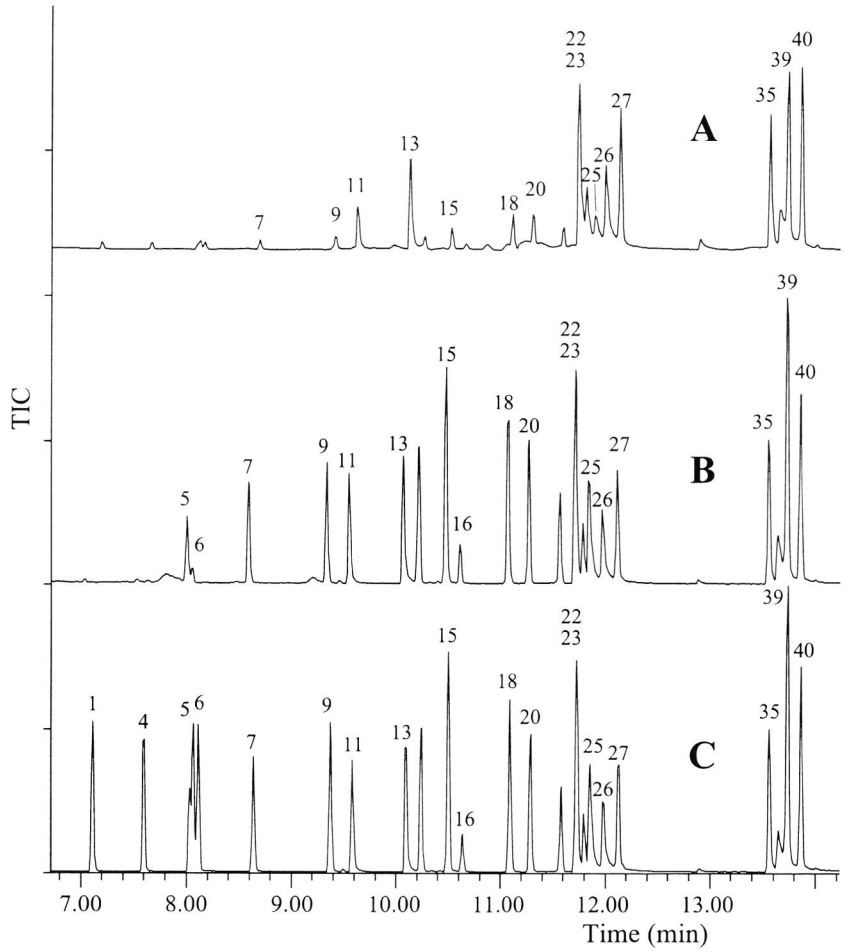

Figure 4
TIC trace of a simulated on-line SPE–GC–MS transfer using (A) no, (B) 20 µl and (C) 50 µl of presolvent prior to desorption with 50 µl of methyl acetate. For further details, see text. For peak assignment, see Table 6.

When no presolvent was introduced before the 6-µl sample plug, most of the volatile and semi-volatile analytes were at least partly lost in all set-ups and essentially quantitative recovery started with methylnaphthalene (No. 51). As Table 5 shows, the type of retaining precolumn used was not particularly important. Even without a retaining precolumn, methylnaphthalene and later eluted analytes were quantitatively recovered, either with or without using a presolvent. The mutual differences found if no presolvent was used (No. 27 vs. No. 51), may well be caused by different delays in the formation of the solvent film at the start of the injection.

When 20 µl of presolvent were introduced, methoxybenzene (No. 7) was the first quantitatively recovered analyte in nearly all cases. With 50 µl of presolvent, all volatile analytes were quantitatively recovered irrespective of the set-up selected.

Table 5
Dependence of loss of volatile analytes for several set-ups using various amounts of presolvent.

Retention gap [a]	Retaining precolumn		First recovered compound [b] using volume of presolvent of		
	type	film (μm)	0 μl	20 μl	50 μl
DPTMDS [c]	no	no	51	7	1
DPTMDS [c]	HP-5-MS	0.25	27	7	1
DPTMDS	PS-264	0.25	51	7	1
DPTMDS	PS-264	0.5	51	7	1
DPTMDS	PS-264	1.0	27	7	1
DPTMDS	DB-1701	0.25	51	7	1
OV-1701	DB-1	1.0	51	11	1

[a] DPTMDS, diphenyltetramethyldisilazane-deactivated; OV-1701, coated with OV-1701-OH.

[b] First test compound of Table 4 with at least 90% recovery compared with 5-μl on-column injection; for compound number, see Table 4. On-line SPE–GC transfer simulated with LVI; in total 100 μl of methyl acetate were injected in all experiments.

[c] If no retaining precolumn was used, a home-made 'flooding' detector was used for optimization and control of the injection [30]. The injection rate was chosen so that the flooded zone, which is further pushed into the GC after the end of the injection, reached the point where the 'flooding' detector was installed, i.e. after 3 m of retention gap, shortly after the end of the injection. To verify correct functioning, the 'flooding' detector was also used for one configuration containing a retaining precolumn.

In conclusion, the introduction of presolvent prior to the transfer of the analytes is much more efficient in the trapping of volatile analytes than the use of a retaining precolumn. The increased recoveries in the presence of a presolvent are due to increased trapping by the solvent film in front of the analytes and not to increased phase soaking of the retaining precolumn, because similar results were obtained without a retaining precolumn. Here, it should be kept in mind that we used a rather polar solvent, because the desorption of polar as well as apolar analytes was our goal. With a different type of solvent, phase soaking may well have a larger influence on the trapping of the more volatile analytes.

Methyl acetate vs. ethyl acetate

When ethyl acetate rather than methyl acetate was used for the (simulated) on-line SPE–GC analysis of volatiles (50 μl of presolvent prior to desorption with 50 μl of solvent; no retaining precolumn), the first compound that was quantitatively recovered was o-chlorotoluene. The recoveries of monochlorobenzene and p/m-xylene were a mere 45% and 34%, respectively, rather than the 95–97% obtained with methyl acetate (experiments of Table 5). Therefore, methyl acetate was preferred as desorption solvent.

On-line SPE–GC–MS analysis of river water using a presolvent

The optimized on-line SPE–GC–MS procedure was applied to the analysis of 10 ml of river Rhine water samples (sampled at Lobith, the Netherlands; 26 April 1995) spiked at the 0.5 µg/l level (**Figure 5**A), with Figure 5B showing the trace of the non-spiked sample. After drying of the SPE cartridge, the cartridge was nearly completely filled with methyl acetate, 50 µl of presolvent were injected into the GC and, then, the analytes were desorbed with 50 µl of methyl acetate [for details, cf. Table 1]. According to our expectations, all analytes showed up in the chromatogram due to the use of 50 µl of presolvent.

For most analytes, recoveries were satisfactory (70–115%; 76 out of the 86 test compounds) or even very good (90–105%; 48 out of 86 test analytes) (**Table 6**). Lower recoveries can generally be attributed to adsorption to capillary walls and/or valves during sampling (compound Nos. 49, 63, 69–72 and 85) [17], early breakthrough during trace enrichment (No. 79) [25] or inefficient trapping by the solvent film (No. 3) [26]. The recoveries of the analytes which were partly lost due to adsorption could be increased by adding 30% of methanol to the sample prior to analysis. To quote two examples, the recovery of chlorodecane increased from 25 to 76%, and that of hexachlorobenzene from 51 to 99%. However, the recoveries of the more polar analytes such as compound Nos. 11–14 then, of course, decreased. Actually, if analytes spanning such a wide polarity range have to be monitored, two different SPE–GC–MS runs are the best solution to obtain high recoveries for all, apolar and polar, analytes. As the aim of this study was to devise a method for monitoring

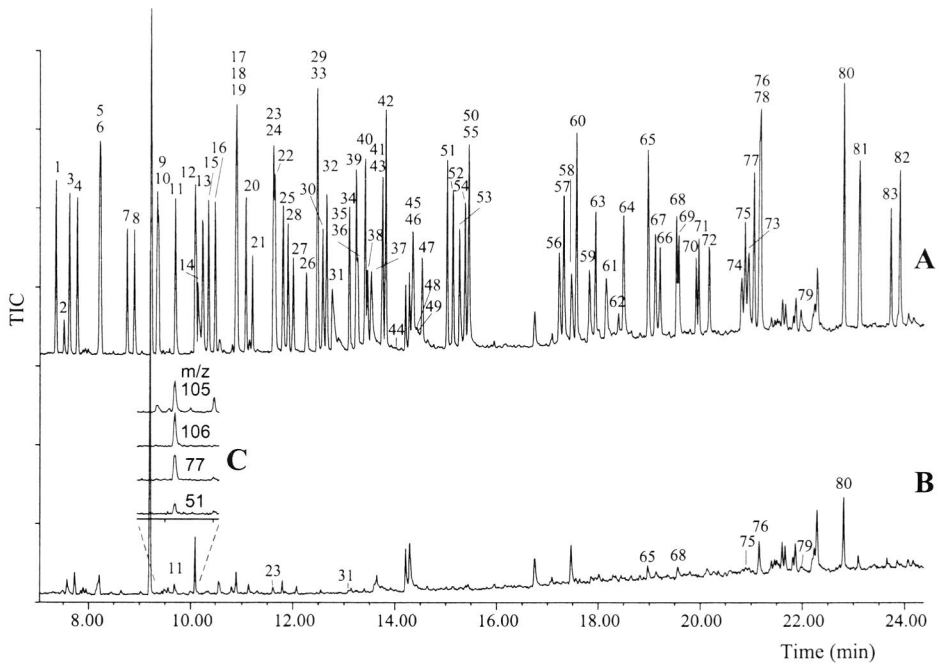

Figure 5

TIC chromatogram for SPE–GC–MS of 10 ml of river Rhine water (B) non-spiked and (A) spiked at the 0.5 µg/l level with 86 microcontaminants. 50 µl of methyl acetate were used as presolvent. For peak assignment, see Table 6; all peaks up to No. 83 are shown. The insert (C) shows the mass chromatograms of four characteristic masses of benzaldehyde (m/z 51, 77, 105 and 106). The time scale for the mass chromatogram is twice as large as for the TIC chromatogram.

Table 6
Analyte recoveries and RSD data for on-line SPE–GC–MS of 10 ml of river Rhine samples spiked at the 0.5 µg/l level.

No.	Compound	Recovery (RSD) [a]		No.	Compound	Recovery (RSD) [a]	
		%	(%)			%	(%)
1	Monochlorobenzene	100	(4)	45	Quinoline	100	(14)
2	Chlorohexane	80	(4)	46	1-Chloro-4-nitrobenzene	107	(4)
3	Ethylbenzene	62	(8)	47	1-Chloro-2-nitrobenzene	103	(8)
4	*p/m*-Xylene	102	(7)	48	Isoquinoline	90	(16)
5	Styrene	103	(1)	49	Chlorodecane	25	(25)
6	*o*-Xylene	100	(2)	50	1H-Indole	101	(3)
7	Methoxybenzene	99	(9)	51	Methylnaphthalene	94	(2)
8	1,2,3-Trichloropropane	98	(2)	52	1,4-Diethoxybenzene	98	(2)
9	*o*-Chlorotoluene	94	(2)	53	2-Methylisoquinoline	93	(19)
10	Propylbenzene	97	(8)	54	Ferrocene	96	(14)
11	Benzaldehyde	107	(3)	55	1,2,4,5-Tetrachlorobenzene	76	(3)
12	Trimethyl thiophosphate	98	(2)	56	3,4-Dichlorobenzeneamine	87	(4)
13	Benzonitrile	100	(2)	57	Dimethyl phthalate	101	(3)
14	2,4,6-Trimethylpyridine	90	(7)	58	1,3-Dinitrobenzene	110	(4)
15	1,3-Dichlorobenzene	94	(2)	59	4-Butoxyphenol	104	(1)
16	1,4-Dichlorobenzene	94	(1)	60	Acenaphthene	98	(1)
17	5-Ethyl-2-methylpyridine	110	(8)	61	3-Nitroaniline	83	(5)
18	1,2-Dichlorobenzene	97	(1)	62	1-Naphthalenol	99	(4)
19	Indane	97	(1)	63	Pentachlorobenzene	65	(1)
20	Indene	99	(1)	64	2,5-Diethoxyaniline	77	(2)
21	Butylbenzene	79	(3)	65	Diethyl phthalate	106	(1)
22	*N*-Methylaniline	95	(1)	66	1-Nitronaphthalene	108	(1)
23	Acetophenone	105	(2)	67	Sorbofuranose derivative [b]	102	(2)
24	1-Octanol	92	(12)	68	Tributyl phosphate	105	(1)
25	2-Methylbenzeneamine	83	(9)	69	1-Chlorotetradecane	61	(6)
26	*m/p*-Methylphenol	82	(15)	70	Trifluralin	57	(4)
27	Nitrobenzene	101	(3)	71	1,4-Dibutoxybenzene	57	(2)
28	*N,N*-Dimethylaniline	98	(2)	72	Hexachlorobenzene	51	(1)
29	*N,N*-Dimethylphenol	95	(5)	73	Dimethoate	108	(8)
30	Isoforon	98	(13)	74	Simazine	109	(8)
31	Triethyl.phosphate	97	(19)	75	Atrazine	108	(2)
32	*N*-Ethylaniline	95	(2)	76	Tris(2-chloroethyl) phosphate	112	(3)
33	1,3,5-Trichlorobenzene	86	(3)	77	Phenanthrene	88	(1)
34	1,4-Dimethoxybenzene	99	(3)	78	Diazinon	103	(1)
35/36	2,4+2,6-Dimethylaniline	82	(13)	79	Caffeine	29	(8)
37	2,4-Dichlorophenol	94	(12)	80	Dibutyl phthalate	102	(1)
38	Methoxyaniline	84	(10)	81	Metolachlor	100	(1)
39	1,2,4-Trichlorobenzene	88	(3)	82	Fluoranthene	73	(1)
40	Naphthalene	100	(2)	83	Chlorooctadecane	74	(6)
41	*m*-Nitrotoluene	97	(3)	84	Pyrazone	113	(8)
42	1,2,3-Trichlorobenzene	92	(4)	85	Di-2-ethylhexyl phthalate	66	(2)
43	Hexachlorobutadiene	75	(7)	86	Dioctyl phthalate	74	(5)
44	*α,α,α*-Trichlorotoluene	9	(40)				

[a] RSD: n = 7.
[b] 1,2:4,6-bis-*O*-(1-methylethylidene)-*α*-L-Sorbofuranose.

river water in one run, no modifier was added to the sample. The low recovery for α,α,α-trichlorotoluene can be attributed to a slow reaction with water [27]. Analyte recoveries were fully comparable with those obtained using ethyl acetate as desorption solvent [28].

For a large majority of all analytes (73 out of the 86 compounds) the repeatability was good with RSD values of 1–9% (n = 7). Interestingly, good repeatability was even obtained for the apolar analytes yielding low recoveries, such as trifluralin (RSD, 4%) and hexachlorobenzene (RSD, 1%). Higher RSD values were observed when the recovery was below 30% (compound Nos. 44 and 49) and for some rather polar and slightly tailing compounds (Nos. 24, 26, 38, 45, 48 and 53). In the latter case integration problems were the main cause.

The linearity was determined by spiking river water in the 0.15–1 μg/l range (four data points). It was satisfactory for 76 out of the 86 compounds (regression coefficient better than 0.98), but less good for some apolar compounds (Nos. 49, 69, 80 and 83; probably due to adsorption on the capillary walls and valves), dibutyl phthalate (blank problem), caffeine (probably due to low recovery) and some volatile compounds (Nos. 2–4 and 10).

Data analysis was automated by means of the standard procedure of the GC–MS software package (for details, see [29]). For each compound the mass chromatograms of the target ion and three characteristic qualifier ions were reconstructed and integrated in the appropriate retention time window (expected retention time ± 0.5 min). When detecting a peak in the target ion trace at the expected retention time, the presence of the target compound was considered confirmed if the ratio of responses of the target ion and each of the three qualifier ions at the corresponding retention time did not deviate more than 30% from that of the target compound.

Using the automated procedure for the river water sample, nine compounds were identified at the 0.02–0.2 μg/l level (**Table 7**). As an example, the mass chromatograms of the target ion (m/z 105) and qualifier ions (m/z 106, 77 and 51) of benzaldehyde at the expected retention time (9.7 ± 0.5 min) are shown in Figure 5C. The target and qualifier ions had a retention time of 9.69 min, and the three qualifier ion ratios met the reference values. The limit of detection (S/N=3) for the mass chromatograms of the target and qualifier ions of benzaldehyde was 4–8 ng/l.

For the total set of analytes tested, the limits of detection were between 2 ng/l and 0.1 μg/l, the individual results being determined by the nature of the mass spectrum and the presence of interferences. In general, compounds present at the 0.02–0.05 μg/l level were detected in the target ion trace, and at 0.05–0.2 μg/l in the total ion current (TIC) trace. Above 0.1 μg/l, usually all qualifier criteria were met, as is true for tris(2-chloroethyl) phosphate and dibutyl phthalate in Table 7. The less good result for caffeine can be attributed to its low recovery of about 25%. At the 0.02–0.1 μg/l level, all qualifier ion ratios still gave the proper results for three out of the six compounds detected. If not all criteria are met, the qualifier value tends to become rather low (cf. Table 7), and identification should be done by comparing the full mass spectra. Actually, the presence of all nine compounds detected in the river water was then confirmed satisfactorily. To show an example, the mass spectrum acquired at 13.11 min for the non-spiked sample (**Figure 6**A) is closely analogous to the reference spectrum of triethyl phosphate (Figure 6B), i.e. all nine major mass peaks of the reference spectrum show up in the acquired spectrum, confirming the presence of triethyl phosphate.

The system proved to be robust and was used for the analysis of more than 200 tap and river water samples.

Table 7
Result of automated data analysis of 86 micropollutants in 10-ml river water sample.

No.	Compound	Identification		Concentration (µg/l)
		Correct qualifier ion ratios[a]	Qualifier value[b]	
11	Benzaldehyde	3	94	0.04
23	Acetophenone	3	81	0.02
31	Triethyl phosphate	1	41	0.02
65	Diethyl phthalate	2	81	0.04
68	Tributyl phosphate	3	89	0.03
75	Atrazine	2	74	0.05
76	Tris(2-chloroethyl) phosphate	3	96	0.10
79	Caffeine	2	70	0.11
80	Dibutyl phthalate	3	99	0.21

[a] The calculated ratio of the responses of each qualifier ion and the target ion was considered correct if it did not deviate more than 30% from that of the target compound.
[b] Qualifier value compares qualifier ion ratios with those of target compound in reference database on scale of 100 (for details, see [29]).

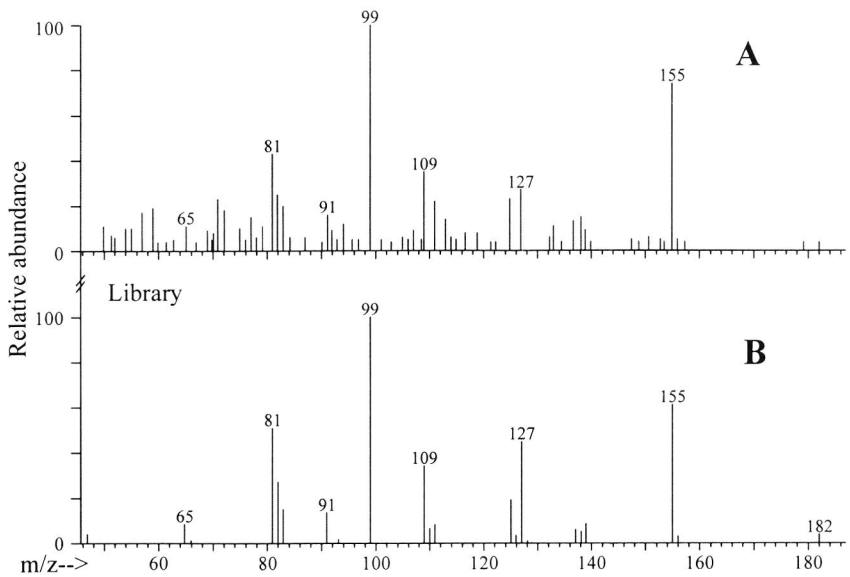

Figure 6
Mass spectrum of peak (A) observed at 13.11 min in the SPE–GC–MS chromatogram of Figure 5B and (B) library mass spectrum of triethyl phosphate.

3.1.4 Conclusions

The application range of on-line SPE–GC–MS of aqueous samples has been extended to include volatile analytes down to monochlorobenzene. The introduction of about 30–50 µl of methyl acetate as a presolvent prior to the desorption of the analytes from the SPE cartridge with 50 µl of organic solvent is sufficient to recover the volatile analytes when using an on-column interface. Methyl acetate is superior to ethyl acetate as presolvent and desorption solvent, because more volatile analytes can be determined, while the desorption efficiency is the same. Actually, when using 50 µl of presolvent, the use of a retaining precolumn did not have any significant influence on the recovery of the volatile analytes. Over eighty microcontaminants which covered a wide range of volatility and polarity were determined in 10 ml of spiked and non-spiked surface water samples down to the 0.02–0.05 µg/l level using full-scan mass selective detection. For a large majority of the analytes studied, the recovery and repeatability data at the trace-level were highly satisfactory. Actually, with conventional off-line SPE the loss of volatiles like 1,4-xylene during sampling, drying and elution is rather critical [18], whereas with the present on-line SPE–GC system, losses do not occur because of the closed nature of the set-up.

In summary, the present system appears to be well suited for the screening of rather volatile as well as high(er)-boiling compounds, e.g., for the automated monitoring of the quality of river water.

References

[1] J.J. Vreuls, A.-J. Bulterman, R.T. Ghijsen and U.A.Th. Brinkman, *Analyst*, 117 (1992) 1701.
[2] A.J.H. Louter, U.A.Th. Brinkman and R.T. Ghijsen, *J. Microcol. Sep.*, 5 (1993) 3031.
[3] Th.H.M. Noij and M.M.E. van der Kooi, in P. Sandra and G. Devos (Editors), *Proc. 17th Intern. Symp. Cap. Chromatogr., Riva del Garda, September 1994*, Hüthig, Heidelberg, Germany, 1994, 1421.
[4] A.J.H. Louter, C.A. van Beekvelt, P. Cid Montanes, J. Slobodník, J.J. Vreuls and U.A.Th. Brinkman, *J. Chromatogr. A*, 725 (1996) 67.
[5] Th. Hankemeier, A.J.H. Louter, F.D. Rinkema and U.A.Th. Brinkman, *Chromatographia*, 40 (1995) 119.
[6] J.J. Vreuls, H.G.J. Mol, J. Jagesar, R. Swen, R.E. Hessels and U.A.Th. Brinkman, in P. Sandra and G. Devos (Editors), *Proc. 17th Intern. Symp. Cap. Chromatogr., Riva del Garda, September 1994*, Hüthig, Heidelberg, Germany, 1994, 1181.
[7] K. Grob, Jr. and H.P. Neukom, *J. High Resolut. Chromatogr.*, 9 (1986) 405.
[8] D.R. Deans, *Anal. Chem.*, 43 (1971) 2026.
[9] J. Roeraade and S. Blomberg, *Chromatographia*, 17 (1983) 387.
[10] K. Grob Jr. and M.-L. Riekkola, *Chromatographia*, 18 (1984) 197.
[11] S. Blomberg and J. Roeraade, *J. High Resolut. Chromatogr.*, 12 (1989) 294.
[12] V. Pretorius, K. Lawson and W. Bertsch, *J. High Resolut. Chromatogr.*, 6 (1983) 419.
[13] Y. Picó, J.J. Vreuls, R.T. Ghijsen and U.A.Th. Brinkman, *Chromatographia*, 38 (1994) 461.
[14] K. Grob, H.-G. Schmarr and A. Mosandl, *J. High Resolut. Chromatogr.*, 12 (1989) 375.
[15] S. Ramalho, Th. Hankemeier, M. de Jong, U.A.Th. Brinkman and J.J. Vreuls, *J. Microcol. Sep.*, 7 (1995) 383.
[16] M.L. Mayer and C.F. Poole, *Anal. Chim. Acta*, 294 (1994) 113.
[17] J. Norberg, J. Slobodník, J.J. Vreuls and U.A.Th. Brinkman, *Anal. Methods. Instrum.*, 5 (1995) 266.
[18] I.S. Deans, C.M. Davidson, D. Littlejohn and I. Brown, *Analyst*, 118 (93) 1375.
[19] R.C. Weast (ed.), *Handbook of Chemistry and Physics*, CRC Press, Boca Raton, FL, USA, 66th edition, 1985.
[20] P. Chartier, P. Gareil, M. Caude, R. Rosset, B. Neff, H. Borgognon and J.F. Husson, *J. Chromatogr.*, 349 (1985) 55.

[21] K. Grob, Jr., J. Chromatogr., 279 (1983) 225.
[22] K. Grob, in W. Bertsch, W.G. Jennings and P. Sandra (eds.), *On-line coupled LC–GC*, Hüthig, Heidelberg, Germany, 1991.
[23] Th. Hankemeier, S.J. Kok, J.J. Vreuls and U.A.Th. Brinkman, *J. Chromatogr. A*, 811 (1998) 105.
[24] K. Grob and E. Müller, *J. High Resolut. Chromatogr.*, 11 (1988) 388.
[25] I. Liska, E.R. Brouwer, A.G.L. Ostheimer, H. Lingeman, U.A.Th. Brinkman, R.B. Geerdink and W.H. Mulder, Intern. *J. Environ. Anal. Chem.*, 47 (1992) 267.
[26] K. Grob, *On-column Injection in Capillary Gas Chromatography*, Hüthig, Heidelberg, Germany, 1987, Chapter BII.
[27] *Merck Index*, ed. by P.G. Stecher, Merck & CO., Inc., Rayway, NJ, USA, 8th edition, 1968.
[28] J.J. Vreuls, W.J.G.M. Cuppen, E. Dolecka, F.A. Maris, G.J. de Jong and U.A.Th. Brinkman, *J. High Resolut. Chromatogr.*, 12 (1989) 807.
[29] *MS Chemstation Users's guide*, HP G1034C MS Chemstation Software, Hewlett Packard, Palo Alto, CA, USA, 1st edition, 1993.
[30] Appendix of Chapter 2.2 of this thesis.

3.2 On-line SPE–GC–MS of aqueous samples using a self-controlled system

Summary

The conventional solid-phase extraction–gas chromatography–mass spectrometry (SPE–GC–MS) procedure was significantly improved by (i) substantially reducing the amount of organic solvent transferred during SPE-to-GC transfer of the analytes, (ii) (automated) detection of the start of the transfer into the GC by monitoring of the helium carrier gas flow, (iii) opening of the solvent vapour exit (SVE) only after the transfer of the desorption solvent, (iv) (automated) closure of the SVE at the very end of the evaporation process and (v) the use of a retention gap oven. The novel system is self-controlled, i.e., no correction for differences of the dead volumes of SPE cartridges and optimization of the injection speed and SVE closure time are necessary any more. In addition, the quality of the retention gap was much less critical than before, the precision of the retention times of volatile analytes was improved and the system was more tolerant to variations of, e.g., the desorption solvent flow rate. Even without the introduction of a presolvent, analytes as volatile as toluene and chlorobenzene were recovered without significant losses. The analytical characteristics were fully satisfactory (typical values: recoveries, 70–110% with RSDs of 1–9%; full-scan MS detection limits, 2–15 ng/l) and the same as in conventional SPE–GC.

3.2.1 Introduction

The on-line coupling of solid-phase extraction (SPE) and gas chromatography (GC) for the (automated) analysis of aqueous samples at or below the 1 μg/l level has been described in many papers [1, 2]. The interfaces used are the on-column interface (partially concurrent solvent evaporation during injection) [2, 3], the loop-type interface (concurrent evaporation of all solvent during injection) [1] and the programmed temperature vaporizer (PTV) injector [4]. For the analysis of volatile analytes, on-column interfacing is preferred provided the sample extract is not too dirty [5, 6]. However, despite the excellent results published for real-life samples, the seeming complexity of the set-up and/or the procedure appears to discourage many potential users. It is, therefore, most interesting that several improvements were recently made [7] which make on-column large-volume injections (LVI) simpler and LVI–GC more robust: after all, LVI is the basic step in an SPE-to-GC transfer.

Most importantly, it was demonstrated that the solvent vapour exit (SVE) closure can be performed in an automated fashion, at the very end of the evaporation process, by monitoring the helium gas flow: the sharp increase of that flow observed when evaporation is completed is used to trigger SVE closure [7]. As an additional advantage, the capacity of the retention gap is significantly larger when the SVE is closed at the last possible moment [8]. Furthermore, our understanding of the processes involved in the on-column LVI–GC [7–10] and on-line SPE–GC [3] analysis of volatile analytes has improved. Due to the pressure drop along the solvent film in the retention gap which occurs when an SVE is used, solvent evaporation takes place not only at the rear end, but also along the whole length and even at the front of the solvent film [7–9]. The larger the pressure drop, the more solvent will evaporate from the front part of the solvent film. In the most extreme situation, the boiling point will be reached at the front end, which will result in fully concurrent solvent evaporation. This is also reflected by the increase of the evaporation rate found during injection. Analyte losses can therefore be severe, especially in SPE–GC, because the analytes are mainly present in the front part of the desorption solvent and, during transfer, in the front part of the solvent film. Loss of volatiles can be prevented by introducing some pure organic solvent, the so-called presolvent, into the retention gap prior to the desorption solvent. A film of pure solvent is then created in front of the analyte-containing film [3]. Admittedly, one may argue that this makes the procedure more complicated.

The performance of the retention gap is a rather critical aspect in the analysis of polar analytes in on-column LVI: the introduction of dirt into the retention gap can result in bad peak shapes of the more polar analytes after a limited number of real-life analyses. Alternatively, one can use a PTV injector for LVI [11]. However, the separation of volatile analytes from the solvent is less efficient than in a retention gap [6]. Grob et al. used the combination of a hot packed vaporizing chamber, a retention gap and SVE [6, 12]. However, with this system degradation of labile compounds in the hot packed liner can be expected to occur and the determination of very volatile analytes will probably not be successful. Another option is independent heating of the retention gap prior to starting the temperature programme of the analytical column. This can be done by putting the retention gap in a second GC oven [13, 14] or by wrapping it with heating wire in the GC oven itself [15].

The recent improvements in knowledge about and instrumentation of LVI–GC briefly indicated above, were used to re-design earlier on-line SPE–GC procedures [3]. The SPE–GC transfer procedure was optimized, especially with regard to the required volumes of

Table 1
Goals of present study.

Parameter	'Conventional' SPE–GC	Envisioned 'self-controlled' SPE-GC
Automation	Full	full
LOD [a]	20–50 ng/l	20–50 ng/l
Optimization	- SVE - injection speed - cartridge volume	not required
Retention gap	quality critical	quality not critical because of separate RG oven
Volatiles	presolvent required to prevent large losses	no significant losses even without presolvent

[a] Limit of detection in full-scan MS detection; 10-ml sample.

presolvent and desorption solvent, and automated SVE closure was implemented. Our goal was to set up a 'self-controlled' SPE–GC system as outlined in **Table 1** that can handle volatile (e.g., toluene, chlorobenzene and xylenes) as well as higher-boiling (e.g., atrazine and trifluralin) analytes without any optimization being required after exchanging the retention gap or the SPE cartridge. In addition, a separate retention gap oven was installed to facilitate the handling of relatively dirty samples without having to exchange the retention gap too frequently.

3.2.2 Experimental

Chemicals

HPLC-grade water and p.a. grade methyl acetate and isopropanol were from J.T. Baker (Deventer, The Netherlands). The organic solvents were glass-distilled prior to use. A 20 μg/ml stock solution of all test compounds in dichloromethane, which was a gift from the Institute for Inland Water Management and Waste Water Treatment (RIZA, Lelystad, the Netherlands), was kept at –20°C. For the microcontaminants used as test analytes one is referred to Table 6 below. River water samples were filtered through 0.45 μm membrane filters (Schleicher & Schüll, Dassel, Germany).

Equipment

The integrated SPE–GC–MS system has been described in some detail in Chapter 3.1 and ref. [3]. Briefly, the set-up was as follows (see **Figure 1**). The Prospekt (Spark Holland, Emmen, the Netherlands) system consisted of three pneumatic 6-port valves, an automated cartridge exchanger and a solvent delivery unit equipped with a 6-port solvent selection valve and a single-piston HPLC pump. All timed events were programmed via a software package (Hewlett Packard, Waldbronn, Germany) into the Prospekt controller unit. Additional equipment was programmed via auxiliary contact closure events of the Prospekt. A Phoenix 30 syringe pump (Carlo Erba Strumentazione, Milan, Italy), used to deliver the organic desorption solvent, was modified to switch the flow on/off by an auxiliary event. An electronically controlled 6-port valve (Valco Instruments, Houston, TX, USA) was used as

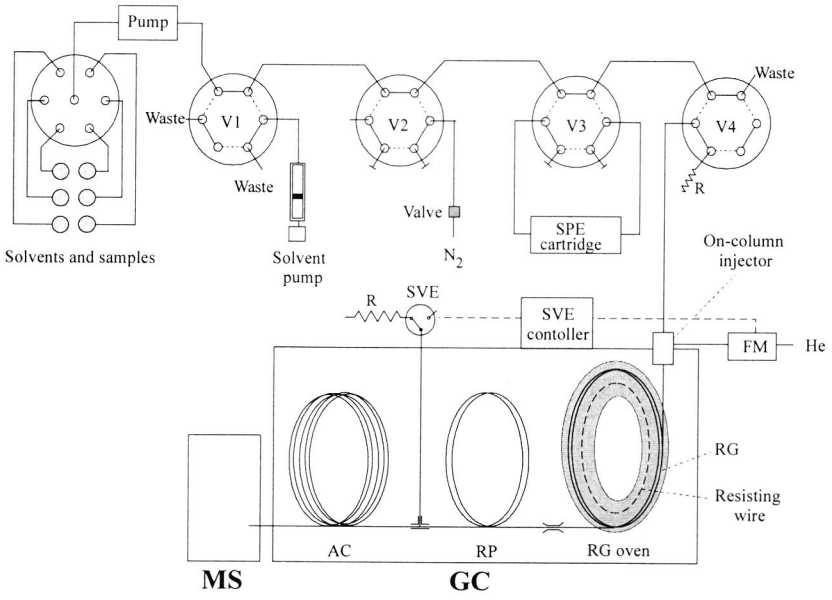

Figure 1
Scheme of on-line SPE–GC–MS system. Abbreviations: FM, flow meter, AC, analytical column; RG, retention gap; RP, retaining precolumn; R, restriction.

transfer valve, and a 24 V solenoid gas valve for actuating the nitrogen flow for drying of the SPE cartridges. The water samples were preconcentrated on a 10 mm x 2 mm I.D. cartridge packed with 20 μm, 100 Å PLRP-S styrene–divinylbenzene copolymer (Spark Holland). One cartridge could be used for at least fifty analyses. The tubing between valves V3 and V4 had a dead volume of 6 μl, and was occasionally used as sample loop for the simulation of an SPE–GC transfer. The SPE module was connected to the GC on-column injector via a 0.25 m x 75 μm I.D. deactivated fused silica capillary.

A Hewlett Packard Model 5890 Series II gas chromatograph equipped with a pressure-programmable on-column injector and a Model 5972 mass selective (MS) detector was used. MS ionization was achieved by electron ionization, ions with m/z 16–335 being monitored at 1.5 scans/sec (electron multiplier voltage, 1800 V). The injector was connected to a 2 m x 0.53 mm I.D. DPTMDS-deactivated retention gap (BGB Analytik, Zürich, Switzerland) and a 1.5 m x 0.32 mm I.D. retaining precolumn containing PS-264 (5% diphenylpolysiloxane and 95% dimethylsiloxane; film thickness, 0.25 μm; BGB Analytik). The retention gap was put in a low-weight retention gap oven which was placed in the GC oven (cf. below). An SVE was inserted between the retaining precolumn and the GC column (HP5MS, 27 m x 0.25 mm I.D., 0.25 μm film) to vent most of the solvent vapour. It was connected to a press-fit T-splitter between the retaining precolumn and GC column. The home-made SVE was installed on the top of the split/splitless injector and kept at 150°C to prevent solvent condensation. If conditions were different than those described above, this is mentioned in the text. For the experiments of Section *Influence of injection conditions on analyte loss*, a 7 m x 0.53 mm I.D. rather than a 2 m x 0.53 mm I.D. DPTMDS-deactivated retention gap was used and no retention gap oven was used.

Retention gap (RG) oven
The circular RG oven (Figure 1) was constructed from aluminum and weighed only 5 g to minimize the heat capacity. Retention gaps were inserted via an opening in the front side. Several metres of resisting wire in the oven were used for heating via a 42-V, 6-A power supply. Heating was controlled by a thermocouple and was started upon a contact closure event of the GC programme. The oven was to some extent thermally isolated by glass fibre isolation tape to the outside.

Procedures

SPE procedure
In the final procedure, each run was started with conditioning of the SPE cartridge with 120 µl of methyl acetate and 2.5 ml of HPLC-grade water. During conditioning with methyl acetate, the HPLC pump was cleaned with 2.5 ml of isopropanol to remove all air to prevent malfunctioning. The HPLC pump and all connecting capillaries up to valve V3 were then flushed with 5 ml of sample in order to cover active sites and, thus, reduce analyte losses due to adsorption. Next, 10 ml of sample were loaded on the cartridge at 2.5 ml/min. After flushing the cartridge with 1.5 ml of HPLC-grade water, it was dried for 30 min with 75 ml/min of nitrogen at ambient temperature. After analyte desorption (cf. below) and cleaning of the cartridge with 250 µl of methyl acetate, pretreatment of the next sample was started. This reduced the sample throughput time from 60 to 45 min.

SPE-to-GC transfer
In the final procedure, the analytes were desorbed with 16 µl of methyl acetate into the GC at 120 µl/min by switching valve V4. During the transfer, the SVE was closed and the oven temperature was 54°C. After the start of the transfer was detected (i.e. as soon as the decrease of the first derivative of the helium flow exceeded the pre-set threshold value of 8 ml/min^2) and a 8-sec delay to allow the introduction of 16 µl of methyl acetate for desorption, valves V3 and V4 were simultaneously switched to clean the tubing between these valves (but not the cartridge) with 26 µl of methyl acetate. Next, the SVE controller was started which, in its turn, opened the SVE and switched valve V4 to introduce 5 µl of pure methyl acetate into the GC. After switching valve V4 again, the helium flow monitoring was started (with a 5-sec delay) to allow detection of the end of the evaporation process. As soon as the first derivative of the helium flow exceeded the pre-set threshold value of 30 ml/min^2, the SVE was closed and the GC programme started (for more details, cf. [7]). After 0.01 min, the programme initiated the heating of the retention gap oven and, after 2 min, the GC oven temperature was increased at 20°C/min to 280°C, which was held for 2 min. If not stated otherwise, the head pressure (He) of the GC was 60 kPa during the transfer. It was programmed to provide constant flow during the GC oven temperature programme. MS acquisition was started 2.5 min after the start of the GC programme. When the oven temperature of 280°C was reached, the heating of the retention gap oven was switched off.

The same temperature/pressure programme was used for 2-µl or 5-µl on-column injections carried out for reference purposes.

3.2.3 Results and discussion

Use of a retention gap oven

If too much 'dirt' is introduced into an SPE–GC or LVI–GC system, the performance of the retention gap will deteriorate rapidly. As a result, the peak shapes of more polar analytes will become distorted. To study this phenomenon, a large number of surface water samples were analyzed by SPE–GC–MS using various types of retention gaps. In **Figure 2**, a series of chromatograms obtained with an OV 1701-OH-coated retention gap are shown as an example. For the second river water analysis, the peak shapes of several polar and 'critical' (as regards their peak shapes) analytes (selected from the 87-analyte test set of Figure 6 below) were satisfactory at the 0.5 µg/l level (Figure 2A). Some tailing was visible only for

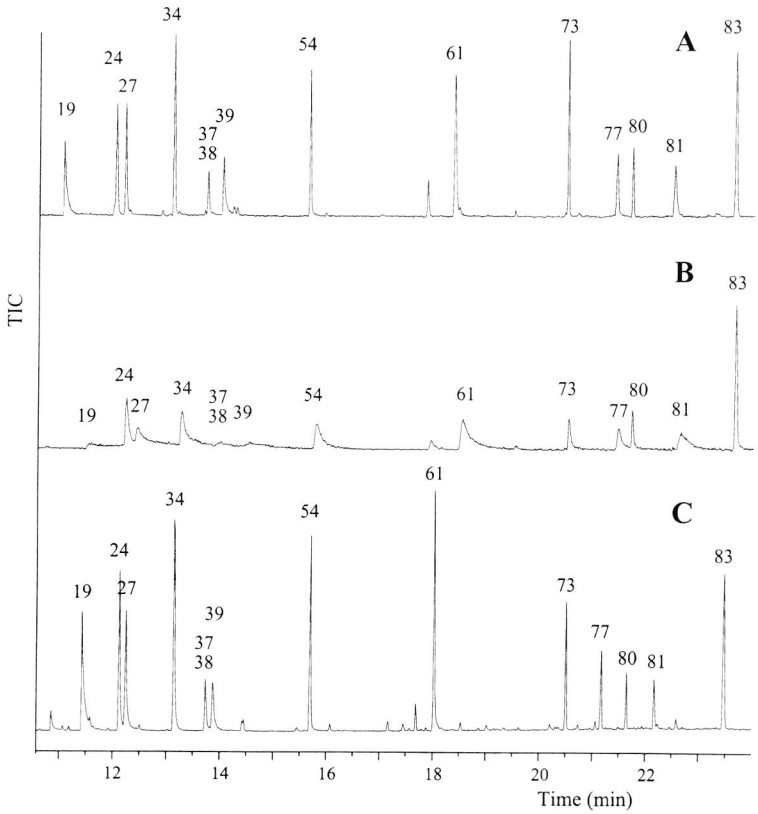

Figure 2
Reconstructed SPE–GC–MS chromatogram of ions m/z 106, 110, 162, 194, 200, and 304 of 10 ml of river Rhine water spiked at the 0.5 µg/l. The second (A) and fortieth (B) analysis of a river sample without using a RG oven are shown; (C) shows the third next analysis carried out after having inserted the retention gap into a RG oven [the slight differences in retention times and peak heights are mainly due to the use of another retaining precolumn; in addition, although the analytical column was the same, 100 river water analyses had been carried out in between]. 50 µl of presolvent and 50 µl desorption solvent (both methyl acetate) were used according to [3]; a 5 m x 0.32 mm I.D. retention gap coated with a thin film of OV 1701-OH (BGB Analytik) was used. For peak assignment, see Table 6.

5-ethyl-2-methylpyridine and 2,4-dichlorophenol (Nos. 19 and 39). However, after forty analyses, most of the polar analytes showed serious tailing and some peaks, such as that of 5-ethyl-2-methylpyridine, had essentially disappeared. Obviously, the deactivation of the retention gap had been seriously affected by the river water samples and/or dirt had been deposited in the retention gap. Similar results were obtained with other retention gaps, such as DPTMDS-deactivated retention gaps and a deactivated retention gap of Hewlett-Packard. Results for the same type of retention gap sometimes varied from batch to batch. However, in the final analysis, the outcome was the same, insufficient robustness: the peak shapes of most of the more polar analytes seriously deteriorated after some 20–30 analyses.

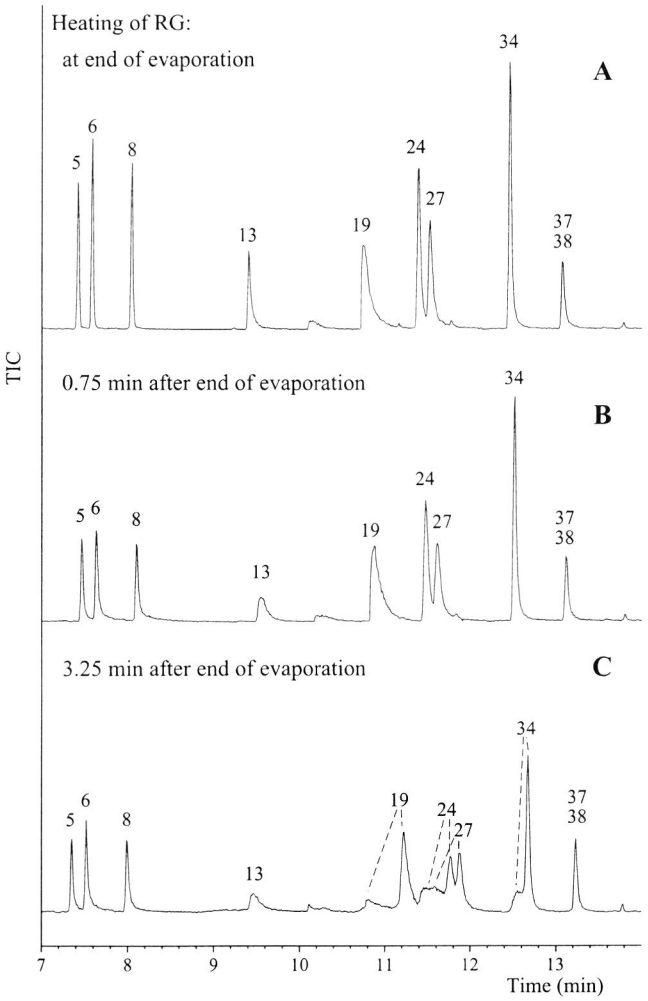

Figure 3

Reconstructed GC–MS chromatogram of ion m/z 106 of a 10-µl injection of a 10-µg/ml standard solution. The SVE was closed during and after injection. Heating of the RG oven was started (A) immediately, (B) 0.75 min and (C) 3.25 min after the end of the evaporation of the solvent. The retention gap had been used for 40 analyses of river water prior to this experiment. For peak assignment, see Table 6.

From among the several options open to overcome this problem, heating of the retention gap prior to the start of the temperature programme of the analytical column was our first choice because it will still allow the analysis of volatile and thermolabile analytes. A low-heat-capacity RG oven was constructed and placed in the GC oven; this keeps the change of the total set-up small; no heated transfer line is required and no cold spots can occur, because the RG oven was placed inside rather than outside the GC oven. Besides, if required, e.g. for partial concurrent solvent evaporation during injection, precise thermostating by the GC oven during analyte transfer (when the heating of the RG oven is not switched on) is possible. Heating of the RG oven was started by a contact closure signal of the GC. Within 2 min, the temperature of the RG oven was 150°C higher than that of the GC oven, and within 4 min, 200°C higher. The transfer line was introduced into the heated zone of the retention gap, and the press-fit connection to the retaining precolumn was positioned just outside the RG oven.

The retention gap of Figure 2B that had been used for 40 river water analyses, was put in the RG oven. The SPE–GC–MS chromatogram of Figure 2C - which was obtained for the third next sample - clearly demonstrates that the peak shapes of all analytes improved dramatically: peak shapes are essentially the same as those of the second river water analysis of Figure 2A. If the analysis of volatile polar compounds is the goal, it is important that heating of the RG oven is started just at the end of the solvent evaporation: **Figure 3** shows that the peak shapes of the volatile and semi-volatile polar analytes were satisfactory if this was indeed done (Figure 3A), but that the peak shapes of, e.g., benzaldehyde and 5-ethyl-2-methylpyridine (Nos. 13 and 19, respectively) distinctly suffered if heating of the RG oven was begun 0.75 (Figure 3B) or 3.25 min (Figure 3C) later. In the latter case one can also observe the formation of broad pre-peaks for 5-ethyl-2-methylpyridine, *N*-methylaniline, 2-methylaniline and N-ethylaniline (Nos. 19, 24, 27 and 34, respectively). Therefore, the SVE was closed and the retention gap heating started, as soon as the SVE controller detected the end of the evaporation.

Influence of injection conditions on analyte losses

In a previous paper [3], the influence of the injection and SPE desorption conditions on analyte recoveries was studied in some detail. For the present project, a 0.53 mm I.D. rather than a 0.32 mm I.D. retention gap coupled to a 0.32 mm I.D. retaining precolumn retention gap was used because the pressure drop along the solvent film then is smaller. As discussed in the *Introduction*, this should result in less evaporation of the solvent from the front end of the solvent film and in less loss of volatile analytes. For a brief (re-)assessment of the dependence of the loss of volatiles on the injection speed and SVE position (open/closed), 10-ml HPLC-grade water samples spiked at the 1-µg/l level were analyzed using injection speeds of 50, 100 or 200 µl/min, and with the SVE (i) open during the SPE–GC transfer and closed a few seconds before the completion of the evaporation process or (ii) closed during the transfer and opened after the transfer (**Table 2**). The results show that, with the SVE open during analyte transfer from the SPE cartridge to the GC, the volatile and some of the semi-volatile analytes are completely lost or recovered only partly. Only the high-boiling analytes with elution temperatures of 120°C or more above the injection temperature showed good recoveries of 85–110%. The results are similar to those earlier obtained for a 0.32 mm I.D. retention gap.

When increasing the injection speed from 100 to 200 µl/min, with the SVE still open, the amount of solvent that is concurrently evaporated during injection decreases and calculation (see footnote of Table 2) shows that about 28 µl rather than 6 µl of solvent film are left in the retention gap at the end of the injection. This causes a significant increase of the recoveries of the volatile analytes: the recovery of, e.g., chlorobenzene increases from 8 to 49%. A similar, though less dramatic, increase is observed for the semi-volatiles, e.g. for benzaldehyde from 73 to 92%. If the SVE is closed during the transfer and only opened afterwards, the overall results for the volatile and semi-volatile analytes were slightly better, but the injection speed – which was varied from 50 to 200 µl/min – then did not have a noticeable influence. Obviously, the loss of (semi-)volatile analytes can be reduced by reducing the amount of solvent evaporating during injection. If less solvent evaporates (for the same injection volume), the solvent film will be longer and, as the solvent evaporates mainly from the rear end, more solvent will be present ahead of the analytes. This is also important because some evaporation of solvent occurs at the front end of the solvent film, especially if the pressure drop along the solvent film is large [8, 9] – which is the reason why a 0.53 mm I.D. retention gap was chosen in this study.

Table 2
Influence of injection speed and SVE position on on-line SPE–GC analysis [a].

Compound	Elution temperature (°C)	SVE:	Recovery (%)			
			open		closed	
		injection speed:	100 µl/min	200 µl/min	50 µl/min	200 µl/min
Volatile						
Toluene	71		0	14	15	21
Tetrachloroethylene	79		0	7	8	10
Chlorobenzene	89		8	49	61	65
p/m-Xylene	94		12	52	62	59
Styrene	99		27	69	75	71
o-Xylene	99		16	59	71	67
Methoxybenzene	104		48	81	88	89
o-Chlorotoluene	112		39	78	81	72
Semi-volatile						
Benzaldehyde	114		73	92	95	99
1,2-Dichlorobenzene	129		75	90	93	88
Indene	131		78	95	97	95
Nitrobenzene	138		100	106	105	108
Naphthalene	156		96	98	96	97
High-boiling						
Methylnaphthalene	173		99	99	100	97
Acenaphthene	199		98	98	98	96
Phenanthrene	235		86	86	84	90
Metolachlor	252		102	102	102	105

[a] 10 ml HPLC-grade water spiked at the 1-µg/l level; desorption, 50 µl of methyl acetate. "open": SVE open at start of transfer and closed a few seconds before end of evaporation process; evaporation rate with SVE open, 88 µl/min; "closed": SVE closed during transfer and opened after transfer; head pressure during injection, 80 kPa; n = 2. Recoveries calculated using a 2-µl on-column injection as reference. Amount of solvent left in RG at end of injection, V_s, (see text) calculated from: $V_s = (\upsilon_{inj} - \upsilon_{evap}) \times t_{inj}$, with υ_{inj}, injection speed; t_{inj}, injection time, υ_{evap}, evaporation rate. For the experiments of this table and Table 4 below, only a limited number of the 87 test analytes were used.

Influence of SVE

To investigate the role of the SVE, an SPE–GC transfer using the presolvent option was simulated by transferring 10 µl of presolvent, next a 5-µl plug containing the test analytes and, finally, 15 µl of solvent [3]. When the SVE was not opened at all, all analytes of Table 2 but one (tetrachloroethylene, 78%), and with toluene as the most volatile compound, were quantitatively recovered (95–105%; comparison with 2-µl on-column injection). This result was according to expectations, because in this case there is no significant pressure drop along the retention gap and evaporation occurs mainly from the rear end: if there is a sufficient length of solvent film ahead of the non-fully-trapped analytes, these analytes will not be lost. When opening the SVE only at the end of the solvent transfer and closing it (automatedly) at the very end of the evaporation process, the recoveries of the analytes of Table 2 are essentially the same, viz. 95–105%, and 84% for tetrachloroethylene. The precision found with the latter procedure were good with RSD values of 1–4% and 3–7% for toluene and tetrachloroethylene (n=4) - the same as was found when keeping the SVE closed.

In conclusion, opening the SVE at the end of the transfer and automated closure just at the end of the evaporation does not have any adverse effect on analyte recovery or precision.

Table 3

Recoveries of test analytes in on-line SPE–GC using various desorption volumes of methyl acetate [a].

Compound	Recoveries (%) for various desorption volumes (in µl)					
	3 µl	6 µl	9 µl	12 µl	15 µl	40 µl
Toluene	85	88	80	86	76	32
Tetrachloroethylene	53	61	49	43	41	10
Chlorobenzene	68	87	85	80	88	52
Methoxybenzene	76	95	88	100	99	94
1,2-Dichlorobenzene	63	87	94	89	95	95
Nitrobenzene	77	93	98	93	96	98
Triethyl phosphate	84	96	102	100	100	96
Naphthalene	55	87	94	98	104	104
Ferrocene	55	81	89	90	103	109
Tributyl phosphate	70	87	92	97	91	87
Trifluralin [b)]	39	48	49	56	47	42
Atrazine	87	104	110	110	111	112
Diazinon	80	97	104	108	104	104
Metolachlor	89	105	102	111	113	114
Acenaphthene	40	73	87	93	105	106

[a] 10 ml HPLC-water spiked at 0.67 µg/l; injection speed, 120 µl/min; SVE closed during transfer; after transfer, SVE opened for experiments with desorption volumes of 12–40 µl and closed by SVE controller; transfer line removed and cleaned with pure solvent after GC run. For the sake of convenience, not all analytes present in the test mixture are given in this table and Table 5. Individual data available on request.

[b] Recovery of trifluralin known to be about 50% due to losses on capillary walls during sampling due to its hydrophobicity [3].

Optimization of desorption step

Optimization of desorption volume

The amount of solvent (methyl acetate) required for analyte desorption was optimized for (i) quantitative desorption from the cartridge and (ii) minimum loss of volatiles. In an earlier study it was observed that most of the analytes were desorbed in the first 10 µl [3], but steps smaller than 10 µl were not used and the loss of volatiles was not studied. In that study, the final compromise was 50 µl in order to clean the transfer line after desorption to prevent memory effects.

For nearly all analytes more than 50% was desorbed with the first 3 µl of methyl acetate and, for all analytes except acenaphthene (15 µl), 9–12 µl were sufficient for quantitative (>80–90%) or 'plateau' (tetrachloroethylene and trifluralin) desorption (**Table 3**). As expected, the recoveries of the volatile, but not of the other, analytes started to decrease if the desorption volume became too large (>15–40 µl). In other words, a smaller desorption volume than was used before, will cause distinctly better results.

Strategies to reduce transfer volume

Minimizing the volume of solvent transferred to the GC in order to minimize the loss of volatiles should include minimizing the solvent volume required for cleaning the (fixed) transfer line and, consequently, reliably assessment of the start of the transfer.

Detection of start of transfer. When solvent enters the retention gap via the transfer line, the helium flow rate decreases steeply mainly because of the presence of solvent vapour in the gas phase. This decrease can be detected by the SVE controller, which then in its turn stops the transfer after a pre-programmed delay time by switching the transfer valve. **Figure 4**

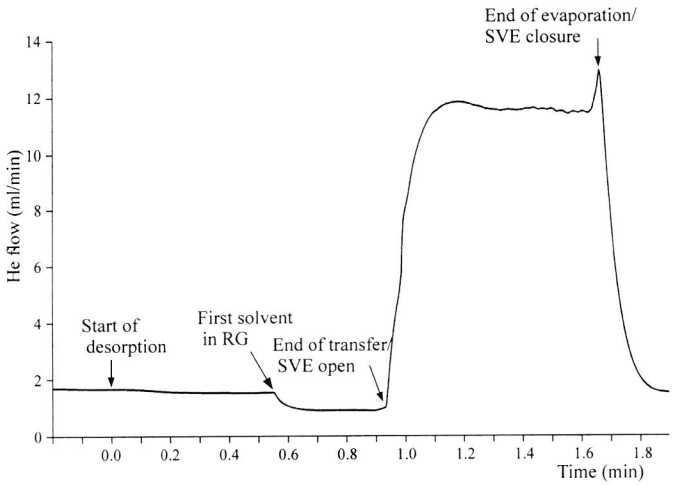

Figure 4

Helium flow rate profile of on-line SPE–GC transfer. Start of introduction of solvent into retention gap was detected by SVE controller. After introduction of 20 µl of desorption solvent at 60 µl/min, the SVE was opened. When the end of the evaporation was detected, the SVE was automatedly closed. For more details, see text. Conditions: retention gap, 3 m x 0.53 mm I.D. DPMDS-deactivated; retaining precolumn, 1.5 m x 0.32 mm I.D. PS-264 (film thickness, 0.25 µm; GC column, 28 m x 0.25 mm I.D DB5-XLB (0.25 µm film); capillary to SVE, 2.5 m x 0.25 mm I.D.; head pressure, 100 kPa.

shows the helium flow profile for the desorption of an SPE cartridge with the SVE being closed during the transfer. Desorption was started by switching valves V3 and V4 of Figure 1. After 0.50 min, the introduction of solvent into the retention gap was detected (decrease of first derivative of helium flow exceeded preset threshold value of 8 ml/min^2). After a 20-sec delay to allow the introduction of the first 20 µl of desorption solvent into the GC at 60 µl/min, the transfer valve was switched to direct the solvent to waste and the SVE was opened. At 1.61 min, the end of the evaporation process was detected by the SVE controller and the SVE closed. Detection of the start of the transfer appeared to be very reliable: during a series of 50 transfers no starts of the transfer were missed or detected too early. Obviously, detection of the start of the transfer by this method will not be possible when introducing pure presolvent into the GC system prior to the desorption of the analytes.

Optimizing cleaning of transfer line. To avoid memory effects and minimize the volume of solvent required to clean the transfer line, the transfer line should be as short as possible and have a small I.D.. A fused silica capillary of 0.25 m x 75 µm I.D. was selected, because a smaller diameter resulted in too high a backpressure during transfer. In addition, the connections to valve V4 were made such that the small channel within the rotor, which connects valve V3 and the transfer line during the transfer, connects valve V3 and waste after the transfer. This was done to effect flushing of the proper internal channel of V4 after the transfer.

The memory effect was studied for eight compounds by determining which percentage was left in the transfer line after a 10-µl injection of a 20 µg/ml solution in methyl acetate through the transfer line and flushing of the dried transfer line with 5–40 µl of methyl acetate (**Table 4**). If there was no flushing after the injection, 5–7% of most compounds was left in the transfer line (naphthalene, acenaphthene and phenanthrene, 0.3–1.5%). Flushing the

Table 4
Memory effect of several test compounds left in the transfer line after previous transfer of 10 µl of 20 µg/ml solution and subsequent flushing of transfer line with methyl acetate [a].

Compound	Per cent memory from previous transfer after flushing with				
	0 µl	5 µl	10 µl	20 µl	40 µl
Naphthalene	0.3	0.0	0.0	0.0	0.0
Acenaphthene	0.4	0.0	0.2	0.1	0.0
Atrazine	6.9	0.6	0.2	0.3	0.1
Phenanthrene	1.5	0.2	0.4	0.4	0.2
Caffeine	6.4	0.2	0.2	0.2	0.2
Metolachlor	6.7	0.3	0.3	0.4	0.1
Fluoranthene	5.4	0.2	0.3	0.3	0.0
Triphenyl phosphate	6.4	0.2	0.2	0.3	0.2

[a] Transfer line removed from injector and 10 µl of 20 µg/ml solution led through transfer line at 60 µl/min; transfer line inserted into injector and dried with He; transfer line removed and 5–40 µl of methyl acetate led through it; then inserted into injector and 50 µl of methyl acetate transferred; internal volume of transfer line, 1.5 µl. As example: 6.9% of atrazine corresponds with 2.1 ng detected in next transfer of 50 µl methyl acetate.

transfer line with 5 µl of solvent (which is about three times its dead volume) or, at the highest, 10 µl sufficed to essentially eliminate all memory effects. As the analyte concentration in the last microlitres of an on-line SPE–GC transfer is much less than 20 µg/ml, flushing with 5 µl of pure solvent after an SPE–GC transfer was considered sufficient for all further work.

Improved SPE–GC–MS procedure

On the basis of the above results, the SPE-to-GC transfer was changed as follows (cf. Figure 1). After detection of the start of the transfer, 16 µl of solvent (methyl acetate) was used to effect desorption of the analytes to the GC; next, valve V3 was switched so that the solvent was not directed through the SPE cartridge any more. The tubing up to valve V4 was cleaned with 26 µl of solvent, V4 was switched and the transfer line flushed with 5 µl of solvent in order to remove analytes from the transfer line to the retention gap. In contrast to earlier procedures, the SVE was closed during the transfer and opened when flushing of the transfer line was started (and closed automatedly by the SVE controller). Closure of the SVE during the transfer is possible because (i) less solvent is introduced, (ii) the capacity of the retention gap is larger if the SVE is closed at the very end of the evaporation process and (iii) the length of the retention gap (and, consequently, the number of active sites) is less critical due to the use of a RG oven. An injection speed of 120 µl/min was chosen, which was above the evaporation rate of methyl acetate when the SVE was open.

The recoveries of a large set of test analytes with the new SPE–GC procedure were determined using 16 or 26 µl of solvent for desorption and 5 µl of solvent for flushing. In addition, the beneficial influence of using of 10 µl of presolvent for the volatile analytes was studied. Not unexpectedly, **Table 5** shows that flushing with 5 µl did not influence recoveries significantly and that better results – i.e., for the volatiles – were obtained with 16-µl compared with 26-µl desorption. The 63–88% recoveries for the first seven analytes (excepting tetrachloroethylene) compare favourably with the 10–50% recoveries typically observed in 'conventional' SPE–GC [3]. The use of presolvent further improves the recoveries, viz. to 89–93% for the same test set. Generally speaking, the recoveries of 70–90% for volatile compounds like chlorobenzene are considered satisfactory for an SPE–GC–MS system which is used for screening purposes, and where a purge-and-trap system is used in addition for the very volatile analytes. Therefore, 16 rather than 26 µl of solvent for desorption and no presolvent (to allow the detection of the start of the transfer!) were used in the final SPE–GC procedure.

The performance of the novel on-line SPE–GC–MS procedure was tested by the analysis of 10-ml samples of river Meuse water (sampled at Eysden, The Netherlands) spiked at 0.6 µg/l with each of the 87 test analytes. All volatile analytes including toluene showed up in the chromatogram (**Figure 5**). The recoveries of the volatile analytes Nos. 1–12 were 70–100% except for tetrachloroethylene (26%) and chlorohexane (43%). The recoveries of the semi-volatiles (Nos. 13–51) were 85–105% with a few lower values for more apolar analytes due to adsorption losses (**Table 6**). Not unexpectedly, recovery data for the semi-volatile and high-boiling microcontaminants were comparable to those reported earlier (recoveries, 70–110% except for very polar and very apolar analytes due to early breakthrough and adsorption losses, respectively). The precision data were comparable to those obtained earlier (RSD, 1–9% for 82 out of 87 compounds). The precision of the retention times of especially

Table 5
Dependence of analyte recovery in SPE–GC–MS on volumes of desorption, flushing and pre-solvent [a].

Compound			Recoveries (%)			
No.	Name	Desorption + flushing:	16 + 5 µl		26 + 5 µl	
		Presolvent:	0 µl	10 µl	0 µl	10 µl
1	Toluene		63	91	27	42
2	Tetrachloroethylene		29	61	12	30
3	Chlorobenzene		77	90	63	89
5	Ethylbenzene		71	89	59	75
6	*p/m*-Xylene		78	93	65	88
7	Styrene		88	93	82	97
8	*o*-Xylene		83	93	72	98
9	Methoxybenzene		95	98	90	105
11	*o*-Chlorotoluene		85	95	80	91
13	Benzaldehyde		100	103	97	105
20	1,2-Dichlorobenzene		94	94	92	100
21	Indene		100	94	96	97
29	Nitrobenzene		101	102	106	95
33	Triethyl phosphate		104	103	102	107
42	Naphthalene		100	97	100	93
56	Ferrocene		97	98	96	96
62	Acenaphthene		98	94	101	104
70	Tributyl phosphate		84	90	88	84
72	Trifluralin		54	49	49	46
77	Atrazine		101	102	101	99
80	Diazinon		98	103	96	96
83	Metolachlor		100	101	104	99

[a] 10 ml HPLC-grade water spiked at 0.5 µg/l was analyzed (n=2); 4 m x 0.53 mm I.D. DPTMDS-deactivated retention gap.

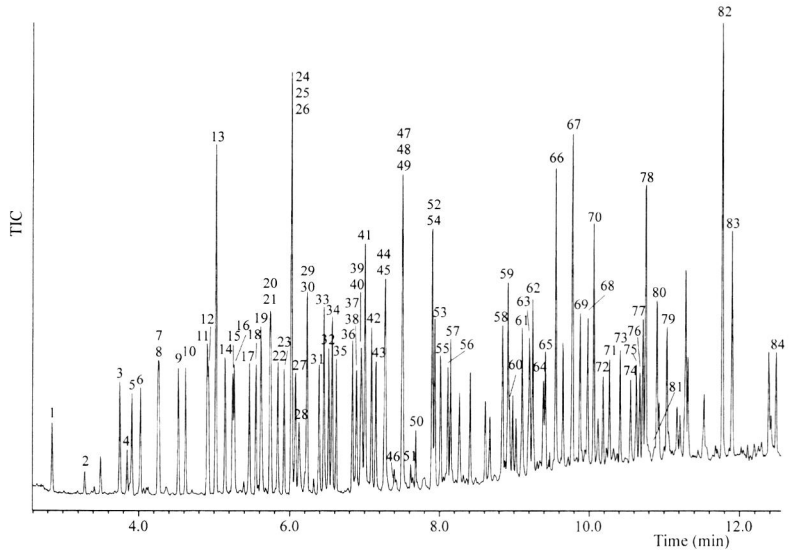

Figure 5
SPE–GC–full-scan MS chromatogram of 10 ml of river Rhine water spiked with 0.6 µg/l level of each of 87 microcontaminants (cf. Table 6). For all other conditions, see Experimental.

Table 6
Analyte recoveries and RSD [a] data for on-line SPE–GC–MS of 10 ml of river Meuse water spiked at the 0.6 µg/l level.

No.	Compound	Recovery [b] %	No.	Compound	Recovery [b] %
1	Toluene	70	45	Hexachlorobutadiene	65
2	Tetrachloroethylene	26	46	α,α,α-Trichlorotoluene	2
3	Monochlorobenzene	77	47	Quinoline	98
4	Chlorohexane	43	48/49	1-Chloro-4-nitrobenzene	101
5	Ethylbenzene	71	50	Isoquinoline	59
6	*p/m*-Xylene	76	51	Chlorodecane	14
7	Styrene	88	52	1H-Indole	105
8	*o*-Xylene	79	53	Methylnaphthalene	91
9	Methoxybenzene	96	54	1,4-Diethoxybenzene	95
10	1,2,3-Trichloropropane	97	55	2-Methylisoquinoline	99
11	*o*-Chlorotoluene	89	56	Ferrocene	96
12	Propylbenzene	78	57	1,2,4,5-Tetrachlorobenzene	77
13	Benzaldehyde	100	58	3,4-Dichlorobenzeneamine	88
14	Trimethylthiophosphate	99	59	Dimethyl phthalate	113
15	Benzonitrile	99	60	1,3-Dinitrobenzene	117
16	2,4,6-Trimethylpyridine	90	61	4-Butoxyphenol	102
17	1,3-Dichlorobenzene	92	62	Acenaphthene	88
18	1,4-Dichlorobenzene	94	63	3-Nitroaniline	89
19	5-Ethyl-2-methylpyridine	86	64	1-Naphthalenol	91
20	1,2-Dichlorobenzene	97	65	Pentachlorobenzene	62
21	Indane	97	66	2,5-Diethoxyaniline	93
22	Indene	96	67	Diethyl phthalate	105
23	Butylbenzene	72	68	1-Nitronaphthalene	104
24	*N*-Methylaniline	99	69	Sorbofuranose derivative[2]	108
25	Acetophenone	99	70	Tributyl phosphate	108
26	1-Octanol	95	71	1-Chlorotetradecane	41
27	2-Methylbenzeneamine	90	72	Trifluralin	61
28	*p*-Methylphenol	85	73	1,4-Dibutoxybenzene	58
29	Nitrobenzene	103	74	Hexachlorobenzene	43
30	*N,N*-Dimethylaniline	98	75	Dimethoate	95
31	*N,N*-Dimethylphenol	98	76	Simazine	99
32	Isoforon	101	77	Atrazine	97
33	Triethyl phosphate	94	78	Tris(2-chloroethyl) phosphate	104
34	*N*-Ethylaniline	99	79	Phenanthrene	77
35	1,3,5-Trichlorobenzene	83	80	Diazinon	99
36	1,4-Dimethoxybenzene	99	81	Caffeine	33
37/38	2,4+2,6-Dimethylaniline	90	82	Dibutyl phthalate	90
39	2,4-Dichlorophenol	75	83	Metolachlor	102
40	Methoxyaniline	94	84	Fluoranthene	51
41	1,2,4-Trichlorobenzene	81	85	Chlorooctadecane	67
42	Naphthalene	99	86	Pyrazone	102
43	*m*-Nitrotoluene	96	87	Di-2-ethylhexyl phthalate	55
44	1,2,3-Trichlorobenzene	95			

[a] RSD, 1–9% except for Nos. 1, 2, 50, 51 (10–15%) and 46 (30%) (n = 6).

[b] Lower recoveries of Nos. 2 and 4 can be attributed to their volatility, of Nos. 51, 65, 71–74, 84, 85 and 87 to adsorption losses, of No. 81 to early breakthrough and of No. 46 to degradation in water sample.

the volatile and semi-volatile analytes were improved compared to the earlier system, because the SVE was always closed at the very last moment of the evaporation. For the volatiles the standard deviations of the retention times were 0.015–0.05 min, for the semi-volatiles, 0.003–0.011 min and for the high-boiling analytes, 0.001–0.002 min. This is a gratifying result if automation of data handling is required. More importantly, the chromatogram of Figure 5 was acquired after 50 tap water samples and 25 river water samples had been analyzed on the SPE–GC–MS system. The good peak shapes of all, i.e. also the polar, analytes demonstrate the robustness of the system. Further work showed that at least 200 river water analyses (10 ml each) could be run without any part of the system being replaced, except for the automated exchange of the SPE cartridge every 20 analyses. Detection limits (S/N = 3) with full-scan MS acquisition and subsequent extraction of the appropriate reconstructed ion chromatograms, were generally 2–5 ng/l, and for a few less favourable analytes, 5–15 ng/l [due to higher fragmentation or low recovery]. The novel on-line SPE–GC–MS procedure requires no optimization: the injection speed does not have to be optimized and the SVE is closed automatedly. Only once, when setting up the system, one

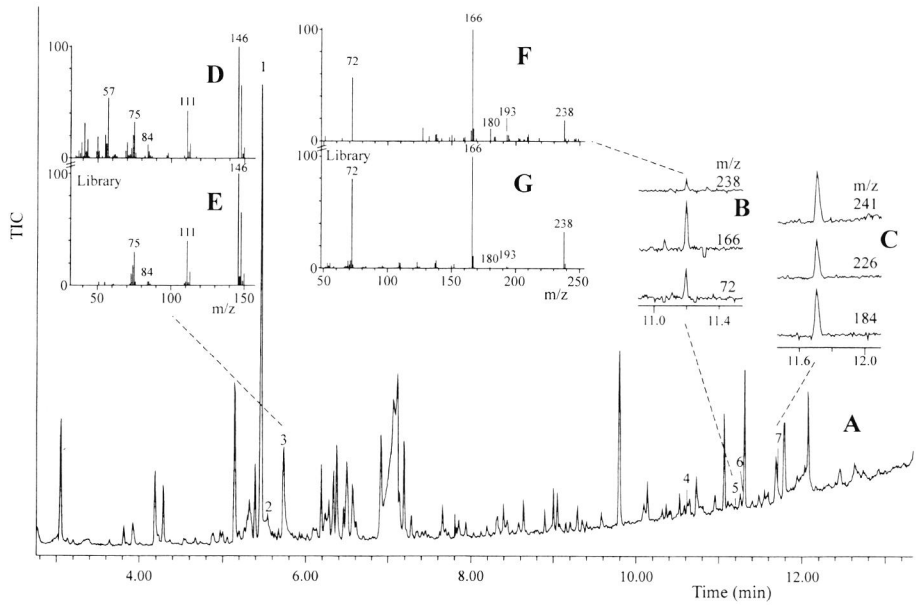

Figure 6

SPE–GC–full-scan MS chromatogram (A) of 10 ml of ground water collected at Esposende South (Portugal, January 1996); sampled at site on SPE cartridge and stored in freezer until analysis. Conditions: cartridge taken from freezer, conditioned to room temperature for 2 h, analyzed according to present SPE–GC–MS procedure starting with cleaning with 1.5 ml of water and drying with nitrogen. Inserts show reconstructed ion chromatograms of three characteristic masses of pirimicarb (B) and prometryn (C) with time scale for the mass chromatogram being twice as wide as for the full-scan chromatogram, and mass spectra of 1,2-dichlorobenzene (D) and pirimicarb (F) and their library spectra (E and G, respectively). The following micropollutants were detected: 1,3-dichlorobenzene (No. 1; 2.9 µg/l), 1,4-dichlorobenzene (No. 2; 0.24 µg/l), 1,2-dichlorobenzene (No. 3; 0.39 µg/l), dimethoate (No. 4; 0.49 µg/l), pirimicarb (No. 5; 0.07 µg/l), caffeine (No. 6; 0.90 µg/l level; low recovery taken into account) and prometryn (No. 7; 0.20 µg/l).

has to determine the dead volume between valves V2 and V4 which includes the SPE cartridge and that of the transfer line to the GC; this can actually be done with the SVE controller. A 2 m x 0.53 mm I.D. retention gap was chosen because its capacity is 32 µl when closing the SVE exactly at the end of the solvent evaporation. This is amply sufficient for the introduction of 16 µl of desorption, and 5 µl flushing solvent without danger of flooding the retaining precolumn. The repeatability of the SVE closure time was found to be satisfactory (RSD, 5%; n = 10). Actually, some variation of the injection speed and larger variations in the internal volume of the SPE cartridge (because of detection of start of transfer) and the evaporation rate (because of SVE controller) can be tolerated. This, in its turn, reduces the demands on the precision of the solvent pump, which means that, in the future, it will not be necessary any more to use an (expensive) syringe pump.

The system is well suited for the analysis of at-site sampled SPE cartridges, because the dead volume of the cartridge is not really important (cf. above). As one example, the analysis of an SPE cartridge which was loaded with 10 ml of ground water at Esposende South (Portugal), stored in the freezer and, then, subjected to SPE–GC–MS, is shown in **Figure 6**. Several micropollutants were detected at the 0.007–2.9 µg/l level. As an example, the reconstructed ion chromatograms of pirimicarb and prometryn are shown (Figures 6B and C, respectively). The presence of all micropollutants detected was confirmed by comparison of their mass spectra with reference spectra. Relevant spectra of 1,2-dichlorobenzene and pirimicarb are included in Figure 6.

3.2.4 Conclusions

The conventionally used on-line SPE–GC procedure was improved by (i) automated control of critical steps via the monitoring of the helium carrier gas flow as was done earlier for LVI–GC, and (ii) re-evaluating each single step in the SPE-to-GC transfer. To quote two examples, a 0.53 mm I.D. retention gap was preferred over a 0.32 mm I.D. retention gap because of the simpler helium flow profile. The lower pressure drop along the solvent film, if a 0.25 or 0.32 mm I.D. capillary is used to connect the retention gap and SVE, results in less evaporation of solvent from the front end of the solvent film, and, therefore, less loss of volatiles. Secondly, the solvent volume transferred to the GC was reduced from the conventional 50–100 µl to 21 µl, i.e. 16 µl for desorption, and only 5 µl for subsequent cleaning of the transfer line. This improvement could be effected because of precise detection of the start of the transfer, and first flushing the 'priority capillaries' after desorption, respectively. As a result, the envisioned self-controlled SPE–GC set-up of Table 1 has been realized: (i) no optimization is required, (ii) the quality of the retention gap is much less critical and (iii) no significant losses of volatiles occur even without presolvent. The new set-up is more robust than the conventional one, as it is more tolerant to variations of, e.g., injection speed and internal volume of the SPE cartridge. In addition, the precision of the retention times of the volatile analytes is improved. Monitoring of the (automatically registered) SVE closure times, which are influenced by the injection volume (which, in its turn, is influenced by the injection speed) and the evaporation rate, can be used to check the performance of the SPE–GC system. The other, analytical, characteristics were as good as with conventional SPE–GC. Finally, because the present procedure is not adversely affected by variations of the dead volume, it is ideally suited for the analysis of SPE cartridges

sampled elsewhere. The simplification introduced by using a flow meter as sensor and the rationalization of the general procedure discussed above will considerably facilitate the use of SPE–GC–MS for routine applications.

References

[1] Th.H. M. Noij and M.M.E van der Kooi, *J. High. Resolut. Chromatogr.*, 18 (1995) 535.
[2] A.J.H. Louter, U.A.Th. Brinkman and R.T. Ghijsen, *J. Microcol. Sep.*, 5 (1993) 3031.
[3] Th. Hankemeier, S.P.J. van Leeuwen, J.J. Vreuls and U.A.Th. Brinkman, *J. Chromatogr. A*, 811 (1998) 117.
[4] J. Staniewski, H.-G. Janssen, C.A. Cramers and J.A. Rijks, *J. Microcol. Sep.*, 4 (1992) 331.
[5] J.J. Vreuls, H.G.J. Mol, J. Jagesar, R. Swen, R.E. Hessels and U.A.Th. Brinkman, in P. Sandra and G. Devos (Editors), *Proc. 17th Intern. Symp. Cap. Chromatogr., Riva del Garda, September 1994*, Hüthig, Heidelberg, Germany, 1994, p. 1181.
[6] K Grob and M Biedermann, *J. Chromatogr. A*, 750 (1996) 11.
[7] Th. Hankemeier, S.J. Kok, J.J. Vreuls and U.A.Th. Brinkman, *J. Chromatogr. A*, 811 (1998) 105.
[8] Th. Hankemeier, S.J. Kok, J.J. Vreuls and U.A.Th. Brinkman, *J. Chromatogr. A*, 841 (1999) 75.
[9] E. Boselli, B. Grolimund, K. Grob, G. Lercker and R. Amadò, *J. High Resol. Chromatogr.*, 21 (1998) 355.
[10] B. Grolimund, E. Boselli, K. Grob, R. Amadò and G. Lercker, *J. High Resol. Chromatogr.*, 21 (1998) 378.
[11] H.G.J. Mol, M. Althuizen, H.-G. Janssen, C.A. Cramers and U.A.Th. Brinkman, *J. High Resolut. Chromatogr.*, 19 (1996) 69.
[12] T. Hyötyläinen, K. Grob, M. Biedermann and M-L. Riekkola, *J. High Resol. Chromatogr.*, 20 (1997) 410.
[13] E.C. Goosens, D. de Jong, J.H.M. van den Berg, G. J. de Jong and U.A.Th. Brinkman, *J. Chromatogr.*, 552 (1991) 489.
[14] G. Hagman and J. Roeraade, *J. Microcol. Sep.*, 5 (1993) 341.
[15] J.F. Hiller, T. McCabe and P.L. Morabito, *J. High Resol. Chromatogr.*, 16 (1993) 5.

4

At-line SPE–GC using the PrepStation

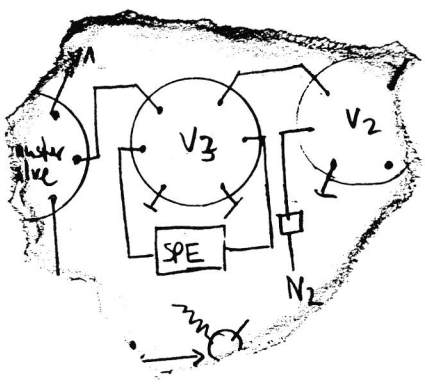

4.1 Automated at-line SPE–GC analysis of micropollutants in water

Summary

A fully automated at-line solid-phase extraction–gas chromatography procedure has been developed for the analysis of aqueous samples using the PrepStation. The sample extract is transferred from the sample preparation module to the gas chromatograph via an autosampler vial. With flame-ionization detection, limits of determination (S/N = 10) of 0.05–0.3 μg/l were obtained for the analysis of HPLC-grade water when modifying the PrepStation by (i) increasing the sample volume to 50 ml, (ii) increasing the injection volume up to 50 μl and (iii) decreasing the desorption volume to 300 μl. The HP autosampler had to be modified to enable the automated 'at-once' on-column injection of up to 50 μl of sample extract. The amount of packing material in the original cartridge had to be reduced to effect the decrease of the desorption volume. The total set-up did not require any further optimization after having set up the method once.

The analytical characteristics of the organonitrogen and organophosphorus test analytes, i.e., recoveries (typically 75–105%), repeatability (2–8%) and linearity (0.09–3.0 μg/l), were satisfactory. The potential of the system was demonstrated by determining triazines and organophosphorus pesticides in river Rhine water at the 0.6 μg/l level using flame-ionization and mass-selective detection. No practical problems were observed during the analysis of more than 100 river water samples.

4.1.1 Introduction

The determination of micropollutants in environmental samples is generally achieved by means of chromatographic analysis. Sample preparation is usually necessary prior to the actual determination step because of the complexity of the samples and the low determination levels which have to be achieved. Unfortunately, sample preparation, which is usually done off-line, and often manually, is generally time consuming [1]. For the determination of micropollutants in water samples by means of gas chromatography (GC), solid-phase (SPE) or liquid–liquid extraction (LLE) are primarily used to transfer the analytes from the water into an organic solvent prior to analysis. Obviously, integration of sample preparation and method of analysis into one set-up is desirable. This can be achieved by on-line or at-line coupling. In on-line interfacing the extract obtained after sample preparation is directly and completely transferred to the chromatographic system. In recent years several on-line SPE–GC systems have been developed and utilized [2–5]. When using an on-column interface for the transfer of 50–100 µl of desorption solvent, a critical parameter is the total amount of solvent transferred to the GC; changes in the dead volume of the SPE cartridge have to be considered. In an at-line approach the sample extract is transferred from the sample preparation module to the chromatographic system via, e.g. an autosampler vial, from which an aliquot (constant volume!) is injected, and no optimization is necessary. The at-line (and also the on-line) set-up offers advantages such as good precision and low contamination due to the closed nature of the system. In addition, the amount of organic solvent used is small, sample throughput is increased and it becomes relatively easy to achieve automation which will help to reduce the cost per analysis. Additionally, the at-line approach allows the injection of (part of) the extract into another GC system with a different detection mode, the addition of an internal standard, the injection of organic extracts or standard solutions for calibration next to the analysis of aqueous samples, and at-line analyte derivatization prior to injection.

To achieve good analyte detectability with an at-line system, it is necessary to analyze a substantial portion (equivalent of the original sample) in the final GC run. Typical sample extract volumes obtained with miniaturized SPE procedures are 100–1000 µl. Today, in GC the injection of sample volumes up to 100 µl is increasingly being used to enhance sensitivity, e.g. by using an on-column interface [6–8]. Recently, Hewlett Packard introduced their so-called PrepStation, which comprises an SPE module for analyte enrichment, desorption with an organic solvent, and a loading/transfer-to-GC module. In the integrated system, the concentrated sample extracts are transported at-line in a vial via a robotic arm from the SPE unit to the autosampler of the GC system, and, finally, an aliquot is injected into this system [9].

The goal of this study was to develop a fully automated PrepStation–GC method for the at-line SPE–GC determination of micropollutants in 1–50 ml of aqueous samples at the 0.1–1 µg/l level. The total set-up should be simple and require essentially no optimization. Modification of the commercial system, if required to achieve our aims, was part of the plans. Several triazines and organophosphorus pesticides were selected as test compounds.

4.1.2 Experimental

Chemicals

HPLC-grade water (J.T. Baker, Deventer, the Netherlands) was used for the conditioning and clean-up steps. Ethyl acetate and methanol (both p.a., J.T. Baker) were distilled before use. Chloroform (p.a.) for Soxhlet extraction of the septa and cartridges was purchased from J.T. Baker. The ten organophosphorus pesticides (OPPs) and six triazines were purchased from Riedel-de Haën (Seelze, Germany). Stock solutions of the OPPs and triazines were stored in the dark at 4°C. Water samples were spiked just before analysis. 4,4′-Difluorobiphenyl (Aldrich, Axel, the Netherlands) or *N,N*-dibenzylaniline (ICN, Costa Mesa, CA, USA) was used as internal standard. River water samples were filtered through 0.45 µm membrane filters (Schleicher & Schüll, Dassel, Germany).

Set-up of PrepStation–GC system

A schematic of the PrepStation–GC system is shown in **Figure 1**. The whole set-up consists of an HP 7686 PrepStation with SPE module (Hewlett Packard, Waldbronn, Germany), a (modified) HP 7673 autosampler with an HP 7673B autosampler tray and an HP 5890 Series II gas chromatograph with electronic pressure control, an on-column injector and a flame-ionization detector (FID). The PrepStation itself consists of a 10-port solvent selection valve, a 2.5-ml syringe pump, a nitrogen 3-port valve, an SPE valve and three drop-off positions, one for an SPE cartridge and two for autosampler vials.

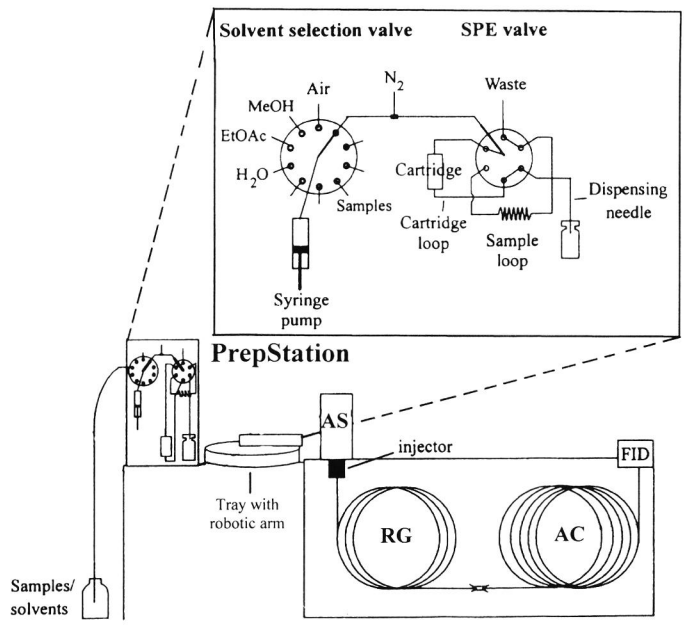

Figure 1
Set-up of the PrepStation–GC–FID system. Abbreviations: AC, analytical column; AS, autosampler; EtOAc, ethyl acetate; H_2O, water; MeOH, methanol; N_2, nitrogen; RG, retention gap.

A total of eight samples and solvents can be positioned at the selection valve; in our case, there were five samples next to HPLC-grade water, methanol and ethyl acetate. A solvent or sample is pumped through the nitrogen purge valve to the SPE valve by the syringe pump. The SPE valve allows one to choose different flow paths which are a combination of the sample loop, the SPE cartridge loop and the waste or dispensing needle as outlet (see **Figure 2** for flow paths used in SPE procedure to be discussed below). The SPE cartridge is sealed by two sealing probes at the top and bottom within the cartridge loop. The SPE cartridge and the autosampler vial are transported by a robotic arm from the sample tray to the drop-off positions of the PrepStation (or vice versa). For an exchange of the SPE cartridge and/or the autosampler vial, the top sealing probe of the SPE cartridge and the dispensing needle are lifted. The needle height of the dispensing needle within the autosampler vial can be programmed. The whole flow system or a part of it can be cleaned with solvent by lowering the dispensing needle into the needle rinser in such a way that also the outside of the dispensing needle is cleaned.

In the present study, an HP G1296A Mixer/Bar Code Reader was used to mix solutions; it was mounted next to the autosampler tray. The drop-off position for an autosampler vial for preparation processes such as heating and evaporation was not used. The SPE cartridge was packed in-house with 20 µm, 100 Å PLRP-S, a polystyrene–divinylbenzene copolymer (Polymer Laboratories, Church Stretton, UK). To this end, the commercial SPE cartridge filled with 100 mg C18-bonded silica, was disassembled, repacked and closed with special home-made tools. Before repacking, the disassembled SPE cartridge was cleaned by 6-h Soxhlet extraction with chloroform to reduce the amount of plasticizers present in the cartridge material that can be extracted by the desorption solvent. To decrease the internal volume of 200 µl of the commercial 14.3 mm x 4.2 mm I.D. SPE cartridge, a 17.1 x 2.0 mm I.D. insert made of teflon was introduced into the cartridge. Two 1.6 mm thick frits were inserted at both ends to keep the stationary phase in place. This modification resulted in an

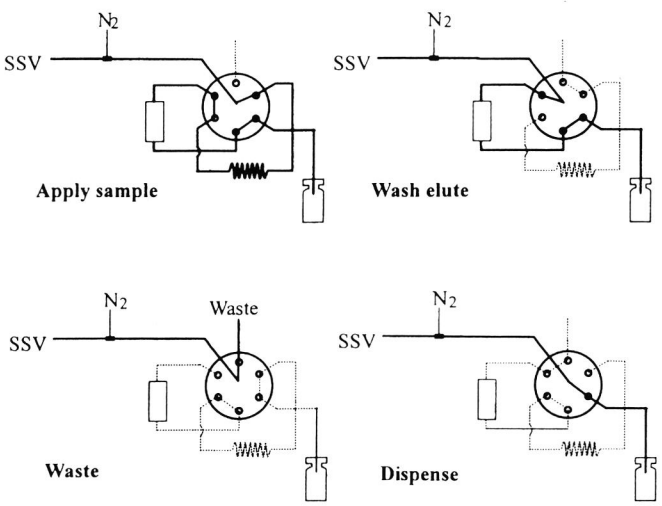

Figure 2
Flow paths of the PrepStation used during the SPE procedure. Abbreviations: N_2, nitrogen, ; SSV, solvent selection valve.

internal volume of only 44 µl. The frits and the insert were also Soxhlet extracted prior to use as described above. A carbon trap (20/40 mesh Carbotrap C, Supelco, Bellefonte, PA, USA) was inserted before the nitrogen purge valve to purify the nitrogen.

On-column injections were done into a 0.53 mm I.D. diphenyltetramethyldisilazane-deactivated retention gap (BGB Analytik, Zürich, Switzerland). The length of the retention gap was 0.7 m for a 5-µl injection, 3 m for a 25-µl injection and 6 m for a 50-µl injection. The retention gap was connected to the GC column (SPB 5, 25 m x 0.32 mm I.D., 0.25 µm film; Supelco, Bellefonte, PA, USA) by means of a press-fit connector. Injection was done at 70°C, which was kept for 2, 3.5 or 6 min for a 5-, 25- or 50-µl injection, respectively. The temperature was programmed to 280°C at 10°C/min and finally held at 280°C for 5 min. The pressure was 90 kPa and was programmed to provide constant flow. The temperature of the on-column injector was always kept 3°C above the oven temperature, and the temperature of the FID was 300°C. For the 25- and 50-µl injections the HP autosampler was equipped with a new EPROM (Hewlett Packard, Wilmington, DE, USA) to enable the programming of a pre- and post-injection delay time of 4 sec and 6 sec, respectively. The slow injection speed was chosen, but the injection was still finished in less than 2 sec.

One software package controls both the PrepStation and the GC system. This allows simultaneous sample preparation of the next, and GC analysis of the previous, sample.

At-line SPE–GC procedure

The procedure of an at-line SPE–GC analysis is summarized in **Table 1**. After rinsing the total system with methanol, the cartridge is conditioned with 10 ml of ethyl acetate and 10 ml of HPLC-grade water. As one 2.5-ml syringe pump is used for all solvents, the pump has to be flushed with methanol between the change-over from ethyl acetate to water. After preflushing of the sample tubing and the pump with 10 ml of sample, 50 ml of sample are sampled through the SPE cartridge. After flushing of the syringe with water, clean-up is effected with 5 ml of HPLC-grade water. Next, the cartridge is dried for 30 min with nitrogen at ambient temperature. Initially, the water left in the tubing between the solvent selection valve and the nitrogen purge valve was removed before the 30 min of drying by pumping air to waste with the syringe pump. However, this step appeared not to be necessary and was therefore omitted.

After flushing the syringe pump with methanol and ethyl acetate to remove all water, the analytes are desorbed with ethyl acetate into an autosampler vial; 10 µl of internal standard are added from a vial to the autosampler vial containing the extract. The contents of the latter vial are mixed using the Mixer/Bar Code Reader and, finally, delivered to the GC autosampler for injection. During the whole procedure, i.e. from the conditioning of the cartridge to the desorption, the cartridge remained in the drop-off position of the PrepStation. Sample preparation took about 90 min.

GC–MS analysis

GC analyzes using mass selective (MS) detection were done with an HP 5890 Series II GC with on-column injector, electronic pressure control and an HP 5972 MSD detector. Manual 50-µl 'at-once' injections were done within 2 sec into a 6 m x 0.53 mm I.D. diphenyltetramethyldisilazane-deactivated retention gap (BGB Analytik). The syringe was

Table 1
Procedure of at-line SPE–GC analysis of aqueous samples with PrepStation

Step	Solvent [a]	Flow path [b]	Volume (ml)	Flow rate (ml/min)
Rinsing of whole system	MeOH	Apply sample	7.5	10
Conditioning of cartridge	EtOAc	Wash elute	10	5
Priming syringe	MeOH	Waste	7.5	10
Conditioning of cartridge	H_2O	Apply sample	10	5
Preflushing with sample	Sample	Waste	10	10
Sample enrichment	Sample	Wash elute	50	5
Priming syringe	H_2O	Waste	5	10
Clean-up	H_2O	Wash elute	5	5
Drying of cartridge for 30 min		Apply sample		
Priming syringe	MeOH	Waste	7.5	10
Priming syringe	EtOAc	Waste	5	10
Desorption of cartridge to vial [c]	EtOAc	Wash elute	0.9	0.2
Addition of internal standard to extract	Standard (vial)	Dispense	0.01	0.1
Mixing of extract				
Injection into GC by autosampler				

[a] Abbreviations: MeOH, methanol; EtOAc, ethyl acetate.

[b] For flow paths, see Figure 2.

[c] A small home-made cartridge with an internal volume of 44 µl was used.

removed 4 sec after the end of the injection. The retention gap was connected via a press-fit connector to a 1.5 x 0.25 mm I.D. section of the GC column (HP5MS, 0.25 µm film, Hewlett Packard), which served as retaining precolumn. An early solvent vapour exit (SVE) was inserted between the retaining precolumn and the GC column (HP5MS, 28 m x 0.25 mm I.D., 0.25 µm film) to remove most of the solvent vapour, as described earlier [3]. A 0.32 mm I.D. fused silica capillary was used to connect the press-fit T-splitter (BGB Analytik) between the retaining precolumn and GC column with the SVE. The home-made SVE was installed on the top of the split/splitless injector and kept at 150°C to prevent solvent condensation. The SVE was closed just before the last microlitres of solvent were evaporated. The GC oven temperature was kept at 75°C for 3 min, and then increased to 280°C at 20°C/min, and kept at 280°C for 5 min. The initial head pressure was 90 kPa and was programmed to provide constant flow. Ionization was achieved by electron impact, and ions with m/z 47–335 were monitored at 1.5 scans/sec. The electron multiplier voltage was set at 1800 V.

4.1.3 Results and discussion

Development of at-line SPE–GC procedure

The set-up of the SPE module of the PrepStation (cf. Figure 1) resembles an on-line SPE–GC system apart from the transfer module to the GC. The size of the SPE cartridge (14.3 mm x 4.2 mm I.D.) is 2–6-fold larger than those typically used in on-line SPE–GC approaches. In on-line SPE–GC [2–4], the SPE procedure for the determination of micropollutants in aqueous samples involves (i) preconditioning of the SPE cartridge with ethyl acetate and water, (ii) sampling, (iii) clean-up with water, (iv) drying of the SPE cartridge with nitrogen and (v) desorption with ethyl acetate. Contrary to on-line SPE–GC, in at-line SPE–GC after addition of an internal standard, an aliquot of the extract is injected into the GC system by the autosampler.

A polystyrene–polyvinylbenzene copolymer, PLRP-S, was preferred as packing material for the SPE cartridge because of its (i) high breakthrough volumes for more polar analytes and (ii) a shorter drying time necessary to remove water compared to silica-based materials. As only commercial SPE cartridges containing silica-based material were available for the PrepStation, it was necessary to use laboratory-packed cartridges. Ethyl acetate was chosen as desorption solvent, because it desorbs analytes covering a wide range of polarity from PLRP-S-packed SPE cartridges [10]. A drying time of 30 min with a nitrogen pressure of 270 kPa was necessary to remove all water from the SPE cartridge. This is a critical aspect because no traces of water can be tolerated in the extract to be injected into the GC. The efficient removal of water was checked by transferring ethyl acetate through the dried cartridge into hexane [11]. No formation of small water droplets or opaque colouring was observed. FID detection was preferred for method development as it is a universal detection mode and its sensitivity is comparable with that of full-scan MS detection.

When the PrepStation was introduced on the market, it was intended for samples taken from 1.8 ml autosampler vials with 5-µl injections out of the extract finally obtained. Therefore, in a first experiment intended to explore the potential of the instrument, a 1.5-ml HPLC-grade water sample was analyzed which had been spiked at the 170 µg/l level with four triazines, atrazine, trietazine, terbutryn and cyanazine. As the dead volume between the SPE cartridge and the tip of the PrepStation needle is about 0.25 ml and the internal volume of the SPE cartridge 200 µl, the analytes had to be desorbed with 600 µl of ethyl acetate. A 5-µl aliquot was injected via the autosampler into the GC–FID. All four triazines showed up with recoveries of 90–95% (see Figure 3C below). The RSD values were 1–3% (n = 6), and the determination limit (S/N = 10) was 130 pg injected into the GC or 15–30 µg/l for a 1.5-ml HPLC-grade water sample.

Since the determination of micropollutants in surface and drinking water is required at the 0.1–1 µg/l level, the analyte detectability of the whole SPE–GC procedure obviously had to be improved. This required three steps: (i) increase the sample volume, (ii) inject a larger aliquot of the extract and (iii) decrease the desorption volume. Increasing the sample volume to 50 ml was a viable approach, because for most analytes no breakthrough will occur with the cartridge in use. Ideally, this 30-fold increase in sample volume should lead to a determination limit of 0.4–0.9 µg/l. By increasing the injected volume of the extract from 5 to 50 µl, the determination limit can be improved another 10-fold to below 0.1 µg/l, i.e. 0.04–0.09 µg/l. Obviously, in this calculation it is assumed that the recoveries and the absolute

Table 2
Recoveries, repeatability (n = 6) and limits of determination (S/N = 10) for at-line SPE–GC–FID analysis of 50 ml HPLC-water spiked at 5 µg/l level; 5 µl out of 600 µl of organic extract were injected.

Analytes	Recovery (%)	RSD (%)	Determination limit (µg/l)
Desethylatrazine	91	2	1.0
Atrazine	94	3	0.4
Trietazine	95	2	0.4
Simetryn	91	3	0.7
Terbutryn	94	2	0.4
Cyanazine	93	6	0.8

detection limit will remain constant, i.e. that the noise will not increase. Finally, a 2-fold decrease of the desorption volume allows a further 2-fold improvement of the determination limit or, alternatively, a 2-fold reduction of the sample size or injection volume (e.g. 25 µl instead of 50 µl).

As regards the practical implementation of the above suggestions, the autosampler will require some modification to increase the injection volume to 25 or 50 µl, as the original autosampler is designed only for the injection of up to 5 µl. A reduction of the desorption volume will be possible by decreasing the size of the SPE cartridge and, thus, the amount of stationary phase.

Increase of sample volume
Sampling of volumes larger than 1.5 ml has to be done via the solvent selection valve of the PrepStation and the syringe pump. Six triazines were now used as test compounds instead of four. **Figures 3**A and B indicate that the determination limit is 1 µg/l or better, when analyzing 50 ml or river Rhine water (sampled at Lobith, the Netherlands; August 2, 1994). This increase of sample volume did not lead to a breakthrough of all six triazines, the recoveries were 91–95% (**Table 2**). Comparable peak areas were obtained as for the analysis of a 1.5-ml sample (Figure 3C), in which the same absolute amounts of four triazines were preconcentrated. For the analysis of 50-ml of HPLC-grade water the analyte detectability showed the expected 30-fold improvement compared with a 1.5-ml sample, i.e. from 15–30 µg/l to 0.4–1.0 µg/l (S/N = 10). 5 µl were injected out of the 600 µl of organic extract. When using non-selective FID detection, the determination limit for river water appeared to be 0.6–1 µg/l due to the presence of interfering compounds (Figures 3A and B). Repeatability was good with RSD values of 2–6% (n = 6) (Table 2).

OPPs. Next to the analysis of the medium polar triazines, the trace-level determination of the OPPs which cover a wider polarity range is of distinct importance in environmental analysis. When analysing a 50-ml HPLC-grade water sample spiked at the 5 µg/l level, five out of the ten OPPs showed recoveries of 92–96% (method 1; **Table 3**). The recoveries were somewhat lower for fenchlorphos, pyrazophos and coumaphos (81–85%), and significantly lower for bromophos-ethyl and ethion (66–67%). The recovery decreased with decreasing polarity of the analytes, which implies that this is due to adsorption on the walls of the tubing between sample bottle and sample valve [3]. Actually, the losses due to the well-known adsorption

Table 3
Recoveries of selected OPPs and triazines using four methods [a] to overcome analyte loss due to adsorption.

Compound	log K_{ow} [b]		Recovery (%) using four methods			
			1	2	3	4
		Preflush volume (ml):	0	25	0	0
		MeOH (%, sample):	0	0	0	30
		MeOH (%, clean-up):	0	0	30	0
OPPs						
Sulfotep			96	92	91	91
Diazinon	3.3 [c]		93	94	94	99
Fenchlorphos	4.9 [c]		83	85	87	95
Parathion-ethyl	3.8 [c]		92	92	93	94
Bromophos-ethyl	5.9 [c]		66	67	72	92
Tetrachlorvinphos	3.5 [c]		97	97	96	95
Ethion	5.1 [c]		67	72	79	95
Triazophos	3.6 [c]		93	93	93	97
Pyrazophos			81	83	91	91
Coumaphos			85	87	92	95
Triazines						
Desethylatrazine	1.5 [c]		84			0
Atrazine	2.7 [d]		94			95
Cyanazine	2.2 [d]		92			71

[a] Sample, 50 ml HPLC-water spiked at 5 µg/l level; 5 µl out of 600 µl of organic extract injected.
[b] K_{ow} = octanol/water coefficient.
[c,d] Values taken from refs. [15] and [16], respectively.

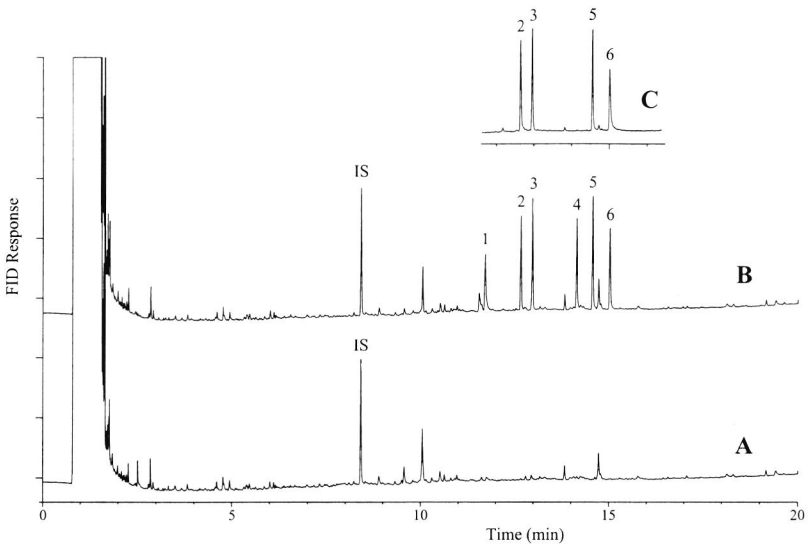

Figure 3
PrepStation–GC–FID chromatogram obtained after preconcentration of 50 ml of (A) river Rhine water and (B) river Rhine water spiked at the 5 µg/l level with six triazines. The insert (C) shows a PrepStation–GC–FID chromatogram of a 1.5-ml HPLC-grade water sample spiked at the 170 µg/l level with four triazines. In all cases, 5 µl out of the 600 µl of organic extract were injected. Peak assignment: IS, internal standard (4,4`-difluorobiphenyl); 1, desethylatrazine; 2, atrazine; 3, trietazine; 4, simetryn; 5, terbutryn; 6, cyanazine.

correlated rather well with the octanol/water partition coefficients (Kow), which reflect the hydrophobicity of the analytes (Table 3).

Three options were tested to prevent the losses due to adsorption. Preflushing of the tubing with sample up to the sample valve before the sampling step increased the recoveries of the more apolar OPPs 1–5% (method 2;. Table 3). The tubing between the sample bottle and the solvent selection valve had been shortened as much as possible, but this did not have a significant influence on the recoveries. Flushing the syringe and the tubing between the solvent selection valve and the sample valve with 5 ml of methanol/water 30/70 (v/v) after the sampling step gave an even better result (1–12% increase of recoveries) (method 3; Table 3). Recoveries over 90% could be achieved for all OPPs by adding 30 vol.% of methanol to the sample solution prior to sampling (method 4; Table 3). However, as is to be expected, the addition of an organic modifier to the sample decreased the breakthrough volumes which had adverse effects especially for the more polar analytes: for a 50-ml sample and with the cartridge in use, cyanazine showed a recovery of only 71%, and desethylatrazine was completely lost. Obviously, if apolar analytes have to be determined in one run next to rather polar ones, no modifier should be added to the sample and preflushing the tubing with sample prior to sampling probably is the best option. Admittedly, the recoveries of the more apolar analytes then inevitably will be somewhat lower - but they will still be quite reproducible, as is demonstrated by the results reported in Table 5 below.

Increase of injection volume

The HP autosampler is in principle designed for on-column injections of up to 5 µl only. Such an injection is done in less than 2 sec. However, this is also the case when injecting a larger volume, e.g. 25 or 50 µl. Therefore, the latter type of injection is so-called 'at-once', i.e. only a small part of the sample solvent is evaporated during the injection, while the major part is spread as a film in the retention gap and evaporated after the injection. The retention gap has to be long enough to prevent the solvent film from reaching the analytical column, otherwise distorted peaks will be obtained [12]. A 3- or 6-m long retention gap was used when injecting 25 or 50 µl, respectively, as the flooded zone of ethyl acetate for a DPTMDS-deactivated retention gap with 0.53 mm I.D. is about 11 cm/µl [10, 13].

Two aspects appeared to be critical for large-volume injections with the HP autosampler and were therefore studied, (i) the occurrence of solvent backflush into the injector during

Table 4

Comparison of repeatability of large-volume injections [a] with autosampler.

Alkane	RSD (%, n = 10) for injection volume of:	
	40 µl (manual)	50 µl (autosampler [b])
C_9	2.0	0.8
C_{10}	2.0	0.4
C_{11}	2.0	0.8
C_{12}	2.0	0.3
C_{13}	2.0	0.3
C_{14}	1.5	0.3
C_{15}	0.5	0.4

[a] Post-injection delay time, 6 sec.

[b] Autosampler with modified EPROM and injection needle with 0.27 mm I.D.

injection or after injection during withdrawal of the syringe, and (ii) the repeatability of the large-volume injections. To study the former aspect, 50-µl injections were made manually. The syringe was withdrawn either immediately after the injection, as is done by the unmodified HP autosampler, or with a post-injection delay time of 6 sec between the end of injection and withdrawal of the syringe. Solvent backflush, which caused a tailing solvent peak and a noisy baseline of the FID chromatogram, was observed in the former case, whereas with a post-injection delay of 6 sec, no solvent backflush was observed for more than 50 injections. The solvent backflush is to all probability due to solvent which is left between the syringe and the retention gap with large-volume injections, and which is pulled back into the injector, if the syringe is withdrawn immediately after the injection [14]. When a post-injection delay is introduced, this solvent is pushed further into the retention gap by the carrier gas. Satisfactory repeatability (RSD less than 2%; n = 10) was obtained for an alkane standard in ethyl acetate (**Table 4**). However, it is not possible to program any post-injection delay time with the original HP autosampler, because the syringe is immediately withdrawn after the injection. A post-injection delay time could only be programmed using an autosampler with a modified EPROM, which was obtained from Hewlett Packard. With this autosampler and a post-injection delay time, no solvent backflush was observed (**Figure 4**).

One further remark should be made. A small gas bubble of ca. 5 µl was left in the syringe after filling the syringe for a 50`-µl injection. Even though the size of the gas bubble was found to be reproducible, its formation was thought not to be convenient. Further study showed that the use of a syringe needle with an internal diameter of 0.27 mm I.D. instead of 0.09 mm I.D. nearly completely eliminated the formation of a bubble. It should be added that the PTFE-tipped plunger of the syringe should be always at least slightly wet, that is,

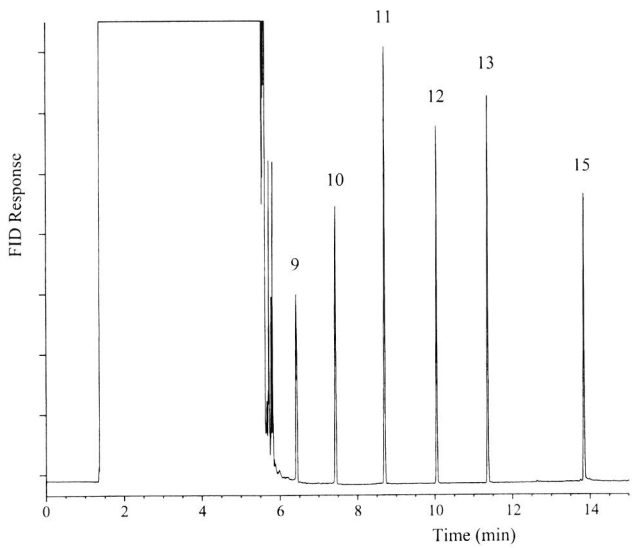

Figure 4
GC–FID chromatogram of a 50-µl injection of a solution of *n*-alkanes in ethyl acetate using the autosampler. A post-injection delay time of 6 sec was used. The eleventh injection is shown. Peak assignment: the numbers indicate the number of carbon atoms.

preflushing with sample or solvent during the autosampler procedure is recommended. During the rest of the study, only syringes with wide-bore needles were used. The repeatability for 50-µl injections was good with RSD values around 0.5% (n = 10) (Table 4).

Unfortunately, when injecting a larger aliquot of the extract into the GC system, e.g. 50 µl out of 600 µl, peaks of compounds extracted from either the SPE cartridge or the septum of the autosampler vial, increasingly showed up in the chromatogram. As an example, **Figure 5** shows GC–FID chromatograms obtained for 50-µl injections out of 600 µl of ethyl acetate. In Figure 5B, the solvent passed the dispensing needle of the PrepStation which pierced the septum. Obviously during the piercing some material of the septum remained at the end of the needle, which in its turn produced peaks in the chromatogram. As a result, the increase in analyte detectability expected on the basis of the increase of the injection volume could not be achieved completely. Various types of septa from other manufacturers were also tested, but with none of them a good blank chromatogram was obtained. The blank problem could be drastically decreased by 6-h Soxhlet extraction of the septa with chloroform (Figure 5A).

In Figure 5D, the solvent was transferred through the untreated SPE cartridge into a septum-less autosampler vial prior to injection. The interfering groups of peaks showing up in the chromatograms are mainly due to plasticizers present in the polymeric constituents of the SPE cartridge. As a consequence, increase of the injection volume did not result in the expected increase of analyte detectability. 6-h Soxhlet extraction was successfully used to clean the cartridge prior to use, which resulted in a good blank chromatogram (Figure 5C). The cartridge used for this test was an empty one and it was disassembled for the Soxhlet extraction.

With pre-cleaned septa and cartridges going from 5- to 50-µl injections typically effected a 5–10-fold increase in analyte detectability.

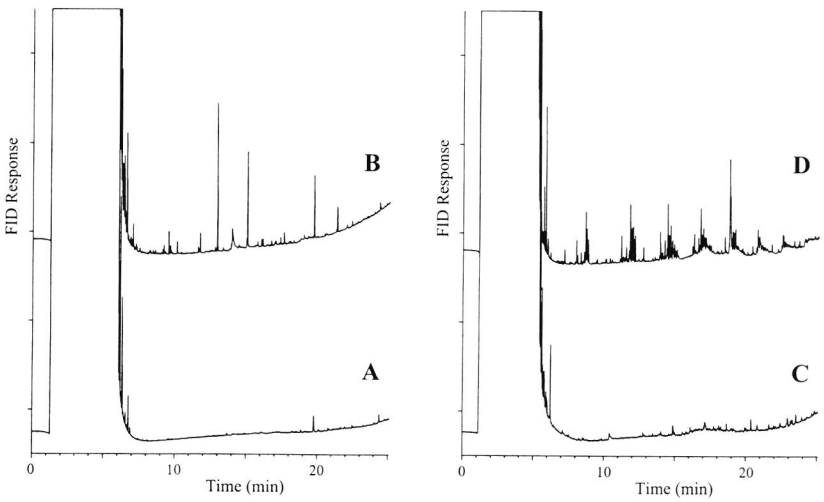

Figure 5

PrepStation–GC–FID chromatograms obtained by transferring 600 µl of ethyl acetate by means of the PrepStation to an autosampler vial through a septum (A) with and (B) without precleaning, and through an empty SPE cartridge (C) with and (D) without precleaning. In the latter two instances, there was no septum on the autosampler vial. 50 µl were injected into the GC–FID system.

Decrease of desorption volume

The desorption volume was determined for the larger, commercial cartridge (internal volume of 200 µl) and the smaller home-made one (44 µl). 50-ml HPLC-grade water samples spiked at 25 µg/l with the test mixture of OPPs were analyzed, and 5 µl of the extract injected.

When using the larger, commercial cartridge, almost all OPPs were recovered quantitatively with 200 µl of ethyl acetate. However, compounds as apolar as bromophos-ethyl, required 400 µl. In practice, 600 µl of solvent were used to be on the safe side. With the smaller home-made cartridge, 150 µl of ethyl acetate were sufficient to desorb all OPPs quantitatively, only bromophos-ethyl required 200 µl of ethyl acetate; in practice, 300 µl were used. Since the desorption volume with the smaller cartridge was 2-fold lower, this cartridge was preferred for further work, as it allows a 2-fold decrease of the injection volume or, in the ideal case, a 2-fold improvement of the determination limit.

Final at-line SPE–GC procedure

Several further parameters of the at-line SPE–GC procedure had to be optimized using the smaller home-made cartridge, i.e. the preflushing volume and the sampling and desorption speed. The main criteria were high recoveries and short analysis times, the former one being considered more important. The smaller home-made cartridge was used. A 0.6 µg/l test mixture of triazines and OPPs (same analytes as in Table 5 below) was analyzed and 25 µl of the extract injected.

The preflushing volume was varied from 5 to 20 ml at a flow rate of 5 ml/min. At the 0.6 µg/l level preflushing had a somewhat larger effect than at the 5 µg/l level discussed above. The recoveries of the more apolar OPPs, bromophos-ethyl, pyrazophos and coumaphos, increased about 10% to 58%, 71% and 88%, respectively, when increasing the preflushing volume from 5 to 10 ml; a further increase to 20 ml did not cause a significant improvement anymore. A preflushing volume of 10 ml was therefore selected for all further work.

Varying the sampling flow rate from 1 to 10 ml/min did not influence the recoveries of the test compounds. A flow rate of 5 ml/min was finally selected to prevent the back-pressure due to the SPE cartridge becoming too high.

A desorption flow rate of 100 to 200 µl/min did not influence the recoveries. Actually, no effects were observed for flow rates up to 800 µl/min for any test compound except bromophos-ethyl. For this analyte, the recovery decreased some 20% upon going from 200 to 800 µl/min. A flow rate of 200 µl/min was therefore selected.

The time required for the total sample preparation procedure of the PrepStation was about 90 min. This comprised a sampling time of 20 min and a drying time of 30 min; the other steps of the procedure took about 20 min. The difference between the 70 min so calculated and the actual SPE time is due to the fact that some operations of the PrepStation are rather slow, e.g. positioning and transport of vials or the cartridge, lifting the sealing probe of the SPE cartridge and the dispensing needle for exchange of the cartridge and/or vial or flushing of the dispensing needle. During the PrepStation procedure the analysis of the previous extract plus an injection of a standard solution were performed.

Performance of at-line SPE–GC

The performance of the at-line SPE–GC procedure was tested by analysing 50-ml HPLC-grade water samples spiked with 0.6 µg/l of several triazines and OPPs (**Figure 6**). 25 rather than 50 µl out of the 300 µl extract were injected. The repeatability was good for all analytes with RSD values of 2–8% (**Table 5**). A 25-µl on-column standard injection was used as reference for the calculation of the recoveries. Slight variations of the extract volume were compensated by the use of an internal standard, which was added to the extract before injection.

The recoveries were above 85% for nine out of the twelve test compounds. The somewhat lower results for pyrazophos and coumaphos (70–80%) and especially bromophos-ethyl (56%) can be explained on the basis of their hydrophobicity (cf. above). The linearity over the relevant range of 0.09–3 µg/l was satisfactory for all tested analytes (see Table 5). The analyte detectability of the total procedure was studied by analysing 50 ml of HPLC-grade water spiked at the 0.09 µg/l level. The limits of determination (S/N = 10) were between 0.05 and 0.1 µg/l for all analytes except tetrachlorvinphos (0.2 µg/l) and desethylatrazine (0.3 µg/l) (Table 5). The determination limit of desethylatrazine is higher because this compound is easily adsorbed on the walls of the retention gap, when the deactivation layer is partly destroyed. The improvement of the determination limit found experimentally is similar to that calculated: analyte detectability has been improved from 15–30 µg/l to 0.05–0.2 µg/l upon a 30-fold sample volume increase, a 5-fold increase of the injection volume and a 2-fold decrease of the desorption volume.

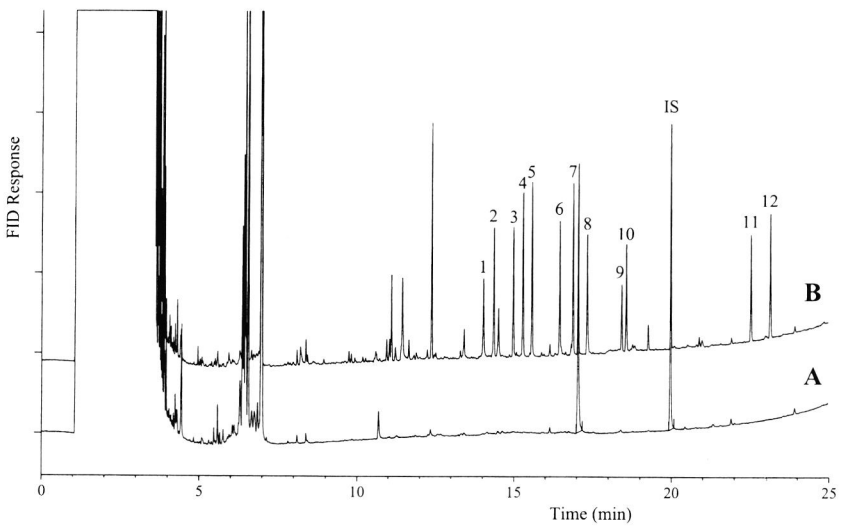

Figure 6
PrepStation–GC–FID chromatogram obtained after preconcentration of 50 ml HPLC-grade water (A) without and (B) with spiking at the 0.6 µg/l level. 25 µl out of 300 µl extract were injected. Peak assignment: IS, internal standard (*N,N*-dibenzylaniline); 1, desethylatrazine, 2, sulfotep, 3, atrazine; 4, trietazine; 5, diazinon; 6, simetryn; 7, terbutryn; 8, cyanazine; 9, bromophos-ethyl; 10, tetrachlorvinphos; 11, pyrazophos; 12, coumaphos.

Table 5
Analytical characteristics of at-line SPE–GC–FID of HPLC-grade water spiked at 0.6 µg/l level; 25 µl out of 300 µl organic extract injected.

Analyte	Recovery (%)	RSD (n = 6) (%)	Linearity [a] R^2	LOD [b] (µg/l)
Desethylatrazine	87	5	0.9971	0.3
Sulfotep	86	3	0.9978	0.1
Atrazine	97	2	0.9995	0.1
Trietazine	105	3	0.9998	0.05
Diazinon	97	2	0.9980	0.05
Simetryn	101	3	0.9995	0.1
Terbutryn	91	2	0.9996	0.05
Cyanazine	90	3	0.9999	0.1
Bromophos-ethyl	56	4	0.9954	0.1
Tetrachlorvinphos	103	4	0.9951	0.2
Pyrazophos	70	5	0.9987	0.1
Coumaphos	78	6	0.9963	0.1

[a] Concentration range: 0.09–3 µg/l, six data points.
[b] Calculated from sample spiked at 0.09 µg/l level, LOD = limit of determination (S/N = 10).

Application: analysis of river water

The potential of the at-line SPE–GC system was demonstrated by determining OPPs in 50 ml of river Meuse water (sampled at Eysden, the Netherlands; September 6, 1994), spiked at the 0.5 µg/l level. In this instance, a large SPE cartridge was used and a 50-µl aliquot out of the 600 µl extract injected into the GC–FID system. All OPPs except bromophos-ethyl (57%) and ethion (69%) showed recoveries of 90% or better. Although the detection of the test analytes is obviously hampered by the presence of many interfering compounds in the surface water sample – which all show up in FID detection –, the limits of determination (S/N = 10) typically were 0.2–0.7 µg/l (**Figure 7**). None of the spiked OPPs were found to be present in the samples at this level. Compared to the limits of determination for the analysis of HPLC-grade water of 0.05–0.2 µg/l, an about 5-fold loss of sensitivity is found, as is to be expected for real-life work using FID detection.

Obviously, a more selective detector is preferred for the determination of micropollutants in river water at a level of around 0.5 µg/l or below. One example is the analysis of 50 ml of river Meuse water (sampled at Eysden, the Netherlands; September 6, 1994) spiked with 0.5 µg/l of several triazines. 50 µl out of the 600 µl extract were injected into a GC–MS system.

Again it is clear that the compounds present in the river water will start to interfere with the determination of the test analytes in the full-scan GC–MS chromatogram at around the 0.1–0.3 µg/l level (**Figures 8**A and B). When using the reconstructed ion chromatogram of a characteristic mass of each analyte instead, the determination limits improve about 10-fold. As an example, the reconstructed ion chromatograms of ion m/z = 200 for the spiked and non-spiked sample are shown in Figures 8C and D, respectively. From these chromatograms the limits of determination for atrazine and trietazine can be calculated to be ca. 0.03 µg/l, and the presence of atrazine in the river water sample is clearly revealed (concentration, 0.07

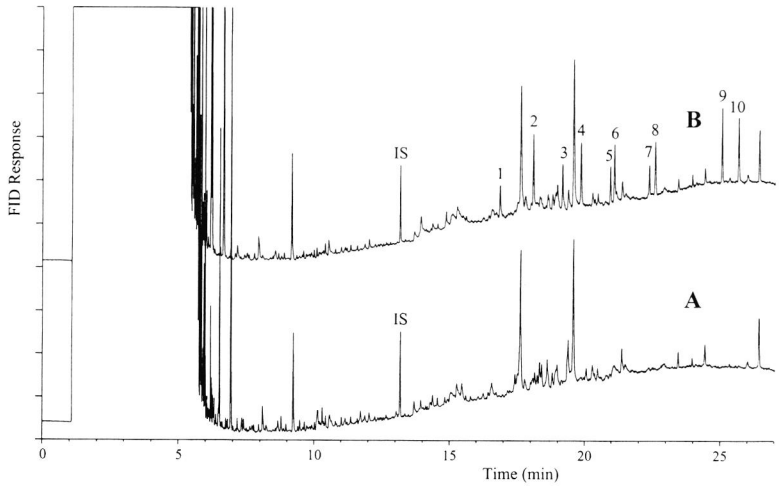

Figure 7

PrepStation–GC–FID chromatogram of 50 ml river Meuse water (A) without and (B) with spiking at the 0.5 µg/l level with OPPs. 50 µl out of 600 µl extract were injected. Peak assignment: IS, internal standard (4,4′-difluorobiphenyl); 1, sulfotep; 2, diazinon; 3, fenchlorphos; 4, parathion-ethyl; 5, bromophos-ethyl; 6, tetrachlorvinphos; 7, ethion; 8, triazophos; 9, pyrazophos; 10; coumaphos.

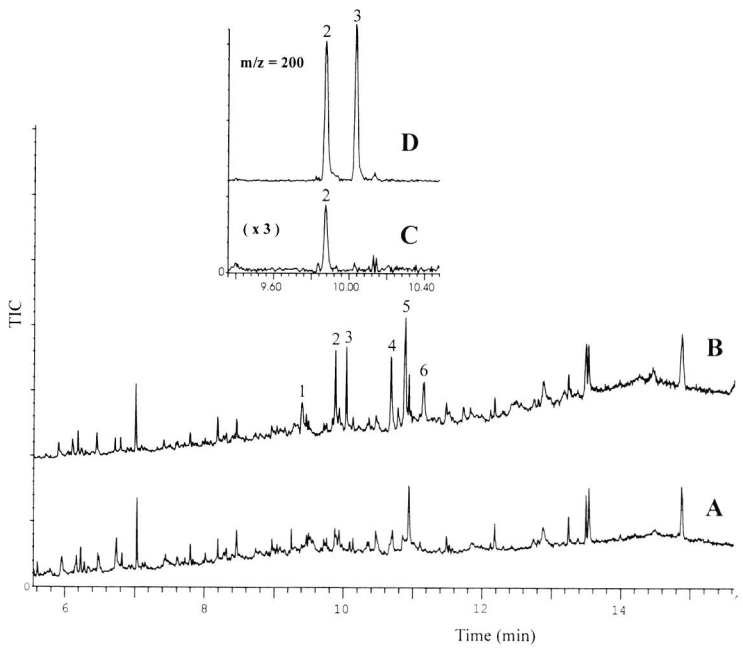

Figure 8

Full-scan PrepStation–GC–MS chromatogram of 50 ml river Meuse water (A) without and (B) with spiking at the 0.5 µg/l level. 50 µl out of 600 µl extract were injected. The insert shows the reconstructed ion chromatogram of m/z 200 (C) without and (D) with spiking at the 0.5 µg/l level. The time scale of the reconstructed ion chromatogram of the non-spiked water sample is 3 x blown up. Peak assignment: 1, desethylatrazine; 2, atrazine; 3, trietazine; 4, simetryn; 5, terbutryn; 6, cyanazine.

µg/l; Figure 8C). The presence of atrazine could be confirmed by the presence of all four characteristic diagnostic ions of atrazine (m/z = 200, 202, 215 and 217).

No experimental problems with the PrepStation–GC were observed during the analysis of more than 100 river water samples were observed.

4.1.4 Conclusions

A fully automated at-line SPE–GC–FID procedure was developed for the determination of micropollutants in aqueous samples using the PrepStation. The system combines several advantages of on-line and off-line SPE–GC: an integrated and closed system is used and, because only an aliquot is injected, although a large one, the remaining extract is available for another GC analysis. Once the SPE–GC procedure has been developed, no reoptimization is necessary, e.g. with regard to compensation of slight changes of the dead volume of the cartridge or of the evaporation rate. The obvious disadvantage of the commercial unit is that the typically determination limits required for environmental analysis of 0.1–1 µg/l can not be obtained. Therefore the sample volume was increased to 50 ml, the injection volume was increased to 25–50 µl and the extract volume decreased to 300 µl. This means that, per injection into the GC, up to 15–20% of the mass of the analytes in the aqueous sample are transferred to the GC. For an increase of the injection volume the HP autosampler had to be adapted such that a post-injection delay time could be used. The injection of volumes up to 50 µl was 'at-once' and required no further optimization, except for the use of retention gap up to 6 m length. No (usually critical) evaporation of a part of the extract was necessary.

The analytical data of the PrepStation–GC–FID were satisfactory. To quote an aspect of primary importance, the determination limits (S/N = 10) for a series of well-known pesticides were between 0.05–0.2 µg/l for the analysis of HPLC-grade. As was to be expected, with river water these values increased, viz. to 0.2–0.7 µg/l. Still, these are below the threshold value of 1 µg/l commonly used as the alert level for surface water. Much improved performance can be obtained with a selective detector, and preliminary work using a PrepStation–GC–MS indeed showed determination limits of 0.02–0.04 µg/l for the determination of the same analytes in river water.

The modified at-line SPE–GC system with its rather robust set-up and ease of operation offers a promising route to determine, and identify, micropollutants in aqueous samples at the sub-µg/l level using moderate sample volumes only. Research focused on the determination of micropollutants at low levels using primarily MS detection is reported in Chapter 4.2. In that chapter an attempt is described to improve the set-up in such a way that no precleaning of the cartridges and/or septa of the autosampler vials is necessary anymore.

References

[1] I. Liska, *J. Chromatogr. A*, 655 (1993) 163.
[2] A.J.H. Louter, U.A.Th. Brinkman and R.T. Ghijsen, *J. Microcol. Sep.*, 5 (1993) 3031.
[3] Th. Hankemeier, A.J.H. Louter, F.D. Rinkema and U.A.Th. Brinkman, *Chromatographia*, 40 (1995) 119.
[4] A.J.H. Louter, C.A. van Beekevelt, P. Cid Monañes, J. Slobodník, J.J. Vreuls and U.A.Th. Brinkman, *J. Chromatogr. A*, 725 (96) 67.

[5] H.G.J. Mol, H.-G. Janssen, C.A. Cramers, J.J. Vreuls, U.A.Th. Brinkman, *J. Chromatogr.*, 703 (1995) 277.
[6] K. Grob, in W. Bertsch, W.G. Jennings and R.E. Kaiser (eds.), *On-column injection in capillary GC*, Hüthig, Heidelberg, Germany, 1987.
[7] F. Munari, P.A. Colombo, P. Magni, G. Zilioli, S. Trestianu and K. Grob, J. Microcol. Sep., 7 (1995) 403.
[8] S. Ramalho, Th. Hankemeier, M. de Jong, U.A.Th. Brinkman and J.J. Vreuls, *J. Microcol. Sep.*, 7 (1995) 383.
[9] K.D. Fogelman, *Laboratory robotics and automation*, 5 (1993) 103.
[10] J.J. Vreuls, W.J.G.M. Cuppen, G.J. de Jong and U.A.Th. Brinkman, *J. High Resolut. Chromatogr.*, 13 (1990) 157.
[11] J.J. Vreuls, R.T. Ghijsen, G.J. de Jong and U.A.Th Brinkman, *J. Chromatogr.*, 625 (1992) 237.
[12] K. Grob Jr., G. Karrer and M.-L. Riekkola, *J. Chromatogr.*, 334 (1985) 129.
[13] K. Grob, in W. Bertsch, W.G. Jennings and P. Sandra (eds.), *On-line coupled LC–GC*, Hüthig, Heidelberg, Germany, 1991, p. 209–211.
[14] K. Grob Jr., *J. Chromatogr.*, 283 (1984) 21.
[15] A. Noble, *J. Chromatogr.*, 642 (1993) 3.
[16] D. Brown and E. Flagg, *J. Environ. Qual.*, 10 (1981) 382.

4.2 At-line SPE–GC–MS of micropollutants in water using the PrepStation

Summary

An automated at-line SPE–GC–MS system for the determination of micropollutants in aqueous samples which is based on the PrepStation and uses large-volume on-column injections, has been redesigned. A cartridge made of stainless steel and polychlorotrifluoroethylene, and a 2-needle system were constructed which allow the determination of micropollutants at the low ng/l level without interferences from impurities extracted from the septa of the vials or the commercial cartridges. No time-consuming pre-cleaning of the cartridges or septa is required. The SPE sample extract (300 µl) is transferred from the sample preparation module to the autosampler of the GC–MS and 50 or 100 µl are injected. The analytical characteristics of the integrated procedure such as analyte recovery (typically 80–105%) and repeatability (RSDs, 2–9%) were satisfactory. Several micropollutants were detected in (unfiltered) river water at the 0.2–400 ng/l level using full-scan MS acquisition. The system proved to be robust during the analysis of more than 100 tap and river water samples.

4.2.1 Introduction

In recent years, the automated analysis of aqueous samples has increasingly been performed by systems which integrate sample preparation and gas chromatographic (GC) separation-plus-detection [1]. In many cases, solid-phase extraction (SPE) is preferred over liquid–liquid extraction (LLE), as it allows the preconcentration of more polar analytes next to apolar analytes and is less time-consuming [2]. On-line or at-line combination of SPE and GC into one system allows the miniaturization of SPE [3]. This results in the use of less sample and less solvent, and automation of the whole procedure is achieved more easily.

Recently, several groups used the PrepStation system [4–9], which allows the at-line analysis of aqueous samples in a closed system. After sample preparation in this system, the extract is at-line transferred by a robotic arm to the autosampler for injection. Three typical examples are as follows. Namera et al. [8] used the PrepStation for automated SPE–GC–MS of seven barbiturates in urine. As they injected only 1 µl out of their 1-ml SPE extract, the limits of detection were about 0.2 µg/ml of urine when using full-scan MS acquisition. At the concentration levels studied, disturbances in the chromatogram due to impurities from the cartridge were reported. Bengtsson and Lehotay [9] determined organic acids by LLE or SPE enrichment, derivatization with *N,O*-bis(trimethylsilyl)trifluoro-acetamide-trimethylchlorosilane and GC–MS analysis using 1-µl injections. The authors reported sensitivity problems, but did not present any detection limits. They remarked that the limited number of SPE columns supplied by the manufacturer is disadvantageous. Soriano et al. [7] reported the determination of several drugs in urine with automated LLE–GC–NPD using 2-µl injections and detection limits of 0.1–0.5 µg/ml.

In an earlier study, we found that the original set-up of the PrepStation–GC–FID system had to be modified to achieve detection limits of 0.1 µg/l which are required in the European Union for the determination of pesticides in tap and surface water. To this end, (i) the sampling volume was increased from 1.5 ml to 50 ml, (ii) the injection volume was increased from 5 µl to 50 µl and (iii) the desorption volume was decreased from 600 µl to 300 µl [5]. However, when injecting a larger aliquot of the extract into the GC system, compounds extracted from either the SPE cartridge or the septum of the autosampler vial, increasingly showed up in the chromatogram. As a result, the improved analyte detectability expected on the basis of the increase of the injection volume was not fully achieved. The blank problem could be drastically reduced by pre-cleaning of the septa and the cartridges; however, this was time-consuming. The aim of this study was to redesign the original set-up in order to prevent any blank problems. To this end, a new cartridge and a new dispensing needle were designed which make pre-cleaning superfluous. The potential of the system was studied by analyzing micropollutants at the 0.001–0.6 µg/l level using full-scan MS detection in order to allow confirmation/identification.

4.2.2 Experimental

Chemicals

HPLC-grade water, ethyl acetate and methanol, all of p.a. grade, were purchased from J.T. Baker (Deventer, The Netherlands). The organic solvents were glass-distilled prior to use. The seven organophosphorus pesticides and six triazines used to study the analytical characteristics and the effect of filtration (cf. Tables 1 and 2) were from Riedel-de Haën (Seelze, Germany). A stock solution of all test compounds of Table 3 at a concentration of about 20 ng/µl in dichloromethane was obtained as a gift from the Institute for Inland Water Management and Waste Water Treatment (RIZA, Lelystad, The Netherlands). Stock solutions were stored in the dark at –20°C. Water samples were spiked just before analysis. When filtering river water samples, 0.45 µm membrane filters (Schleicher & Schüll, Dassel, Germany) were used.

Set-up of the PrepStation–GC system

The system consisted of a Model 7686 PrepStation with SPE module (Hewlett-Packard, Waldbronn, Germany), a (modified) HP 7673 autosampler with a HP 7673B autosampler tray and a HP 5890 Series II gas chromatograph with an on-column injector and an FID detector (FID). A scheme of the PrepStation–GC system is shown in **Figure 1**. The SPE module resembles an on-line SPE–GC system apart from the transfer module; for a more detailed description of the system one is referred to Chapter 4.1 and [5]. Different from the commercial system and the system described in [5], a home-made SPE cartridge and a home-made 2-needle dispensing system were used to prevent the extraction of impurities from the cartridge or septa; for more details, cf. Sections 3.1 and 3.2.

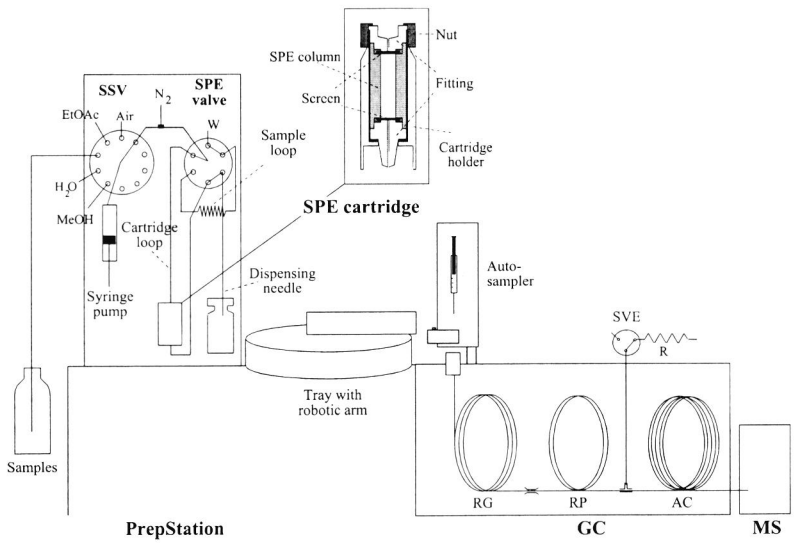

Figure 1
Set-up of PrepStation; insert shows design of new cartridge. Abbreviations: AC, analytical column; EtOAc, ethyl acetate; H_2O, water; MeOH, methanol; N_2, nitrogen gas; R, restriction; RG, retention gap; RP, retaining precolumn; SSV, solvent selection valve; SVE, solvent vapour exit; W, waste.

50-µl 'at-once' on-column injections were done into a 6 m x 0.53 mm I.D. diphenyltetramethyldisilazane-deactivated retention gap (DPTMDS; BGB Analytik, Zürich, Switzerland). The retention gap was connected to the GC column (SPB 5, 25 m x 0.32 mm I.D., 0.25 µm film; Supelco, Bellefonte, PA, USA) by means of a press-fit connector. Injection was done at 70°C and 90 kPa, and 5 min after the injection the oven temperature was programmed to 290°C at 10°C/min and finally held at 290°C for 5 min. The HP autosampler was equipped with a new EPROM (Hewlett Packard, Wilmington, DE, USA) to enable the programming of a pre- and post-injection delay time of 4 sec and 6 sec, respectively (for more details, cf. [5]).

For PrepStation–GC–MS the sample vials were (manually) transferred to the autosampler tray of a Carlo Erba Series 8000 gas chromatograph equipped with an on-column injector, an AS800 autosampler and an MD 800 (CE Instruments, Milan, Italy) mass spectrometer. A 2 m x 0.53 mm I.D. DPTMDS deactivated retention gap (BGB Analytik) was connected to an 1-m retaining precolumn and a 25-m analytical column (both HP5MS, 0.25 mm I.D., film thickness 0.25 µm; HP) via a press-fit connector and a T-piece, respectively. A solvent vapour exit (SVE), an electronically controlled 6-port valve (Valco Instruments, Houston, TX, USA), was connected to the T-piece so that most of the solvent vapour did not reach the MS detector [10]. 50 or 100 µl of extract were on-column injected using partially concurrent solvent evaporation (PCSE) conditions at 60 µl/min and 60 kPa. Optimization of the injection conditions was achieved by large-volume injections (50 or 100 µl) of a solution of *n*-alkanes (C_{10}–C_{20}) in ethyl acetate by varying the injection temperature according to ref. [11]. The SVE was generally closed 0.17 min after the end of the injection to prevent the loss of volatile analytes (for more details, see [11]). After a delay time of 5 min, the temperature was programmed to 290°C at 10°C/min and finally held at 290°C for 5 min. The mass selective detector was operated in the electron impact ionization mode at 70 eV in full-scan acquisition, and the mass range was 45–400 amu.

With both GC systems, helium 5.0 (Hoekloos, Schiedam, The Netherlands) was the carrier gas.

At-line SPE–GC procedure

After rinsing of the whole SPE module system with 7.5 ml of methanol, the SPE cartridge was conditioned with 7.5 ml of ethyl acetate and 7.5 ml of water. For sample volumes larger than 1.5 ml sampling was done via the solvent selection valve and the syringe pump of the PrepStation. After preflushing of the sample tubing and the syringe pump, 50 ml of sample were sampled through the SPE cartridge. Next, some clean-up was effected with 5 ml of water. After drying of the cartridge with nitrogen for 30 min at ambient temperature and 270 kPa, 780 µl of ethyl acetate were transferred for desorption through the cartridge loop to obtain 300 µl of extract in a vial. After addition of 10 µl of a solution of *N,N*-dibenzylaniline in ethyl acetate as internal standard and mixing of the extract using the Mixer/Bar Code Reader, an aliquot of 50 or 100 µl was injected into the GC system. When changing the solvent from ethyl acetate to water or vice versa within the procedure, the syringe pump was primed with 7.5 ml of methanol in between. The flow rate used was 5 ml/min, but rinsing of the whole system or priming of the syringe was done at 10 ml/min. Sample preparation took about 87 min, and the sample preparation of the next sample was started during GC analysis of the previous sample.

4.2.3 Results

Design of new dispensing needle system

In the original set-up, the dispensing needle pierces through the septum of the autosampler vial (**Figure 2**B) and, then, dispenses the sample through the needle or sucks in solvent. However, in our earlier study we observed peaks in the GC–FID traces when dispensing solvent through a septum compared to dispensing of solvent without a septum being present. Obviously, during the piercing some material of the septum sticks to the tip of the needle, and gradually dissolves in the solvent in the vial. Only after the dispensing step the outside of the needle is cleaned by flushing with solvent in the needle rinser (Figure 2D). To solve the problems so generated, a 2-needle system was designed: the outer needle pierces the septum, and the inner needle, which protrudes further into the autosampler vial than the outer needle, is used to dispense the solvent (Figure 2A). After the dispensing step, both needles can be cleaned by flushing their inner and outer walls in the needle rinser (Figure 2C). As it was not possible to modify the PrepStation software, the needle system was designed in such a way that all desired operations could be performed without any modification of the software. With the new set-up, no additional peaks were observed when dispensing solvent (50 µl) into an autosampler vial which was closed with a septum compared to dispensing without a septum

In order to study the occurrence of memory effects, 0.5 ml of a 100 µg/ml solution of *n*-alkanes in ethyl acetate was dispensed into a vial via the needle. Next, 0.5 ml of ethyl acetate was dispensed into another vial, and 50 µl were injected into the GC. Without cleaning of

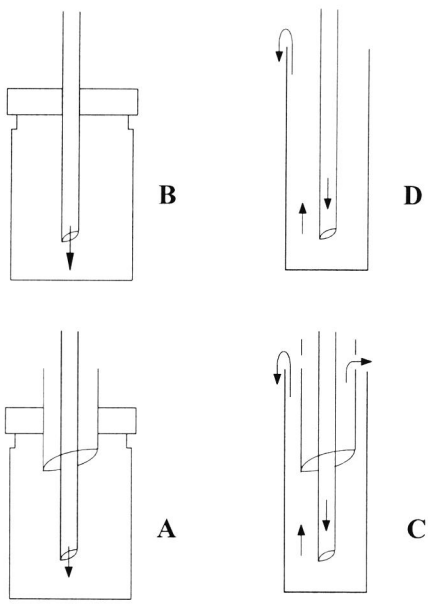

Figure 2
Schemes of the original (B, D) and new (A, C) dispensing needle system. The position of the needle used to dispense solvent into an autosampler vial is shown for the old (B) and new (A) situation. The cleaning of the needle system in the rinser is also shown for the old (D) and new (C) situation.

the. needle prior to the dispensing of pure ethyl acetate, each alkane showed up in the GC–FID chromatogram at a concentration level of about 0.05 μg/ml. However, after cleaning of the needle system according to the procedure of Figure 2C, no memory effect was observed down to the 0.002 μg/ml level; that is, there was an at least 25-fold improvement. The new needle system was used without any problems for more than 300 analyses.

Design of new cartridge

The aim was to design a cartridge which can be easily (re)packed manually, which will not cause blank peaks and, of course, can be transported by the PrepStation tray. A scheme of the final design is shown in Figure 1. The SPE column was made of stainless steel and the fittings were made of polychlorotrifluoroethylene in order to prevent extraction of impurities during SPE. The same cartridge holder was used as with the original SPE cartridges. The internal dimensions of the new SPE column were chosen to be 12.9 mm x 1.8 mm I.D. rather than the 14.3 x 4.2 mm I.D. of the commercial 100 mg version, because in earlier studies 10 x 2 mm I.D. columns proved to be sufficient for SPE enrichment of analytes from up to 100 ml of aqueous sample [12, 13]. In addition, with a smaller column the elution volume is also smaller. A device which fits onto the stainless-steel column was designed to slurry-pack easily the home-made column with a suitable sorbent by means of a syringe. In this study, a polystyrene–divinylbenzene copolymer, 100 Å, 20 μm PLRP-S, was used as sorbent. The packed cartridge proved to be leak-tight at flows of up to 5 ml/min for more than 100 SPE analyses. When transferring ethyl acetate through the packed cartridge, and injecting 50 μl into either a GC–FID or a GC–MS system, no peaks from the cartridge showed up at a level corresponding to about 1 ng/ml of the extract (also see Figure 3 B).

Only when changing the type of cartridge, e.g. when replacing the commercial by the redesigned home-made cartridge, the dead volume had to be determined and the elution volume had to be optimized once. The dead volume of the cartridge loop (including the SPE cartridge) was determined to be 480 μl. Next, 50-ml HPLC-grade water samples spiked at the 0.6 μg/l level with a test mixture of 13 analytes (for their names, see Table 1) were analyzed by PrepStation–GC–FID using desorption volumes of 25–600 μl. 150 μl of ethyl acetate proved to be sufficient to desorb all analytes quantitatively (> 95%) from the cartridge. To be on the safe side, and to allow the use of conventional autosampler vials, 300 μl of ethyl acetate were routinely used for desorption. An internal standard, *N,N*-dibenzylaniline, was added to the extract prior to injection. In this way, slight variations in the desorption volume or injection volume or evaporation of solvent out of the vial are compensated.

Analysis of aqueous samples

Tap water

The system was tested by analysing 50 ml of Amsterdam tap water spiked at the 0.1 μg/l level with 13 micropollutants. 50 μl out of the 300 μl of extract were injected into the GC–MS system (**Figure 3**C). Figure 3 also compares the full-scan GC–MS chromatogram of ethyl acetate (Figure 3A) with the PrepStation–GC–MS chromatogram of a complete 'blank' sample preparation procedure (Figure 3B), i.e. including drying of the cartridge and transferring ethyl acetate through the new cartridge and 2-needle system, but without preconcentration of a water sample. It is obvious that there are no significant disturbances

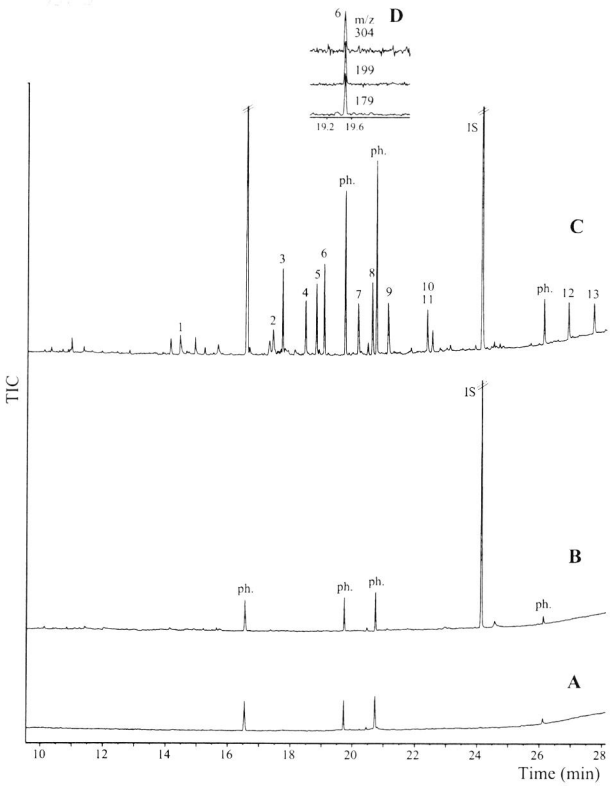

Figure 3

Full-scan PrepStation–GC–MS obtained after preconcentration of 50 ml of tap water spiked at the 0.1 µg/l level; 50 µl out of the 300 µl extract were injected (C). For comparison, the PrepStation–GC–MS chromatogram obtained for (A) ethyl acetate and (B) a complete 'blank' sample preparation procedure is shown; 50 µl were injected. Insert (D) shows the reconstructed ion chromatograms of three characteristic masses of diazinon (peak No. 6; m/z 179, 199 and 304) obtained after analysis of 50 ml tap water spiked at the 0.01 µg/l level (time scale twice as large as for full-scan chromatogram). Peak assignment: IS, internal standard (*N,N*-dibenzylaniline); 1, mevinphos; 2, desethylatrazine, 3, sulfotep, 4, atrazine; 5, trietazine; 6, diazinon; 7, simetryn; 8, terbutryn; 9, cyanazine; 10, bromophos-ethyl; 11, tetrachlorvinphos; 12, pyrazophos; 13, coumaphos. Peaks present in trace A are the IS and impurities present in the ethyl acetate used [ph., phthalate ester].

from the septa of the vial or the cartridge above a level corresponding to about 1 ng/ml of the extract. The four peaks showing up in Figure 3B next to the internal standard were phthalate esters present in the ethyl acetate used (Figure 3A). The recoveries of 12 out of the 13 analytes were fully satisfactory (80–110%) and the repeatability was good for all but one analyte (1–9%) (**Table 1**). The recovery of bromophos-ethyl was 75%, which can be attributed to losses due to its well-known adsorption to tubing walls caused by its high hydrophobicity [13]. With the polar mevinphos, there was some peak tailing which resulted in a rather poor repeatability (19%). The detection limits generally were 5–30 ng/l when using the

Table 1
Analyte recovery, repeatability and detection limits for PrepStation–GC–MS of tap water spiked at the 100 ng/l (recovery) or 10 ng/l (LODs) level.

Compound	Recovery (%)	RSD (%, n = 3)	LOD [a] (ng/l)
Mevinphos	110	19	10
Desethylatrazine	86	6	2
Atrazine	99	4	2
Trietazine	101	3	1
Sulfotep	98	2	2
Diazinon	97	4	2
Cyanazine	98	9	10
Simetryn	99	4	1
Terbutryn	97	4	1
Bromophos-ethyl	75	3	3
Pyrazophos	84	5	3
Coumaphos	87	7	10
Tetrachlorvinphos	95	7	4

[a] Limit of detection (S/N = 3) using appropriate reconstructed ion chromatogram (three m/z per analyte).

full-scan GC–MS chromatograms. When the reconstructed ion chromatograms of the appropriate (two or three) ions were used, the detection limits were at the 1–4 ng/l level. As an example, the reconstructed ion chromatograms for three characteristic masses of diazinon are shown in Figure 3D for an analysis at the 10 ng/l level

River water

The system was also used to determine micropollutants in river water. As an example, a large number of micropollutants were determined in 50 ml of unfiltered river Meuse water (Eysden, The Netherlands; July 11, 1995). To increase sensitivity, 100 µl rather than 50 µl out of the 300 µl of extract were injected into the GC–MS system. In the full-scan PrepStation–GC–MS chromatogram, 36 out of the 37 compounds spiked to the water sample at the 0.18 µg/l level showed up (**Figure 4**A); the recoveries of 35 out of the 37 compounds were good (75–110%). Lower recoveries were found for decamethyl-cyclopentasiloxane (40%, No. 4) and caffeine (16%, No. 32; not visible in full-scan trace). The lower recovery for caffeine can be ascribed to breakthrough due to its high polarity [14].

In order to detect and identify, the compounds present in the (non-spiked) river water sample (Figure 4B), reconstructed ion chromatograms of the appropriate characteristic masses of each compound rather than the full-scan chromatogram were used. Three examples are shown as inserts in Figure 4 (C–E). 24 of the test compounds were detected in the non-spiked sample at concentration levels from 0.2 up to 450 ng/l (**Table 2**). In one case, a small peak (No. 2) in the reconstructed ion chromatograms of two characteristic masses of 1,3-dichlorobenzene, m/z 146 and 148, shown in Figure 4C, indicates the presence of 1,3-dichlorobenzene at a level of 0.2 ng/l. Actually, two more peaks (Nos. 2' and 2'') show up at retention times closely similar to that of 1,3-dichlorobenzene. These indicate the presence of 1,4-dichlorobenzene and 1,2-dichlorobenzene, respectively. The presence of all three congeners could be confirmed by their mass spectra and a library search. In **Figure 5**, this is

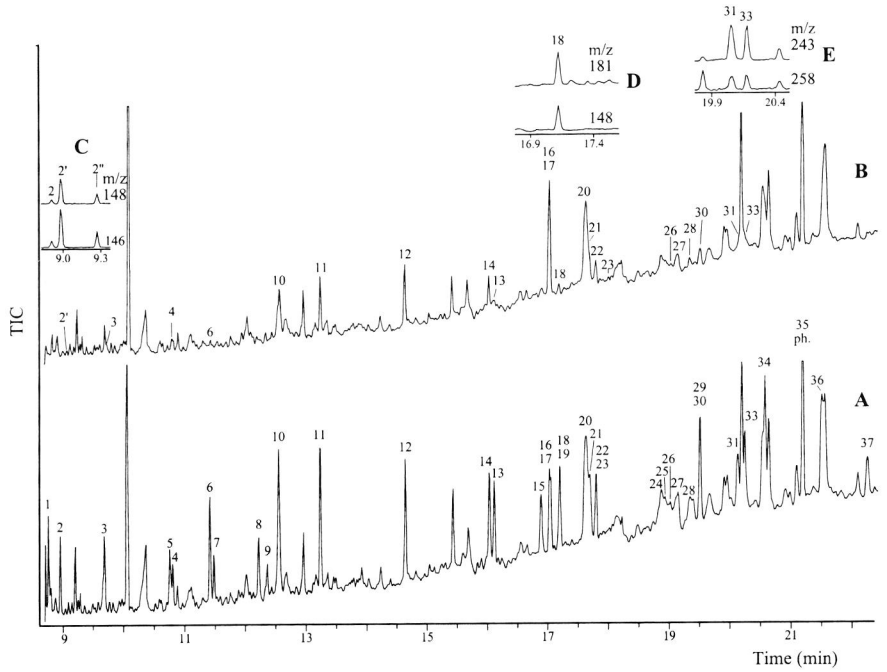

Figure 4

Full-scan PrepStation–GC–MS obtained after preconcentration of 50 ml of river Meuse water (B) without and (A) with spiking with 37 micropollutants at the 0.18 µg/l level. 100 µl out of the 300 µl extract were injected. The inserts show the reconstructed ion chromatograms of two characteristic masses of 1,3-dichlorobenzene (C), 2-methylthiobenzothiazole (D) and Musk G and T (E); the time scale is enlarged 2-fold compared to the full-scan chromatogram. The response scales for each of the two reconstructed ion chromatograms of the same compound are identical except for the mass trace m/z 258, which is enlarged twice compared to m/z 243. Peak assignment: 1, 2,4,6-trimethylpyridine; 2, 1,3-dichlorobenzene; 2', 1,4-dichlorobenzene; 2'', 1,2-dichlorobenzene; 3, acetophenone; 4, decamethyl-cyclopentasiloxane; 5, 2,5-dimethylphenol; 6, naphthalene; 7, α-terpineol; 8, quinoline; 9, dichlorvos; 10, isoquinoline; 11, 2-methylquinoline; 12, 2,4,7,9-tetramethyl-5-decyne-4,7-diol; 13, dibenzofuran; 14, triisobutyl phosphate; 15, *N,N*'-diethyl-3-methylbenzamide; 16, 2,2,4-trimethylpentane-1,3-dioldiisobutyrate; 17, diethyl phthalate; 18, 2-methylthiobenzothiazole; 19, diisopropylidenesorbofuranose; 20, tetraacetylethylenediamine; 21, tributyl phosphate; 22, ethyl citrate; 23, desethylatrazine; 24, dimethoate; 25, simazine; 26, atrazine; 27, tris(2-chloroethyl) phosphate; 28, *N*-butylbenzenesulfonamide; 29, diazinon; 30, tris(2-chloroisopropyl) phosphate; 31, Musk G; 32, caffeine; 33, Musk T; 34, *N,N*'-diethyl-*N,N*'-diphenylurea; 35, ethofumesate; 36, metolachlor; 37, metazachlor; ph., phthalate ester.

demonstrated for 1,4-dichlorobenzene; all relevant peaks of the library spectrum showed up in the acquired spectrum, and the (reversed) hit factor was 963, with 1000 being the maximum. As similar response factors can be assumed for the three dichlorobenzenes [15], the two additional congeners could be provisionally quantified, with levels of 1.5 ng/l for 1,4-dichlorobenzene and 0.6 ng/l for 1,2-dichlorobenzene. With 1,3-dichlorobenzene, the four most abundant mass peaks showed up in the mass spectrum even at 0.2 ng/l.

Table 2
PrepStation–GC–MS of micropollutants in 50 ml of unfiltered river Meuse water.

No.	Compound	Concentration (ng/l)
2	1,3-Dichlorobenzene	0.2
2'	1,4-Dichlorobenzene	1.5
2''	1,2-Dichlorobenzene	0.6
3	Acetophenone	6
4	Decamethyl-cyclopentasiloxane	7
6	Naphthalene	4
10	Isoquinoline	74
11	2-Methylquinoline	30
12	2,4,7,9-Tetramethyl-5-decyne-4,7-diol	190
13	Dibenzofuran	7
14	Triisobutyl phosphate	52
15	*N,N'*-Diethyl-3-methylbenzamide	15
16	2,2,4-Trimethylpentane-1,3-dioldiisobutyrate	110
17	Diethyl phthalate	75
18	2-Methylthiobenzothiazole	9
20	Tetraacetylethylenediamine	430
21	Tributyl phosphate	33
22	Ethyl citrate	145
23	Desethylatrazine	42
25	Simazine	10
26	Atrazine	37
27	Tris(2-chloroethyl) phosphate	46
28	*N*-Butylbenzenesulphonamide	40
30	Tris(2-chloroisopropyl) phosphate	66
31	Musk G	3
33	Musk T	3

Together with another example, the detection and identification of 2-methylthiobenzothiazole at the 9 ng/l level (Figures 4D and 5C and D, respectively; (reversed) hit factor, 951) , the combined information should suffice to illustrate that the detection limits were, typically, 0.5–2 ng/l, and the identification limits, 1–4 ng/l. The detection limits were closely similar to those found for tap water, with the higher injection volume (100 vs. 50 µl) offsetting the disadvantage of a higher background/noise level.

Since the PrepStation uses a syringe pump for loading of the cartridges, it is possible to analyze unfiltered water samples, as was done in the previous example. As a final illustration of the potential of PrepStation–GC–MS, we studied the loss of analytes which may occur if river water samples are filtered through a 0.45 µm membrane filter prior to analysis. A river Meuse water sample (Eysden, Netherlands; September 26, 1995) was spiked with 13 micropollutants at the 0.6 µg/l level. First, the unfiltered sample was analyzed; the sample was left standing for some 30 min prior to analysis to allow the largest particles to precipitate in the sample. In a second analysis, part of the spiked sample was filtered through a 0.45 µm membrane filter prior to analysis. For further comparison, another sample taken at the same time was filtered first, and then spiked.

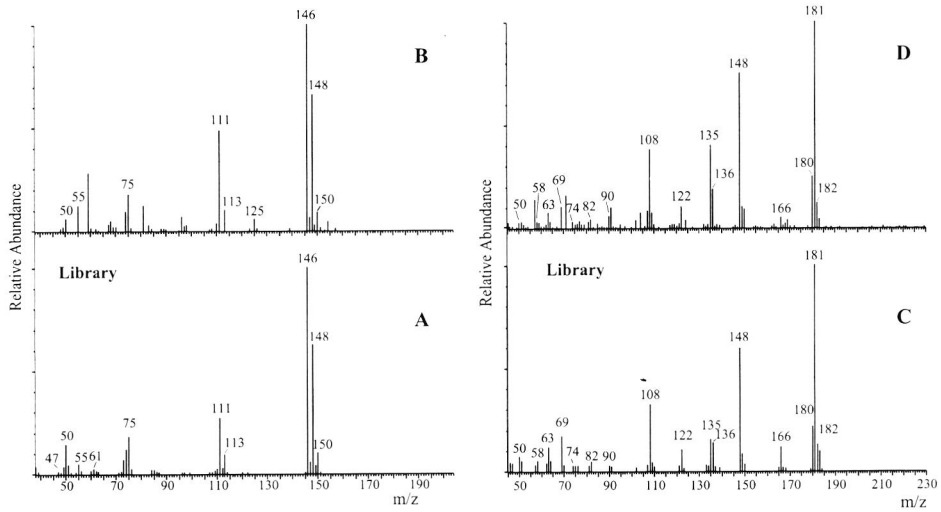

Figure 5
Mass spectra of peaks at (B) 8.97 min and (D) 17.12 min obtained from the PrepStation–GC–MS analysis of 50 ml of non-spiked river Meuse water (Figure 4B). For further details, see legend of Figure 4 and text. For comparison, the library spectra of (A) 1,4-dichlorobenzene and (C) 2-methylthiobenzothiazole are shown.

Table 3
Effect of filtering of river water sample on the recovery of several micropollutants using PrepStation–GC–MS.

Compound	log K_{OW} [a]	Recovery (%) after:		
		no filtration	filtration after spiking	filtration prior to spiking
Mevinphos	0.1	89	97	82
Desethylatrazine	1.5	82	82	77
Atrazine	2.7	103	102	102
Trietazine		103	99	108
Sulfotep	4.0	105	74	121
Diazinon	3.3	96	79	106
Cyanazine	2.2	89	78	85
Simetryn	2.6	97	94	96
Terbutryn	3.7	111	99	113
Bromophos-ethyl	5.9	69 [b]	0	81
Pyrazophos	3.8	105	0	110
Coumaphos	4.1	92	0	91
Tetrachlorvinphos	3.5	106	72	114

[a] K_{OW}, octanol–water coefficient, values taken from refs. [16–18].

[b] For explanation, see text and ref. [13].

Scrutiny of the data of **Table 3** (while keeping in mind the RSD values reported in Table 1) rapidly shows the reliability of the analytical procedure: the 'no filtration' and 'filtration. prior to spiking' data are essentially the same for all test compounds.

Table 3 shows that for seven out of the thirteen compounds, the recoveries were comparable with a mutual difference of 10–15%. Sulfotep, diazinon and tetrachlorvinphos showed somewhat lower recoveries of 70–80% upon filtration after spiking, while bromophos-ethyl, pyrazophos and coumaphos were not recovered at all. Although there is no direct correlation between analyte recovery and log K_{ow} (octanol–water coefficient), it is obvious from the data in Table 3 that appreciable losses due to adsorption of the analytes on the particulate matter in the water sample start to occur if log K_{ow} is about 3.5. Obviously, if one is especially interested in the total amount of the more apolar analytes in a water sample, it should not be filtered prior to analysis. However, if the analysis is performed in order to assess the quality of water intended for the production of drinking water, filtration prior to analysis is not a real problem, because the particulate matter will be filtered out anyway during processing.

The present system was used without any real maintenance problem for the analysis of a large variety of river and tap water samples.

4.2.4 Conclusions

After further optimization of a PrepStation by redesigning the cartridge and introducing a 2-needle system, all earlier problems regarding interferences due to impurities coming from the septa and cartridges have been eliminated, and time-consuming pre-cleaning is now superfluous. Using large-volume injections (50–100 µl) and full-scan and reconstructed ion MS detection, it is now possible to determine a wide range of micropollutants down to the 1–2 ng/l level in 50 ml of tap and surface water samples. Another advantage of the PrepStation is its ability to analyze unfiltered river water samples.

The present system proved to be robust during the analysis of several hundreds of tap and river water samples.

References

[1] H.G.J. Mol, H.-G. M. Janssen, C.A. Cramers, J.J. Vreuls and U.A.Th. Brinkman, *J. Chromatogr. A*, 703 (1995) 277.
[2] I. Liska J., *Chromatogr. A*, 655 (1993) 163.
[3] A.J.H. Louter, U.A.Th. Brinkman and R.T. Ghijsen, *J. Microcol. Sep.*, 5 (1993) 3031.
[4] K.D. Fogelman, *Lab. Robot. Autom.*, 5 (1993) 103.
[5] Th. Hankemeier, P.C. Steketee, J.J. Vreuls and U.A.Th. Brinkman, *J. Chromatogr. A*, 750 (1996) 161.
[6] A. Polettini, A. Groppi, C. Vignali and M. Montagna, *J. Chromatogr. B*, 713 (1998) 265.
[7] C. Soriano, J. Munoz-Guerra, D. Carreras, C. Rodriguez, A.F. Rodriguez and R. Cortes, *J. Chromatogr. B*, 687 (1998) 183.
[8] A. Namera, M. Yashiki, K. Okada, Y. Iwasaki, M. Ohtani and T. Kojima, *J. Chromatogr. B*, 706 (1998) 253.
[9] I.M. Bengtsson and D.C. Lehotay, *J. Chromatogr. B*, 685 (1996) 1.
[10] K. Grob, H.-G. Schmarr and A. Mosandl, *J. High Resolut. Chromatogr.*, 12 (1989) 375.

[11] S. Ramalho, Th. Hankemeier, M. de Jong, U.A.Th. Brinkman and J.J. Vreuls, *J. Microcol. Sep.*, 7 (1995) 383.
[12] I. Liska, E.R. Brouwer, A.G.L. Ostheimer, H. Lingeman, U.A.Th. Brinkman, R.B. Geerdink and W.H. Mulder, *Intern. J. Environ. Anal. Chem.*, 47 (1992) 267.
[13] Th. Hankemeier, A.J.H. Louter, F.D. Rinkema and U.A.Th. Brinkman, *Chromatographia*, 40 (1995) 119.
[14] Th. Hankemeier, S.P.J. van Leeuwen, J.J. Vreuls and U.A.Th. Brinkman, *J. Chromatogr. A*, 811 (1998) 117.
[15] Th. Hankemeier, *Quantitative Determinations in GC/MS: the Concept of the Molar Response*, M.Sc. thesis, University of Ulm, Ulm, Germany, 1992.
[16] A. Noble, *J. Chromatogr.*, 642 (1993) 3.
[17] D. Brown and E. Flagg, *J. Environ. Qual.*, 10 (1981) 382.
[18] C.D.S. Tomlin, *The Pesticide Manual*, BCPC Publications, Berks, UK, 11th ed, 1997.

5

On-line SPE–GC with atomic emission detection

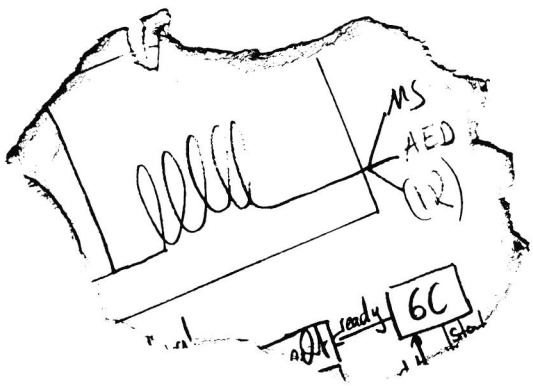

5.1 On-line coupling of SPE and GC with AED

Summary

An on-line solid-phase extraction–gas chromatography–atomic emission detection (SPE–GC–AED) system has been set up using an on-column interface to transfer 100 µl of desorbing solvent to the GC part of the system. Analytical characteristics such as recovery, precision and linearity of the calibration plots were comparable with those of the off-line combination of SPE–GC–AED using organophosphorus pesticides (OPPs) as test compounds. The fully on-line set-up causes a marked increase of detectability because of the quantitative transfer of the analytes from the SPE module to the GC: detection limits are as low as 5–20 ng/l for the analysis of 10-ml raw and spiked surface water samples using the phosphorus channel. Detectability can be further enhanced by processing up to 100-ml samples. The integrated analytical system is robust. The potential of the on-line set-up has been demonstrated for the analysis of surface water and waste water.

5.1.1 Introduction

A relative newcomer in the field of detectors is the atomic emission detector (AED) which was specially designed for capillary gas chromatography (GC). In principle, GC–AED allows the selective detection of any element except helium [1]. With typical detection limits in the order of 0.1 pg/s for organometallics, 0.2 pg/s for carbon and 1 pg/s for sulphur, GC–AED is ideally suited for rapid and selective screening of a wide range of environmental samples. Determination of the elemental composition of unknowns can also provide highly desirable additional information to that obtained from GC with mass-selective detection (GC–MS) [2]. Admittedly, for several elements with environmental relevance such as nitrogen and the halogens, detectability using the AED is less good than when using a thermionic (NPD) or an electron-capture detector, respectively [3]. However, this drawback can be largely overcome by combining GC–AED with large-volume injections.

Today, solid-phase extraction (SPE) is often the preferred sample pretreatment procedure if organic microcontaminants have to be determined at trace level in aqueous samples, and the off-line combination of SPE and GC analysis is well documented in the literature [4, 5]. Unfortunately, a common drawback of these procedures is that a rather small aliquot of, typically, 0.1–2% of the concentrated extract is injected into the GC system. In other words, analyte detectability expressed in terms of concentration units, is seriously reduced in the penultimate step of the total procedure. Although this problem can be overcome by, e.g., even further concentration by means of rigorous evaporation or the use of water samples of ca. 1 litre, disadvantages such as the loss of the more volatile analytes [6] and tedious sample handling often requiring the use of 100–200 ml of organic solvent, respectively, make it increasingly attractive to combine SPE and GC analysis on-line rather than off-line.

The inherent advantages of on-line SPE–GC for the analysis of aqueous samples have repeatedly been discussed in recent years [7] and, based on experience gained in the field of column liquid chromatography – i.e., with SPE–LC [8] – several systems have been designed for semi- and fully automated SPE–GC of aqueous samples with, often, NPD or MS detection [9–11]. In most instances, transfer of the analytes retained by and, then, desorbed from the SPE precolumn, requires only about 100 µl of an organic solvent [12]. In order for such an procedure to be applicable to GC–AED, that is, in order to design a fully on-line SPE–GC–AED system, it is necessary to find out first whether it is possible to use large-volume injections in combination with AED detection, because this detector is generally considered rather vulnerable. Recent work has shown that there is no need for serious concern. Goosens et al. [13] demonstrated that it is possible to introduce up to 100 µl of several organic solvents into a GC–AED system without any real problems. Next, Rinkema et al. [14] reported the successful use of an off-line combination of SPE and GC–AED using injections of 100-µl sample extracts in ethyl acetate (which correspond to an aliquot of 20%) via a loop-type interface. Several real-life samples were analysed.

As a continuation of the earlier work, an on-line and fully automated SPE–GC–AED system has now been set up. For the introduction of the desorption solvent into the GC part of the system an on-column, rather than a loop-type, interface was selected in order to provide a wider application range [7, 15]. The analytical potential of the on-line set-up was studied in some detail, and its performance was compared with that of the earlier off-line combination. Organophosphorus pesticides (OPPs) were used as test compounds, and both raw and spiked surface water samples were analysed.

5.1.2 Experimental

Chemicals

HPLC-grade water (J.T. Baker, Deventer, The Netherlands) was used to condition (removal of ethyl acetate) and to clean-up the trace-enrichment precolumn. Ethyl acetate (99.9%, p. a., J.T. Baker) was distilled before use. Eleven OPPs were chosen as a test set in the whole study. They were purchased from Riedel-de Haën (Seelze, Germany) and were of at least 98% purity. Stock solutions of the OPPs of 10 mg/ml in ethyl acetate were stored in the dark at 4°C. Spiking water samples with those stock solutions was done just before analysis. High-purity helium gas (5.0) was obtained from Union Carbide (Westerlo, Belgium).

Equipment

A schematic of the set-up of the SPE–GC–AED system is shown in **Figure 1**. The SPE module consisted of a Kontron Tracer 670 valve-switching unit (Kontron Analytic, London, U.K.) with four pneumatic six-port valves. The system was controlled by a Model 200 Programmer (Kontron). Ethyl acetate was delivered by a Model 300 (Gynkotek, Germering, Germany) dual-piston pump. A 80 cm x 50 µm I.D. restriction capillary was installed between the pump and valve V2 to provide a constant and pulse-free flow of 76 µl/min. HPLC-grade water was delivered by a Spectroflow 400 (Applied Biosystems, Rotterdam, The Netherlands) pump at 2 ml/min. For the analysis of water samples a 2.2 ml-loop mounted on valve V1 was used, the aqueous sample was flushed into the precolumn with 4 ml by the HPLC-grade water pump. If larger volumes were analysed, the loop was replaced

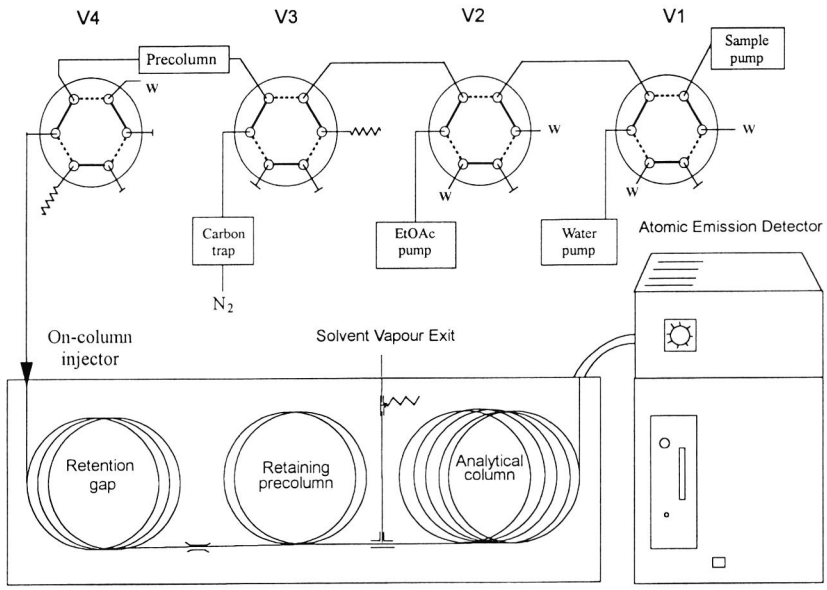

Figure 1
Set-up of the on-line SPE–GC–AED system. Abbreviation: EtOAc, ethyl acetate; W, waste.

by a Gilson (Villiers-le-Bel, France) Model 302 pump; the sample loading speed was then 5 ml/min. The samples were preconcentrated on a 10 mm x 2 mm I.D. stainless-steel precolumn (Chrompack, Middelburg, the Netherlands) inserted between valves V3 and V4. The precolumn was packed with 10 μm particles of 300 Å PLRP-S (Polymer Laboratories, Church Stretton, UK), which is a styrene–divinylbenzene copolymer. Water remaining in the precolumn after sample loading was removed from the precolumn by a nitrogen purge (30 min, 50 ml/min); the nitrogen was purified with a carbon trap (20/40 mesh Carbotrap C, Supelco, Bellefonte, PA, USA).

The GC–AED system (Hewlett Packard, Waldbronn, Germany) consisted of an HP 5890 Series II gas chromatograph with electronic pressure control, an on-column injector and the HP 5921 A AED detector. The SPE unit was interfaced to the GC system *via* a 30 cm x 50 μm I.D. fused silica capillary. This capillary, which was permanently mounted in the on-column injector, was inserted into a 5 m x 0.32 mm I.D. diphenyltetramethyldisilazane-deactivated retention gap (BGB Analytik, Zürich, Switzerland). The retention gap was connected by means of a press-fit connector to a 3 m x 0.32 mm I.D. section of the GC column (SPB 5, 0.25 μm film, 0.32 mm I.D.; Supelco), which served as a retaining precolumn. The analytes were desorbed and transferred to the GC system using 108 μl of ethyl acetate at a flow rate of 76 μl/min. An early solvent vapour exit (SVE) was inserted between the retaining precolumn and the 15 m x 0.32 mm I.D. SPB 5 analytical column to create the desired evaporation rate of 71 μl/min. The SVE consisted of a 24 V pinch solenoid valve (Type S 104; Sirai, Milan, Italy), which closed a 2 mm O.D. silicone tubing and was controlled by the purge B triggering signal of the GC. The oven temperature during analyte transfer was 80°C. After 5 min the temperature was programmed to 280°C at 20°C/min and finally held at 280°C for 2 min. The conditions used for the AED are shown in **Table 1**.

Table 1
AED parameters used for on-line SPE–GC–AED [a].

Element	Wavelength (nm)	Scavenger gas	Make-up flow (ml/min)
C	193.0	H_2,O_2	40
Cl	480.2	O_2	40
P	185.9	H_2	80
N	174.2	H_2,O_2	40

[a] Transfer line temperature, 300°C; cavity temperature, 300°C

Procedure

The various steps of the sample preparation part of the on-line SPE–GC–AED procedure were programmed into the control unit. Except for manual injection of the sample when using a sample loop, the whole procedure – i.e. conditioning of the precolumn, sampling, clean-up with HPLC-grade water, desorption and transfer of the analytes to the GC system, solvent evaporation *via* the SVE and GC–AED analysis of the transferred analytes – was automated.

Each run was started with conditioning the precolumn with 4 ml of HPLC-grade water at 2 ml/min. Next, valve V1 was switched in order to effect preconcentration of the water sample in the 2.2-ml loop, or by means of the additional sample pump which was operated at 5 ml/min. After preconcentration some clean-up was achieved by flushing the precolumn with 1.8 ml of HPLC-grade water. Next, the precolumn was dried for 30 min with a 50 ml/min flow of nitrogen. During drying all connection capillaries were flushed with ethyl acetate in order to remove any water present and to pressurize the ethyl acetate, because the transfer capillary acted as restriction during the transfer [11]. Desorption of the analytes by ethyl acetate and transfer of the first 108 µl of ethyl acetate to the GC system was started by switching valves 3 and 4 simultaneously.

The GC oven temperature during transfer was 80°C and the head pressure was increased from 50 kPa to 160 kPa at 680 kPa/min after starting the transfer. The SVE was closed just before the last drop of ethyl acetate had evaporated. The head pressure was next decreased to 50 kPa at 680 kPa/min, and programmed to provide a constant flow rate. 5 min after the start of the transfer the vent of the AED was closed and the temperature gradient started. When preconcentrating 2.2-ml samples, the total analysis time was 51 min. To increase sample throughput, the next sample pretreatment was started after the end of the transfer into the GC system by flushing the precolumn with ethyl acetate for 5 min at 76 µl/min. This decreased the time needed per sample to 40 min.

River and waste water samples were filtered through 0.20 µm membrane filters (Schleicher & Schüll, Dassel, Germany).

5.1.3 Results

Design and optimization of the on-line SPE–GC–AED system

Using an on-column interface for the transfer of the desorption solvent to the GC system requires a pumping system which provides a constant and non-pulsating flow. Usually, an (expensive) syringe pump is used for this purpose. In this work a conventional dual-piston pump was used, and a constant flow rate was achieved by means of a pulse damper and a long restriction capillary of 50 µm I.D..

The critical parameters in an on-line SPE–GC procedure such as transfer temperature, pressure and the length of the retention gap were chosen to yield an evaporation rate of 71 µl/min which is somewhat lower than the transfer rate of 76 µl/min to ensure that the flooded zone in the retention gap due to the large-volume injection did not reach the retaining precolumn [16].

Although earlier results showed that 100-µl injections of samples in ethyl acetate did not cause any flame-outs of the AED [13], an early solvent vapour exit (SVE) was installed (cf. Figure 1) to increase the solvent evaporation rate [17]. Additionally, the head pressure of the GC was increased during analyte transfer from the precolumn to the retention gap. The SVE was closed just 1–2 sec before completion of the solvent evaporation in order to prevent loss of more volatile compounds. The solvent vent of the AED was closed only after 5 min to make sure that no solvent reached the discharge tube of the AED.

On-line SPE–GC–AED compared with off-line combination

The performance and reliability of the on-line SPE–GC–AED system were tested by determining the recovery, relative standard deviation (RSD), analyte detectability and linearity for eleven organophosphorus pesticides in HPLC-grade and real water samples. The data were compared with results obtained for the same test compounds with the off-line SPE/GC–AED set-up mentioned above [14]. Enhancing the detection limits (in concentration units) was studied for sample volumes up to 100 ml. For quantitation the phosphorus channel of the AED was used, because the AED is more sensitive for phosphorus than for nitrogen or carbon [1]. Other channels were used for provisional compound identification.

Recovery, RSD and linearity

The recoveries of the test compounds for the analysis of spiked HPLC water generally were satisfactory (79–105%) and fully comparable with those obtained in off-line SPE/GC–AED measurements. In both instances, rather low recoveries were observed for bromophos-ethyl (40–45%) and ethion (60–70%). These two compounds are quite apolar and adsorption to capillary walls and/or valves will therefore readily occur during sampling. To prevent such adsorption problems, in a next experiment, 10% methanol was added to the water sample before the sampling step. The recoveries for bromophos-ethyl and ethion now increased to 82% and 90%, respectively, whereas the recoveries of the other compounds did not change. Actually, the only real difference between the on-line and off-line experiments was found with mevinphos, which gave broad peaks (cf. **Figures 2**B and 3B) and therefore was excluded in studies of recovery, RSD and linearity. To all probability this was due to using too adsorptive a retention gap.

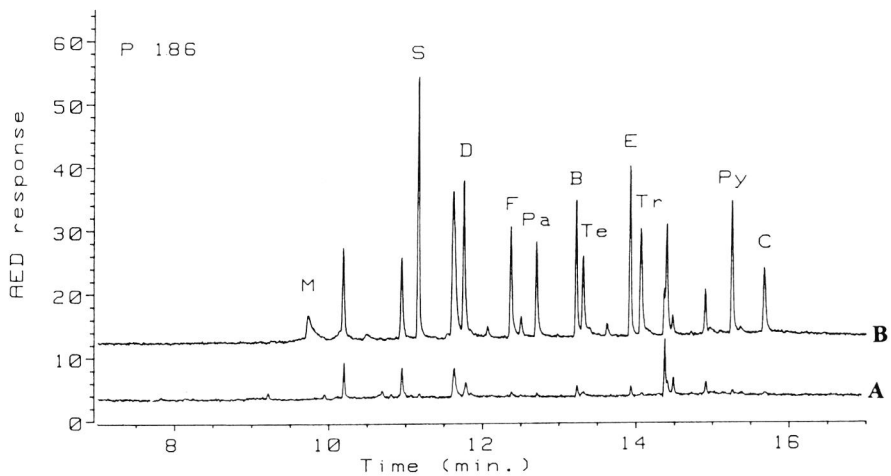

Figure 2

On-line SPE–GC–AED (P channel) of 100 ml of HPLC-grade water, (A) without and (B) with spiking at the 10 ng/l level. Peak assignment of OPPs used for spiking: M, mevinphos; S, sulfotep; D, diazinon; F, fenchlorphos; Pa, parathion-ethyl; B, bromophos-ethyl; Te, tetrachlorvinphos; E, ethion; Tr, triazophos; Py, pyrazophos; C, coumaphos.

The RSDs for the analysis of 2.2-ml HPLC-water samples spiked at the 5 µg/l level were rather good (4–11%) (**Table 2**). Compared with the off-line experiments, the RSD values are comparable or slightly better, as they should be for an on-line procedure.
Linearity in the 0.1–25 µg/l range (6 data points) was satisfactory. The regression coefficients, R^2, were between 0.997 and 0.999 for all OPPs except bromophos-ethyl (0.980) and tetrachlorvinphos (0.987) (Table 2).

Detection limits
With regard to analyte detectability 10-ml samples were analysed in both on-line and off-line SPE–GC–AED. With the off-line method an extract of 500 µl was obtained, of which an aliquot of 100 µl was injected into the GC using a loop-type interface [14], whereas with the on-line method the whole sample extract was injected. The clear increase in detectability so obtained can be read from the data in **Table 3**. To a first approximation, the expected 5-fold enhancement is well borne out by the two ranges of values, of 15–270 ng/l (off-line) and 5–20 ng/l (on-line), respectively.

The above results certainly are not the limit of what can be achieved. By analyzing 100 ml, instead of the earlier 10 ml, of sample, now spiked at the 10 ng/l level, detection limits of 0.5–1.5 ng/l were obtained for all OPPs (except mevinphos; cf. above). The almost invariable 10-fold improvement in detection limits (see **Table 3**) simultaneously demonstrates that breakthrough of the OPPs on the precolumn is essentially absent even with the 100-ml sample. The chromatograms obtained for the analysis of a 100 ml blank (Figure 2A) and a 10 µg/l spiked (Figure 2B) sample monitored using the phosphorus channel demonstrate that detection does not create problems even at this low level.

Table 2
Recovery, RSD (n=5) and linearity (6 data points) data for eleven OPPs by means of on-line and off-line SPE–GC–AED[a].

	Recovery (%)		RSD (%)		Linearity
Compounds	Off-line	On-line	Off-line	On-line	On-line
Mevinphos	87	-	7	-	-
Sulfotep	95	97	6	7	0.9994
Diazinon	110	105	9	4	0.9993
Fenchlorphos	85	86	4	7	0.9984
Parathion	95	92	10	7	0.9970
Bromophos-ethyl	42	44	22	5	0.9801
Tetrachlorvinphos	86	80	9	6	0.9872
Ethion	72	61	11	9	0.9973
Triazophos	104	79	5	7	0.9992
Pyrazophos	96	82	5	5	0.9999
Coumaphos	102	78	18	11	0.9992

[a] Off-line studies: 10 ml of water spiked at 1 µg/l level; on-line studies: 2.2 ml of water at 5 µg/l level. Linearity was tested over 0.1–25 µg/l range.

Table 3
Comparison of detection limits (ng/l; signal-to-noise, 3) for OPPs in aqueous samples using off-line and on-line SPE–GC–AED.

Compounds	Detection limits (ng/l) for:		
	Off-line 10 ml, 1 µg/l sample	On-line 10 ml, 0.1 µg/l sample	On-line 100 ml, 10 ng/l sample
Mevinphos	50	-	-
Sulfotep	15	5	0.5
Diazinon	30	10	1.0
Fenchlorphos	30	10	1.0
Parathion	30	15	1.0
Bromophos-ethyl	150	10	1.0
Tetrachlorvinphos	70	30	1.5
Ethion	40	5	0.5
Triazophos	75	20	1.5
Pyrazophos	130	15	1.0
Coumaphos	275	30	1.5

Analysis of river water and municipal waste water

The present system was used for the analysis of river Meuse water (sampled at Eysden, the Netherlands; July 17, 1993). The sample was spiked at the 0.1 µg/l level with the OPPs used as test compounds. The chromatograms of a raw and a spiked sample are shown in **Figures 3**A and 3B, respectively (P 186 channel). In both cases 50-ml samples were analysed. The detection limits clearly are on the order of 1–30 ng/l; that is, they do not deviate too much from the values for HPLC-grade water included in Table 3. The spiked pesticides were not

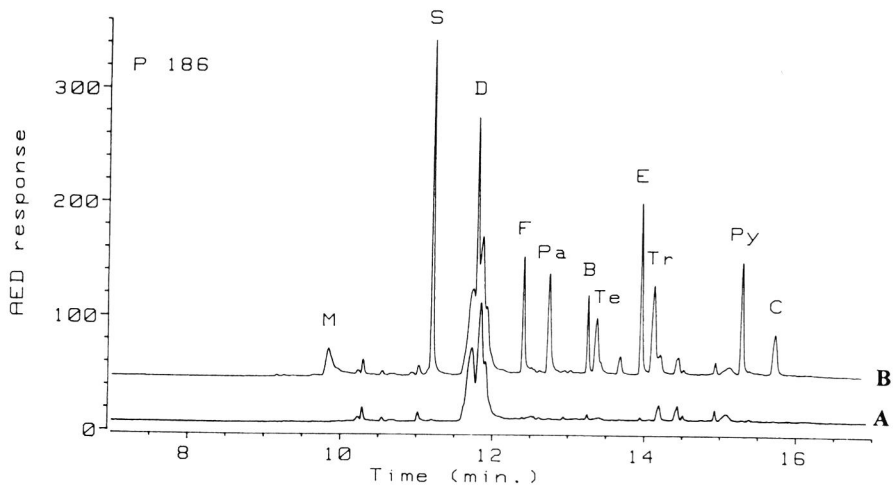

Figure 3
On-line SPE–GC–AED (P channel) of (A) 50 ml Meuse water and (B) 50 ml Meuse water spiked with OPPs at the 0.1 µg/l level. For peak assignment, see Figure 2.

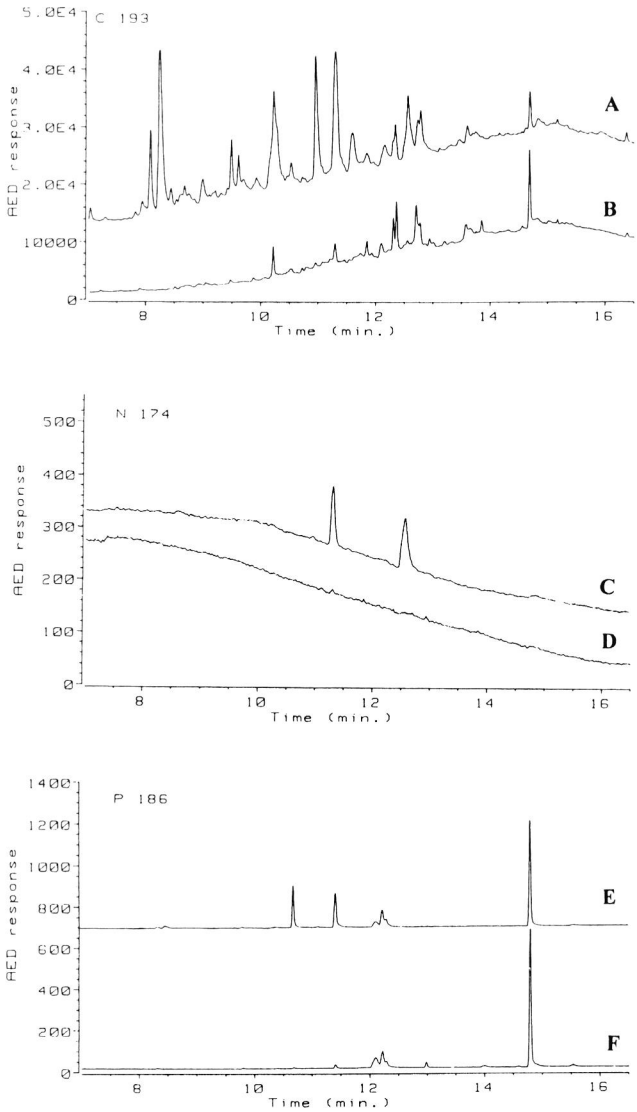

Figure 4
On-line SPE–GC–AED of 10-ml waste water samples using (A, B) the C 193, (C, D) the N 174 and (E, F) the P 186 channel. The influent (A, C, E) and effluent (B, D, F) were analysed.

present in the river Meuse sample at these concentration levels. So far, well over 100 HPLC-grade and river water (cf. below) samples have been analysed without any serious experimental or maintenance problems.

On-line SPE–GC–AED was also used for the analysis of municipal waste water; 10-ml waste water samples were analysed. The samples were taken before and after the biological treatment. **Figure 4** shows typical results for both influents and effluents using the carbon (Figures 4A, B), nitrogen (Figures 4C, D), and phosphorus (Figures 4E, F) channels. Since the influent and effluent samples were taken at the same time, and sampling time was only a

few minutes, no definitive conclusions can be drawn from the several influent and effluent traces; the general 'clean-up' of the treatment procedure is obvious from the carbon and nitrogen traces shown, but not from the phosphorus traces. A more systematic study involving peak identification is reported in Chapters 5.2 and 5.3. The main purpose of the present experiments was to demonstrate that SPE–GC–AED really has a wide application range. Actually, when analyzing the waste water samples, the SPE cartridge had to be exchanged more often (once every 200–300 ml), especially when analyzing the influent, than when analyzing surface water (once every litre). Also the retention gap had to be exchanged more often when analyzing the influent.

5.1.4 Conclusions

The present study shows that on-line SPE–GC–AED is a viable approach for the trace-level determination of environmental pollutants in water samples. With 10–100 ml samples, detection limits of 1–30 ng/l can be obtained, even in real-life samples, when using the phosphorus channel. This indicates that the threshold values of 0.1 µg/l and 1 µg/l, typically set for priority pollutants in drinking and surface water, respectively, can easily be obtained with many other element channels of the atomic emission detector also. With the present set of test compounds, characteristics of the integrated analytical system such as analyte recovery, linearity of calibration plots, and repeatability were found to be fully satisfactory. Maintenance of the system did not present any special problems.

In other words, the scope of on-line, and automated, SPE–GC for which, so far, NPD, MS, flame photometric and flame ionization detection have been used, has again been extended. This is especially interesting because AED detection is well suited for general monitoring and screening purposes of highly complex samples. On the other hand, SPE–GC–AED can also be used to confirm results obtained with selective GC detection or mass-selective detection. Next to extending the applicability range of the present system by studying other element channels, such correlation of on-line SPE–GC data obtained with various detectors, including the atomic emission detector, will be the subject of our future research.

References

[1] P.L. Wylie and B.D. Quimby, *J. High Resolut. Chromatogr.*, 12 (1989) 813.
[2] M. Cooke, D.A. Leathard, C. Webster and V. Rogers, *J. High Resolut. Chromatogr.*, 16 (1993) 662.
[3] H.-J. Stan and M. Linkerhägner, *J. High Resolut. Chromatogr.*, 16 (1993) 548.
[4] H. Kobayashi, K. Ohyama, N. Tomiyama, Y. Jimbo, O. Matano and S.Goto, *J. Chromatogr.*, 643 (1993) 197.
[5] J. Beltran, F.J. Lopez and F. Hernandez, *Anal. Chim. Acta*, 283 (1993) 297.
[6] K. Grob and E. Müller, *J. Chromatogr.*, 404 (1987) 297.
[7] J.J. Vreuls, G.J. de Jong, R.T. Ghijsen and U.A.Th. Brinkman, *J. Assoc. Off. Anal. Chem.*, 77 (1994) 306.
[8] J. Slobodnik, E.R. Brouwer, R.B. Geerdink, W.H. Mulder, H. Lingeman and U.A.Th. Brinkman, *Anal. Chim. Acta*, 268 (1992) 55.
[9] P.J.M. Kwakman, J.J. Vreuls, U.A.Th. Brinkman and R.T. Ghijsen, *Chromatographia*, 34 (1992) 41.
[10] A.J.H. Louter, U.A.Th. Brinkman and R.T. Ghijsen, *J. Microcol. Sep.*, 5 (1993) 303.

[11] A.-J. Bulterman, J.J. Vreuls, R.T. Ghijsen and U.A.Th. Brinkman, *J. High Resolut. Chromatogr.*, 16 (1993) 397.
[12] J.J. Vreuls, W.J.G.M. Cuppen, G.J. de Jong and U.A.Th. Brinkman, *J. High Resolut. Chromatogr.*, 13 (1990) 157.
[13] E.C. Goosens, D. de Jong, G.J. de Jong, F.D. Rinkema and U.A.Th. Brinkman, *J. High Resolut. Chromatogr.*, 18 (1995) 38.
[14] F.D. Rinkema, A.J.H. Louter and U.A.Th. Brinkman, *J. Chromatogr. A*, 678 (1994) 289.
[15] K. Grob Jr. and J.-M. Stoll, *J. High Resolut. Chromatogr.& Chromatogr. Commun.*, 9 (1986) 518.
[16] K. Grob Jr., G. Karrer and M.-L. Riekkola, *J. Chromatogr.*, 334 (1985) 129.
[17] K. Grob, H.-G. Schmarr and A. Mosandl, *J. High Resolut. Chromatogr.*,12 (1989) 375.

5.2 Data correlation in on-line SPE–GC–AED/MS detection of unknown microcontaminants

Summary

A procedure is described for the (non-target) screening of hetero-atom-containing compounds in tap and waste water by correlating data obtained by gas chromatography (GC) using atomic emission (AED) and mass selective (MS) detection. Solid-phase extraction was coupled on-line to both GC systems to enable the determination of microcontaminants at the 0.02–1 μg/l level in 7–50 ml of aqueous sample. The screening was limited to compounds present in at least one hetero-atom-selective GC–AED trace above a predetermined concentration level. These compounds were identified by their partial formulae (AED) and the corresponding mass spectra, which were obtained from the GC–MS chromatogram via the retention index concept. The potential of the approach was demonstrated by the identification of target compounds as well as all unknowns present in tap and waste water above the predetermined threshold of 0.05 μg/l (tap water) or 0.5 μg/l (waste water).

5.2.1 Introduction

Large numbers of environmental samples have to be screened for the presence of organic microcontaminants. Solid-phase extraction (SPE) or liquid–liquid extraction are often used for sample preparation, with subsequent gas chromatographic (GC) separation. Detection is often done with element-selective detectors. However, because of their selectivity, these detectors are not necessarily the proper choice for screening studies. This helps to explain the growing popularity of the atomic emission detector (AED) [1–3]. An additional advantage of this detector is that the response per mass unit of an element is more or less independent of the structure of the analyte of interest [4–7], although this statement is not uncontested [8, 9]. A compound-independent elemental response would allow simplified quantification based on universal calibration with an element calibration curve rather than calibration curves for all analytes.

Even if structure-independent responses would allow the provisional calculation of the elemental composition of a compound, identification will require the additional use of mass spectrometric (MS) detection. It is, however, generally recognized that subjecting complete chromatograms peak-by-peak to full-scan MS screening is not a very realistic option. In addition, the search for analytes of interest, e.g. those containing one or two selected hetero-atoms, conducted in the first (screening, i.e. AED) mode should be directly related to the second (confirmation/identification, i.e. MS) mode. This is what has, as yet, not been done at the 0.05–1 µg/l level in most recent, and otherwise highly interesting papers on the complementarity of AED and MS. Relevant examples are the following. Jiménez et al. identified some major peaks of fluvalinate residues in honey by using the partial formulae obtained by AED as well as the MS spectra [10]. Several authors used GC–AED to locate compound(s) containing a single hetero-atom in their GC traces, for subsequent correlation with MS. Pedersen-Bjergaard et al. used GC–AED to detect sulphur-containing compounds, e.g. for the determination of sulphur compounds in pulp mill effluents [11] and for sulphur- or chlorine-containing compounds in marine sediment [12], and Deruaz et al. for sulphur-containing compounds in garlic [13]. However, none of these papers discussed how unambiguous correlation was obtained. For the determination of sulphurated compounds Bicchi et al. used a sulphur-selective detector to locate seven rather dominant peaks, and used the C/S ratios of GC–AED and mass spectra for identification [14]. They were the only group who used retention index-based data correlation; however, no data on the correlation itself or further quantification were shown. From among the quoted authors, only Pedersen-Bjergaard et al. used the universal calibration concept for the provisional quantification of compounds after their identification at a level of 3 µg/l or higher [11]. However, no confirmation of the results by an independent method was provided. A lack of sensitivity was mentioned for studies carried out at lower levels [12].

In this context, it will of course be highly desirable to focus attention on peaks representing compounds present in the samples at or above a predetermined threshold level of, typically, 0.1 or 1 µg/l. This will require the application of SPE–GC procedures [15, 16] to achieve analyte trace enrichment and, on a quite different level, experimental verification of the validity of the universal calibration concept. Our aim was to develop and apply a concept for the screening for relevant compounds by systematic and unambiguous AED-to-MS correlation of relevant peaks in aqueous samples like tap, surface and waste water and

subsequent (approximate) quantification. The retention index concept was used to establish the unambiguous correlation. The envisioned procedure has been summarized in **Table 1**.

5.2.2 Experimental

Chemicals and reagents

HPLC-grade water (J.T. Baker, Deventer, The Netherlands) was used to condition (removal of ethyl acetate) and to effect clean-up of the trace-enrichment SPE cartridge. Ethyl acetate (99.9%, p. a., J.T. Baker) was distilled before use. The organophosphorus pesticides (OPPs) and triphenylphosphine oxide were of at least 98% purity. Stock solutions of 10 mg/ml were stored in the dark at 4°C. Stock solutions (20 μg/ml) of tris(2-chloroethyl) phosphate and tris(2-chloro-1-methylethyl) phosphate were obtained as a gift from the Institute for Inland Water Management and Waste Water Treatment (RIZA, Lelystad, the Netherlands) and kept at –20°C. High-purity helium gas (5.0) was obtained from Union Carbide (Westerlo, Belgium).

River and waste water samples were filtered through 0.20 μm membrane filters (Schleicher & Schüll, Dassel, Germany).

Table 1
Scheme for (non-target) screening of relevant hetero-atom-containing microcontaminants.

Step	Description
1	Compounds containing at least one hetero-atom and giving at least one element peak above a predetermined threshold concentration level are selected.
2	Partial molecular formulae are calculated for peaks present in several element GC–AED chromatograms at same retention time by using universal calibration.
3	Retention times of corresponding GC–MS chromatogram are calculated by using retention index concept [24] using a spreadsheet programme.
4	Mass spectra are taken at that retention time, and peaks are better located via extracted ion chromatogram; mass spectra are also taken at calculated retention time ± 0.07 and ± 0.15 min to take possible retention time shifts into account. All characteristic mass spectra so obtained are considered for identification.
5	For main peak(s) of mass spectrum/spectra obtained, reconstructed ion chromatograms are plotted. Background-corrected mass spectra at peak maximum/a are subjected to search in spectral library.
6	For acquired mass spectrum hits of library search are compared with partial formula of GC–AED. If partial formula (AED) and formula of first hit (MS) agree, and MS hit score is acceptable, it is checked whether all important mass peaks from reference spectrum are found in acquired spectrum. If yes, provisional identification has been achieved. If this is not the case, this control is repeated for the next hit for which partial formula and formula of mass hit agree until provisional identification is achieved.
7	After identification, compound is quantified by means of AED-based universal calibration.
8	If necessary, and if the reference compound is available, standard addition experiment is done for further confirmation and quantification.

Equipment

The on-line SPE–GC–AED system is shown in **Figure 1**. The set-up of the on-line SPE–GC–MS system was essentially the same.

SPE system

The SPE module of the on-line SPE–GC–AED system consisted of a Kontron Tracer 670 valve-switching unit (Kontron Analytic, London, UK) with four pneumatic six-port valves. All events were programmed and controlled by a Model 200 Programmer (Kontron). The water sample and HPLC water were each delivered at 2.5 ml/min by means of a Gilson (Villiers-le-Bel, France) Model 302 pump; both pumps were programmed via auxiliary contact closure events of the Model 200 Programmer. A Phoenix 30 syringe pump (Carlo Erba Strumentazione, Milan, Italy) was used for the delivery of ethyl acetate. The samples were preconcentrated on a 10 mm x 2 mm I.D. stainless-steel SPE cartridge (Chrompack, Middelburg, The Netherlands) inserted between valves V3 and V4. The SPE cartridge was packed with 10 µm, 300 Å PLRP-S (Polymer Laboratories, Church Stretton, UK), which is a styrene–divinylbenzene copolymer. Water remaining in the SPE cartridge after sample loading was removed by a nitrogen purge (30 min, 70 ml/min); the nitrogen was purified with a carbon trap (20/40 mesh Carbotrap C; Sulpelco, Bellefonte, PA, USA). Prior to loading a new sample, the sample pump and the tubing were flushed with about 5 ml of methanol to prevent memory effects. Next, the tubing was flushed with 5 ml of sample in order to cover active sites and, thus, reduce the loss of apolar analytes due to adsorption on capillary walls and the HPLC pump during sampling.

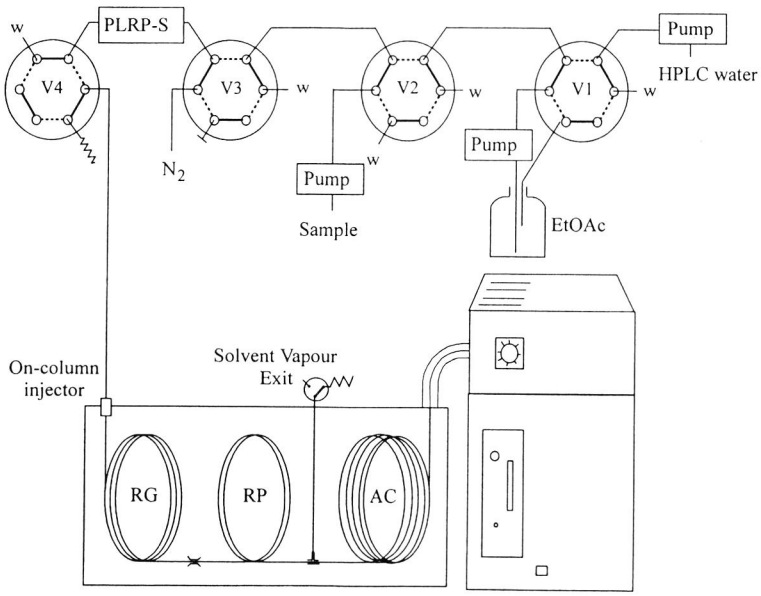

Figure 1

Set-up of the on-line SPE–GC–AED system. Abbreviations: AC, analytical column; EtOAc, ethyl acetate; RG, retention gap; RP, retaining precolumn; w, waste.

The SPE module (Prospekt; Spark Holland, Emmen, The Netherlands) of the on-line SPE–GC–MS system resembled the one described above, except that it contained three pneumatic six-port valves and one six-port solvent selection valve allowing one pump to deliver the aqueous sample, HPLC-grade water and methanol as described in Chapter 3.1.

Both SPE modules were interfaced to the GC system via 0.3 m x 75 µm I.D. deactivated fused silica tubing to the on-column injector. This capillary, which was permanently mounted in the on-column injector, was inserted into the 0.32 mm I.D. retention gap of the GC system (cf. below).

GC–AED system

The GC–AED system (Hewlett Packard, Waldbronn, Germany) consisted of a HP 5890 Series II gas chromatograph with electronic pressure control, an on-column injector and the HP 5921 A AED detector. The injector was connected to a 5 m x 0.32 mm I.D. deactivated retention gap (BGB Analytik, Zürich, Switzerland) and a 2 m x 0.25 mm I.D. section of the GC column (HP5MS; film thickness, 0.25 µm; Hewlett Packard). An early solvent vapour exit (SVE) was inserted between the retaining precolumn and the GC column (HP5MS) to vent most of the solvent vapour [17]. The home-made SVE was connected to the press-fit T-splitter (BGB Analytik) between the retaining precolumn and GC column (see Figure 1); it was installed on the top of the split/splitless injector and kept at 150°C to prevent solvent condensation.

The transfer line to the AED and the temperature of the cavity were kept at 300°C. The cavity pressure was about 10 kPa.

GC–MS system

A HP Model 5890 Series II gas chromatograph equipped with a pressure-programmable on-column injector and a Model 5972 mass selective detector was used for GC–MS analysis. The set-up of the GC system was the same as for the GC–AED system, i.e. the same type of retention gap, retaining precolumn, SVE and GC column were used. The transfer line to the MSD was held at 300°C. Ionization was achieved by electron ionization, and ions with m/z 47–435 were monitored at 1.9 scans/sec. The electron multiplier was set at 1800 V.

Procedure

On-line SPE–GC–AED

Each run was started by conditioning the SPE cartridge with 2 ml of HPLC-grade water at 5 ml/min. Next, valve V2 was switched to effect preconcentration of the water sample at 5 ml/min. Some clean-up was achieved by switching valve V2 and flushing the SPE cartridge with 2 ml of HPLC-grade water. Next, the SPE cartridge was dried for 30 min with a 70 ml/min flow of nitrogen by switching valve V3. During drying all connecting capillaries were flushed with ethyl acetate in order to remove any water present. Desorption of the analytes with ethyl acetate and the transfer of the first 100 µl of ethyl acetate to the GC system were started by switching valves V3 and V4 simultaneously.

The GC oven temperature during transfer was 75°C and the head pressure was increased from 50 kPa to 180 kPa at 680 kPa/min when starting the transfer. After the transfer, the head pressure was decreased to 50 kPa at 680 kPa/min. The SVE was closed just before the last drops of ethyl acetate had evaporated. 5 min after the start of the transfer the vent of the AED

was closed and the temperature gradient started, i.e. the temperature was increased to 300°C at 10°C/min, which was held for 3 min. The head pressure was programmed to provide a constant flow rate during the temperature programme. When preconcentrating 50-ml samples, the analysis time was 72 min. To increase sample throughput, the next sample pretreatment was started after the end of the transfer into the GC system by flushing the SPE cartridge with ethyl acetate for 4 min at 62 µl/min. This decreased the time required per analysis to 47 min. As the AED covers only a limited range of wavelengths and different reagents gases have to be added to the plasma for different elements, three SPE–GC–AED analyses were required to acquire all element traces of interest (run 1: C, S; run 2: H, Cl, Br; run 3: P). For the reagent gases and the make up flow, one should consult Table 2 below.

As the ethyl acetate pump could not be controlled via auxiliary events, the ethyl acetate was pumped back to the solvent reservoir when not directed to valve V2. When changing samples, the sample pump was first flushed with 5 ml of methanol and then with 5 ml of sample.

On-line SPE–GC–MSD

After conditioning the SPE column with water, the sample pump and tubing up to valve V3 were flushed with 5 ml of sample in order to cover active sites to reduce the loss of apolar analytes due to adsorption [18]. The programme for sampling, clean-up and drying of the cartridge was essentially the same as for on-line SPE–GC–AED. The transfer conditions, i.e. the temperature and programming of the pressure were the same as for the GC–AED system except for the pressure after the transfer, which was 60 kPa. As with the GC–AED, the pressure was programmed to yield a constant flow during the temperature programme of the GC oven. After the transfer, the cartridge was flushed with 1 ml of ethyl acetate, and the sample pump with 5 ml of methanol.

Optimization of introduction flow rate

The introduction flow rate was optimized by means of a series of 100-µl injections of an *n*-alkane standard solution. For these (and other) 100-µl injections, the SPE cartridge was replaced by a 150-µl loop between valves V3 and V4. The 150-µl loop was filled by means of a syringe, which was inserted instead of the nitrogen line at valve V3. Next, the sample was pushed into the retention gap by organic solvent from the syringe pump.

The introduction flow rate was stepwise increased until peak distortion of the analytes was observed which indicated flooding of the retaining precolumn [19]. The flow rate selected was 4 µl/min lower than that for which flooding had been observed. This procedure ensured that a solvent film was always created in the retention gap during the transfer without undue risk of flooding of the retaining precolumn. Typical flow rates were 60–80 µl/min.

Optimization of SVE closure

The solvent vapour leaving the SVE was monitored by means of a flame of a gas burner; the SVE was closed when the flame extinguished. Next, a 100-µl injection of the alkane mixture was made, and the SVE closed at the predetermined time. If loss of C_{10} was observed (comparison with 1-µl on-column injection), the SVE closure time was slightly varied and the injection repeated.

5.2.3 Results

Calculation of partial molecular formulae by GC–AED

Retention time shifts for element traces

Reliable calculation of the partial molecular formula of an (unknown) analyte requires the retention times of that compound in the various AED element-selective chromatograms to be identical. However, if each element is detected under its optimal reagent and make-up flow conditions, retention times in the various element traces can differ considerably, i.e. up to 0.04 min, as is shown for bromophos-ethyl in **Table 2**. The imprecision cannot be accepted if two, or more, AED-element traces have to provide combined information (on the same analyte) and a complex matrix like waste water is analysed. The increased retention time due to an increased flow of make-up and reagent gas can be explained by the increase of the cavity pressure (to be read on the manometer) and, therefore, higher back pressure at the outlet of the GC column [20]. The shifts in retention time can be eliminated by manual correction of the pressure of the discharge at the back pressure manometer. However, with the present system this cannot be automated; in addition, manual correction will cause precision to deteriorate. As an alternative, the total flow through the discharge tube can be kept constant by keeping the sum of the flows of reagent gases used and the make-up flow constant. As a maximum we used two reagent gases; if only one reagent gas was used, helium was used as auxiliary gas. The make-up flow was chosen to be 140 ml/min in all runs in order to obtain good peak shapes also in the phosphorus trace. With the total flow through the discharge tube now being constant in all runs, the retention times of bromophos-ethyl in the six element traces studied before now were the same to within ± 0.001 min (Table 2). This considerable improvement is obtained at some loss of sensitivity for those elements for which the total flow through the discharge tube was increased. As the data in Table 2 show the about 2.5-fold increase in flow rate caused a 2-fold loss in analyte detectability for all elements studied except phosphorus; for that element, the flow and, consequently, the detection limit remained essentially the same.

Table 2

Retention times and detection limits (LOD, S/N=3) of bromophos-ethyl in GC–AED for six element traces at different flow conditions.

Element	Conditions [a]	Flow [b] (ml/min)	t_r (min)	LOD (pg)	Conditions	Flow [b] (ml/min)	t_r (min)	LOD (pg)
C 193	H_2, O_2	67	14.476	30	H_2, O_2, F+	154	14.514	55
H 486	O_2	61	14.472	60	O_2, Aux, F+	154	14.515	115
S 181	O_2, H_2	67	14.477	15	O_2, H_2, F+	154	14.514	30
Cl 479	O_2	61	14.472	105	O_2, Aux, F+	154	14.514	250
Br 478	O_2	61	14.473	145	O_2, Aux, F+	154	14.514	285
P 186	H_2, F+	146	14.510	35	H_2, Aux, F+	154	14.515	35

[a] F+, increased flow of make-up gas.

[b] Total flow of reagent gas and make-up gas through plasma; measured at opened ferrule purge and closed window purge.

For further explanation, see text.

Universal calibration

In principle, the molecules eluting from the GC column into the microwave plasma of the AED are decomposed into free atoms, which are then excited and emit light of characteristic wavelength [21]. Therefore, it can be expected that the molar elemental response (i.e. the response per mass unit of element) will be independent of the structure of the compound. Actually, a more or less compound-independent elemental response has been reported for carbon, hydrogen, chlorine, bromine and sulphur with variations of, typically, up to 20% [4–6, 9, 14, 22, 23]. For oxygen, larger variations, i.e. up to 60%, were reported [8]. From limited data published on the molar response of phosphorus, Olson et al. calculated variations of up to 35% [7].

The molar responses of five elements were determined for a series of OPPs, triphenylphosphine oxide and also for several chlorine-containing compounds (**Table 3**). For this study, 10–20 ng of each compound were injected on-column. The results of Table 3 show that for compounds with mutual structural differences as are typically encountered in studies on microcontaminants, the molar responses are essentially independent of the analyte structure with relative standard deviations on the order of 5–10%. Therefore, a mixture containing seven compounds (Table 3) was prepared to be used for all further calibration work.

Data correlation for separate GC systems via retention index

The concept of temperature-programmed retention indices (RI) [24] was used to determine which peaks in the GC–AED and GC–MS chromatograms correspond with each other. The two systems contained identical retention gaps, retaining precolumns and analytical columns. Temperature-programmed retention indices had to be used because a temperature programme was required to separate the analytes of interest which covered a wide volatility range. A

Table 3
Molar response data for five elements using OPPs, triphenylphosphine oxide and Cl-containing test analytes.

Element	OPPs and TPPO [a]			Cl-containing compounds [b]			Calibration mixture [c]		
	n [d]	Range [e]	RSD (%)	n	Range	RSD (%)	n	Range	RSD (%)
C 193	9	0.95–1.10	5	6	0.81–1.15	11	7	0.93–1.09	6
H 486				6	0.90–1.09	8	7	0.88–1.15	11
S 181	7	0.89–1.04	7				3	0.97–1.03	3
P 186	9	0.88–1.11	9				3	0.99–1.01	1
Cl 479	2	1.0		6	0.92–1.13	8	4	0.90–1.07	7

[a] Sulfotep, diazinon, fenchlorphos, parathion-ethyl, bromophos-ethyl, triazophos, triphenylphosphine oxide (TPPO), pyrazophos, coumaphos.

[b] Chlorooctane, chlorododecane, tetrachlorobenzene, pentachlorobenzene, fenchlorphos, bromophos-ethyl, dieldrin.

[c] Chlorooctane, chlorododecane, pentachlorobenzene, diazinon, parathion-ethyl, bromophos-ethyl.

[d] Number of compounds in mixture containing that element.

[e] Lowest and highest value found for molar elemental response divided by average of molar elemental response.

Number of injections: 6 except for Cl-containing compounds (n=2).

series of *n*-alkanes (C_{11}, C_{15}, C_{18}, C_{20}, C_{23}, C_{25} and C_{28}) was used as retention index markers. Using standard injections of several OPPs into the GC–AED system, we found that two parameters have a major influence on the temperature-programmed retention indices. To quote an example, a change in the temperature ramp from 10 to 20°C/min caused the retention indices of the test compounds to shift 10–30 RI units. When increasing the head pressure from 50 to 100 kPa and keeping the other conditions constant, the retention indices of the test compounds shifted 40–80 RI units. Here, it should be noted that the pressure at the end of the GC column differs considerably for the GC–MS and GC–AED systems, it being vacuum or about 111 kPa, respectively. Even when programming the head pressure of both systems such that an identical column flow is obtained, differences of the linear gas flow along the column can be expected due to the different pressure profile along the column in both systems.

When using the same set-up and exactly the same conditions except for the head pressures, which were different in order to obtain an identical column flow, the retention indices calculated from standard injections of the eight OPPs into the GC–AED and GC–MS systems differed 4–15 RI units. This can be probably attributed to minor differences in the column flows, in the different pressure drop along the column and different characteristics of the retention gap and/or analytical column due to a change in activity caused by earlier injections. The latter aspect is important as apolar *n*-alkanes were used as RI marker for the OPPs which cover a wide range of polarity. A retention index difference of 15 corresponds with a difference in retention time of about 0.15 min with the present GC–AED and GC–MS systems. In other words, when searching for a corresponding peak in the GC–MS chromatogram, a window of ± 0.15 min has to be taken into account to cover also the worst-case situation.

System set-up and application

Interfacing SPE and GC for trace analysis

The aim of this study was the determination of microcontaminants at the 0.05–0.1 µg/l level in tap water and at the 0.5 µg/l level in waste water. As was briefly discussed above, the detection limits with the element traces of interest are in the 30–300 pg (of element) range (cf. Table 2). Or, in other words, up to about 3 ng of analyte will be required to achieve detection. If a 50-ml sample is used and sample treatment is by means of on-line SPE–GC, as has been reported for both AED and MS detection [15, 16], so that essentially all analytes in the sample are transported through the system, detection should be possible down to about the 0.1–0.6 µg/l level. For a detailed discussion and description of the two hyphenated systems using an on-column interface, one is referred to Chapters 3.1 and 5.1 and the literature quoted above.

Analysis of tap water

A sample of Amsterdam tap water was spiked with several OPPs (**Table 4**). 50 ml of sample were analysed by on-line SPE–GC–AED (C, H, Br, Cl and S traces) and on-line SPE–GC–MS. For acquisition of the sensitive phosphorus trace only 30 ml were sampled. The molar responses obtained from the analysis of the calibration mixture (cf. Table 3) were used to calculate the partial formulae and (approximate) concentrations of hetero-atom-containing

Table 4
Identification of hetero-atom-containing compounds by means of their partial formulae (AED) and corresponding mass spectra.

SPE–GC–AED			SPE–GC–MS [a]				
No.	RI	Partial formula	RI	Library search [b]			
				Identified compound	Hit No. [b]	Qual. [b]	Formula
1	1707	$P_{0.3}S_{1.0}$	1704	Sulfotep	1 (1)	55 (99)	$C_8H_{20}O_5P_2S_2$
2	1777	$Cl_{2.6}P_{1.0}$	1776	Tris(2-chloroethyl) phosphate	9	10	$C_6H_{12}Cl_3O_4P$
3	1820	$Cl_{2.8}P_{1.0}$	1814	Tris(2-chloro-1-methylethyl) phosphate	– [c]	–	$C_9H_{18}Cl_3O_4P$
4	1818	$P_{0.9}S_{1.0}$	1815	Diazinon	1 (1)	62 (99)	$C_{12}H_{21}N_2O_3PS$
5	1950	$Cl_{2.5}P_{0.9}S_{1.0}$	1936	Fenchlorphos	(1) [d]	(99)	$C_8H_8Cl_3O_3PS$
6	2020	$P_{1.2}S_{1.0}$	2008	Parathion-ethyl	1 (1)	87 (94)	$C_{10}H_{14}NO_5PS$
7	2148	$Br_{1.1}Cl_{1.8}P_{0.8}S_{1.0}$	2134	Bromophos-ethyl	1 (1)	38 (91)	$C_{10}H_{12}BrCl_2O_3PS$
8	2166	$Cl_{3.8}P_{1.0}$	2152	Tetrachlorvinphos	1 (1)	93 (97)	$C_{10}H_9Cl_4O_4P$
9	2315	$P_{0.7}S_{1.0}$	2301	Ethion	1 (1)	97 (99)	$C_9H_{22}O_4P_2S_4$
10	2346	$P_{0.4}S_{1.0}$	2332	Triazophos	1 (1)	94 (96)	$C_{12}H_{16}N_3O_3PS$
11	2576	P	2561	Triphenylphosphine oxide	2	48	$C_{18}H_{15}OP$
12	2670	$P_{0.8}S_{1.0}$	2656	Pyrazophos	1 (1)	91 (97)	$C_{14}H_{20}N_3O_5PS$
13	2774	$Cl_{1.1}P_{1.3}S_{1.0}$	2760	Coumaphos	1 (1)	91 (99)	$C_{14}H_{16}ClO_5PS$

[a] Corresponding mass spectra of peaks in GC–AED and GC–MS found via retention index.
[b] NBS (HPPEST) library used; Qual, match qualifier on a scale of 100.
[c] No matching library spectrum found.
[d] Present only in HPPEST library, not in NBS library.

compounds. The calibration mixture was injected on-column just prior to the analysis of the aqueous samples; no internal standard was used.

Since it was our aim to identify all hetero-atom-containing microcontaminants present at a concentration of 0.05–0.1 µg/l and above, all peaks in the element chromatograms with peak heights higher than that corresponding with an elemental concentration of 0.06 nmol/l were considered relevant. This threshold corresponds with a concentration of 0.02 µg/l of a (hypothetical) compound which contains (i) one of each of the hetero-atoms considered, (ii) has a molecular weight of 300 atomic units and (iii) a peak width at half maximum of 0.035 min. These criteria should ensure that no analytes yielding somewhat broader peaks and/or having a less-than-quantitative SPE recovery, are overlooked. Obviously, if a microcontaminant contains two or more of one of the hetero-atoms selected, it will be included at a correspondingly lower concentration.

All peaks in the sulphur, phosphorus, chlorine and bromine traces present at or above the pre-set concentration levels (see peaks 1–13; **Figure 2**) were treated according to the correlation procedure of Table 1. The starred peak in the sulphur trace eluting at 20.85 min was not considered because it was present in the system blank. At the low analyte levels discussed, disturbances in the carbon and hydrogen trace often interfered with quantification; therefore carbon and hydrogen were not considered when calculating the partial molecular formulae shown in Table 4.

The thirteen corresponding mass spectra of the SPE–GC–MS analysis were obtained via the retention index correlation procedure of Table 1. All compounds except No. 3 could be identified via a library search of their mass spectra. The NBS rather than the HPPEST library was used, because the potential of AED/MS correlation should be studied for microcontaminants other than pesticides also. The NBS library contains much more spectra than the HPPEST library but the difference between the sample and library spectra were

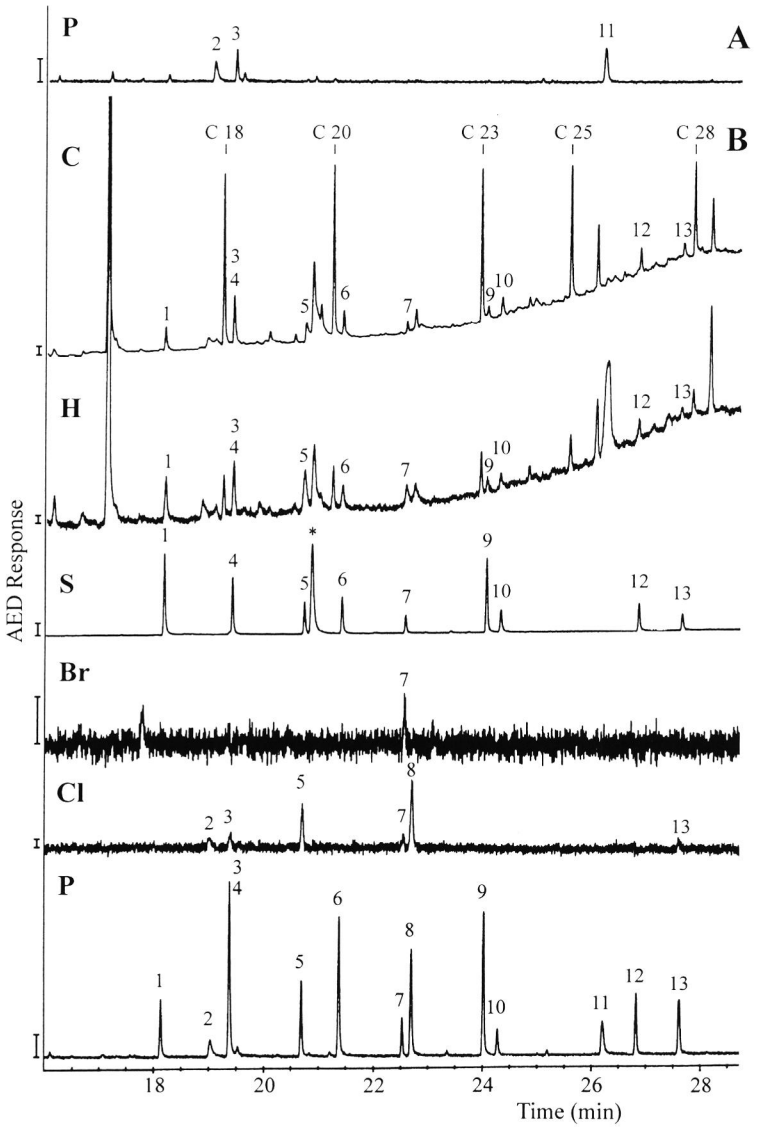

Figure 2

Element-selective SPE–GC–AED chromatograms of 50 ml of tap water (A) without (only P trace) and (B) with spiking of ten OPPs at the 40–70 ng/l level (C, H, S, P, Cl and Br traces) and some *n*-alkanes. For the acquisition of the P trace only 30 ml of tap water were sampled. For peak assignment, see Table 4; starred peak in S trace also present in system blank. The bars indicate the peak height of a (hypothetical) compound containing one of each hetero-atoms at the 0.02 µg/l level (cf. text).

larger for the former library, because only the latter was acquired with a MS detector similar to the one used in this study; besides, the spectra in the NBS library contain a lower number of the less intensive mass peaks. To quote an example, the match qualifier for the similarity of the acquired mass spectrum of bromophos-ethyl was 38 with the reference spectrum of the NBS library, but 91 with that of the HPPEST library, on a scale of 100.

The identification of tris(2-chloroethyl) phosphate illustrates the potential of the present concept. GC–AED data analysis suggests the partial formula $Cl_{2.6}P_{1.0}$ for peak No. 2 (RI 1777). When a library search of the corresponding mass spectrum (**Figure 3**A) was performed, the first compound on the hit list of the MS library containing phosphorus and chlorine search is No. 9, i.e. tris(2-chloroethyl) phosphate (see insert in Figure 3). As is to be expected, due to the low signal the match qualifier is low, i.e. 10. Nevertheless, visual inspection of the sample (Figure 3A) and reference (Figure 3B) spectra shows them to be closely similar, i.e. all major peaks of the reference spectrum are present in the acquired spectrum. The partial formula supported the provisional identification, and, indeed, standard addition of tris(2-chloroethyl) phosphate to the sample and subsequent on-line SPE–GC–MS analysis confirmed its presence.

Compound No. 3 (RI 1820) co-eluted with diazinon. Therefore the non-spiked sample was used to calculate its partial molecular formula. However, the compound could not be identified by the NBS library search. The mass spectrum contains some masses (m/z 81, 99, 117 and 125) which are typical for a chlorinated alkyl phosphate ester. The partial formula obtained by GC–AED suggests that the molecule contains three chlorine and one phosphorus atom(s). Interpretation of the mass spectrum (**Figure 4**A) suggests the compound to be tris(2-chloro-1-methylethyl) phosphate [three alcohols of phosphate ester are probably isomers of

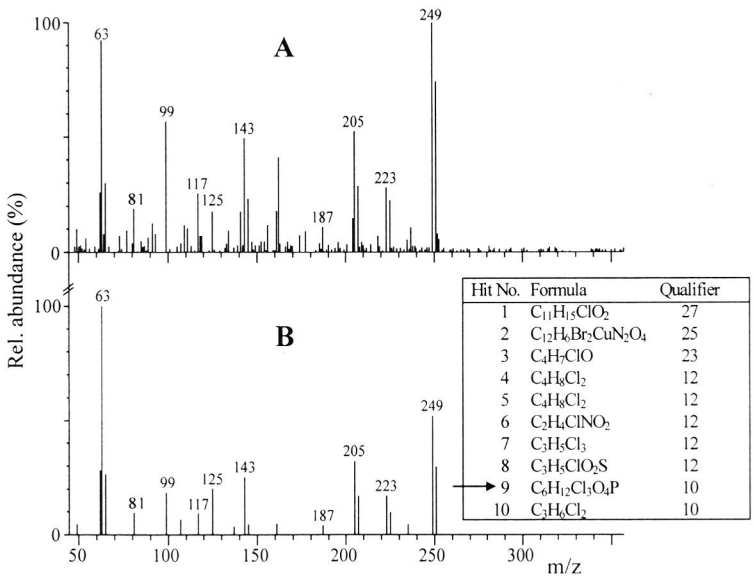

Figure 3

(A) Mass spectrum of peak No. 2 (RI 1776) of Figure 2. Insert shows hit list of library search. (B) Library spectrum of tris(2-chloroethyl) phosphate; hit number, 9; match qualifier, 10 (out of 100).

chloropropanol because of RI and masses present in spectrum; 2-chloro-1-methylethyl is probably only isomer with McLafferty rearrangement and subsequent significant loss of CH_2Cl, resulting in m/z 277, and after repeated loss(es) of chloropropene also m/z 201 and 125]. Final confirmation was obtained from the mass spectrum (Figure 4C) and retention index (RI=1815) of authentic tris(2-chloro-1-methylethyl) phosphate (being first peak of Fyrol PCF [25] obtained from RIZA (Lelystad, The Netherlands).

As regards the partial formulae determined by means of GC–AED, the results for chlorine, bromine and sulphur agreed well with the compounds identified via GC–MS: differences were less than 20%. However, in the case of phosphorus, a less consistent picture emerged. In ten instances the relative error was acceptable (≤ 30%), but in the two remaining cases (sulfotep and triazophos), the differences were 60–70%. The non-linearity of the calibration plot for phosphorus at low concentrations has been reported by Quimby and Sullivan [26]. Olson et al. also observed deviating molar responses of phosphorus at low

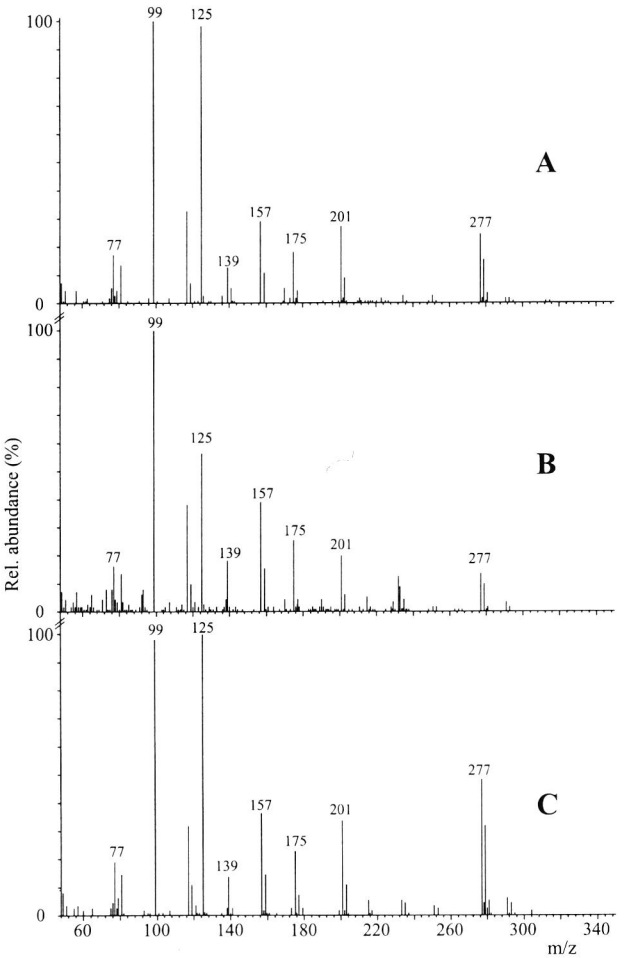

Figure 4

Mass spectrum of (A) peak No. 3 of Figure 2 and (B) of peak No. 5 of Figure 5 (see as below). (C) Reference spectrum of tris(2-chloro-1-methylethyl) phosphate.

levels [7]. They attributed this to a reaction of part of the phosphorus with the wall of the discharge tube, which would be noticeably only at low concentrations. Still, the information on the presence or absence of phosphorus is highly useful for the selection of the proper hits during the MS library search.

A comparable picture was obtained when quantifying identified compounds by GC–AED using the universal calibration concept (**Table 5**). Using the data obtained from the sulphur trace, the OPP recoveries were found to be 70–110% except for bromophos-ethyl (43%) and ethion (64%). These values, and also the two exceptional results, are closely similar to what was found in an earlier study on SPE of OPPs [15]. The low results can be explained on the basis of the apolar character of the analytes considered and the consequent loss caused by sorption to walls and tubing. As is to be expected from the discussion above, the concentrations calculated by using the bromine and chlorine traces were comparable to those calculated with the help of the sulphur trace [even though some of the peaks were close to the detection limit], while the phosphorus trace occasionally gave quite unsatisfactory results. The presence of tris(2-chloroethyl) phosphate and triphenylphosphine oxide was confirmed by standard addition with SPE–GC–MS analysis; the concentrations determined by universal AED calibration were close to those obtained by standard addition.

To summarize, quantification by means of universal calibration was reliable at the 20–70 ng/l level for the sulphur, bromine and chlorine traces. The retention indices observed for an individual compound on the various GC–AED element traces differed less than 0.1 units; differences between the on-line SPE–GC–AED and on-line SPE–GC–MS runs were 3–15 units (cf. Table 4). These differences were similar to those found above for standard injections. As regards analyte identification, one should note that compounds such as tris(2-

Table 5
Quantification of microcontaminants in tap water using universal calibration for four AED element traces and standard addition in case of MS detection.

Compound	Spiking Level (ng/l)	Concentration (ng/l) determined by AED				MS
		S	P	Cl	Br	
Sulfotep	64	54	16			
Tris(2-chloroethyl) phosphate	– [a]		22	20		18
Tris(2-chloro-1-metylethyl) phosphate	– [a]		18	16		
Diazinon	70	76	70			
Fenchlorphos	64	44	40	36		
Parathion-ethyl	54	50	62			
Bromophos-ethyl [b]	31	30	24	28	34	
Tetrachlorvinphos	52		68	64		
Ethion [b]	29	30	42			
Triazophos	40	34	14			
Triphenylphosphine oxide	– [a]		28			34
Pyrazophos	56	46	36			
Coumaphos	36	28	36	32		

[a] Found to be present in the tap water.

[b] Bromophos-ethyl and ethion were spiked at the 72 and 46 µg/l level, respectively. The values given in the table take their known low recovery, i.e. 45 and 65%, respectively, into account.

chloroethyl) phosphate are easily missed when inspecting only the SPE–GC–MS chromatogram, because the peak does not stand out clearly in the chromatogram. This advantage of combined AED/MS detection will, of course, even be larger for more complex samples.

Analysis of waste water

The above approach was also applied for the screening of waste water, which is a more complex matrix than tap water but, generally, also contains higher concentrations of microcontaminants. Therefore, in this instance, only 7 ml of the effluent of a municipal purification plant were taken, and analysed by SPE–GC–AED, and 10 ml by SPE–GC–MS (**Figure 5**). Bromophos-ethyl was added as a 1.86 µg/l spike. In order to identify all hetero-atom-containing compounds present in the sample at a level of 0.5 µg/l, all peaks showing up at or above a level of 0.2 µg/l were considered relevant (peaks Nos. 2–4 and 6 in Figure 5). In addition, also the phosphorus-containing peaks at the 0.07–0.2 µg/l level (peaks No. 1, 5 and 7) were studied because of the non-linearity of the phosphorus response at low concentrations (cf. above). In the sulphur trace, many peaks were found at a level below 0.2 µg/l; no effort was made to identify these compounds. The much larger number of, occasionally even rather prominent, peaks showing up in SPE–GC–MS (Figure 5) clearly indicates that screening without the added benefit of SPE–GC–AED would be much more laborious and time-consuming.

Identification could be achieved for all seven compounds considered relevant on the basis of their partial molecular formulae and the corresponding mass spectra (**Table 6**). In the effluent sample, higher concentrations of tris(2-chloroethyl) phosphate and tris(2-chloro-1-methylethyl) phosphate were found (0.3 and 0.2 µg/l, respectively) than in the tap water

Table 6

Identification and quantification of hetero-atom-containing microcontaminants by means of their partial formula and universal calibration (AED) and corresponding mass spectra and standard addition (MS) in waste water.

SPE–GC–AED			SPE–GC–MS				Concentration (µg/l)				
No.	RI	Partial	RI	Library search [b]			AED				MS
		Formula		Identified compound	Q [b]	Formula	S	P	Cl	Br	
1	1662	P	1663	Tributylphosphoric acid	64	$C_{12}H_{27}O_4P$		0.10			0.21
2	1782	$Cl_{2.5}P$	1781	Tris(2-chloroethyl) phosphate	91	$C_6H_{12}Cl_3O_4P$		0.36	0.30		0.54
3	1792	Cl	1778	Hexachlorocyclohexane [a]	32	$C_6H_6Cl_6$			0.12		
4	1818	$Cl_{2.5}P$	1814	Tris(2-chloro-1-methyl-ethyl) phosphate		$C_9H_{18}Cl_3O_4P$		0.25	0.21		
5	1831	$Cl_{2.3}P$	1828	Bis(2-chloro-1-methyl-ethyl) (2-chloropropyl) phosphate		$C_9H_{18}Cl_3O_4P$		0.09	0.06		
6	2148	$Br_{1.1}Cl_{1.9}P_{1.1}S$	2135	Bromophos-ethyl [c]	38	$C_{10}H_{12}BrCl_2O_3PS$	1.1	1.2	1.0	1.2	
7	2427	P	2425	Tris(2-butoxyethyl) phosphate	40	$C_{18}H_{39}O_7P$		0.07			

[a] Isomer not further identified.

[b] NBS library was used for library search and determination of match qualifier (Q). Identified compounds always were No. 1 on hit list.

[c] Bromophos-ethyl, spike of 1.0 µg/l corrected for low recovery.

(Table 6). Compound No. 3 (RI 1792) was identified as an isomer of hexachlorocyclohexane on the basis of its mass spectrum. The partial formula and the mass spectrum of compound No. 5 (RI 1828) (Figure 4B) are closely analogous to those of tris(2-chloro-1-methylethyl) phosphate. The relative abundances of the masses m/z 277, 201 and 125 in the mass spectrum are lower than those of tris(2-chloro-1-methylethyl) phosphate suggesting that compound No. 5 contains one or two other isomeric chloropropyl groups. Actually, compound No. 5 was

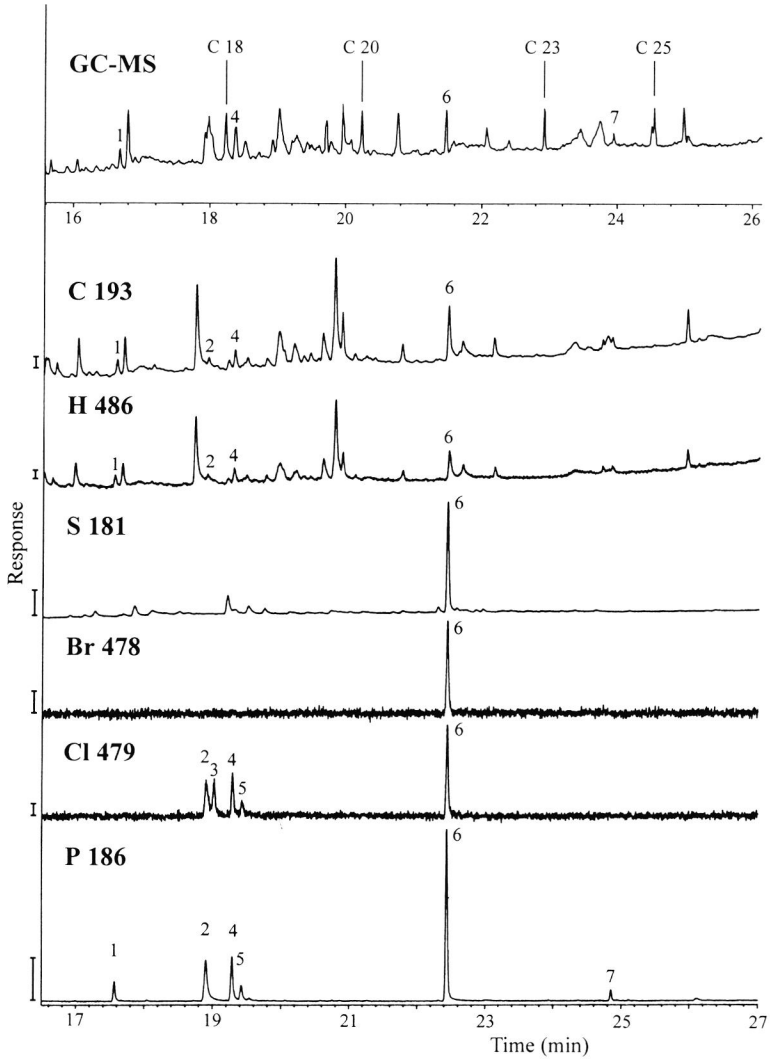

Figure 5

Element-selective SPE–GC–AED chromatograms and full-scan SPE–GC–MS chromatogram of 7 ml of waste water (C, H, S, P, Cl and Br traces). The sample was spiked with bromophos-ethyl at the 1.86 µg/l level. The sample analysed by GC–MS was also spiked with some *n*-alkanes. For peak assignment, see Table 6. The bars indicate the peak height of a (hypothetical) compound containing one of each hetero-atom at the 0.2 µg/l level (for further explanation, cf. text).

found to be identical with the minor peak (RI=1829) observed when injecting Fyrol PCF, and probably is bis(2-chloro-1-methylethyl) (2-chloropropyl) phosphate [25].

Quantification of the five analytes for which the concentration could be calculated by more than a single method yielded rather satisfactory results. This is obvious from the data in Table 6, with bromophos-ethyl as the most striking example. Admittedly, for compounds Nos. 1 and 2 the results calculated from the SPE–GC–MS traces were somewhat high. However, the combined data are still fully acceptable for a screening procedure at the trace level without using a reference compound.

5.2.4 Conclusion

A procedure for the screening of (non-target) hetero-atom-containing compounds in tap and waste water by correlating data obtained by on-line SPE–GC–AED and on-line SPE–GC–MS was set up and applied to real samples. On-line coupling of SPE and GC allowed the determination of microcontaminants at the 0.02–1 µg/l level using only moderate sample volumes, i.e. 7–50 ml. Due to the demonstrated validity of the concept of universal calibration of the AED, it is possible to limit screening to those compounds present in the sample above a predetermined concentration level.

In the examples shown, all spiked analytes and even all non-spiked analytes found to be present at a concentration level above 0.05 µg/l (tap water) or 0.5 µg/l (waste water) could be identified by correlation of their partial formulae (AED) and their mass spectra. Correlation of the AED and MS data was achieved by means of the concept of retention indices. After optimization, differences in retention indices between both systems were found to be only 1–15 RI units. The further reductions of these differences by integrating the AED and MS detectors into a single SPE–GC–(MS/AED) system is presented in Chapter 5.3.

The present successful use of the described approach for identifying unknowns and quantifying trace-level constituents with an imprecision of less than 50% (when using, e.g., various element traces) at the 0.02–1 µg/l range, indicates that this may will become a powerful multidimensional analytical strategy.

References

[1] S. Pedersen-Bjergaard and T. Greibrokk, *J. High. Resol. Chromatogr.*, 19 (1996) 597.
[2] H.-J. Stan and M. Linkerhägner, *J. Chromatogr. A*, 750 (1996) 369.
[3] W. Elbast, J. Guitton, M. Desage, D. Deruaz, M. Manchon and J.L. Brazier, *J. Chromatogr. B,* 696 (1996) 97.
[4] S. Pedersen-Bjergaard, T.N. Asp and T. Greibrokk, *Anal. Chim. Acta*, 265 (1992) 87.
[5] N.L. Olson, R. Carrell, R. Cummings, R. Rieck and S. Reimer, *Journal of APAC International*, 78 (1995) 1464.
[6] T.G. Albro, P.A. Dreifuss and R.F. Wormsbecher, *J. High. Resol. Chromatogr.*, 16 (1993) 13.
[7] N.L. Olson, R. Carrell, R.K. Cummings and R. Rieck, *LC-GC*, 12 (1994) 142.
[8] C. Webster and M. Cooke, *J. High Resol. Chromatogr.*, 18 (1995) 319.
[9] J. Th. Jelink and A. Venema, *J. High Resol. Chromatogr.*, 13 (1990) 447.
[10] J.J. Jiménez, J. Atienza and J.L. Bernal, *J. High. Resol. Chromatogr.*, 18 (1995) 367.
[11] S. Pedersen-Bjergaard, T.N. Asp, J. Vedde, G.E. Carlberg and T. Greibrokk, *Chromatographia*, 35 (1993) 193.

[12] S. Pedersen-Bjergaard, S.I. Semb, J. Vedde, E.M. Brevik and T. Greibrokk, *Chemosphere*, 732 (1996) 337.
[13] D. Deruaz, F. Soussan-Marchal, I. Joseph, M. Desage, A. Bannier and J.L. Brazier, *J. Chromatogr.*, 677 (1994) 345.
[14] C. Bicchi, C. Frattini, G. Pellegrino, P. Rubiolo, V. Raverdiono and G. Tsourpras, *J. Chromatogr.*, 609 (1992) 305.
[15] Th. Hankemeier, A.J.H. Louter, F.D. Rinkema and U.A.Th. Brinkman, *Chromatographia*, 40 (1995) 119.
[16] A.J.H. Louter, U.A.Th. Brinkman and R.T. Ghijsen, *J. Microcol. Sep.*, 5 (1993) 3031.
[17] K. Grob, H.-G. Schmarr and A. Mosandl, *J. High Resolut. Chromatogr.*, 12 (1989) 375.
[18] J. Norberg, J. Slobodník, J.J. Vreuls and U.A.Th. Brinkman, *Anal. Methods. Instrum.*, 5 (1995) 226.
[19] S. Ramalho, Th. Hankemeier, M. de Jong and U.A.Th. Brinkman, J.J. Vreuls, *J. Microcol. Sep.*, 7 (1995) 383.
[20] M. Linkerhägner and H.-J. Stan, *Z. Lebensm. Unters. Forsch.*, 198 (1994) 473.
[21] P.C. Uden, in P.C. Uden (ed.), *Element Specific Detection by Atomic Emission Spectroscopy (ACS Symposium Series, No. 479)*, American Chemical Society, Washington DC, 1992, p. 1.
[22] S. Pedersen-Bjergaard, S.I. Semb, E.M. Brevik and T. Greibrokk, *J. Chromatogr. A*, 723 (1996) 337.
[23] J.J. Sullivan and B.D. Quimby, *J. High Resol. Chromatogr.*, 12 (1989) 282.
[24] H. van den Dook and P.D. Kratz, *J. Chromatogr.*, 11 (1963) 463.
[25] D.F. Othmer, *Kirk-Othmer Enyclopedia of Chemical Technology*, 3rd edition, John Wiley & Sons, New York, USA, 1978, p. 402.
[26] B.D. Quimby and J.J. Sullivan, *Anal. Chem.*, 62 (1990) 1027.

5.3 GC of organic microcontaminants using AED and MS detection combined in one instrument

Summary

The coupling of an atomic emission (AED) and mass spectrometric (MS) detector to a single gas chromatograph (GC) is described. Splitting of the column effluent enables simultaneous detection by AED and MS and yields a powerful system for the target as well as non-target analysis of GC-amenable compounds. Organo microcontaminants are detected via their hetero-atom AED traces, while parallel-acquired mass spectra allow confirmation and identification. Correlation of AED and MS data is straightforward because retention times are the same to within, typically, 0.5 sec. The possibility of compound-independent AED elemental calibration was studied for vegetable and water samples. The AED and MS results were in good agreement with each other. Manual at-line SPE–GC–AED/MS was used for the non-target analysis of river water. A number of hetero-atom-containing microcontaminants were detected, identified and quantified down to the 20 ng/l level.

5.3.1 Introduction

Gas chromatography (GC) with atomic emission detection (AED) is becoming increasingly popular because of its selectivity for, in principle, all elements [1–8]. Additionally, the response per mass unit of an element is more or less independent of the structure of the molecule [5, 9–11], although this statement does not go unchallenged [12–13].
In a previous paper [14], we have extensively discussed the complementarity of data obtained from GC with AED and mass spectrometric (MS) detection. If some compromises are made with regard to the number and flow-rate ratios of the reagent and make-up gases used, and correlation of the results from the two GC systems is done by means of the retention index (RI) concept, the use of an on-line solid-phase extraction (SPE) set-up – i.e. of SPE–GC–AED and SPE–GC–MS – enables the detection and provisional identification of target analytes down to the 50–500 ng/l in 7–50 ml water samples. Several unknowns were also identified.

The published approach, although obviously successful, has a few disadvantages. The main problem is that, even after extensive optimisation, differences in the retention indices of up to 15 RI units are frequently encountered (for discussion, see Section *Characteristics of the GC–AED/MS set-up*). This, of course, limits the applicability range when identification of (ultra) trace-level unknowns is a main goal of a screening procedure and will make the GC–AED plus GC–MS data correlation less reliable.

In an attempt to further improve the performance of our procedure, we have now coupled the AED and MS detectors to a single GC instrument, thereby creating GC–AED/MS. The present paper discusses the design, and the technical and analytical performance, of the integrated system. Next, the analysis of several vegetable and surface water samples is used to demonstrate its potential and limitations.

5.3.2 Experimental

Chemicals and reagents

Solvents (p.a.) were obtained from J.T. Baker (Deventer, the Netherlands); ethyl acetate and methyl acetate were distilled before use. Pesticides were purchased from Riedel de Haen (Seelze, Germany) and were of at least 98% purity. Standards were prepared in ethyl acetate and stored in the dark at –18°C. High-purity (5.0) helium, hydrogen and oxygen were used. The pesticides included in the evaluation of the AED elemental response were: desethylatrazine, desisopropylatrazine, bromophos-ethyl, trifluralin, dimethoate, atrazine, propazine, diazinon, disulfoton, alachlor, fenchlorophos, chlorpyriphos, tetrachlorvinphos, fenamiphos, metamitron, pyrazophos, azinphos-ethyl and coumaphos. Two bromine/fluorine-containing compounds were also included: 5-bromo-2-chloro-trifluoromethylbenzene and 4-bromo-2-fluorobiphenyl.

Sample preparation

Preparation of vegetable extracts
25 g of vegetable (carrot, cauliflower or onion) were homogenised with 50 ml of ethyl acetate in a food processor. The extract was dried over anhydrous Na_2SO_4 and, next, 10-fold concentrated by evaporation under a low flow of nitrogen gas. 1 ml of the final extract corresponded to 6 g of vegetable; 1 µl of this extract was subjected to GC analysis.

Preparation of water extracts
River water was taken from the river Meuse (Eysden, the Netherlands). After filtration over a 0.45 µm filter, the water sample was spiked by adding a concentrated solution of pesticides in ethyl acetate. Next, 75 ml of water were enriched using SPE. This was done using a Prospekt (Spark Holland, Emmen, the Netherlands) sample-handling module equipped with 10 mm x 2 mm I.D. SPE cartridges packed with PLRP-S (Polymer Labs, Church Stretton, UK) styrene–divinylbenzene copolymer) as described for the SPE–GC–MS system in Chapter 5.2. The cartridge was desorbed with 0.75 ml of methyl acetate, which contained 1-chlorododecane as an internal standard, into an autosampler vial. 50 µl of this extract were subjected to GC analysis.

Instrumental

GC–AED
For the determination of the elemental responses the GC column was coupled to the AED only, i.e. the column effluent was not split. The GC–AED system (Hewlett Packard, Waldbronn, Germany) consisted of a HP 5890II gas chromatograph with electronic pressure control, an on-column injector, an HP7673 autosampler and an HP5921A AED detector. The analytical column (28 m x 0.25 mm I.D.; film thickness, 0.25 µm; HP-5-MS; Hewlett Packard) was connected to the on-column injector via a 15-cm piece of DPTMDS-deactivated 0.53 mm I.D. fused silica to enable automated on-column injections (injection volume, 1 µl). The column was directly connected to the AED detector. The system was operated in the constant-flow mode (ca. 2.5 ml/min) using helium as the carrier gas. The GC temperature programme was as follows: initial temperature, 40°C; hold for 1 min; ramp, 10°C/min to 280°C; hold, 2 min.

The AED transfer line and the AED cavity temperature were held at 290°C and 300°C, respectively. Data acquisition and processing were done with an HP AED-Chemstation 5895A using element recipes as provided by the manufacturer. A solvent delay of 4 min was applied. Reagent gases used were H_2 (3.9 bar), O_2 (1.65 bar), and 'AUX' which is 10% CH_4 in N_2 (3.0 bar). A low helium make-up flow (F-) corresponded with 30 ml/min and a high make-up flow (F+) with 180 ml/min. The sets of elements, wavelengths and reagent gases and make-up flows used were as follows. Set 1: C (193 nm), N (174 nm), S (181 nm), O_2/H_2, F-. Set 2: C (496 nm), H (486 nm), Cl (479 nm), Br (478 nm), O_2, F-. Set 3: P (178 nm), O_2/H_2, F+. Set 4: F (690 nm), O_2/H_2, F-. Set 5: O (777 nm), AUX, F-.

The spectrometer was purged with nitrogen at 2 l/min and the window with helium at 30 ml/min. The cooling water temperature was 65°C. The pressure regulator controlling the AED cavity pressure was replaced by an electronic pressure controller. With the original set-up the cavity pressure increases slightly when switching to a high make-up flow, i.e. when

recording the phosphorus trace. As the cavity pressure is also the back-pressure at the end of the GC column, this causes a shift in retention time [14, 15]. With electronic pressure control the cavity pressure could be kept constant at 10 kPa. Constant retention times for all element traces can also be obtained by applying a high make-up flow for all elements but this has an adverse effect on analyte detectability which is undesirable, especially for less sensitive traces such as nitrogen, chlorine and bromine.

GC–AED/MS

The integrated system was set up by combining the GC–AED with an MD 800 (CE Instruments, Milan, Italy) mass spectrometer, which was used in the electron ionization mode over the 35–400 amu range. The set-up is discussed in Section 5.3.3.

In part of the study, large-volume injections were used, and the set-up changed as described in Section *Design of GC–AED/MS system*, below (see also Figure 1). The procedure was as follows. At the start of the injection the GC oven temperature was 50°C and the solvent vapour exit (SVE) was open. Next, 50 µl of sample in methyl acetate were injected at the standard 'on-column' speed of the autosampler. Under these conditions virtually no evaporation of solvent takes place during sample introduction; this, anyway, was not a problem as the retention gap was large enough to accommodate the entire sample. Most of the solvent was eliminated as vapour via the SVE before closure of the valve after 1.1 min. The GC oven temperature was increased after 2 min at a rate of 10°C/min to 290°C, which was held for 9 min. Solvent delays for both the MS and AED were 5 min.

5.3.3 Results and discussion

Design of GC–AED/MS system

When an MD800 mass spectrometer was coupled to the GC–AED set-up, the analytical column was withdrawn from the AED transfer line and connected to both detectors by means of two uncoated deactivated 0.32 mm I.D. transfer capillaries (T_1 and T_2 in **Figure 1**) via a press-fit T-splitter. The transfer capillary leading to the mass spectrometer was connected to a restriction (ca. 32 cm x 0.10 mm I.D., uncoated fused silica, R_1 in Figure 1) via a glass press-fit; the restriction R_1 was almost entirely located in the MS transfer line interface which was maintained at constant temperature (290°C). In this way a constant split ratio of the column effluent to the AED and MS of ca. 2:1 was obtained. The press-fit connection at the MS interface side was prone to leakage due to the MS vacuum which resulted in a high air background. This problem was solved by sealing the press-fit connection with polyimide-glue.

For large-volume injections, the 15-cm piece of deactivated uncoated capillary from the above set-up was replaced by a 6 m capillary (retention gap) of the same material. This capillary was coupled to a so-called retaining precolumn, a 2-m piece of analytical column, by a glass press-fit. The retaining precolumn was connected to the analytical column and a capillary leading to the SVE via a press-fit T-splitter. The capillary from this press-fit to the SVE was a 1.4 m x 0.25 mm I.D. restriction (R_2 in Figure 1). This ensured that a flow through the analytical column was maintained also when the SVE exit was open. If there would be no such flow (i.e. no pressure at the top of the analytical column), the MS will suck

gases from the AED cavity. If oxygen is the AED reagent gas, this will destroy the deactivation of the AED transfer capillary and cause severe adsorption of more polar analytes. At an inlet pressure of 150 kPa, the purge flow through the SVE during solvent elimination was measured to be 34 ml/min.

Characteristics of the GC–AED/MS set-up

The integrated set-up of Figure 1 has the obvious advantage that errors in data interpretation caused by differences in the injection-plus-separation parts of the two GC instruments that had to be used in the earlier set-up, do not occur any more. In addition, AED vs. MS peak correlation is much easier now. Earlier, RIs of organophosphorus pesticides and other micropollutants found in real-life samples were found to differ up to 15 units, corresponding with 0.15 min variation in calculated retention time [at a temperature gradient of 10°C/min]. This was attributed to the different outlet pressures of the MS (vacuum) and AED (10 kPa) and inevitable differences in the condition of the analytical column and the connective capillary tubing (ageing, 'bad' spots, active sites). In the present system, the differences in retention time of a compound found with AED and MS detection were very small, i.e. less than 0.5 sec (ca. 1 scan) in most cases. Relevant data are included in Table 5 below. This virtually eliminates the possibility of mismatching the mass spectrum and the observed AED peak. Data correlation also is less time-consuming because the peak in the MS trace corresponding with a selected peak in an AED trace has to be searched only in a window of ± 1 sec width rather than in a window of ± (10–12) sec as with the earlier set-up. The retention times of the same compound in the various element traces were the same within 1 sec due to the (electronically regulated) constant pressure in the AED cavity without any loss of sensitivity (cf. *Experimental* and Table 5 below).

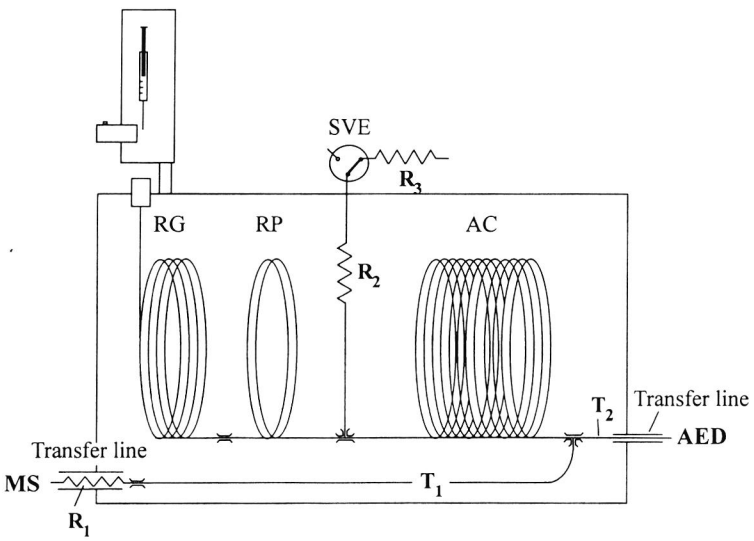

Figure 1
Set-up used for large-volume injection GC–AED/MS. AC, analytical column; RG, retention gap; RP, retaining precolumn; SVE, solvent vapour exit; T_1 and T_2, deactivated uncoated transfer capillaries; R_1, R_2 and R_3, deactivated restrictions, 32 cm x 0.10 mm, 1.4 m x 0.25 mm I.D. and 1 m x 0.075 mm I.D., respectively.

Table 1
AED elemental responses of twenty test analytes [a].

Element and Channel (nm)	n [b]	Average Response [c]	Range	MDM [d] (%)	LOD (S/N=3) [e] (pg E/s)	Average LOD [f] (ng compound)	Linearity [g] (R^2)
C 193	20	0.96	0.93–1.00	4	5.5	0.03	0.9998
H 486	20	0.99	0.93–1.11	8	7.0	0.40	0.9998
O 777	14	1.05	0.75–1.58	14	119	3.0	0.9985
N 174	13	0.94	0.75–1.10	8	39	0.75	0.9997
S 181	10	0.94	0.88–1.00	4	1.5	0.04	0.9998
P 178	11	1.00	0.89–1.16	5	1.0	0.05	0.986
Cl 479	10	0.97	0.92–1.00	3	27	0.75	0.9996
Br 478	3	0.97	0.95–1.00	2	-	0.75	-
F 690	3	0.96	0.79–1.09	12	-	2.4	-

[a] For names of analytes, see *Experimental*. [b] Number of pesticides containing the element. [c] Elemental response relative to chlorpyriphos for C, H, Cl, N, O and P, and to 4-bromo-2-fluorobiphenyl for Br and F. [d] Mean deviation from mean elemental response. [e] LOD (S/N=3) for chlorpyriphos as test compound; E, element. [f] Average LOD (S/N=3) of those of the 20 test analytes containing this element. [g] Linearity over two orders of magnitude (starting from the detection limit) using chlorpyriphos as test compound.

In order to assess the potential of AED screening, twenty pesticides were selected and relevant analytical data collected. Compared with our earlier work, and also with that of others [9, 11–14, 16], a rather wide area was covered, especially regarding the dependence of the elemental response on the molecular structure. Typical results are summarized in **Table 1**. The main conclusions that can be drawn from the data, are as follows. (i) Detection limits (for a compound of 200–400 amu) typically vary from 30–50 pg (S, P, C) to 400–800 pg (Cl, Br, H, N) to 2–4 ng (F, O). Obviously, ca. 1 ng of an analyte will suffice for the identification for most elements of interest, and a few nanograms will be sufficient to include even oxygen and fluorine. (ii) The linearity is fully satisfactory for all elements of chlorpyriphos except phosphorus (which agrees with earlier findings [1, 10]). (iii) The average elemental responses are within relatively small ranges for six of the nine elements tested, and these can certainly be used for compound-independent, or universal, calibration with an element calibration curve for deriving provisional partial molecular formulae (although the carbon and hydrogen traces will, of course, not have any real relevance when analysing real-life samples).

It may be argued that the less-than-satisfactory behaviour of fluorine is relatively unimportant, but the same is certainly not true for nitrogen and oxygen. The data, which generally are in line with those reported in the literature [5, 13], indicate that including nitrogen in partial formulae is justified only if the analyte concentrations are well above the detection limit, whereas with oxygen, it is safe to draw conclusions regarding presence or absence (see Table 2 below), but not about the number of atoms per molecule. [The relatively strong structure dependence found for oxygen has been reported before [13] and was attributed to incomplete breakdown of the compounds in the plasma and/or recombination of atoms (e.g. CO formation). The condition of the plasma cavity discharge tube was also considered to affect the elemental response.] Interestingly, the present data clearly indicate why some workers advocate in favour of, wherever others warn against, deriving partial formulae and using universal calibration [1, 10–13]. The selectivity found for all element channels implies that a presence–absence decision can be confidently made in all instances. For all hetero atoms studied except oxygen, (semi-)quantitation (formulae; concentration

levels) can be expected to include 20–30% errors. This seems to be fully acceptable for trace-level analysis which, moreover, is complemented by an MS-based result.

Practicality of GC–AED/MS

Two types of applications were studied in order to test our above conclusions and to study the practicality of the procedure for the (provisional) identification of unknowns at the trace level.

Vegetables

Carrot, onion and cauliflower extracts were spiked with 1.2 (or 0.2) µg/g of five pesticides and subjected to analysis. Since no large-volume injections were used in this instance, only ca. 6 (or 1.0) ng of each pesticide were injected on the GC column. Results are reported in **Table 2**. At the 1.2 µg/g level, fully satisfactory results were obtained: in all cases except trifluralin in carrot, the partial formula (without oxygen) was correctly predicted. This as well as the selected AED traces shown in **Figure 2** confirm the several positive, and also the negative (oxygen) conclusions of the previous section. As can already be expected on the basis of the AED data of Figure 2, at the 0.2 µg/g level, oxygen and fluorine did not show up any more. However, the results for the other elements, with cauliflower as an example, were still rather satisfactory. This is demonstrated by the quantification data of **Table 3**. The results obtained by universal AED calibration were comparable with the external MS quantification data. It is interesting to add that the few rather large errors are spread over the MS and AED data and not confined to one detector. Finally, it should be admitted that the analysis of onion samples was not really successful at the 0.1 µg/g spiking level. Not unexpectedly, the sulphur peaks were obscured by a large number of interfering peaks caused by the matrix. However, for the same sample, some difficulties were encountered with MS quantification as well, especially with azinphos-ethyl because the ions formed after electron ionization were not very specific. On the other hand, the phosphorus channel still showed undisturbed peaks, and quantification of the three phosphorus-containing analytes, bromophos-ethyl, tetrachlorvinphos and azinphos-ethyl, gave errors of only 10–40% at this less-than-1-ng level.

Table 2
Qualitative analysis using GC–AED: determination of partial molecular formulae.

		AED: partial molecular formula [a]			MS: identification [b]	
Matrix:		Carrot	Onion	Cauliflower	Compound	formula
Spike (mg/kg):		*1.2*	*1.2*	*0.2*		
Analyte [c]	t_r(min) [d]					
3	13.45	$F_{1.0}N_{1.3}O_x$	$F_{1.0}N_{1.0}O_x$	$N_{1.0}O_x$	Trifluralin	$C_{13}H_{16}F_3N_3O_4$
4	15.80	$Cl_{1.0}N_{1.0}O_x$	$Cl_{1.0}N_{1.0}O_x$	$Cl_{1.2}N_{1.0}O_x$	Alachlor	$C_{14}H_{20}ClNO_2$
6	16.91	$Br_{1.0}Cl_{1.9}O_xP_{1.3}S_{1.0}$	$Br_{1.2}Cl_{2.3}O_xP_{1.3}S_{1.0}$	$Br_{1.1}Cl_{2.0}P_{0.8}S_{1.0}$	Bromophos-ethyl	$C_8H_8BrCl_2O_3PS$
7	17.88	$Cl_{1.0}O_xP_{0.23}$	$Cl_{1.0}O_xP_{0.22}$	$Cl_{1.0}P_{0.15}$	Tetrachlorvinphos	$C_{10}H_9Cl_4O_4P$
8	21.93	$N_{1.4}O_xP_{0.6}S_{1.0}$	$N_{1.7}O_xP_{0.7}S_{1.0}$	$N_{1.8}O_xP_{0.6}S_{1.0}$	Azinphos-ethyl	$C_{12}H_{16}N_3O_3PS_2$

[a] 1.0 assigned to element with lowest number of atoms in partial formula; however, if P is that element and Br, Cl, F, N or S are also present, one of these is used instead. For oxygen, only its presence ($_x$) is indicated (cf. text). [b] First hit in library search corresponding with partial formula obtained by AED; compounds identified in all three matrices. [c] Nos. 1, 2 and 5 are internal standards. [d] Retention time t_r for analysis of carrots of Figure 2.

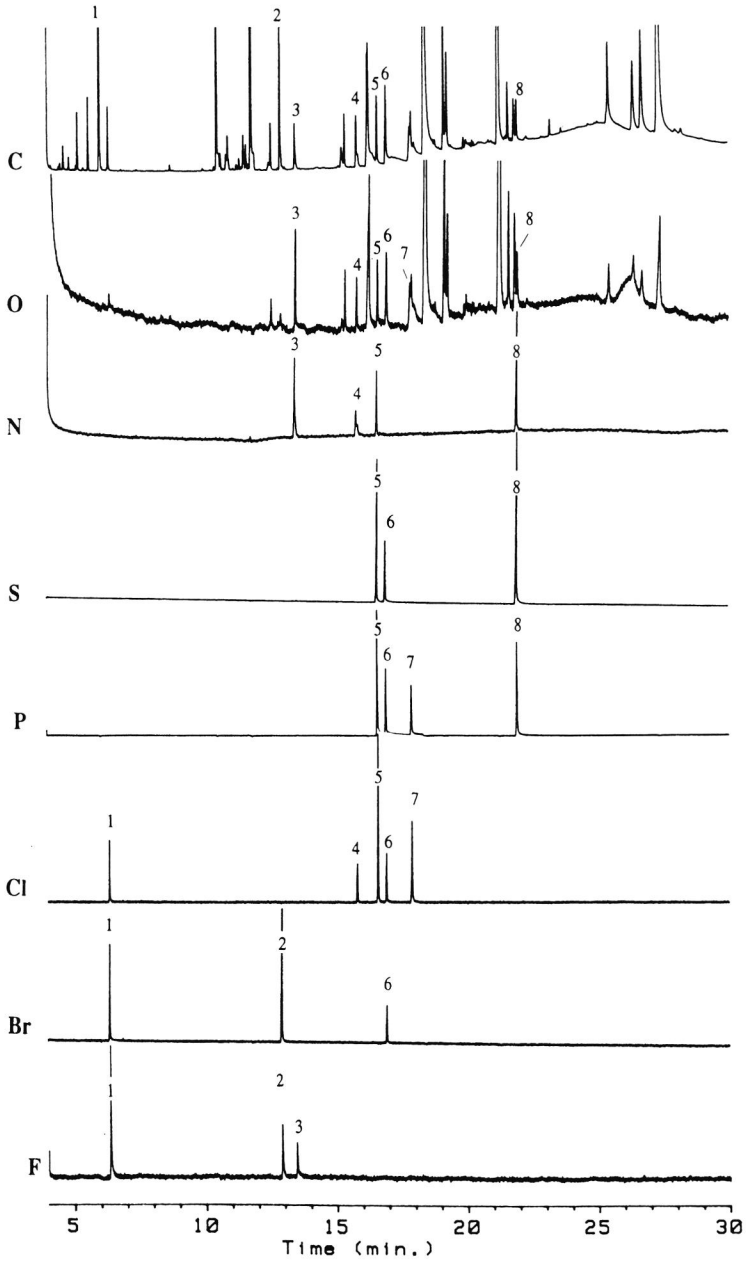

Figure 2
GC–AED chromatograms obtained after injection of a spiked carrot extract (ca. 1 mg/kg). Injection volume, 1 µl (corresponds with ca. 6 ng of each analyte). Peak assignment: 1, 5-bromo-2-chloro-trifluoromethylbenzene; 2, 4-bromo-2-fluorobiphenyl; 3, trifluralin; 4, alachlor; 5, chlorpyriphos; 6, bromophos-ethyl; 7, tetrachlorvinphos; 8, azinphos-ethyl.

Table 3
Comparison of MS and AED detection in quantitative analysis of vegetables [a].

	True value	Experimental concentration (mg/kg)							
		MS [b]		AED					
Analyte	(mg/kg)	m/z 1	m/z 2	Br	Cl	F	N	P	S
Carrot									
Trifluralin	1.24	1.18	1.19			0.98	1.24		
Alachlor	1.31	1.32	1.31		1.35		1.34		
Bromophos-ethyl	1.18	1.19	1.20	1.12	1.07			1.37	1.09
Tetrachlorvinphos	1.24	1.39	1.79		1.18			1.07	
Azinphos-ethyl	1.61	2.00	1.93				1.51	1.87	1.59
Onion									
Trifluralin	1.24	1.53	1.48			1.19	1.24		
Alachlor	1.31	1.31	1.35		1.28		1.31		
Bromophos-ethyl	1.18	1.18	1.11	1.20	1.11			1.27	0.54
Tetrachlorvinphos	1.24	1.30	1.41		1.04			0.95	
Azinphos-ethyl	1.61	1.82	1.79				1.53	1.93	1.38
Cauliflower									
Trifluralin	0.21	0.20	0.20			n.d.	0.20		
Alachlor	0.22	0.22	0.22		0.24		0.20		
Bromophos-ethyl	0.20	0.19	0.20	0.21	0.20			0.16	0.19
Tetrachlorvinphos	0.21	0.22	0.21		0.17			0.10	
Azinphos-ethyl	0.27	0.30	0.30				0.29	0.31	0.25

[a] MS: internal standardization used (chlorpyriphos, m/z 314); AED: universal elemental calibration.
[b] m/z 1 and m/z 2: trifluralin, 306 and 264; alachlor, 188 and 160; bromophos-ethyl, 331 and 125; tetrachlorvinphos, 331 and 109; azinphos-ethyl, 160 and 132.

Table 4
Comparison of MS and AED detection in quantitative surface water analysis [a].

	True value	Experimental concentration (μg/l)						
		MS [b]		AED				
Analyte	(μg/l)	m/z 1	m/z 2	Br	Cl	N	P	S
Trifluralin	0.82 [c]	0.84	0.83			0.77		
Atrazine	0.97	0.96	0.99		0.83	0.84		
Diazinon	0.73	0.69	0.68			0.64	0.83	0.72
Alachlor	1.03	1.02	1.02		0.94	1.12		
Terbutryn	1.05	1.04	1.07			0.88		0.94
Bromophos-ethyl	0.70 [c]	0.77	0.75	0.63	0.71		0.60	0.69
Azinphos-ethyl	1.30	1.52	1.42			1.08	1.33	1.13

[a] MS: internal standardization used (chlorpyriphos, m/z 314); AED: universal elemental calibration.
[b] m/z 1 and m/z 2: atrazine, 215 and 200; diazinon, 179 and 137; terbutryn, 241 and 226; other compounds, see Table 3.
[c] with trifluralin and bromophos-ethyl, their known and experimentally verified low recoveries of ca. 80% and 70%, respectively, were taken into account.

Water

River Meuse water was 100-fold preconcentrated on a 10 mm x 2 mm I.D. SPE cartridge using the SPE module of the SPE–GC system described in Chapter 3.1. 750 µl of methyl acetate used for desorption were transferred into an autosampler vial and (manually) transferred to the autosampler of the GC–AED/MS. An 50-µl aliquot (corresponding with 5 ml of water) was analysed by GC–AED/MS. The data of **Table 4** show that, at the 1-µg/l level, the selectivity of MS and AED were amply sufficient for proper identification and quantification. Universal AED quantification and external MS quantification agree to within about 20%, and correction for the notorious low recoveries of trifluralin and bromophos-ethyl also bring the results for these analytes in line.

The applicability of GC–AED/MS for non-target compound analysis was also studied for river Meuse water. After 100-fold off-line enrichment (cf. above), 50 µl of the methyl acetate extract were analysed. Since the oxygen and fluorine channels could not be expected to provide useful information at the 0.02–0.5 µg/l level aimed at, screening was limited to the C/N/S, C/H/Cl/Br and P traces. A typical set of results is shown in **Figure 3**. The simultaneously acquired total ion current GC–MS trace is also shown in Figure 3. Since the bromine trace (not shown) contained only one peak, viz. for the calibrant added, and most of the peaks in the sensitive sulphur trace represent very small amounts of analytes - and will, therefore, yield very poor MS spectra - peak identification was mainly attempted on the basis of the chlorine and phosphorus channel data, and the subsequent MS confirmation. The data of **Table 5** show that twelve compounds could be identified, and quantified. The concentration levels were from ca. 0.5 µg/l down to as little as 20 ng/l. The mutual agreement of the quantification data (at the sub-µg/l level) can be called fully satisfactory. Quite a number of chlorinated phosphate esters were found to be present, and the excellent fit of the Cl/P elemental ratio in three out of five cases is worth mentioning. These compounds are widely used as flame retardants and plasticizers. Another aspect of interest is that the retention-time data confirm our earlier tentative conclusion regarding a main advantage of the present set-up. With two exceptions, differences are on the order of 0.01 min, and in one case even lower than 0.001 min (peak no. 12).

During acquisition of each AED element set, a range of wavelengths is covered rather than one individual wavelength for each element in the set. Spectra over a range of approx. 20 nm are therefore available. Background-corrected spectra, so-called snapshots, can be used to further confirm element identity. All numbered peaks of the sulphur, chlorine and phosphorus traces were confirmed by snapshot data. An example for the phosphorus channel is given as an insert of Figure 3. The identity of the peak found at 22.19 min, and recorded at 178.3 nm is confirmed by the other two peaks in the snapshot, at 177.5 and 178.8 nm, which together make up the characteristic phosphorus triplet.

Finally, it is fair to give an indication of the limitations of the present approach. In our earlier work [14], we included an example of the analysis of waste water. The results obtained for the effluent (!) studied were rather good. An attempt was now made to analyse the influent of a sewage treatment plant. The spiking solution was the same as used for the surface water analysis at the 1-µg/l spiking level (cf. Table 4). The influent was found to contain many sulphur-containing compounds; as a result, the S trace was extremely noisy, and many peaks showed up which made detection of individual analytes essentially impossible. Detection in the nitrogen trace was complicated by a big hump in the 10–20 min region, which obscured four out of our six relevant test analytes. On the other hand, nitrogen-

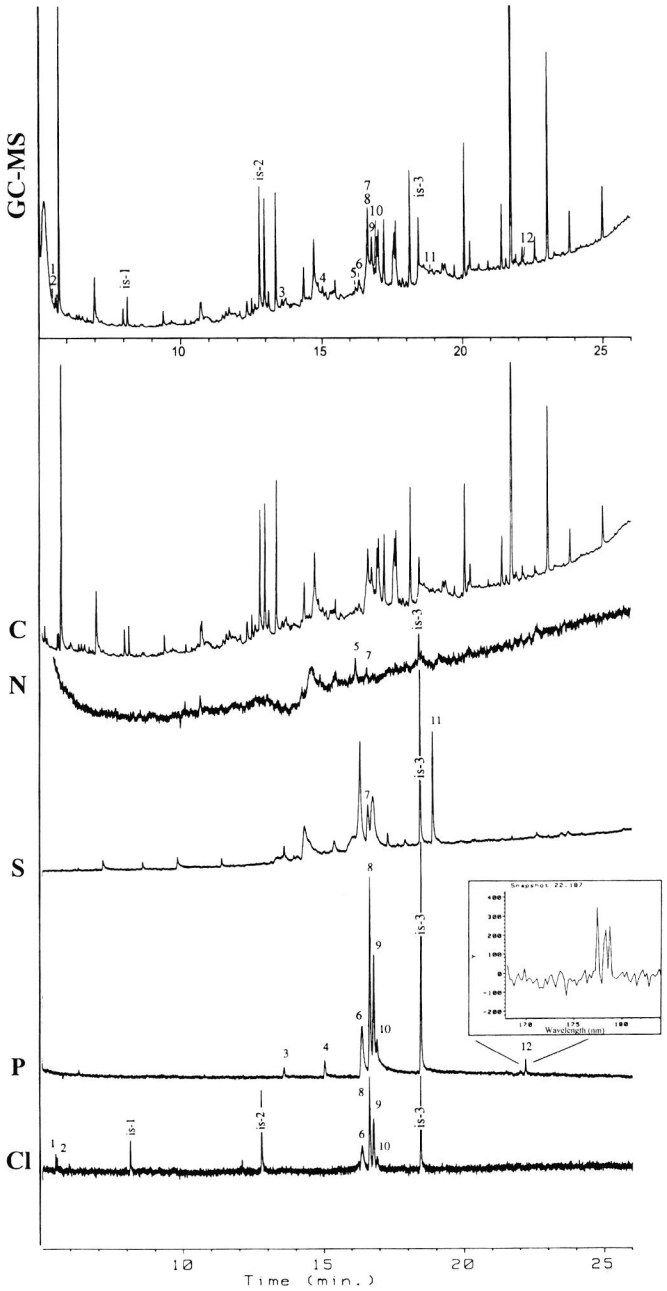

Figure 3
GC–AED/MS chromatograms obtained after injection of 50 µl of a 100-fold concentrated extract of river Meuse water. AED screening: C, N, S, Cl and P traces. Simultaneously acquired total ion MS chromatogram. Peak assignment: is-1, 5-bromo-2-chloro-trifluoromethylbenzene; is-2, 1-chlorododecane; is-3, chlorpyriphos; other peaks, see Table 5. The insert shows the snapshot of the peak found at 22.19 min in the P trace.

trace detection of trifluralin and azinphos-ethyl caused no problems, and the quality of the phosphorus, chlorine and bromine traces was not affected at all. As a result, five out of the seven analytes could still be recognised from (up to three) AED traces and confirmed by the clearly more selective (only one ion missing out of a total of fourteen) MS data. On the other hand, AED detection gives a good impression of the complexity of a sample caused by compounds containing targeted hetero-atoms, which is something MS detection does not do. Not unexpectedly, band broadening was observed after the injection of several waste water extracts due to deterioration of the retention gap. Obviously, the sample introduction plus GC technique requires further optimization if the analysis of samples as contaminated as influent waste water is the goal.

Table 5
Non-target analysis of a river water sample using GC–AED/MS.

Peak	Qualitative analysis						Quantitative analysis (µg/l)	
	AED screening			MS identification			MS.	AED
No.	Element	t_r (min)	Elem. ratio	Compound	t_r (min)	m/z 1 m/z 2	Standard add.	Elemental calc.
1	Cl	5.48	-	Tetrachloroethane	5.49	85	0.01	0.02
					5.49	83	0.01	
2	Cl	5.50	-	Trichloropropane	5.54	110	0.002	0.02
					5.54	75	0.001	
3	P	13.58	-	Tris(*i*-butyl) phosphate	13.58	155	0.03	0.03
					13.58	99	0.03	
4	P	15.05	-	Tributyl phosphate	15.02	211	0.03	0.03
					15.02	99	0.03	
5	N	16.19	-	Atrazine	16.20	215	0.04	0.06
					16.20	200	0.04	
6	Cl	16.39	3.5/1.0	Tris(2-chloroethyl) phosphate	16.34	251	0.16	0.12
	P	16.40			16.34	249	0.11	0.20
7	N	16.60	S/N<3	*n*-Butylbenzene sulphonamide	16.60	170	0.10	S/N < 3
	S	16.59	-		16.60	141	0.12	0.08
8	Cl	16.64	3.1/1.0	Tris(2-chloro-1-methylethyl) phosphate	16.63	277	0.36	0.40
	P	16.64			16.63	201	0.32	0.28
9	Cl	16.79	3.0/1.0	Bis(2-chloro-1-methylethyl) (2-chloropropyl) phosphate [a]	16.77	277	- [b]	0.26
	P	16.78			16.78	201		0.19
10	Cl	16.90	3.0/1.0	(2-Chloro-1-methylethyl) bis(2-chloropropyl) phosphate [a]	16.89	277	- [b]	0.08
	P	16.90			16.89	201		0.06
11	S	18.88	-	Sulphur	18.88	258	- [b]	0.02
					18.89	256		
12	P	22.19	-	Octyl diphenyl phosphate	22.19	251	- [b]	0.02
					22.19	250		

[a] For more details on identification, cf. [14].
[b] No standard available.

5.3.4 Conclusions

Combining GC on-line with simultaneous AED and MS detection provides a powerful means to screen for the presence of hetero-atom-containing microcontaminants (AED) and, next, to identify or confirm their identity (MS) and carry out quantification (MS, and, especially in non-target analysis when no reference compound is available as external standard, AED). The dual-hyphenation set-up largely eliminates data-interpretation problems caused by small differences in retention time, or retention indices and is, therefore, a distinct improvement over a purely conventional GC–AED plus GC–MS approach. Present experience indicates that the analysis of vegetables, tap and surface water and, even, effluent waste water, does not cause undue problems down to analyte concentrations of 20–200 ng/l. Not unexpectedly, with influent waste water, the presence of (too) many chemical compounds at, frequently, high concentrations, easily disturbs part of the AED traces. Although this may be interpreted as providing interesting information about the general pollution profile, the intended information on individual analytes is lost. In other words, further study is required to improve the analytical performance of GC–AED/MS for this sample type.

References

[1] B.D. Quimby and J.J. Sullivan, *Anal. Chem.*, 62 (1990) 1027.
[2] J.J. Sullivan and B.D. Quimby, *Anal. Chem.*, 62 (1990) 1034.
[3] S. Pederson-Bjergaard and T. Greibrokk, *J. High Res. Chromatogr.*, 19 (1996) 597.
[4] H.-J. Stan and M. Linkerhägner, *J. Chromatogr. A*, 750 (1996) 369.
[5] N.L Olson, R. Carrell, R. Cummings, R. Rieck and S. Reimer, *J. Assoc. Off. Anal. Chem. Intern*, 78 (1995) 1464.
[6] Th. Hankemeier, A.J.H. Louter, F.D. Rinkema and U.A.Th. Brinkman, *Chromatographia*, 40 (1995) 119.
[7] E.C. Goosens, D. de Jong, G.J. de Jong, R.D. Rinkema and U.A.Th. Brinkman, J. *High Res. Chromatogr.*, 18 (1995) 38.
[8] S. Pedersen-Bjergaard, T.N. Asp, J. Vedde, G.E. Carlberg and T. Greibrokk, *Chromatographia*, 35 (1993) 193.
[9] P.L. Wylie, J.J. Sullivan and B.D. Quimby, *J. High Res. Chromatogr.*, 13 (1990) 499.
[10] N.L. Olson, R. Carrell, R.K. Cummings and R. Rieck, *LC-GC*, 12 (1994) 142.
[11] S. Pedersen-Bjergaard, T.N. Asp and T. Greibrokk, *Anal. Chim. Acta*, 265 (1992) 87.
[12] J.Th. Jelink and A. Venema, *J. High Res. Chromatogr.*, 13 (1990) 477.
[13] C. Webster and M. Cook, *J. High Res. Chromatogr.*, 18 (1995) 319.
[14] Th. Hankemeier, J. Rozenbrand, M. Abhadur, J.J. Vreuls and U.A.Th. Brinkman, *Chromatographia*, 48 (1998) 273.
[15] H.-J. Stan and M. Linkerhägner, *J. High Res. Chromatogr.*, 16 (1993) 539.
[16] K. Janák, C. Ostman, H. Carlsson, A. Bemgård and A. Colmsjö, *J. High Res. Chromatogr.*, 17 (1994) 135.

6

On-line SPE–GC with IR detection

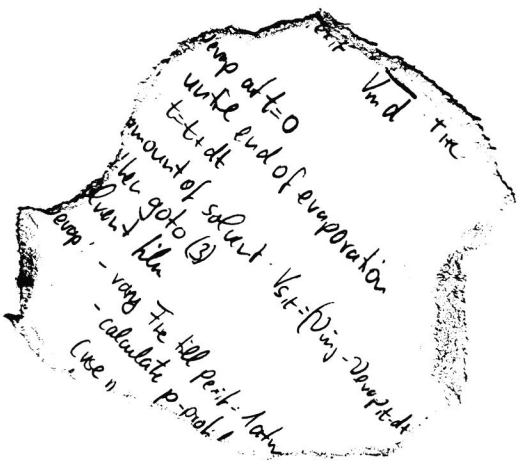

6.1 Detectability enhancement by the use of large-volume injections in GC–cryotrapping-IR

Summary

The use of large-volume injections via a loop-type interface in GC–cryotrapping-IR has been studied. *n*-Alkanes and polyaromatic hydrocarbons (PAHs) were used as test compounds. When using 100-µl injections the analyte detectability was enhanced by two to three orders of magnitude compared with conventional split/splitless injections. For the *n*-alkanes, the absolute detection limits were nearly independent of the injected volume and the mode of injection. With the PAHs a water background (due to press-fit connections and six-port valves) somewhat disturbed the GC–IR chromatograms and the spectra of the PAHs. This detracts from the system performance. Still, upon going from split/splitless injections to 100–200-µl injections, analyte detectability was increased by a factor of 30–500. The repeatability of the total 100-µl GC–cryotrapping-IR procedure was satisfactory.

The potential of the set-up was demonstrated by determining PAHs in river water at the 0.5 µg/l level by means of micro liquid-liquid extraction and 100-µl GC–cryotrapping-IR. The IR spectra obtained matched well with those of standard libraries.

6.1.1 Introduction

The identification and quantitation of environmental pollutants becomes increasingly demanding as threshold values for microcontaminants still tend to be set lower for health and safety reasons. The current alarm level for individual pesticides in surface water and drinking water, for instance, is 1 μg/l and 0.1 μg/l, respectively [1]. Reaching such detection limits is a distinct challenge.

Gas chromatography (GC) is often used for trace analysis because of its high sensitivity, separation efficiency and speed of analysis. Detection is usually carried out by flame ionization detection (FID), the more or less element-selective nitrogen–phosphorus detection and electron-capture detection, or by mass spectrometry (MS) if structural information is required. Unambiguous identification by MS, however, is not always possible, e.g. when one has to distinguish isomers. In such cases, Fourier transform infrared (IR) spectrometric detection is the preferred alternative [2–5].

Coupling of GC and IR can be achieved by the 'light-pipe' flow cell interface [6], and by low-temperature sample storage techniques such as matrix isolation [7] and direct deposition or cryotrapping [8]. The light-pipe is the most straightforward interface but a major drawback is the short residence time of the sample in the cell. The sensitivity is at best 10–100 ng of analyte injected on-column.

The principle of the sample storage techniques is immobilization of the GC chromatogram at cryogenic temperature, typically 4–80 K. The GC eluate is trapped as a small trace on a moving substrate. IR detection is carried out either immediately after deposition (on-the-fly) or after completion of the GC run (post-run scanning). This type of sample storage allows the use of IR microscopy and extended data acquisition of each spot on the substrate. As a consequence, the sensitivity of these techniques is two orders of magnitude better than GC–lightpipe–IR resulting in detection limits of 0.1–1 ng on-column [9]. Admittedly, sample storage interfaces are more complex and require more operator involvement.

So far, sample volumes injected on sample storage GC–IR systems have been limited to 1–2 μl, i.e., to μg/ml levels in terms of concentration in the extract solution. In principle, however, the analyte detectability (in concentration units) can be dramatically increased by injecting a larger volume of the sample solution. Several techniques to inject such volumes into a GC system have been developed, particularly for the on-line coupling of LC and GC. Examples are the on-column interface with partially concurrent solvent evaporation [10] and the loop-type interface using fully concurrent solvent evaporation [11]. Recently, the programmed temperature vaporizer (PTV) has been used for large-volume injection too [12]. Several applications of GC combined with these injection techniques have been reported [13–16].

Occasionally, large-volume injection has been applied to increase the detectability of GC–IR, but only for instruments equipped with a light-pipe interface. *Fehl et al.* reported the development of a two-trap injection system to inject 100-μl volumes [17]. The system resembled a PTV injector with an additional cold trap between the PTV and the analytical column. *Hu et al.* used an on-column interface for 100-μl injections into a light-pipe GC–IR instrument [18] using a 37 m long retention gap. An increase in analyte detectability by a factor of 100 was claimed but quantitative data were not shown. *Full et al.* demonstrated the

use of an on-column interface for injections of up to 550 µl in an on-line LC–GC–lightpipe–IR system [19]. Detection limits were not reported.

Obviously, further improvement of analyte detectability in GC–IR can be achieved by applying large-volume injection on a more sensitive, but also more complex sample storage GC–IR system. We therefore studied large-volume injection combined with GC–cryotrapping-IR. A loop-type injection interface was chosen because of its rather simple optimization. The system was tested and optimized with standard solutions of alkanes and polycylic aromatic hydrocarbons (PAHs). The practicability of the system was tested by the determination of PAHs in river water extracts obtained by means of micro liquid-liquid extraction (micro-LLE).

6.1.2 Experimental

Chemicals

The standard mixture of PAHs in toluene was a Standard Reference Material (SRM 2260) from the National Institute of Standards and Technology (NIST), obtained from C.N. Schmidt (Amsterdam, Netherlands). The certified concentrations were around 60 µg/ml. The stock solution was used for the preparation of diluted standards in hexane and for spiking of river Rhine water samples.

A stock solution containing undecane (C_{11}), tridecane (C_{13}), pentadecane (C_{15}), heptadecane (C_{17}), nonadecane (C_{19}), uneicosane (C_{21}), trieicosane (C_{23}) and pentaeicosane (C_{25}) was prepared in *n*-hexane at a concentration of about 20 µg/ml. For optimization of the large-volume injections the stock solution was diluted to a concentration of 50 pg/µl in *n*-pentane, *n*-hexane, ethyl acetate, acetonitrile and toluene. Ethyl acetate, *n*-pentane and *n*-hexane (all Nanograde) were from Mallinckrodt and were purchased from Promochem (Wesel, Germany). Toluene (glass distilled grade) and acetonitrile (HPLC grade) were obtained from Rathburn Chemicals (Walkerburn, UK). Anhydrous sodium sulfate was obtained from J.T. Baker (Deventer, Netherlands) and dried at 150°C before use. Helium 4.0 was purchased from Hoekloos (Schiedam, Netherlands).

GC equipment

A Carlo Erba MEGA 5160 gas chromatograph (Carlo Erba Strumentazione, Milan, Italy) equipped with a split/splitless injector and an FID detector was used. The large-volume injection system (**Figure 1**) consisted of a loop-type interface with two six-port rotating switching valves. The sample valve contained a sample syringe and a 100-µl loop.

The GC system contained a 5 m x 0.32 mm I.D. diphenyltetramethyldisilazane-deactivated retention gap (BGB Analytik, Zürich, Switzerland), a 1 m x 0.25 mm I.D. CP-Sil-5 CB (Chrompack, Middelburg, the Netherlands) retaining precolumn and a 25 m x 0.25 mm I.D. CP-Sil-5 CB analytical column with a film thickness of 0.25 µm. For the analysis of the real-life water samples a 1 m x 0.25 mm I.D. DB-17 (J&W Scientific, Folsom, CA, USA) retaining precolumn and a 15 m x 0.25 mm I.D. DB-17 analytical column with a film thickness of 0.15 µm were used. An early solvent vapour exit (SVE) was inserted between the retaining and the analytical column. The SVE was opened and closed manually by

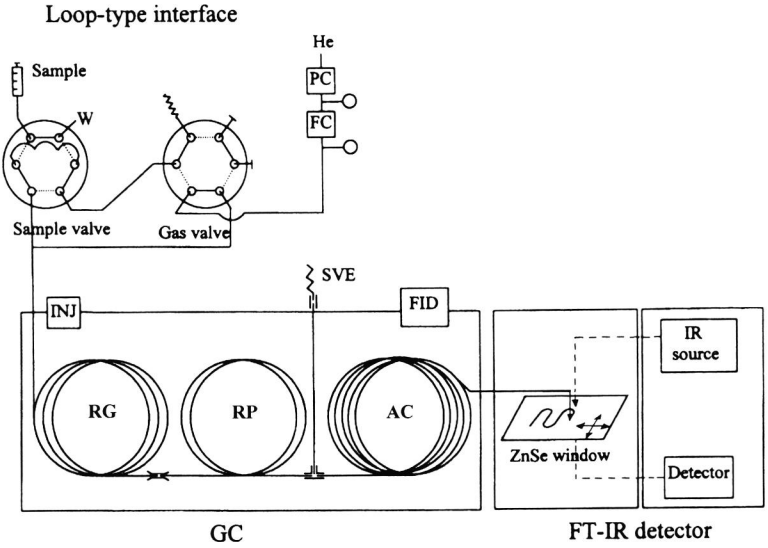

Figure 1
Set-up of the large-volume injection–GC–cryotrapping-IR system. Abbreviations: FC, flow controller; PC, pressure controller; RG, retention gap, RP, retaining precolumn, AC, analytical column, INJ, injector; SVE, solvent vapour exit; W, waste.

removing and attaching a press-fit connector to which a 0.60 m x 50 μm I.D. restriction capillary was connected (see Figure 1).

Large-volume injections of 100, 200 or 400 μl were performed by (i) filling the sample loop using a syringe, (ii) opening the SVE and (iii) simultaneously switching the sample and gas valve so that the carrier gas pushes the sample plug via the retention gap to the GC system. After completion of the transfer, which is indicated by the pressure drop on the manometer inserted after the flow controller, both six-port valves were switched to the default position (shown in Figure 1). The SVE was closed after 30 sec, and the GC temperature programme and the data acquisition were then started.

For the analysis of alkanes, the temperature was increased from the transfer temperature to 290°C (final hold time, 10 min) at 20°C/min. Transfer temperatures for 100-μl injections of various solvents are summarized in **Table 1**. The transfer temperature for the injection of 200- and 400-μl volumes were 3°C higher than for the 100-μl amounts. For the determination of the PAHs the temperature was increased to 180°C at 20°C/min, followed by an increase to 290°C at 5°C/min, with a final 10-min hold. The gas flow was set to 0.9 ml/min, resulting in a head pressure of around 80 kPa at 70°C for the 25-m and 55 kPa for the 15-m analytical column. To remove traces of water present in the helium, a water trap (Supelco, Bellefonte, PA, USA) was installed in front of the pressure and flow control of the GC system. For reference purposes, 1-μl split and splitless injections were carried out. The injector temperature then was 250°C and the head pressure 90 kPa.

Table 1
Minimum transfer temperature and application range for various solvents.

Solvent	Boiling point [°C]	Optimized transfer temperature [°C]	Elution temperature of first *n*-alkane [°C]	First *n*-alkane [a] [C number]
n-Pentane	36	60	200	15
n-Hexane	69	95	240	19
Ethyl acetate	77	100	240	19
Acetonitrile	81	112	260	21
Toluene	111	143	280	23

[a] First *n*-alkane of test mixture, which was quantitatively recovered.

IR spectrometry

The infrared spectrometer used was a Digilab, FTS-40 Fourier transform instrument (Bio-Rad, Cambridge, MA, USA) equipped with a Digilab Tracer cryotrapping GC interface [2]. Data acquisition and processing was done with a SPC 3200 computer (Bio-Rad). The GC column was connected to a 1-m deactivated fused-silica transfer capillary of 150 μm I.D. by means of an aluminum ferrule connector (Bio-Rad). The transfer line was guided into the interface housing through a stainless-steel pipe. The interface housing was held at 1.3 10^{-3} Pa to minimize condensation of compounds present in the ambient air. A fused-silica deposition tip of 60 μm I.D. was fixed to the end of the transfer line and located 30 μm above the surface of a moving IR transparent ZnSe window, which was cooled to 80 K with liquid nitrogen. The tip and the transfer line were kept at 250°C.

Eluting compounds were trapped as solids on the ZnSe slide, which was moved continuously by an X–Y stepping motor. A few seconds after deposition the trapped spots passed through the beam of an IR microscope. The immobilized chromatogram was thus scanned on-the-fly by averaging four spectra recorded at 2 scans/s for each step. After completion of the GC run extended post-run scanning of certain retention times was performed by repositioning the corresponding coordinates of the ZnSe window into the IR beam. Post-run spectra were acquired by averaging 256 scans. The optical resolution of on-the-fly and post-run spectra was 8 cm^{-1}.

GC–IR chromatograms of the integrated IR absorption as a function of retention time were constructed by standard Gram–Schmidt vector orthogonalization. Functional-group GC–IR chromatograms of preselected wavelength regions were applied to reduce interferences of compounds not showing absorption in that wavelength region [3]. The interval 2820–2980 cm^{-1} was chosen for the alkanes, and 700–950 cm^{-1} for the PAHs, as the strongest absorption bands of these compounds occur in these regions.

Liquid-liquid extraction

A 1-l water sample held in a 1-l Erlenmeyer-flask was extracted twice with 0.6 ml of n-hexane. After shaking for 5 min, a laboratory-made micro-extraction adapter modified slightly from ref. [20] was placed on top of the 1-l flask via an NS 24 connection. The flask was tilted and water added via the wider glass tubing so that the hexane layer was pushed

into the glass capillary, and could then be removed with a pipette. After removing about 30 ml of water from the Erlenmeyer flask, another 0.6 ml of n-hexane was added and the extraction process repeated. A total of about 1 ml of hexane was recovered. The extract was dried over anhydrous sodium sulfate.

6.1.3 Results and discussion

Optimization of large-volume injections

Large-volume injections via a loop-type interface require optimization of two basic parameters: (i) the transfer temperature and (ii) the closing time of the SVE necessary to minimize the amount of solvent reaching the IR detector.

Optimization of transfer temperature for various solvents
When injecting large volumes of solvent into the GC system via a loop-type interface, the solvent is evaporated under fully concurrent evaporation conditions. The only parameter to be optimized is the transfer temperature, which has to be above the boiling point of the solvent. At too low a transfer temperature the solvent evaporation is too slow and the solvent film will reach the retaining precolumn; this will result in severe peak distortion. If the transfer temperature is too high, the more volatile analytes will be (partly) lost. The minimal transfer temperatures to avoid flooding the retaining precolumn for various solvents were optimized with a 50 pg/µl solution of the uneven (C_{11}–C_{25}) *n*-alkanes in *n*-pentane, *n*-hexane, ethyl acetate, acetonitrile and toluene. For reasons of simplicity, FID was used for optimization. The SVE was closed 30 sec after completion of the transfer which was indicated by the pressure drop as described above. The first *n*-alkane which was quantitatively recovered with the various solvents is listed in Table 1. The difference between the boiling point and the optimized transfer temperature is around 25°C for *n*-pentane, *n*-hexane and ethyl acetate, and around 31°C for acetonitrile and toluene. The difference between the transfer temperature and the elution temperature of the first alkane is about 140°C. *n*-Hexane was used as solvent in all further work for reasons of practicability. That is, C_{19} can be determined without, and C_{17} with some loss.

Optimization of closure of SVE
Obviously, 1-µl splitless injections into GC will cause a vapour cloud at the end of the deposition tip that may be partly spread over the deposition window of the IR detector. It is known from previous GC–cryotrapping-IR experiments that part of this solvent cloud may crystallize on the window, despite the high vacuum [3]. As a consequence, the chromatogram as well as the IR spectra may be obscured by solvent absorption. Similar problems can be expected when applying large-volume injections. In this set-up solvent vapour can reach the IR detector in two ways:

(i) during solvent transfer, via the T splitter; most of the vapour is led to waste through the SVE, but a small part is directed to the IR interface as a result of the vacuum at the end of the transfer line;

(ii) if the SVE is closed too early: solvent that is left in the retention gap and retaining precolumn will reach the IR detector.

In principle, the amount of solvent reaching the IR detector during analyte transfer can be decreased by reducing the transfer time, i.e. by increasing the transfer temperature. However, this option was discarded, since it would result in a loss of more volatile compounds.

The optimal time delay between completion of the transfer and closure of the SVE was established for 100-µl injections of the uneven *n*-alkanes in *n*-hexane. FID was used for this study, since the amount of solvent transferred can not be monitored by the IR detector. The solvent peak width was recorded as a function of the time delay to provide a measure of the amount of solvent transferred to the detector. The solvent peak width did not decrease any further when closing the SVE later than 30 sec after completion of the transfer. With a time delay longer than 30 sec, loss of alkanes, e.g. C_{17} and C_{19} was observed. As no significant difference in the recovery of C_{17} was observed when closing the SVE either immediately after completion of the transfer or 30 sec later, the SVE was always closed with a time delay of 30 sec.

Performance of large-volume injection–GC–cryotrapping-IR

The performance of large-volume injection–GC–cryotrapping-IR in terms of analyte detectability and repeatability was studied for injection volumes of 100–400 µl. The *n*-alkanes and PAHs were used as test compounds.

Repeatability

The repeatability was tested for 100-µl injections of an *n*-alkane standard solution in hexane at the 50 pg/µl level. Quantitation with GC–IR can be accomplished by using the peak height of (i) the Gram Schmidt chromatogram, (ii) the functional-group GC–IR chromatogram and (iii) the strongest band in the IR spectra. The results for the latter two methods are shown in **Table 2**. The relative standard deviation (RSD) was 15% or less (n = 6) for all *n*-alkanes when using the functional-group chromatogram. Significantly higher RSD values were obtained for C_{17} and C_{19} when using the strongest band in the spectrum. This effect can be attributed to variations in the background and background subtraction, and to a somewhat larger discrimination during the transfer.

Table 2
Repeatability of 100-µl injections (n = 6) of *n*-alkanes (50 pg/µl) in GC–cryotrapping-IR.

	RSD (%) for response [a] obtained from	
Alkane	Functional group chromatogram	Highest peak in IR spectra
C_{17}	15	27
C_{19}	13	29
C_{21}	11	15
C_{23}	9	15
C_{25}	8	15

[a] Response obtained from functional-group GC–IR (2820–2980 cm^{-1}) chromatogram and highest peak in IR spectra (2820–2980 cm^{-1} range).

Detection limit

The absolute detection limit of a GC system is determined by the amount of analyte passing through the detector, the sensitivity and noise of the detector and the peak shape of the analyte. In the ideal situation all material injected will reach the detector. Consequently, the detectability of an analyte in an extract can be enhanced with a factor that is directly proportional to the injected volume. It follows that the limit of detection of a total procedure, i.e. sample preparation and separation-cum-detection, can be dramatically improved by injecting a larger portion of the extract. In order to study the analyte detectability with large-volume injection–GC–cyrotrapping–IR, injections of 100-, 200- and 400-µl amounts were compared with that of 1-µl (split 1:10 and splitless).

Using GC–FID, the theoretically expected increase in analyte detectability in concentration units was indeed observed, or, in other words, the absolute detection limits were independent of the injection volume and the injection method used (**Table 3**). It should be noted, that the solvent must be very pure to prevent reduced performance as a result of interfering solvent contaminants in case of large-volume injection.

The situation was marginally less good when using the functional-group GC–IR chromatogram. No problems were observed up to, and including, 100-µl injections, even though some baseline distortion due to solvent contamination was observed for the 100-µl injections (**Figure 2**). A noticeable loss of performance, and, consequently, a modest increase of the absolute detection limits (from 250 to 300 pg) was found with the 200- and 400-µl injections. Actually, during the transfer, the formation of a distinct solvent spot on the

Table 3

Detection limits expressed in concentration units (pg/µl) (S/N = 3) of alkanes and PAHs in GC–cryotrapping-IR and GC–FID using split, splitless and large-volume injection. The numbers given in brackets are absolute detection limits (pg).

Analytes	Detector	Detection limit [pg/µl or (pg)]				
		Split	Splitless	Large-volume injection		
		1 µl (1:10)	1 µl	100 µl	200 µl	400 µl
n-Alkanes	FID	200	20	0.2	0.1	0.05
		(20)	(20)	(20)	(20)	(20)
	IR	2500	250	2.5	1.5	0.75
		(250)	(250)	(250)	(300)	(300)
PAHs	FID	700	70	1	0.5	
		(70)	(70)	(100)	(100)	
	IR	30,000	3,000	90	60	
		(3,000)	(3,000)	(9,000)	(12,000)	

Detection limits were obtained from GC–FID or functional-group GC–IR chromatogram (700–950 cm^{-1} for PAHs and 2820–2980 cm^{-1} for alkanes). Detection limits are average values for all alkanes, and for the PAHs from fluoranthene to benzo[*k*]fluoranthene (peaks 4–9, see Figure 3).

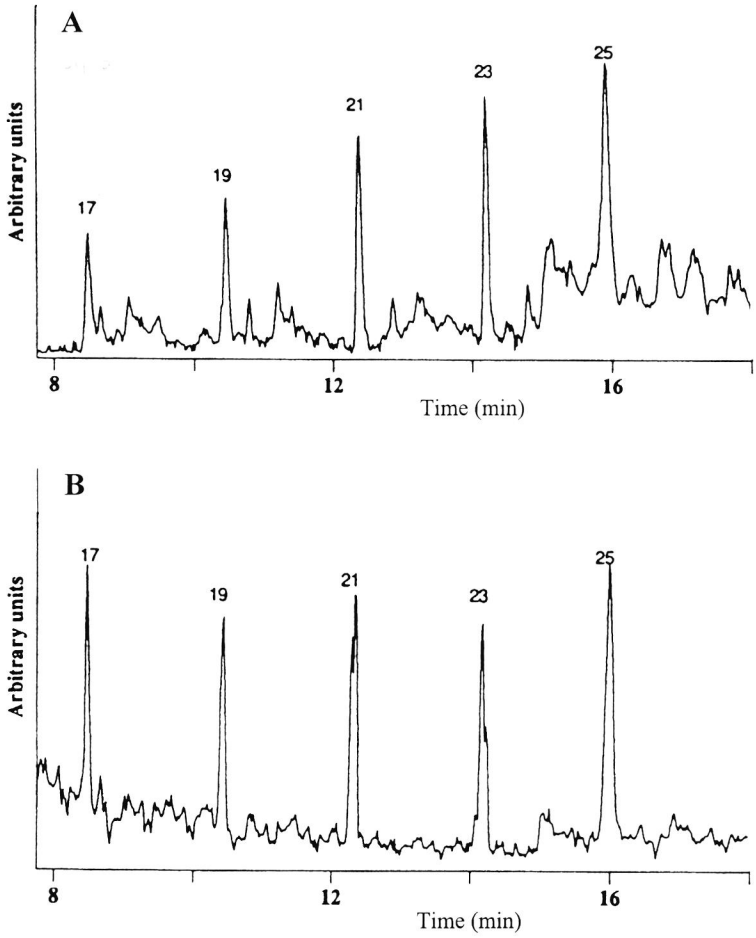

Figure 2
Functional-group GC–IR chromatogram (2820–2980 cm^{-1}) of uneven *n*-alkanes. (A) 100-µl injection of a 10 pg/µl per compound standard solution in hexane, (B) 1-µl splitless injection of a 1000 pg/µl standard solution in hexane.

deposition window was observed (cf. above). As the position of the deposition tip can not be changed during the transfer, 100-µl injections were considered to be most appropriate for routine work. It should be noted that use of the cryotrapping interface might result in some loss of chromatographic resolution. To mention an example, the peak width at half height of nonadecane obtained with a 1-µl splitless injection of a 5 ng/µl standard solution was 2 sec with GC–FID and 5 sec with GC–cryotrapping-IR.

As the data included in Table 3 show, somewhat larger problems were encountered with the PAHs. Still, the overall picture is highly encouraging. With GC–FID, the gain in analyte detectability expressed in concentration units effected by going from split to 200-µl injections was 1,500-fold rather than the theoretical 2,000-fold, or, in other words, the absolute detection limits increased some 50%. The reduced performance was attributed to somewhat broader peaks with large-volume injections than with split injection. After

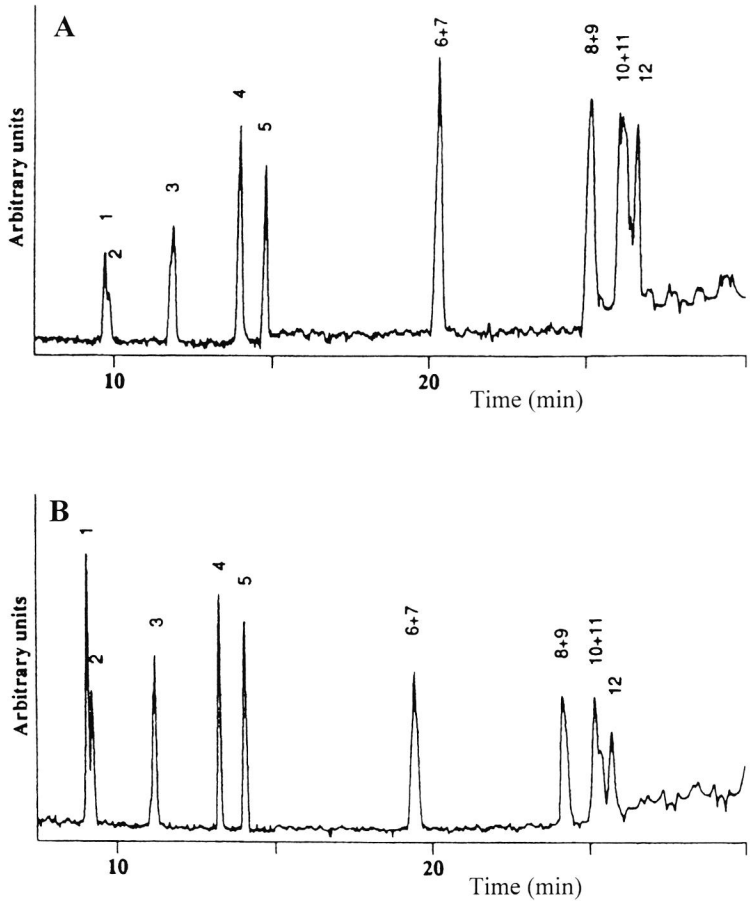

Figure 3

Functional-group GC–IR chromatogram (700–950 cm^{-1}) of PAHs. (A) 100-µl injection of a 600 pg/µl per compound standard solution in hexane; (B) 1-µl splitless injection of a 60,000 pg/µl standard solution. Peak assignment: 1, phenanthrene; 2, anthracene; 3, 1-methylphenanthrene; 4, fluoranthene; 5, pyrene; 6, benz[*a*]anthracene; 7, chrysene; 8, benzo[*b*]fluoranthene; 9, benzo[*k*]fluoranthene; 10, benzo[*e*]pyrene; 11, benzo[*a*]pyrene; 12, perylene. Phenanthrene, anthracene and 1-methylphenanthrene were partly lost with the 100-µl injection (A).

injection the analytes are spread over the retention gap prior to refocusing by the phase-ratio effect [21]. If the retention gap displays some retention towards the PAHs due to the presence of active places on the inner wall or the surface of the deactivation layer, peaks will be somewhat broadened already at the start of the separation in the analytical column.

As was to be expected, detecting PAHs by means of GC–IR was less straightforward than that of the *n*-alkanes. A larger wavenumber interval (700–950 cm^{-1}) had to be taken for the functional-group chromatogram while the detector noise in this region is relatively high. Besides, the extinction coefficients of the aromatic C–H out-of-plane absorption bands are smaller. Additionally, it should be noted that at the time of this study the obtained absolute

detection limit for split/splitless injections of PAHs were somewhat worse than those reported earlier [3]. This has to be attributed to a decrease in performance of the IR detector.

As regards GC–IR of the PAHs, the justified concern about the ca. 4-fold loss in absolute analyte detectability is distinctly outweighed by the impressive 500-fold gain effected by using a 200-µl rather than a split injection (Table 3). As regards the somewhat deteriorated performance, next to some decrease in retention gap performance, the higher water background in the large-volume injection system is a plausible explanation. As reported earlier, the performance of GC–cryotrapping-IR is very sensitive to traces of water and this effect is particularly apparent if the analytes absorb in the same wavelength region as ice [3, 22]. This is the case in the PAH-specific region of 700–950 cm^{-1}. In the present set-up, the press-fit connections and the six-port valves appeared to be the most critical items.

It should be added that the detection limits reported for the PAHs in Table 3 were calculated on the basis of the data for fluoranthene to benzo[*k*]fluoranthene (peaks 4–9 in **Figure 3**). The detection limits for benzo[*e*]pyrene, benzo[*a*]pyrene and perylene are about 2–3-fold higher than for these PAHs irrespective of the injection mode used. This is due to some peak broadening at high retention times and the higher background caused by column bleeding. Consequently, the gain in analyte detectability achieved upon going from splitless to large-volume injection was the same as for the earlier eluting compounds.

The detection limits of most PAHs were found to be around 10-fold better when quantifying by means of a peak in the IR spectrum rather than by the peak in the functional-group chromatogram. To quote an example, the detection limit of fluoranthene for a 100-µl injection was 10 pg/µl for the strongest peak in the spectrum (**Figure 4**), while it was 100 pg/µl when using the functional-group chromatogram (Figure 3A).

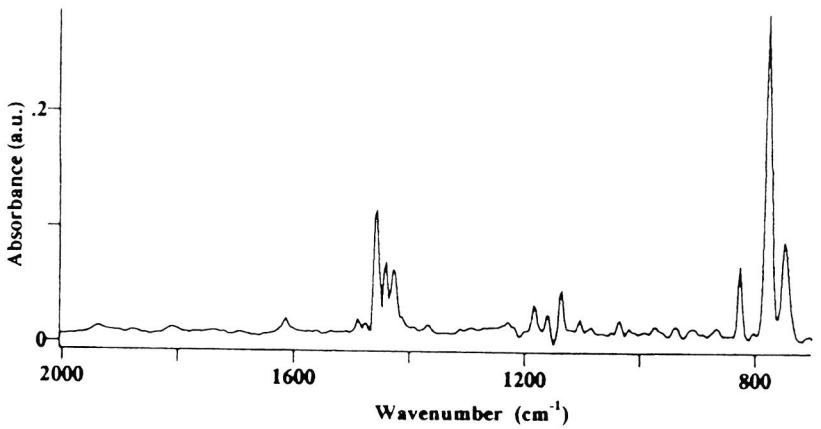

Figure 4
GC–cryotrapping-IR spectrum of fluoranthene obtained with a 100-µl injection at the 600 pg/µl level.

Micro-LLE/GC–cryotrapping-IR

The practical usefulness of GC–cryotrapping-IR with 100-µl injections was demonstrated by the off-line combination with micro-LLE. 1 l of river Rhine water, sampled at Lobith, Netherlands, September 5, 1994, and spiked with PAHs at the 0.5 µg/l level, was extracted twice with 0.6 ml *n*-hexane which resulted in 1 ml of extract. The sample preparation was simple and rapid, since it only involved micro-LLE with no further need of evaporation of part of the solvent.

All PAHs showed up in the functional-group GC–IR chromatogram (700–950 cm^{-1}) (**Figure 5**A) with recoveries between 80 and 90% when using the absorbance of the strongest peak in the spectra. Characteristic IR spectra of all PAHs were obtained, as is illustrated for the isomers benzo[*a*]pyrene and benzo[*e*]pyrene in **Figure 6**. Although these compounds were not completely separated in the functional-group GC–IR chromatogram (Figure 5A), interference-free IR spectra were obtained from the wings of the GC peaks (Figures 6A and C). The significant differences between the IR spectra of both isomers clearly demonstrate the potential of GC–cryotrapping-IR in the identification of molecules with closely related structures. Besides, the acquired GC–IR spectra could easily be identified using a library with reference cryotrapped spectra (Figures 6B and D). The GC–cryotrapping-IR spectra were also found to closely resemble reference spectra obtained with the conventional KBr pelleting technique. This endorses earlier conclusions on the usefulness of standard libraries for the identification of cryotrapped spectra [3, 22].

Detection limits for the PAHs in the river water sample were determined at 0.1–0.25 µg/l for fluoranthene, pyrene, benz[*a*]anthracene and chrysene (PAH peaks 4–7 in Figure 5), and around 0.4 µg/l for benzo[*b*]fluoranthene, benzo[*k*]fluoranthene, benzo[*e*]pyrene benzo[*a*]pyrene and perylene (PAH peaks 8–12 in Figure 5), despite the fact that the baseline

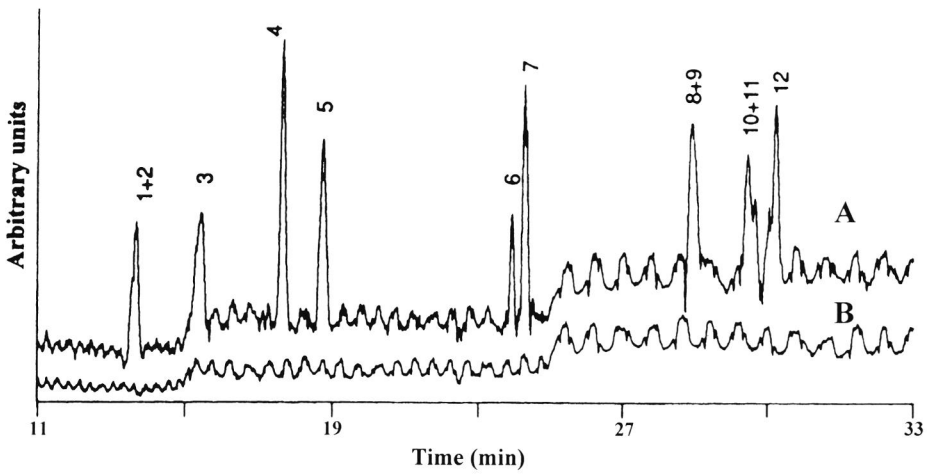

Figure 5
Functional-group GC–IR chromatogram (700–950 cm^{-1}) obtained after injection of a 100-µl aliquot (10%) of a hexane extract obtained with micro-LLE of 1 l of river Rhine water (A) spiked at the 0.5 µg/l level and (B) non-spiked. For peak assignment, see Figure 3.

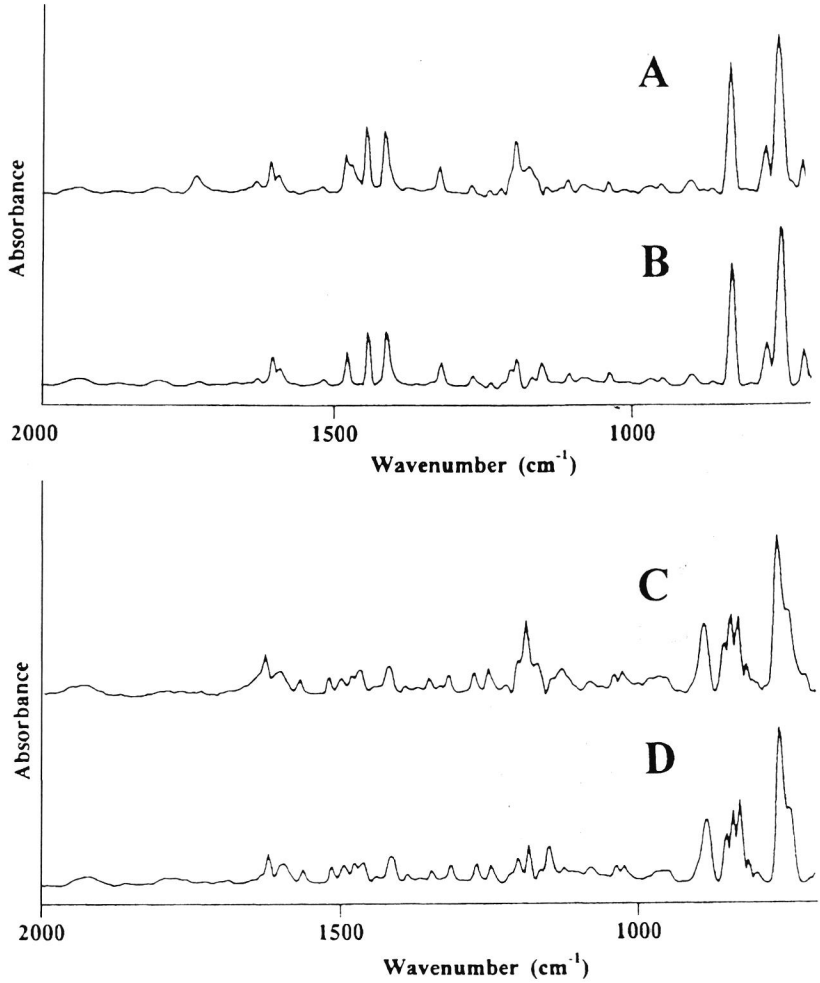

Figure 6
IR spectra of benz[*e*]pyrene (A) and benz[*a*]pyrene (C) from the spiked river Rhine water extract (Figure 5A, peaks 10 and 11, respectively). For comparison, the library spectra are added (B, D).

of the functional-group GC–IR chromatogram showed some distortion due to a water background (cf. Figure 5). Detection limits were again about 10-fold better when using spectra instead of functional-group chromatograms. PAHs were not detected in the unspiked river water, neither in the functional-group chromatogram (Figure 5A) nor in the spectra acquired by extended post-run scanning at the appropriate retention times. This example demonstrates that it is possible to detect microcontaminants with GC–cryotrapping-IR not only below the alert level of 1 μg/l for river water but even down to the maximum allowed level of 0.1 μg/l in drinking water.

6.1.4 Conclusions

Large-volume injection by means of a loop-type interface can be carried out successfully in conjunction with GC–cryotrapping-IR. The hyphenation permits enhanced detectability of analytes by about two orders of magnitude compared to conventional split/splitless GC–cryotrapping-IR. Injected volumes of 100 µl prove to be most appropriate. Injection of larger amounts causes interfering solvent crystallization, inherent to the principle of trapping the GC eluate at cryogenic temperatures. More effective solvent elimination techniques should reduce this drawback and are discussed in Chapter 6.2.

Optimization of the experimental set-up is relatively simple but the system is sensitive to traces of water. Small leaks turned out to be highly detrimental; in this respect, press-fit connections and six-port valves are the most critical parts.

For *n*-alkanes concentration levels of 2.5 pg/µl can be determined when using 100-µl injections and on-the-fly detection. The increase in analyte detectability for the PAHs was smaller than for the alkanes, due to reduced instrument performance and ice interference. Still, 30–500 fold improvements for 100–200-µl injections compared with 1-µl split (1:10) and splitless injections were readily achieved. The repeatability for 100-µl injections was satisfactory with RSD values of 10–20% (n = 6) at the 50 pg/µl level.

The applicability of large-volume injection GC–cryotrapping-IR to real-life analysis is promising. As demonstrated, the determination and identification of PAHs in river water is possible down to a level of 0.5 µg/l, even when using simple micro-LLE as sample preparation technique. The IR-spectra obtained match well with those of standard libraries, which facilitates identification and unambiguous discrimination of isomers. The present system may therefore be considered a viable approach to trace-level environmental analysis. Research directed at setting up a fully on-line SPE–GC–cryotrapping-IR system is reported in Chapter 6.2, and a number of real-life studies are described which convincingly demonstrate this claim.

References

[1] *EEC drinking water guidelines, 80/779/EEC, EEC No. L229/11-29,* EEC, Brussels, August 30, 1980.
[2] N.R. Smyrl, D.M Hembree, W.E. Davis, D.M. Williams and J.C. Vance, *Appl. Spectrosc.*, 46 (1992) 277.
[3] T. Visser, M.J. Vredenbregt and A.P.J.M. de Jong, *J. Chromatogr. A*, 687 (1994) 303.
[4] R.P. Griffiths, *Science*, 222 (1983) 297.
[5] J.W. Childers, N.K. Wilson, R.L. Harless and R.K. Barbour, *Chemosphere*, 25 (1992) 1285.
[6] P.R. Griffiths, *Appl. Spectrosc.*, 31 (1977) 284.
[7] G.T. Reedy, D.G. Ettinger, J. Schneider and S. Bourne, *Anal. Chem.*, 57 (1985) 1602.
[8] K.H. Shafer and P.R. Griffiths, *Anal. Chem.*, 58 (1986) 3254.
[9] P. Jackson, G. Dent, D. Carter, D.J. Schofield, J.M. Chalmers, T. Visser and M. Vredenbregt, *J. High Resolut. Chromatogr.*, 16 (1993) 515.
[10] K. Grob, D. Fröhlich, B. Schilling, H.-P. Neukom and P. Nägeli, *J. Chromatogr.*, 295 (1984) 55.
[11] K. Grob and J.-M. Stoll, *J. High Resolut. Chromatogr.*, 9 (1986) 519.
[12] H.G.J. Mol, H.-G. Janssen, C.A. Cramers and U.A.Th. Brinkman, *J. High Resolut. Chromatogr.*, 18 (1995) 19.
[13] S. Ramalho, Th. Hankemeier, M. de Jong, U.A.Th. Brinkman and J.J. Vreuls, *J. Microcol. Sep.*, 7 (1995) 383.
[14] J.F. Hiller, T. McCabe and P.L. Morabito, *J. High Resolut. Chromatogr.*, 16 (1993) 5.

[15] H.G.J. Mol, H-G. M. Janssen, C.A. Cramers, J.J. Vreuls and U.A.Th. Brinkman, *J. Chromatogr. A*, 703 (1995) 277.
[16] P.L. Morabito, T. McCabe, J.F. Hiller and D. Zakett, *J. High Resolut. Chromatogr.*, 16 (1993) 91.
[17] A.J. Fehl and C. Marcott, *Anal. Chem.*, 58 (1986) 2578.
[18] H. Hu, M. Zhu, Y. He and K. Sun, *J. Chromatogr.*, 547 (1991) 494.
[19] G. Full, G. Krammer and P. Schreier, *J. High Resolut. Chromatogr.*, 14 (1991) 160.
[20] D.A.J. Murray, *J. Chromatogr.*, 177 (1979) 135.
[21] K. Grob Jr., G. Karrer, M.-L. Riekkola, *J. Chromatogr.*, 334 (1985) 129.
[22] T. Visser and M.J. Vredenbregt, *Vibr. Spectrosc.*, 1 (1990) 205.

6.2 On-line SPE–GC–cryotrapping-IR for the trace level determination of microcontaminants in aqueous samples

Summary

A large-volume on-column GC–cryotrapping-IR system was developed for injections of up to 100 µl of organic extracts. Considerable reduction of the solvent-and-water background and enhanced analyte detectability was achieved by using a column-switching device between the GC column and the IR detector and improving the leaktightness of the system.

The system was combined with solid-phase extraction (SPE) to yield on-line SPE–GC–IR. With this set-up, sample volumes of only 20 ml sufficed to detect, and identify, microcontaminants in tap and surface water at the 0.1–1 µg/l level. Detection limits were on the order of 15 ng/l for tap water when using appropriate functional-group chromatograms. Or, in other words, SPE–GC–IR is a suitable technique for the screening of environmental water samples for functional groups, i.e. classes of compounds, of interest.

6.2.1 Introduction

Sensitivity is a crucial point when applying gas chromatography (GC) with infrared (IR) detection as a tool in environmental analytical chemistry. Coupling of GC and IR is generally achieved by using a light-pipe interface [1]. This interface is easy to handle, but has a rather limited sensitivity with detection limits of typically 10–100 ng on-column. Sensitivity can be increased by using a sample storage interface such as cryotrapping; the GC effluent is immobilized on a ZnSe window at 80 K and IR detection is carried out immediately after deposition (on-the-fly) [2–4]. Post-run scanning after completion of the GC run further improves the sensitivity to an analyte detectability of 0.1–1 ng on-column [5]. However, the interface is rather sensitive to disturbances like an ice background due to the presence of water or solvent crystallization [5].

The analyte detectability (in concentration units) can be further increased by making more efficient use of the sample extract, i.e. by injecting 100 µl rather than the conventional 1–5 µl [6, 7]. In the most efficient set-up, the total extract is transferred to the GC system. To quote an example, in on-line SPE–GC (SPE, solid-phase extraction) the complete SPE desorption solvent volume of about 100 µl is transferred to the GC system [8, 9].

Recently, we developed a large-volume injection–GC–cryotrapping-IR system based on loop-type interfacing [10]. The results were promising and a 30–500-fold increase of sensitivity was obtained. However, two problems adversely affecting the spectral quality and detection limits were encountered: (i) an relatively high ice background and (ii) interferences due to solvent crystallization. The latter problem was also encountered with 1-µl splitless injections [5]. A drawback of the set-up was the loss of some more volatile analytes, as was to be expected when using a loop-type interface [11]. By using an on-column interface, the application range can be extended to more volatile analytes [12]. The ice background can be reduced by eliminating leaks due to press-fit connections and six-port valves. The solvent vapour can be eliminated by using a column-switching device or an open-split interface between the GC column and the GC detector [13–18].

The aim of this study was to develop solutions as suggested above and to design a robust large volume injection–GC–IR system using an on-column interface. Regarding the set-up of the column-switching device, we aimed at a fully inert transfer and at preventing any trace of solvent to reach the detector. Therefore, a coaxial rather than a perpendicular flow system and an inert all-glass flow path were preferred. However, the coaxial open-split interfaces reported [13, 18] were designed for mass spectrometric detection and not to meet the more demanding requirements of cryotrapping IR, i.e. complete removal of solvent and no water background at all. Therefore, a new design was developed. In addition, the leaktightness of the total system was optimized. The second goal was to use the developed system for the on-line SPE–GC–IR determination of microcontaminants in tap and harbour water at the 0.1–1 µg/l level. To promote the overall efficiency of the procedure, 20 ml of sample were preconcentrated on an SPE cartridge, which was brought to the GC–IR facility and there on-line desorbed with 100 µl of organic solvent into the GC–IR.

6.2.2 Experimental

Chemicals

Ethyl acetate (Nanograde, Mallinckrodt) was purchased from Promochem (Wesel, Germany). HPLC-grade water (J.T. Baker, Deventer, The Netherlands) was used to condition and clean-up the SPE cartridge. Diethylphthalate (Merck-Schuchardt, Darmstadt, Germany), caffeine (Sigma-Aldrich, Zwijndrecht, The Netherlands), atrazine, diazinon, metolachlor, simetryn, sulfotep and triazophos (all Petanal-grade, Riedel-de Haën, Seelze, Germany) were used as test compounds. Stock solutions of 1 mg/ml were stored in the dark at 4°C. A mixture of 50 µg/ml was diluted to a concentration of 0.2 µg/ml for large-volume injections, and to 0.1 and 1 µg/ml for spiking of the water samples. A stock solution containing decane, undecane, dodecane, tridecane, tetradecane, pentadecane, heptadecane, octadecane, nonadecane and eicosane (all alkanes from Polyscience Cooperation and purchased from Chrompack, Middelburg, The Netherlands) was prepared in ethyl acetate at a concentration of about 20 µg/ml per compound. The stock solution was diluted to a concentration of 0.2 µg/ml in ethyl acetate or *n*-hexane for optimization of the large-volume injections. Helium 4.0 was purchased from Hoekloos (Schiedam, The Netherlands) and used as carrier gas.

GC–IR system

GC equipment

The experimental set-up is schematically depicted in **Figure 1.** A Carlo Erba MEGA 5160 gas chromatograph (Carlo Erba Strumentazione, Milan, Italy) equipped with a split/splitless injector, an on-column injector and a flame ionization detector was used. For the on-column interface a 1/16 inch Swagelok T-piece replaced the original on-column injector, as the latter was found to be less reliable regarding leaktightness. The helium line coming from the pressure regulator of the original on-column injector was connected to the T-piece. The head pressure was 60 kPa. The sample was transferred by an automated syringe pump (Harvard Apparatus 22, So. Natick, MA, USA) pump via a Rheodyne (Cotati, CA, USA) 6-port valve and the transfer line into the GC. The transfer line, which was permanently mounted on the T-piece, was inserted into a 3 m x 0.53 mm I.D. DPTMDS-deactivated retention gap (BGB Analytik, Zürich, Switzerland). An early solvent vapour exit (SVE) was placed between the retention gap and the analytical column. For this purpose, another 1/16 inch Swagelok (Solon, OH, USA) T-piece was used to insert the analytical column 5 mm into the retention gap. A 70 cm x 0.25 mm I.D. fused silica capillary connected the T-piece with a Rheodyne HPLC 6-port valve just outside the GC oven. This capillary was connected to a 50 cm x 50 µm I.D. restriction in one position, and to a short metal capillary with 1 mm I.D. in the other. The restriction itself was placed close to the hot split/splitless injector to prevent condensation of solvent vapour. The 25 m x 0.25 mm I.D. HP5MS (Hewlett Packard, Waldbronn, Germany) analytical column was connected to the column-switching device.

Column-switching device

The column-switching device is schematically represented in the top half of Figure 1. It consisted of a 1/16 inch Swagelok T-piece (T) and X-cross (X), metal capillaries of 0.25 mm I.D. (between T and R3, and between X and R1), fused silica restrictions of 50 µm I.D. (R1

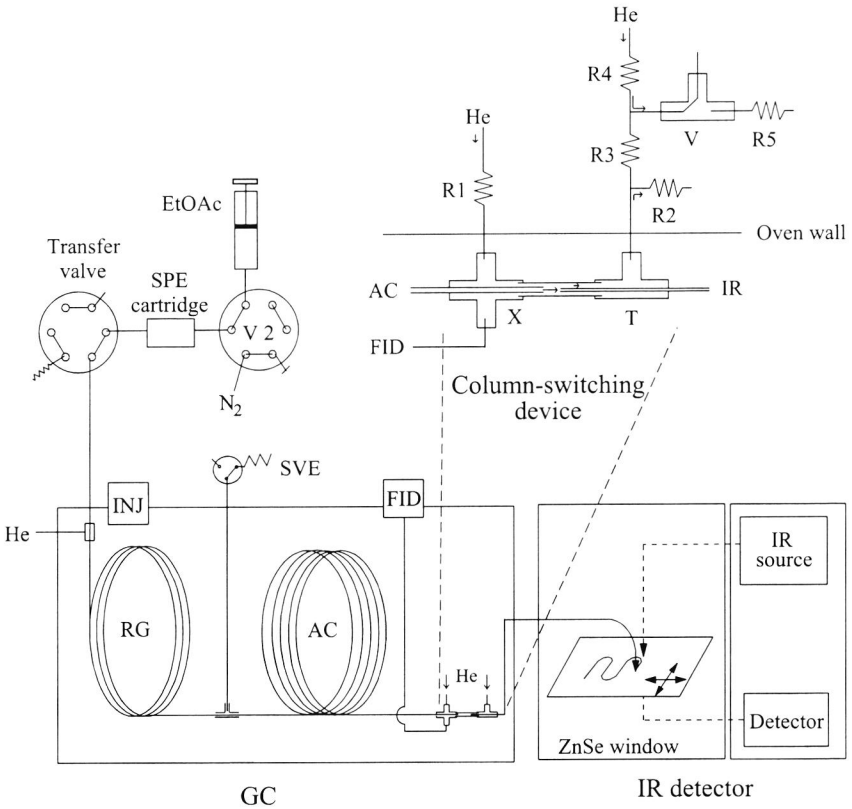

Figure 1

Set-up of the on-line SPE–GC–cryotrapping-IR system. The HPLC 6-port valves are shown in the position for injection into GC or desorption of the SPE cartridge into the GC. The insert shows the column-switching device. The gas valve V is shown in the position for transfer of the column effluent to the IR detector. Abbreviations: AC, analytical column; EtOAc, ethyl acetate; He, helium; INJ, standard on-column injector; N_2, nitrogen; RG, retention gap; R1–R5, restrictions; SVE, solvent vapour exit; T, T-piece; V2, sample HPLC 6-port valve; V, switching gas valve; X, cross piece.

and R5) and 100 μm I.D. (R2, R3 and R4) and a 24 V solenoid valve (V). The connection between the X-cross and the FID was by 70 cm of a 0.25 mm I.D. deactivated fused silica capillary. T and X were connected via a 70 mm x 0.53 mm I.D. metal capillary internally coated with a DB-PS1 film of 0.15 μm thickness (J&W, Folsom, CA, USA). The transfer line to the IR detector (1 m x 0.15 mm I.D. deactivated fused silica; Bio-Rad, Cambridge, MA, USA) and the analytical column were inserted via T and X, respectively, into this capillary and held at a distance of 5 mm from each other. A piece of metal tubing was welded on the T-piece and the X-cross to fix their positions in the GC oven. All connections to the T-piece and X-cross were tightened by means of laboratory-made silver ferrules and Swagelok pieces and nuts. This was also the case for the T-pieces of the on-column interface and SVE. The connections outside the GC oven were tightened by standard Vespel/Graphite (90/10) ferrules. The purge flow through capillary R2 was checked by holding the capillary into a solvent and checking the flow of bubbles.

IR spectrometry

The infrared spectrometer was a Digilab FTS-40 Fourier transform instrument (Bio-Rad) equipped with a Digilab Tracer cryotrapping GC interface [2]. Data acquisition and processing was performed with a Bio-Rad SPC 3200 computer. The column-switching device was connected to the IR detector by a transfer line using aluminum ferrules. The transfer line was guided into the interface housing through a stainless-steel pipe. The interface housing was held at $1.3 \cdot 10^{-5}$ Pa to minimize condensation of compounds present in the ambient air. A fused-silica deposition tip of 150 μm I.D. was fixed to the end of the transfer line and located 30 μm above the surface of a moving IR-transparent ZnSe window, which was cooled to 80 K with liquid nitrogen. The tip and the transfer line were kept at 275°C.

Eluting compounds were trapped as solids on the ZnSe window. The window was continuously moved by an X–Y stepping motor. A few seconds after deposition the trapped spots passed through the beam of an IR microscope and were scanned on-the-fly by averaging four spectra recorded at 2 scans/sec. After completion of the GC run extended post-run scanning of certain retention times of the immobilized chromatogram was performed by repositioning the corresponding coordinates of the ZnSe window into the IR beam. Post-run spectra were acquired by averaging 256 scans. The data point resolution of on-the-fly and post-run spectra was 4 cm^{-1}.

GC–IR chromatograms of the integrated IR absorption as a function of the retention time were constructed by standard Gram–Schmidt vector orthogonalization. Several functional-group GC–IR chromatograms of preselected wavenumber regions (2820–2980 cm^{-1}, 1640–1670 cm^{-1}, 1520–1580 cm^{-1} and 1000–1050 cm^{-1}) were used to enhance selectivity and, consequently, analyte detectability [5].

Large-volume injections

Two types of injections were used, (i) large-volume injections of a sample by means of a syringe and (ii) desorption of an SPE cartridge with 100 μl of ethyl acetate. In the first case, the syringe pump replaced the SPE cartridge at the transfer valve. The 250-μl syringe was filled and inserted into the syringe pump. Next, the line to the transfer valve was flushed, the SVE opened and the column-switching device switched to direct the GC effluent to the FID. The transfer valve was switched so that the sample was introduced via the transfer line into the retention gap at, typically, 125 μl/min. The oven temperature during the injection was the boiling point of the solvent used under normal pressure, i.e. for ethyl acetate, 77°C and for *n*-hexane, 68°C. The SVE was closed 3 sec after the end of the injection and the solvent peak monitored with the FID. At the end of the solvent peak, the GC oven temperature programme and the data acquisition was started and, after a further 30 sec, the column-switching device was switched to direct the GC effluent to the IR detector. The oven temperature was programmed from the injection temperature to 290°C at 10°C/min and finally held at 290°C for 10 min.

The injection rate for large-volume injections was optimized by injection of a mixture of ten *n*-alkanes starting with C_{10}. Subsequent injections were carried out at increasing injection rates at a constant injection temperature until the volatile analytes starting with C_{10} were quantitatively recovered in the chromatogram without visible peak deformation [19]. The FID detector was used for optimization.

Preconcentration and on-line desorption of SPE cartridges

The water samples were preconcentrated on commercial 10 mm x 2 mm I.D. cartridges packed with 20 μm, 100 Å PLRP-S styrene–divinylbenzene copolymer (Spark Holland, Emmen, The Netherlands). The SPE preconcentration of the aqueous samples was automated by using a Prospekt sample preparation system (Spark Holland) as described in Chapter 3.1. After conditioning the SPE cartridge with 2 ml of methanol and 2.5 ml of HPLC-grade water, 20 ml of sample were loaded at 2.5 ml/min. Clean-up to remove salts and very polar compounds was effected by flushing the SPE cartridge with 2 ml of HPLC-grade water. Next, the SPE cartridge was dried for 5 min at a nitrogen flow of 70 ml/min at ambient temperature.

For analysis, the preconcentrated SPE cartridge was inserted in a laboratory-made cartridge holder between the transfer valve and an additional Rheodyne 6-port HPLC-valve V2 (Figure 1). The cartridge was dried for a further 10 min with a nitrogen flow of 80 ml/min at ambient temperature. In the meantime, the SVE was opened, the 250-μl syringe was filled with ethyl acetate, placed in the syringe pump and, subsequently, the tubing up till valve V2 was flushed. The pump was started and the transfer valve and valve 2 were simultaneously switched to desorb the analytes into the GC with 100 μl of ethyl acetate at a flow rate of 125 μl/min. After 73 sec (the time required to fill the empty tubing and SPE cartridge with solvent, and then to transfer 100 μl), the transfer valve was switched again and the solvent peak was monitored as described above.

6.2.3 Results and discussion

Prior to testing the potential of on-line SPE–GC–IR, the design and performance of the column-switching and large-volume injection interfaces had to be optimized, i.e. the ice background and interferences due to solvent crystallization observed in an earlier study, had to be overcome by improving the set-up.

Column-switching device

The aim of the column-switching device was to enable direction of the GC effluent either to the IR detector or quantitatively to the FID in order to prevent the transfer of solvent to the IR detector. In addition, a set-up was desired in which almost each connection can be exchanged without having to disassemble the whole system.

The developed flow-controlled column-switching device is shown in Figure 1. In the position shown in Figure 1 the column effluent and some helium make-up gas (via R1) are transferred for the main part to the IR via the transfer line (about 1 ml/min) and for a small part purged through restriction R2. If the flow exiting from the analytical column is higher than the flow to the IR and the purge through R2, a part of the GC effluent is directed to the FID. Directing the GC eluent completely to the FID is achieved by switching valve V into the other position so that a helium flow of 4.9 ml/min is directed via R3 and T to X. As a result, only helium will enter the IR detector. The efficiency of the system was tested with conventional 1-μl splitless injections; when directing the solvent vapour to the FID during elution of the solvent peak, no solvent background was observed when performing parallel

data acquisition with the IR detector. The set-up was found to be a significant improvement over the original one, where even a 1-µl splitless injections lead to solvent condensation on the ZnSe window [5, 10].

As mentioned above, it is very important to have leaktight connections. Leaks could easily be located by using acetone and monitoring the FID signal or the IR detector pressure. Several possibilities of making the connections within the GC oven were tested. Home-made silver ferrules and Swagelok connections proved to be leaktight for long periods of time. With other types of connections and Vespel ferrules leakage was observed after a few runs. A solenoid valve in the purge flow appeared to be sensitive to leakage of water vapour, too. For that reason, such a valve was not used in the flow path to the IR detector. In the final set-up, the water background of the IR detector was found to be within the specifications of the unmodified GC–IR instrument (i.e., less than 0.02 absorption units).

On-column large-volume injection interface

The use of the standard on-column injector on the GC appeared to be attended with the introduction of a relatively high amount of water. Therefore, a new on-column interface was constructed by using a Swagelok T-piece equipped with home-made silver ferrules for connections (cf. Figure 1). Due to the presence of the column-switching device, optimization of the SVE closure time was no longer critical. The SVE was closed at the end of the injection and the column effluent was monitored with the FID. When passage of the solvent peak had been registered by the FID, the GC effluent was directed to the IR detector and data acquisition was started.

The only parameter which had to be optimized for large-volume injections was the injection rate. Optimization was achieved by injections of *n*-alkanes and using FID detection as described above (cf. Section *Large-volume injection* above and [19]). When injecting C_{10}–C_{20} in *n*-hexane, all *n*-alkanes from C_{10} were recovered quantitatively. This is a distinct extension of the application range compared to the earlier set-up using a loop-type interface, where only *n*-alkanes from C_{19} could be recovered quantitatively [10].

Interfering absorptions due to ice formation caused by water or solvent condensation were not observed during the many injections performed. This is a significant improvement of the robustness of the system and the sensitivity.

Screening of microcontaminants by SPE–GC–IR

The potential of the system was tested by screening microcontaminants in tap and Rotterdam harbour water spiked at levels of 1.0 and 0.1 µg/l. 20 ml of aqueous sample were preconcentrated on a 10 x 2 mm I.D. SPE cartridge. Next, the SPE cartridge was transported to the IR laboratory and inserted into the SPE–GC–IR system (cf. above). After 10-min drying with nitrogen at ambient temperature, the cartridge was desorbed with 100 µl of ethyl acetate directly into the GC–IR system.

In the tap water sample spiked at the 1.0 µg/l level, all analytes were detected in the Gram–Schmidt GC–IR chromatogram (**Figure 2**). The recoveries were 80–110% for all microcontaminants except caffeine (20%; due to breakthrough during sample enrichment because of its high polarity [20]). The sensitivity with which a compound can be detected in a Gram–Schmidt GC–IR chromatogram is mainly determined by the summed absorption, and

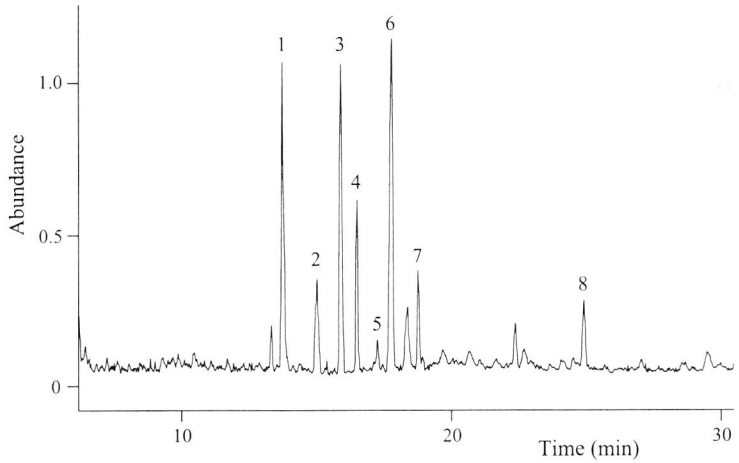

Figure 2
On-line SPE–GC–IR analysis of 20 ml tap water spiked at the 1.0 µg/l level with several microcontaminants. The Gram–Schmidt chromatogram is shown. Peak assignment: 1, diethylphthalate; 2, sulfotep; 3, atrazine; 4, diazinon; 5, caffeine; 6, simetryn; 7, metolachlor; 8, triazophos.

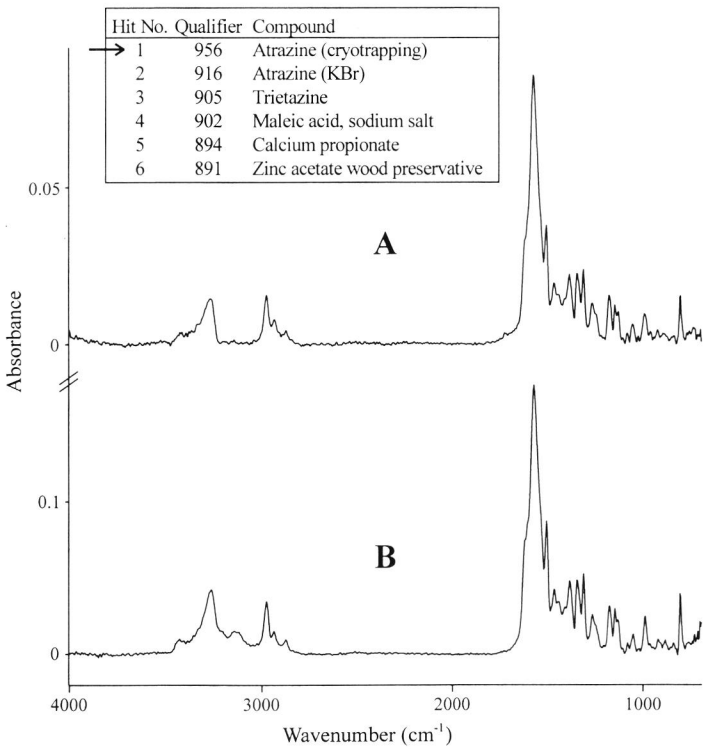

Figure 3
(A) IR spectrum taken at apex of peak No. 3 of Figure 2. (B) Library cryotrapping spectrum of atrazine. The insert shows the hit list of the library search; match qualifier on a scale of 1000; all spectra except for the first hit are KBr standard spectra.

thus by the sum of the absorption coefficients in the 700–4000 cm^{-1} region. This explains the different peak heights and areas of the test compounds (except caffeine due to its low recovery). The IR spectra corresponding with the eight peaks could all be identified by library search using the Euclidean distance algorithm and a library of cryotrapping and KBr standard spectra (first on hit list in all cases). The result for atrazine is shown as an example in **Figure 3**.

With tap water that was spiked at the 0.1 µg/l level with the same eight microcontaminants, the peaks in the Gram–Schmidt GC–IR chromatogram self-evidently were less pronounced. However, an attractive feature of IR detection is the use of so-called functional-group chromatograms, which can be recorded simultaneously with the Gram–Schmidt chromatogram. These chromatograms can be used to monitor compounds with a structural element absorbing in a specific wavenumber region and, thus, improve selectivity. When using this approach, the results indeed improved considerably and all contaminants except caffeine (again, low SPE recovery) could be detected. As an example, **Figure 4** shows the 1520–1580 cm^{-1} chromatogram of the region which is correlated with the C=N structural features of triazines. Only two major peaks, atrazine and simetryn (Nos. 3 and 6), showed up; their detection limits were about 15 ng/l. The much smaller peak at 15.85 min and the very small peak at 17.75 min can be assigned to the organophosphorus pesticides diazinon and triazophos, which also have a C=N bond. The high noise level of the 'on-the-fly' spectra of

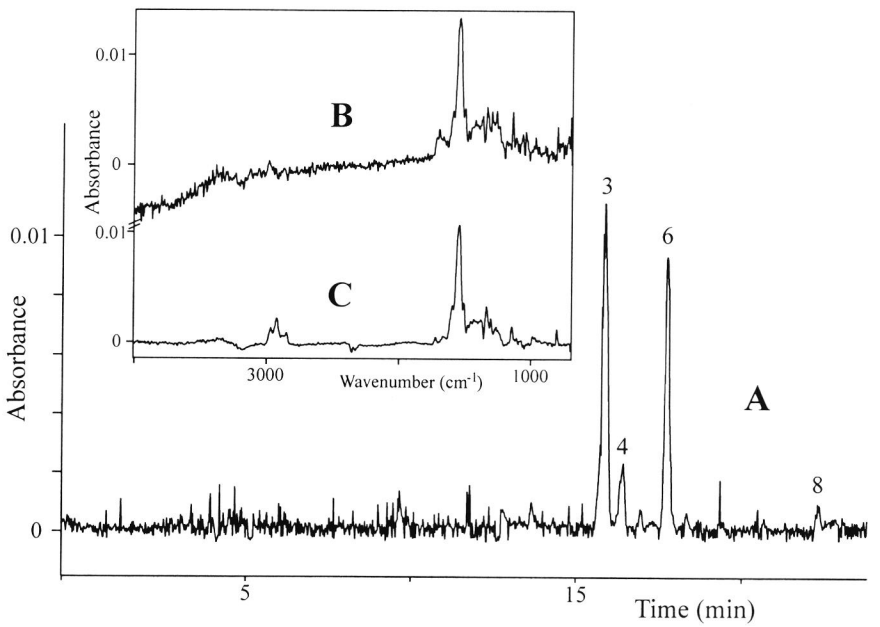

Figure 4
On-line SPE–GC–IR analysis of 20 ml tap water spiked at the 0.1 µg/l level with several microcontaminants. (A) The functional-group (1520–1580 cm^{-1}) chromatogram and (B) 'on-the-fly' IR spectrum of peak No. 6 are shown. The spectral quality could be improved by extended post-run acquisition (256 scans) (C), and the compound identified as simetryn. For peak assignment, see Figure 2.

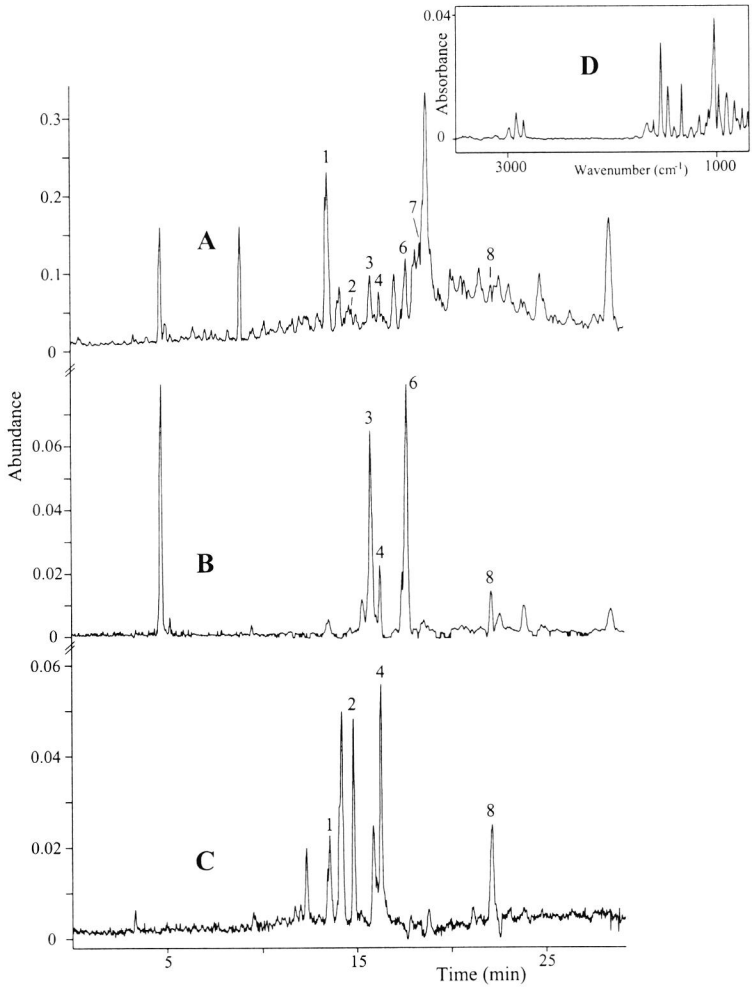

Figure 5
On-line SPE–GC–IR analysis of 20 ml harbour water spiked at the 1.0 µg/l level with several microcontaminants. The (A) Gram–Schmidt, two functional-group chromatograms, (B) (1520–1580 cm^{-1}) and (C) (1000–1050 cm^{-1}), and the (D) 'post-run' IR spectrum of peak No. 8 (triazophos) are shown. For peak assignment, see Figure 2.

analytes at the 0.1 µg/l level (Figure 4B) hampered direct identification by a library search. However, the spectral quality was considerably improved by post-run acquisition of the immobilized chromatogram, and the spectrum of e.g. peak No. 6 (Figure 4C) now could easily be identified by library search as simetryn.

As another application, 20 ml of Rotterdam harbour water spiked at the 1 µg/l level were analysed. Because of the chemical noise which is, of course, much higher for harbour water than for tap water, the spiked microcontaminants do not show up too clearly in the Gram–Schmidt chromatogram (**Figure 5**A) [the large peak No. 1 was due to presence of diethylphthalate in non-spiked sample]. However, by selecting the appropriate functional-

group chromatograms, all microcontaminants but caffeine could be clearly detected. Figures 5B and 5C illustrate the selective detection of triazines (1520–1580 cm^{-1}) and organophosphorus pesticides (1000–1050 cm^{-1}), respectively. Despite the complexity of the matrix, the IR spectra obtained after extended post-run acquisition were of good quality. An example is given in Figure 5D.

6.2.4 Conclusions

The present large-volume on-column GC–cryotrapping-IR system allows the injection of 100 µl of organic extracts. Due to the use of a column-switching device between the GC column and the IR detector and the enhanced leaktightness of the system, the solvent-and-water background is considerably reduced. Optimization of the SVE closure time is not necessary. These improvements make the system more robust and more sensitive than the loop-type set-up described earlier [10].

The optimized system was combined with SPE-type sample handling to yield an on-line SPE–GC–IR set-up. The potential of this approach is demonstrated by the fact that sample volumes of only 20 ml sufficed to detect, and identify, microcontaminants in tap and surface water at the 0.1–1 µg/l level. When using appropriate functional-group chromatograms rather than the Gram–Schmidt chromatogram, detection limits were on the order of 15 ng/l for tap water.

Because of its inherent sensitivity, SPE–GC–IR appears to be a suitable technique for the screening of environmental water samples. The SPE cartridges can be loaded with samples sent to the laboratory or, alternatively, they can be loaded at the sampling site and, then, be transported to a GC–IR facility. Screening for functional groups, i.e. classes of compounds, of interest will indicate whether or not distinct peaks are present in the IR traces. These can then be identified on the basis of their full spectrum by means of a library search.

Finally, even though our practical experience still is limited, it seems justified to state that the present developments of SPE–GC–IR, or large-volume injection–GC–IR in general, make it a promising complementary or even alternative technique to screening systems such as SPE–GC with mass spectrometric or atomic emission detection [21, 9].

References

[1] P.R. Griffiths, *Appl. Spectrosc.*, 31 (1977) 284.
[2] G.T. Reedy, D.G. Ettinger, J. Schneider and S. Bourne, *Anal. Chem.*, 57 (1985) 1602.
[3] K.H. Shafer and P.R. Griffiths, *Anal. Chem.*, 58 (1986) 3254.
[4] P. Jackson, G. Dent, D. Carter, D.J. Schofield, J.M. Chalmers, T. Visser and M. Vredenbregt, *J. High Resolut.Chromatogr.*, 16 (1993) 515.
[5] T. Visser, M.J. Vredenbregt and A.P.J.M. de Jong, *J. Chromatogr. A*, 687 (1994) 303.
[6] H.G.J. Mol, H.-G. Janssen, C.A. Cramers, J.J. Vreuls, U.A.Th. Brinkman, *J. Chromatogr.*, 703 (1995) 277.
[7] S. Maeno and P.A. Rodriguez, *J. Chromatogr. A.*, 731 (1996) 201.
[8] A.J.H. Louter, U.A.Th. Brinkman and R.T. Ghijsen, *J. Microcol. Sep.*, 5 (1993) 3031.
[9] Th. Hankemeier, A.J.H. Louter, F.D. Rinkema and U.A.Th. Brinkman, *Chromatographia*, 40 (1995) 119.
[10] Th. Hankemeier, H.T.C. van der Laan, J.J. Vreuls, M.J. Vredenbregt, T. Visser and U.A.Th. Brinkman, *J. Chromatogr. A*, 732 (1996) 75.
[11] K. Grob, Jr. and J.-M. Stoll, *J. High Resolut. Chromatogr.*, 9 (1986) 519.

[12] J.J. Vreuls, H.G.J. Mol, J. Jagesar, R. Swen, R.E. Hessels and U.A.Th. Brinkman, in P. Sandra and G. Devos (Editors), *Proc. 17th Intern. Symp. Cap. Chromatogr., Riva del Garda, September 1994*, Hüthig, Heidelberg, Germany,1994, 1181.
[13] D. Henneberg, U. Henrichs and G. Schomburg, *Chromatographia*, 8 (1975) 449.
[14] L. Hathcock, Q.W. Zhang and W. Bertsch, *J. High Resolut. Chromatogr.*, 13 (1990) 656.
[15] D. Henneberg, U. Henrichs, H. Husmann and G. Schomburg, *J. Chromatogr.*, 167 (1978) 139.
[16] S. Bourne and W.R. Croasmun, *Anal. Chem.*, 60 (1988) 2172.
[17] J.F. Pankow and L.M. Isabelle, *J. High Resolut. Chromatogr.*, 10 (1987) 617.
[18] R.F. Arrendale, R.F. Severson and O.T. Chortyk, *Anal. Chem.*, 56 (1984) 1533.
[19] S. Ramalho, Th. Hankemeier, M. de Jong, U.A.Th. Brinkman and J.J. Vreuls, *J. Microcol. Sep.*, 7 (1995) 383.
[20] Th. Hankemeier, S.P.J. van Leeuwen, J.J. Vreuls and U.A.Th. Brinkman, *J. Chromatogr. A*, 811 (1998) 117.
[21] A.J.H. Louter, C.A. van Beekvelt, P.C. Monatanes, J. Slobondník, J.J. Vreuls and U.A.Th. Brinkman, *J. Chromatogr. A*, 725 (1996) 67.

Samenvatting

Om te onderzoeken of een monster, zoals oppervlaktewater, stoffen bevat die schadelijk zijn voor mens en/of milieu, is het nodig meetsystemen ter beschikking te hebben die relevante verbindingen kunnen identificeren. Tegelijkertijd moeten deze verbindingen ook gekwantificeerd worden, om zo te bepalen of deze stoffen aanwezig zijn in concentraties boven voor hen gestelde grenswaarden. Zuivere verbindingen kunnen met spectrometrische methoden als massaspectrometrie (MS) en infrarood spectrometrie (IR) nauwkeurig worden gekarakteriseerd en vaak ook geïdentificeerd. Door de veelal grote hoeveelheid verbindingen in een monster is het echter moeilijk deze verbindingen met behulp van spectrometrische technieken direct op een laag concentratieniveau in het monster te bepalen. Voordat spectrometrische detectie mogelijk is, moeten de verbindingen eerst gescheiden worden van de matrix en bij voorkeur ook van elkaar. Het is dus nodig scheidingsmethoden te koppelen met spectrometrische detectie. Men spreekt dan van *hyphenated* of gekoppelde technieken.

Dit proefschrift beschrijft de ontwikkeling van systemen voor wateranalyse die berusten op de koppeling van gaschromatografie (GC) als scheidingstechniek, met spectrometrische detectie zoals MS, IR en atomaire emissie detectie (AED). Het uiteindelijke doel was een geautomatiseerd, gevoelig systeem te ontwikkelen dat robuust en gebruikersvriendelijk is, en bovendien toepasbaar voor de bepaling van verbindingen met een verschillende mate van vluchtigheid. Dit kan bereikt worden door monstervoorbewerking, GC scheiding en universele maar toch selectieve detectie in één systeem te integreren.

GC is een veelgebruikte methode die de scheiding van een breed scala aan vluchtige en minder vluchtige verbindingen mogelijk maakt. Een probleem is dat water niet rechtstreeks in een GC geïntroduceerd kan worden. Er is voorbewerking van het monster nodig, zodanig dat een groot gedeelte van de storende matrix-verbindingen geëlimineerd wordt. Er is voor vaste-fase extractie (SPE, solid-phase extraction) gekozen vanwege het brede bereik aan verbindingen dat hiermee verrijkt kan worden. De meest efficiënte koppeling van SPE en GC is in-lijn (in het Engels *on-line*): de in het monster aanwezige en op de SPE kolom aangerijkte analieten worden rechtstreeks en kwantitatief met behulp van een geschikt organisch oplosmiddel in de GC gebracht. Hierdoor kan het systeem geminiaturiseerd en geautomatiseerd worden en is een minimale hoeveelheid oplosmiddel nodig. Om de hoeveelheid oplosmiddel nodig voor desorptie van de SPE-extractiekolom direct in de GC te kunnen introduceren, is een interface nodig. In dit onderzoek is voor een *on-column* interface gekozen vanwege zijn brede toepassingsbereik, van vluchtige tot minder vluchtige verbindingen. Maar, zoals vaker wordt gezien bij het zoeken naar een interface tussen geheel verschillende analysetechnieken, de onderliggende principes werden niet volledig begrepen, en er was een tijdrovend vooronderzoek nodig voordat met het geoptimaliseerde systeem een grotere hoeveelheid monster efficiënt en geautomatiseerd kon worden gemeten.

Als detectietechniek is in eerste instantie voor MS gekozen vanwege de universaliteit, de gevoeligheid, de selectiviteit en de mogelijkheid tot identificatie. Bij de ontwikkeling van strategieën om doelgericht de aanwezigheid van bepaalde klassen van verbindingen te vinden

en deze vervolgens te identificeren, zijn ook andere spectrometrische detectietechnieken onderzocht. Voor de *screening* van monsters naar bepaalde hetero-atoom-bevattende verbindingen is de koppeling van SPE–GC met AED gebruikt, en voor het onderzoek van verbindingen die bepaalde functionele groepen bevatten, IR-detectie.

In **Hoofdstuk 1** wordt een overzicht gegeven van de huidige stand van zaken betreffende SPE–GC in de literatuur, waarbij de resultaten van het onderzoek beschreven in dit proefschrift in de beschouwing worden betrokken. Algemene aspecten en problemen van de in-lijn koppeling van LC en GC worden aan de orde gesteld en er worden verschillende toepassingen beschreven. Verwante technieken worden kort beschreven en hun mogelijkheden worden met die van SPE–GC vergeleken. Verwachte trends voor de toekomst worden geschetst. Tot slot wordt het uitgangspunt voor en de strekking van het onderzoek in dit proefschrift gepresenteerd.

In **Hoofdstuk 2** wordt het optimaliseren van de injectie van een grote volumina met de on-column injector behandeld. Bij deze techniek wordt geïnjecteerd in een *retention gap*, een niet-gecoate kolom, geplaatst voor de analytische kolom in de GC. Hierbij verdampt een deel van het oplosmiddel terwijl het andere deel een film vormt in de retention gap. Deze film zorgt ervoor dat vluchtige verbindingen worden vastgehouden. Door gebruik te maken van een zgn. *solvent vapour exit* (SVE) kan het oplosmiddel sneller verdampen, terwijl tevens voorkomen wordt dat het de GC detector bereikt. Als al het oplosmiddel verdampt is, moet de SVE gesloten worden en kan de gewone GC-scheidings/detectie-procedure beginnen. Er worden methoden beschreven om de juiste injectiecondities (injectiesnelheid, injectietemperatuur en druk van het draaggas) te kiezen zonder dat het systeem behoeft te worden omgebouwd. Daarnaast wordt een methode beschreven om het tijdstip te bepalen waarop de SVE gesloten moet worden (Hoofdstuk 2.1). Omdat deze procedures tijdrovend zijn, is er een alternatief ontwikkeld waarbij de SVE op het juiste tijdstip sluit zonder enige voorafgaande optimalisatie. Hierbij wordt de draaggasstroom gemonitord met een stromingsmeter: bij toename van de gasstroom aan het eind van de verdamping regelt een nieuw ontwikkelde controller automatisch de sluiting (Hoofdstuk 2.2). Vervolgens zijn procedures ontwikkeld om de juiste injectiecondities met slechts enkele injecties van puur oplosmiddel te vinden (Hoofdstuk 2.3). Hierbij is rekening gehouden met het feit dat de verdampingssnelheid van het oplosmiddel tijdens de injectie verandert. Dit was tot dan toe nog niet in de literatuur vastgesteld, hetgeen de keuze van injectiecondities negatief kan beïnvloeden Deze veronderstelling is onderbouwd met een mathematisch model, dat het verloop van de verdamping in de retention gap tracht te beschrijven.

In **Hoofdstuk 3** wordt beschreven hoe de in-lijn koppeling van SPE en GC is onderzocht en verbeterd. Met de voorheen gebruikelijke SPE–GC procedures waren vluchtige verbindingen zoals monochloorbenzeen niet te bepalen. Tijdens desorptie van een SPE-kolom wordt het grootste deel van elke verbinding namelijk met de eerste microliters oplosmiddel in de retention gap geïntroduceerd. Er is tijdens de verdamping niet voldoende oplosmiddelfilm aanwezig vóór de verbindingen om deze vast te houden. Ter verbetering van de bestaande methode werd, voorafgaand aan de desorptie, zuiver oplosmiddel in de GC geïntroduceerd. Op deze manier kan monochloorbenzeen in 10 ml water op een niveau van 0,01–0,05 µg/l worden bepaald (Hoofdstuk 3.1). De methode is verder verbeterd door de gebruikte hoeveelheid desorptievloeistof te verlagen met behulp van maatregelen zoals in Hoofdstuk 2.2 beschreven. Uiteindelijk 'controleert het systeem zichzelf': optimaliseren van

injectietemperatuur, snelheid en druk, en correctie voor variaties in het dode volume van de SPE kolommen is niet meer nodig. Bovendien is het systeem robuuster omdat de retentietijd van vluchtige verbindingen minder varieert en het systeem toleranter is met betrekking tot variaties in factoren als de stroomsnelheid van het oplosmiddel. Verder is de kwaliteit van de retention gap minder kritisch aangezien deze in een aparte oven wordt verwarmd. Zelfs vluchtige analieten kunnen nu zonder presolvent goed worden bepaald (Hoofdstuk 3.2).

Hoofdstuk 4 beschrijft onderzoek naar de *at-line* koppeling van SPE en GC met behulp van een commercieel systeem, het PrepStation. Dit systeem combineert de voordelen van in-lijn en uit-lijn SPE–GC: het SPE verrijkingssysteem is geïntegreerd, redelijk geminiaturiseerd en gesloten zoals bij de in-lijn koppeling. Doordat het extract van de SPE kolom bij dit systeem niet direct, maar via een autosamplervaatje naar de GC wordt overgebracht, is het systeem minder gecompliceerd dan in-lijn SPE–GC maar, in zijn originele vorm, bij lange na niet gevoelig genoeg. De gevoeligheid van de procedure is door ons aanzienlijk verbeterd door de hoeveelheid watermonster te verhogen, het injectievolume in de GC te vergroten (tot 50 µl) en het desorptievolume te verminderen (Hoofdstuk 4.1). De bij de hogere gevoeligheid optredende storingen uit de SPE kolom en septa werden vervolgens geëlimineerd met behulp van een nieuw ontworpen SPE kolom van roestvast staal en polychloortrifluoretheen en een 2-naalds systeem. Zonder voorafgaande reiniging lag het blanconiveau nu op slechts enkele ng/l. De analytische karakteristieken waren goed en vergelijkbaar met die van een in-lijn systeem, zij het dat de gevoeligheid iets minder en de analysetijd iets langer was.

Het gebruik van de AED voor SPE–GC wordt in **Hoofdstuk 5** beschreven. De voordelen van een AED zijn de hoge selectiviteit voor alle elementen en een responsfactor per element die min of meer onafhankelijk is van de structuur van de verbinding. Ondanks de voor sommige elementen niet al te grote gevoeligheid van een AED detector, kan door in-lijn koppeling van SPE en GC–AED de voor wateranalyse benodigde gevoeligheid wel bereikt worden (Hoofdstuk 5.1). Er is een procedure uitgewerkt om onbekende (*non-target*) verbindingen met één of meer hetero-atomen boven een bepaald concentratieniveau met SPE–GC–AED te detecteren en deze vervolgens door combinatie van de SPE–GC–AED en SPE–GC–MS gegevens te karakteriseren. Contaminanten boven het niveau van 0,05 µg/l (kraanwater) of 0,5 µg/l (afvalwater) zijn geïdentificeerd met behulp van hun partiële formule (verkregen met de AED) en het juiste (zelfde retentie-index) bijbehorende massaspectrum (Hoofdstuk 5.2). Zelfs bij identieke opbouw en procedures blijven er echter kleine verschillen in de retentie-indices van beide SPE–GC systemen bestaan, voornamelijk als gevolg van drukverschillen aan het einde van de kolom bij GC–AED en GC–MS. De gehele procedure kan vereenvoudigd worden door AED en MS in één SPE–GC systeem te integreren. De verschillen in retentietijd bedragen nu ten hoogste 0,5 sec (Hoofdstuk 5.3). Het systeem is met succes gebruikt voor het opsporen van hetero-atoom-bevattende verontreinigingen in groenten en kraan- en oppervlaktewater.

Ofschoon IR detectie relatief ongevoelig is, wordt sporenbepaling van (non-target) verbindingen met een bepaalde functionele groep in water mogelijk als GC–IR gekoppeld wordt met groot-volume injectie of SPE (**Hoofdstuk 6**). Er wordt gebruik gemaakt van een van de meest gevoelige GC–IR interfaces, een cryotrapping interface. Hierbij wordt het chromatogram op een ZnSe-plaat vastgevroren. Een nadeel van dit interface is dat het zeer gevoelig is voor storingen veroorzaakt door het kristalliseren van water en organisch oplosmiddel op de ZnSe-plaat. Inleidende experimenten lieten zien dat 100-µl (in plaats van

de conventionele 1-µl) injecties inderdaad leidden tot de gehoopte aanzienlijke detectiegrensverbetering (Hoofdstuk 6.1). Vervolgens werd de lekdichtheid van het systeem verbeterd, en werden storingen veroorzaakt door organisch oplosmiddel, voorkomen door gebruik te maken van een kolom-schakel systeem tussen GC en IR detector (Hoofdstuk 6.2). De gevoeligheid werd verder verhoogd door in-lijn koppeling met SPE. Dit leidde er toe dat microcontaminanten met een bepaalde functionele groep tot op een niveau van 0,1–1 µg/l in 20 ml kraan- of oppervlaktewater aangetoond konden worden.

Glossary of symbols and abbreviations

Some symbols which are used only once are not included.

AC	analytical column
AED	atomic emission detection
$\mathcal{G}$	ratio (injection time/evaporation time)
DAD	diode array detection
d_f	film thickness
DPTMDS	diphenyltetramethyldisilazane
ECD	electron capture detector
EI	electron ionization
EtOAc	ethyl acetate
f	length of solvent film expressed as fraction of the total length of the retention gap
FCSE	fully concurrent solvent evaporation
FID	flame ionization detector
FM	flow meter
FPD	flame photometric detector
FS	full scan
FZ	flooded zone
GC	gas chromatography
He	helium
IASPE	immunoaffinity solid-phase extraction
ICP	inductively coupled plasma
I.D.	internal diameter
IR	infrared spectrometry
ITD	ion-trap detection
K_d	distribution constant between stationary phase and mobile phase
K_{ow}	octanol–water coefficient
LC	liquid chromatography
LLE	liquid–liquid extraction
LOD	limit of detection
LVI	large-volume injection
MeOAc	methyl acetate
MS	mass spectrometer
NCI	negative chemical ionization
n.d.	not detectable
NPD	nitrogen–phosphorus detector
NPLC	normal-phase liquid chromatography
O.D.	outer diameter
OPP	organophosphorus pesticide
OTT	open tubular trapping
PAH	polycyclic aromatic hydrocarbons
PB	particle beam
PCI	positive chemical ionization
PCSE	partially concurrent solvent evaporation
PrOH	propanol
PTFE	polytetrafluoroethylene
PTV	programmed temperature vaporizer
R	regression coefficient
RG	retention gap
RP	retaining precolumn
RPLC	reversed-phase liquid chromatography

RSD	relative standard deviation
SFE	supercritical fluid extraction
SIM	selected ion monitoring
SPE	solid-phase extraction
SPETD	solid-phase extraction thermal desorption
SPME	solid-phase micro extraction
SVE	solvent vapour exit
TD	thermal desorption
TIC	total ion chromatogram
t_r	retention time
μLLE	micro liquid–liquid extraction
UV	ultraviolet
v_{evap}	evaporation rate
v_{inj}	injection speed

Dankwoord

Het heeft wat geduurd, maar na vele lange avonden en weekeinden is het boekje af! Dit is niet alleen het werk van één persoon, maar veel personen hebben direct of indirect een bijdrage geleverd aan de totstandkoming van dit proefschrift. Het is bijna onmogelijk al deze mensen passend te bedanken, maar ik wil het hier toch proberen.

Udo Brinkman, die in snelheid soms bijna niet te volgen is, al bij onze eerste ontmoeting in Amsterdam nodigde hij me uit toch al de volgende week te beginnen. Zijn interesse (niet alleen voor het werk) en inbreng was groot, de veelal lange discussies heel productief (soms had ik erna werk voor maanden). De bijna lichtsnelheid, waarmee hij stukken zorgvuldig gecorrigeerd per fax weer terugstuurde, zal hem waarschijnlijk niemand na doen. Zo hielp hij mij door te zetten, ook al was er altijd veel voor TNO te doen of wachtte er weer een TOP tentamen. En *Jacqueline Brinkman*, die ook nog 's avonds laat een vriendelijk en warm woord had voor een hardwerkende promovendus, die eigenlijk naar haar man vroeg.

René Vreuls, zijn Nederlands kon ik het eerst verstaan, en van hem heb ik vele kunstjes in groot-volume injectie en SPE–GC geleerd. Tijdens ons filosoferen over hoe het eigenlijk zou moeten zijn vele nieuwe ideeën geboren. Ook was hij altijd voor gekke dingen op de lange conferentieavonden te vinden, denk aan de open haard in Wintergreen!

Gerhard Werner, er hat mich vor allem am Anfang mit gutem Rat unterstützt, und auch mein Interesse für Leipzig geweckt. Ich werde nicht vergessen wie wir während der Suche nach einem Stipendium und Interessierten für unser Forschungsprojekt mit dem Trabi durch Leipzig rasten, und, wir haben ein Stipendium gefunden!

Tom Visser, zijn enthousiasme heeft me aangestoken (niet alleen op het gebied van IR), door zijn positivisme (hoeveel transfer lijnen waren het ook al weer?) heb ik me graag laten aansteken.

De leden van de leescommisie, *Hubi Irth*, *Hans-Gerd Janssen*, *Peter Schoenmakers* en *Tom Visser*, bedankt voor al die nuttige commentaren en het toch snelle lezen van het manuscript.

Dick van Iperen, *Klaas van Altena* en *Roald Boegschoten* van de Instrumentmakerij, ze hebben niet alleen kleinere problemen verholpen, maar wisten ook al die ontwerpen op vaak een klein velletje papier tot een echte retention gap oven of een nieuw design van het PrepStation te brengen, er was bijna niets te moeilijk!

Lex van der Gracht, die ook na het bouwen van de SVE controller met veel geduld al onze ideeën voor verbeteringen van het programma iedere keer weer geïmplementeerd heeft. *Joost Buijs*, hoeveel controllers hij heeft gebouwd weet ik zelfs bijna niet meer.

Heel veel heb ik aan de studenten te danken, zonder hun grote inzet waren vele mooie resultaten, maar ook vele leuke en gezellige momenten er niet geweest. De Dream Team leden *Jens Dallüge*, der mit größter Präzision die unterschiedlichsten Aufgaben löste (nicht zu vergessen die Karl-Fischer Aufstellung), und der mir später als AIO-Kollege mit Rat und Tat bei den letzten Experimenten half, *Philip Steketee*, een creatieve geest, die zelfs het tropenrooster eigenwillig wist te interpreteren, en *Stefan van Leeuwen*, wiens geheime Nuts voorraad ik toch kon vinden. *Sylvia Ramalho*, it was not only your temperament, but also

your warmth what was making working with you pleasant. *Marco de Jong*, altijd even opgewekt. *Sander Kok*, die niet alleen de laatste ideeën over flow meters nauwkeurig uitvoerde, maar ook goed documenteerde, en van wiens aanwezigheid ik nu nog dagelijks mag genieten. *Mohammed Abhadur*, hoewel we beiden het Nederlands nog nauwelijks beheersten, kregen wij de SPE–GC–AED werkend.

Feddy Rinkema, voor wie het verwisselen van discharge tubes nooit teveel was, en *Johan Rozenbrand*, die mij op de hoogte van de Nederlandse cultuur probeerde te brengen.

En de post-doc *Hans Mol*, die met behulp van retention gaps zelfs HP en Interscience apparatuur in één systeem kon integreren.

Rickie van der Laan, die me de voordelen van GC–IR leerde, en *Edwin Hooijschuur*, die zich niet door brekende transferlijnen en al die lekkage problemen heeft laten weerhouden het AIO bestaan te ondergaan.

Jaroslav Slobodník, who not only shared his house for the first months with another foreigner, but with whom, and sometimes in the company of *Nikolay Grebentchikov*, I discussed all the Dutch habits during many, many beers. De mede-leden van de LC–GC groep *Arjan Louter*, die toch uiteindelijk van Zwitserland naar Nederland terugkeerde, en *Vincent Goudriaan*. De (voormalige) leden van de vakgroep AAC die de tijd aan de VU altijd weer plezierig maakten: *Henk Lingeman*, *Nel Velthorst*, *Cees Gooijer*, *Elise Goosens*, *Pim Voogt*, *Gerard Hoornweg*, *Dick Kamminga*, *Ben Van Baar*, *Rudy Ghijsen*, *Ariadne Hogenboom*, *Bart Zegers*, *Rob Veraart* (nu mede-TNOer), *Harm Niederländer*, *Freek Ariese*, *Arjan Mank* (hij overtuigde me van de voordelen van een laser diode), *Steven Kok*, *Ronald van der Nesse*, *Nico van de Merbel*, *Tjijpke de Beer*, *Marco Beekman*, *Wilfried Niessen*, *Govert Somsen*, *Eric Brouwer*, *Dick Schouten*, *Reijer Dijkstra*, en *Gisèle Cassee*. The visiting scientists *Habib Bagheri*, *Igor Kozin*, *Ulrike Malmquist*, *Eva Pocurull*, *Rosa Herráez Hernández*, *Jan Norberg*, *Ebrahim Noroozian*, *Yolanda Pico*, *Krishna Verma*. En al die studenten die juist tijdens borrels en gebaksessies de groep vol leven wisten te brengen.

The persons involved in the SIVEGOM/Rhine Basin Program, *K.-Peter Hupe*, *Piet van Hout* (HP), *Wim-Herbert Mulder*, *Ab van Luin*, *Alie Sijpersma* en *Henk Barreveld* (RIZA), *Jan Steevens* (de software-man), who stimulated me not only to build a working water analyser, but also a really robust one.

All the manufacturers and suppliers, *Jan Brands* (Supelco), meneer *Goedknecht* (Bester), *Richard Slot* (LC Service), *Beat Schilling* and *Bernhard Fischer* (BGB Analytik), *John van Brussel* (Merck) and *René Leenderts* (Interscience), who supplied this project with new products; especially new retention gaps were much wanted in the hope that somewhere the breakthrough in the retention gap technology had been achieved!

Martin van der Vaart, die met een koffie in de hand mee filosofeerde aan het ontwerp van een leuk omslag, en *Miriam Verwei*, zonder wie het concept niet op tijd bij de leescommissie was geweest.

Al die begripvolle *TNO-ers*, die mij 's ochtends, na al die nachtelijke computer-sessies, weer met wat kleine oogjes bij het koffieautomaat aantroffen.

Al mijn *goede vrienden*, die me hielpen van Amsterdam en Nederland te leren houden, en voor wie ik de laatste tijd helaas veel te weinig tijd had, en die altijd hetzelfde excuus moesten aan horen, 'het proefschrift'...

Ingrid und Martin, meine lieben Eltern, denen ich sehr dankbar bin für ihre Unterstützung und Vertrauen nicht nur am Beginn des 'Abenteuers Amsterdam'. Ingrid, leider hast du den erfolgreichen Abschluß nicht mehr erleben dürfen. Auch mein *Großvater Alfred*, der mich

mit ersten chemischen Experimenten über dem Gasherd in der Küche inspiriert hat, hat uns leider schon verlassen.

Lieve *Peet*, jouw steun in de laatste maanden, jouw liefde, maar ook je vaardigheden achter de computer hielpen om het allemaal tot een goed eind te brengen. Je had je het begin van ons relatie zeker anders voorgesteld, maar vanaf nu hoort die tijd ons!

Bedankt allemaal!

Curriculum Vitae

Thomas Hankemeier was born on 9 December 1966 in Detmold (Germany). In 1986, he obtained his 'Abitur' at the Gymnasium Lage. In the same year he started his Chemistry studies at the University of Bielefeld, which he continued from 1989 at the University of Ulm. In 1990 he spent three months at the National Institute of Standards and Technology, Gaithersburg (USA) to carry out a project on LC–MS. Work for his Master's thesis on quantification with GC–MS was conducted in the Department of Analytical and Environmental Chemistry of prof.dr. Karlheinz Ballschmiter at the University of Ulm, where he received his Master's in Chemistry in 1992.

In 1993 he started his Ph.D. work in the Department of Analytical Chemistry at the Free University in Amsterdam under supervision of prof.dr. Udo A.Th. Brinkman. He participated in research studies on the development of an early-warning/monitoring system for the trace-level determination of organic micropollutants in surface water using a gas chromatography-based analyzer. This work was sponsored by, first, a scholarship from the State of Saxony (Germany) and, next, a Human Capital and Mobility grant from the EU.

Since 1996 he is working in the Packaging Department of TNO Voeding (Zeist, the Netherlands) as product manager for packaging research and polymer analysis.

List of publications

Parts of this thesis have been or will be published in the following papers:

Chapter 1.1 Th. Hankemeier and U.A.Th. Brinkman, in: W.M.A. Niessen (ed.), *Current Practice of Gas Chromatography–Mass Spectrometry*, Marcel Dekker, New York, NY, USA 2000;
and
U.A.Th. Brinkman, Th. Hankemeier and J.J. Vreuls, *Chem. Anal. (Warsaw)*, 40 (1995) 495-509.

Chapter 2.1 S. Ramalho, Th. Hankemeier, M. de Jong, U.A.Th. Brinkman and J.J. Vreuls, *J. Microcol. Sep.*, 7 (1995) 383.

Chapter 2.2 Th. Hankemeier, S.J. Kok, J.J. Vreuls and U.A.Th. Brinkman, *J. Chromatogr. A*, 811 (1998) 105.

Chapter 2.3 Th. Hankemeier, S.J. Kok, R.J.J. Vreuls and U.A.Th. Brinkman, *J. Chromatogr. A*, 841 (1999) 75.

Chapter 3.1 Th. Hankemeier, S.P.J. van Leeuwen, J.J. Vreuls and U.A.Th. Brinkman, *J. Chromatogr. A*, 811 (1998) 117.

Chapter 3.2 Th. Hankemeier, S. Ramalho, S.J. Kok, J.J. Vreuls and U.A.Th. Brinkman, *J. High Resolut. Chromatogr.*, submitted.

Chapter 4.1 Th. Hankemeier, P.C. Steketee, J.J. Vreuls and U.A.Th. Brinkman, *J. Chromatogr. A*, 750 (1996) 161.

Chapter 4.2 Th. Hankemeier, P.C. Steketee, J.J. Vreuls and U.A.Th. Brinkman, *Fresenius J. Anal. Chem.*, 364 (1999) 106.

Chapter 5.1 Th. Hankemeier, A.J.H. Louter, F.D. Rinkema and U.A.Th. Brinkman, *Chromatographia*, 40 (1995) 119.

Chapter 5.2 Th. Hankemeier, J. Rozenbrand, M. Abhadur, J.J. Vreuls and U.A.Th. Brinkman, *Chromatographia*, 48 (1998) 273.

Chapter 5.3 H.G.J. Mol, Th. Hankemeier and U.A.Th. Brinkman, *LC–GC Int.*, 12 (1999) 108.

Chapter 6.1 Th. Hankemeier, H.T.C. Van der Laan, J.J. Vreuls, M.J. Vredenbregt, T. Visser and U.A.Th. Brinkman, *J. Chromatogr. A,* 732 (1996) 75.

Chapter 6.2 Th. Hankemeier, E. Hooijschuur, R.J.J. Vreuls, U.A.Th. Brinkman and T. Visser, *J. High Resolut. Chromatogr.*, 21 (1998) 341.

Additional papers on related subjects:

'On-line coupling of immunoaffinity-based solid-phase extraction and gas chromatography for the determination of s-triazines in aqueous samples'
J. Dallüge, Th. Hankemeier, J.J. Vreuls, U.A.Th. Brinkman, *J. Chromatogr. A*, 830 (1999) 377.

'Use of a drying cartridge in on-line solid-phase extraction gas chromatography mass spectrometry'
Th. Hankemeier, A.J.H. Louter, J. Dallüge, J.J. Vreuls, U.A.Th. Brinkman, *J. High Res. Chromatogr.*, 21 (1998) 450.

'Trace analysis GC–IR by injection of large sample volumes'
Th. Hankemeier, U. Brinkman, M. Vredenbregt and T. Visser,
Microchim. Acta [Suppl.], 14 (1997) 719.

'Improvements in environmental trace analysis by GC–IR and LC–IR'
T. Visser, M.J. Vredenbregt, A.P.J.M. de Jong, G.W. Somsen, Th. Hankemeier, N.H. Velthorst, C. Gooijer, U.A.Th. Brinkman,
J. Molecular Structure, 408/9 (1997) 97.

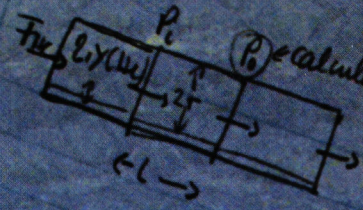

$$F_{He} = y_{He} \frac{600 \pi r^4}{16 \eta L} \frac{P_i^2 - P_o^2}{P_o} \frac{p_o}{p_{ref}} \frac{T_{ref}}{T}$$

$$V_{evap} = 1000 \frac{1 - y_{He,exit}}{y_{He,exit}} \frac{M}{V_{mol}} F_{He}$$

Programme:

(1) Calculate V_{evap} at $t=0$

(2) Loop: repeat until end of evaporation

- (a) increase $t = t + dt$
- (b) calculate amount of solvent $V_{sol,t} = (V_{inj} - V_{evap,t-dt}) / \dots$
- (c) if $V_{sol,t} = 0$, then goto (3)
- (d) calculate solvent film
- (e) calculate V_{evap} using F_{He}, $P_{exit} = 1\,atm$
  - calculate p-profile along R6 (Equal
  - (use η, y_{He}, r, P_i of previous segment)
  - if $p_{out} < 1\,atm$: $F_{He} = F_{He} + dF_{He}$
  - calculate V_{evap}, P_i
  - write V_{evap} in database

(3) end